LA-UR -83-3182

TP 8402100418

Los Alamos National Laboratory is operated by the University of California for the United States Department of Energy under contract W-7405-ENG-36

TITLE: TRAC ANALYSES OF SEVERE OVERCOOLING TRANSIENTS FOR THE OCONEE-1 PWR

AUTHOR(S): B. Bassett, B. Boyack, M. Burkett, J. Ireland, J. Koenig, J. Lime, and R. Nelton

Compiled by J. Ireland

SUBMITTED TO: Nuclear Regulatory Commission
Division of Accident Evaluation
Nuclear Regulatory Research
Washington, DC

Los Alamos National Laboratory
Los Alamos, New Mexico 87545

FORM NO 836 R4
ST NO 2629 5/81

CONTENTS

ABSTRACT 1

I. INTRODUCTION AND SUMMARY 2

II. TRAC INPUT MODEL DESCRIPTION AND STEADY-STATE RESULTS 4
A. Primary Side 6
1. Vessel 6
2. Hot Legs 8
3. Steam Generators 9
4. Cold Legs 11
5. Emergency Core-Cooling System (ECCS) 11
B. Secondary Side 11
1. Feedwater Train 11
2. Steam-Generator Control Valves 12
3. Emergency Feedwater 14
4. Steam Lines 14
C. Control System 15
1. Trips 15
2. Integrated Control System 20
D. Steady-State Calculation 30

III. TRAC TRANSIENT CALCULATIONS 35
A. Oconee-3 Turbine Trip 35
1. Introduction 35
2. Model Description and Assumptions 36
3. Transient Calculation 36
4. Summary 44
B. Main Steam-Line Break 44
1. Introduction and Summary 44
2. Model Description 47
3. Results 48
a. Base Case (Case 1) 48
b. Parametric case - Case 2 70
c. Parametric case - Case 3 79
d. Parametric case - Case 4 90
4. Conclusions 103
C. PORV LOCA 105
1. Introduction and Summary 105
2. Model Description and Assumptions 105
3. Transient Calculation 107
4. Summary 112
D. Turbine Bypass-Valve Failures 119
1. One Bank of Two TBVs 119
a. Introduction and Summary 119
b. Model Description 119
c. Results 120
i. Base Case 120
ii. Parametric Case 1 128
iii. Parametric Case 2 137

d. Conclusions..... 138
2. Two Banks of Two TBVs..... 139
a. Introduction and Summary..... 139
b. Results..... 140
i. Base Case..... 140
ii. Parametric Case 1..... 148
iii. Parametric Case 2..... 156
c. Conclusions..... 157
E. Hot-Leg Break LOCAs..... 159
1. 2 in. Break..... 159
a. Introduction and Summary..... 159
b. Model Description and Assumptions..... 160
c. Transient Calculations..... 160
d. Analysis of the Loop-Flow Oscillations..... 171
2. 4 in. Break..... 174
a. Introduction and Summary..... 174
b. Model Description and Assumptions..... 175
c. Transient Calculation..... 175
d. Summary..... 182
F. Rancho-Seco Type Transient (SG Dryout Followed by EFW Overfeed)..... 188
1. Introduction and Summary..... 188
2. Model Description and Assumptions..... 189
3. Results..... 190
4. Conclusions..... 197

IV. CONCLUSIONS AND RECOMMENDATIONS..... 197

REFERENCES..... 201

APPENDIX A OCONEE ICS CONTROLLER FOR LOOP-A..... 202

APPENDIX B EXTRAPOLATIONS..... 213

APPENDIX C UNCERTAINTIES IN OCONEE PTS CALCULATIONS..... 234

LIST OF FIGURES

1. Primary-side model for Oconee-1 7
2. Vent-valve model 8
3. Secondary-side model for Oconee-1 10
4. Detail of feedwater-heater model (cross-section) 13
5. Steam-generator control-valve schematic 13
6. Reactor trip system 17
7. HPI, RCP, and MFW realignment trip system 18
8. Hotwell, condensate-booster, and main feedwater pumps trip system 19
9. SG isolation trip system 20
10. Emergency feedwater trip system 21
11. ICS organization 22
12. Feedwater-control section of the ICS 23
13. BTU-limiter control blocks 24
14. Neutron-power cross-limiter control blocks 25
15. Feedwater-flow control blocks 27
16. Level-limiter control blocks 29
17. Feedwater-valve adjustment control blocks 29
18. MFW-pump-speed control blocks 31
19. Main-steam safety-valve modeling for Oconee-3 transient 37
20. Measured main feedwater flow rates 38
21. TRAC-calculated decay power and Oconee-3 measured thermal power 38
22. Calculated and measured primary pressures 39
23. Calculated and measured pressurizer water levels 39
24. Calculated and measured hot- and cold-leg temperatures for loop A 42
25. Calculated and measured hot- and cold-leg temperatures for loop B 42
26. Calculated and measured steam-generator A secondary pressures 43
27. Calculated and measured steam-generator B secondary pressures 43
28. Calculated and measured water levels in steam-generator A 45
29. Calculated and measured water levels in steam-generator B 45
30. Pressurizer pressure (0-900 s) - base case 51
31. Pressurizer pressure (0-7200 s) - base case 51
32. Pressurizer water level (0-900 s) - base case 52
33. Pressurizer water level (0-7200 s) - base case 52
34. Downcomer liquid temperatures (0-900 s) at vessel axial level 6 (all azimuthal sectors) - base case 53
35. Downcomer liquid temperatures (0-7200 s) at vessel axial level 6 (all azimuthal sectors) - base case 53
36. Total vent-valve flow into downcomer - base case 55
37. Hot-leg liquid subcooling (0-900 s) - base case 55
38. Hot-leg liquid subcooling (0-7200 s) - base case 56
39. Hot-leg mass flows (0-900 s) - base case 56
40. Hot-leg mass flows (0-7200 s) - base case 57
41. Candy-cane void fractions - base case 57
42. Upper-plenum liquid volume fraction - base case 58
43. Loop-A cold-leg mass flows - base case 58
44. Loop-A cold-leg liquid temperatures - base case 59
45. Loop-B cold-leg mass flows - base case 59
46. Loop-B cold-leg liquid temperatures - base case 61
47. SG A secondary-side water inventory - base case 61
48. SG A secondary-side pressure - base case 62

49. SG A steam-line flow - base case..... 62
50. CCFL phenomena in affected steam generator (SG A) - base case..... 63
51. SG B secondary-side water inventory (0-900 s) - base case..... 63
52. SG B secondary-side water inventory (0-7200 s) - base case..... 64
53. SG B secondary-side pressure (0-900 s) - base case..... 64
54. SG B secondary-side pressure (0-7200 s) - base case..... 66
55. MFW pump speed - base case..... 66
56. MFW liquid temperature - base case..... 67
57. MFW mass flows - base case..... 67
58. EFW mass flows (0-900 s) - base case..... 68
59. EFW mass flows (0-7200 s) - base case..... 68
60. EFW liquid temperature at pump discharge - base case..... 69
61. EFW liquid temperatures at injection locations - base case..... 69
62. Loop-A HPI flows - base case..... 71
63. Loop-B HPI flows - base case..... 71
64. Accumulator water levels - base case..... 72
65. Accumulator liquid volume discharged - base case..... 72
66. PORV mass flow - base case..... 73
67. Pressurizer pressure - Case 2..... 73
68. Pressurizer water level - Case 2..... 75
69. Downcomer liquid temperatures at vessel axial level 6 (all azimuthal sectors) - Case 2..... 75
70. Hot-leg mass flows - Case 2..... 76
71. Candy-cane void fractions - Case 2..... 76
72. Loop-A cold-leg mass flows - Case 2..... 77
73. Loop-B cold-leg mass flows - Case 2..... 77
74. Loop-A cold-leg liquid temperatures - Case 2..... 78
75. Loop-B cold-leg liquid temperatures - Case 2..... 78
76. SG A secondary-side water inventory - Case 2..... 80
77. SG A secondary-side pressure - Case 2..... 80
78. SG A steam-line flow - Case 2..... 81
79. SG B secondary-side water inventory - Case 2..... 81
80. SG B secondary-side pressure - Case 2..... 82
81. MFW pump speed - Case 2..... 82
82. HPI flows - Case 2..... 83
83. Pressurizer pressure - Case 3..... 83
84. Pressurizer water level - Case 3..... 85
85. Downcomer liquid temperatures at vessel axial level 6 (azimuthal sectors) - Case 3..... 85
86. Hot-leg mass flows - Case 3..... 86
87. Candy-cane void fractions - Case 3..... 86
88. Loop-A cold-leg mass flows - Case 3..... 87
89. Loop-B cold-leg mass flows - Case 3..... 87
90. Loop-A cold-leg liquid temperatures - Case 3..... 88
91. Loop-B cold-leg liquid temperatures - Case 3..... 88
92. SG A secondary-side water inventory - Case 3..... 89
93. SG A secondary-side pressure - Case 3..... 89
94. SG A steam-line flow - Case 3..... 91
95. SG B secondary-side water inventory - Case 3..... 91
96. SG B secondary-side pressure - Case 3..... 92
97. MFW pump speed - Case 3..... 92
98. System pressure for Case 4 and base case..... 95
99. Downcomer liquid temperatures at vessel axial level 6 for Case 4 and base case..... 95
100. Break flow for Case 4..... 96
101. SG-A secondary pressure for Case 4..... 96
102. SG-B secondary pressure for Case 4..... 97

103. EFW flow (SG A and SG B) for Case 4..... 97
104. SG A total feedwater flow for Case 4..... 98
105. SG B total feedwater flow for Case 4..... 98
106. SG-A tube-bundle-region mass inventory for Case 4..... 99
107. SG-B tube-bundle-region mass inventory for Case 4..... 99
108. Hot-leg A and B mass flows for Case 4..... 100
109. Hot-leg A and B liquid temperatures for Case 4..... 100
110. Loop A cold-leg mass flows for Case 4..... 101
111. Loop A cold-leg liquid temperatures for Case 4..... 101
112. Loop B cold-leg mass flows for Case 4..... 102
113. Loop B cold-leg liquid temperatures for Case 4..... 102
114. Total HPI flow for Case 4..... 104
115. Total mass flow through vent valves for Case 4..... 104
116. Upper plenum liquid temperature for Case 4..... 105
117. SG A secondary pressure..... 108
118. SG B secondary pressure..... 108
119. Main-feedwater flow - loops A and B..... 109
120. Main-feedwater liquid temperature - loops A and B..... 109
121. Realignment mass flow - loop A (negative flow is into SG)..... 110
122. Realignment mass flow - loop B (negative flow is into SG)..... 110
123. Steam-generator secondary inventory - loop A..... 111
124. Steam-generator secondary inventory - loop B..... 111
125. Pressurizer pressure..... 111
126. Pressurizer water level..... 113
127. PORV mass flow..... 114
128. PORV vapor fraction..... 114
129. Hot-leg mass flows - loops A and B..... 115
130. Hot-leg liquid temperatures - loops A and B..... 115
131. Cold-leg mass flows - loops A1 and A2..... 116
132. Cold-leg mass flows - loops B1 and B2..... 116
133. Cold-leg liquid temperatures - loops A1 and A2..... 117
134. Cold-leg liquid temperatures - loops B1 and B2..... 117
135. Candy-cane void fractions - loops A and B..... 118
136. Vessel upper-plenum void fractions - all azimuthal cells..... 118
137. Downcomer liquid temperatures at vessel axial level 6 (all azimuthal sectors)..... 119
138. Pressurizer pressure..... 121
139. Steam-generator-secondary pressure - loop A..... 121
140. Steam-generator-secondary pressure - loop B..... 122
141. Main-feedwater flow - loop A..... 122
142. Main-feedwater flow - loop B..... 124
143. Main-feedwater liquid temperatures - loop A..... 124
144. Main-feedwater liquid temperatures - loop B..... 125
145. Flow through emergency-feedwater header - loop A..... 125
146. Flow through emergency-feedwater header - loop B..... 126
147. Liquid temperatures in the emergency-feedwater header - loop A..... 126
148. Liquid temperatures in the emergency-feedwater header - loop B..... 127
149. Steam-generator-secondary inventory - loop A..... 127
150. Steam-generator-secondary inventory - loop B..... 129
151. Hot-leg flow - loop A..... 129
152. Hot-leg flow - loop B..... 130
153. Cold-leg flow - loop A1..... 130
154. Cold-leg flow - loop A2..... 131
155. Cold-leg flow - loop B1..... 131
156. Cold-leg flow - loop B2..... 132

157. Cold-leg liquid temperatures - loop B1..... 132
158. Cold-leg liquid temperatures - loop B2..... 133
159. Cold-leg liquid temperatures - loop A1..... 133
160. Cold-leg liquid temperatures - loop A2..... 134
161. Candy-cane vapor fraction - loop A..... 134
162. Candy-cane vapor fraction - loop B..... 135
163. Pressurizer water level..... 135
164. Downcomer liquid temperatures (base case) at vessel axial level 6 (all azimuthal sectors)..... 136
165. Downcomer liquid temperatures (parametric case 1) at vessel axial level 6 (all azimuthal sectors)..... 136
166. Downcomer liquid temperatures (parametric case 2) at vessel axial level 6 (all azimuthal sectors)..... 139
167. Pressurizer pressure..... 141
168. Steam-generator-secondary pressure - loop A..... 141
169. Steam-generator-secondary pressure - loop B..... 142
170. Main-feedwater flow - loop A..... 142
171. Main-feedwater flow - loop B..... 144
172. Main-feedwater liquid temperatures - loop A..... 144
173. Main-feedwater liquid temperatures - loop B..... 145
174. Emergency-feedwater flow - loop A..... 145
175. Emergency-feedwater flow - loop B..... 146
176. Emergency-feedwater liquid temperatures - loop A..... 146
177. Emergency-feedwater liquid temperatures - loop B..... 147
178. Steam-generator-secondary inventory - loop A..... 147
179. Steam-generator-secondary inventory - loop B..... 149
180. Hot-leg flow - loop A..... 149
181. Hot-leg flow - loop B..... 150
182. Cold-leg flow - loop A1..... 150
183. Cold-leg flow - loop A2..... 151
184. Cold-leg flow - loop B1..... 151
185. Cold-leg flow - loop B2..... 152
186. Cold-leg liquid temperature - loop A1..... 152
187. Cold-leg liquid temperature - loop A2..... 153
188. Cold-leg liquid temperature - loop B1..... 153
189. Cold-leg liquid temperature - loop B2..... 154
190. Candy-cane vapor fraction - loop A..... 154
191. Candy-cane vapor fraction - loop B..... 155
192. Pressurizer water level..... 155
193. Downcomer liquid temperatures (base case) at vessel axial level 6 (all azimuthal sectors)..... 158
194. Downcomer liquid temperatures (parametric case 1) - vessel axial level 6 (all azimuthal sectors)..... 158
195. Downcomer liquid temperatures (parametric Case 2) - vessel axial level 6 (all azimuthal sectors)..... 159
196. Steam generator secondary-side pressure - loop A..... 161
197. Steam generator secondary-side pressure - loop B..... 161
198. Steam generator secondary-side inventory - loop A..... 162
199. Steam generator secondary-side inventory - loop B..... 162
200. MFW mass flows - loops A and B..... 164
201. MFW liquid temperatures - loops A and B..... 164
202. Emergency/realigned mass flows - loops A and B..... 165
203. Emergency/realigned liquid temperatures - loops A and B..... 165
204. Pressurizer pressure..... 166
205. Pressurizer water level..... 166
206. Break mass flow..... 167
207. Break void fraction..... 167

208. Candy-cane void fractions - loops A and B..... 168
209. Cold-leg mass flows - loops A1 and A2..... 168
210. Cold-leg mass flows - loops B1 and B2..... 169
211. Cold-leg liquid temperatures - loops A1 and A2..... 169
212. Cold-leg liquid temperatures - loops B1 and B2..... 170
213. Hot-leg mass flows - loops A and B..... 170
214. Hot-leg liquid temperatures - loops A and B..... 172
215. Downcomer liquid temperatures - vessel axial level 6 (all azimuthal sectors)..... 172
216. Downcomer liquid temperature comparison for 2-in. break case (vent valves versus no vent valves)..... 173
217. Total vent valve mass flow..... 173
218. Steam generator secondary-side pressure - loop A..... 176
219. Steam generator secondary-side pressure - loop B..... 176
220. Steam generator secondary-side inventory - loop A..... 177
221. Steam generator secondary-side inventory - loop B..... 177
222. MFW flows - loops A and B..... 178
223. MFW liquid temperatures - loops A and B..... 178
224. Realigned mass flows - loops A and B..... 179
225. Realigned liquid temperatures - loops A and B..... 179
226. Pressurizer pressure..... 180
227. Pressurizer water level..... 180
228. Break mass flow..... 181
229. Break void fraction..... 181
230. Candy-cane void fractions - loops A and B..... 183
231. Hot-leg mass flows - loops A and B..... 183
232. Hot-leg liquid temperatures - loops A and B..... 185
233. Cold-leg mass flows - loops A1 and A2..... 185
234. Cold-leg mass flows - loops B1 and B2..... 186
235. Cold-leg liquid temperatures - loops A1 and A2..... 186
236. Cold-leg liquid temperatures - loops B1 and B2..... 187
237. Total positive vent-valve vapor mass flow..... 187
238. Downcomer liquid temperatures - vessel axial level 6 (all azimuthal sectors)..... 188
239. Primary system pressure..... 191
240. Pressurizer water level..... 191
241. PORV mass flow..... 192
242. SG-A secondary-side pressure..... 192
243. SG-B secondary-side pressure..... 193
244. EFW mass flows..... 193
245. EFW liquid temperatures at injection point..... 194
246. SG-A secondary-side inventory..... 194
247. SG-B secondary-side inventory..... 195
248. Loop A cold-leg liquid temperatures..... 195
249. Loop B cold-leg liquid temperatures..... 196
250. Hot-leg liquid temperatures..... 196
251. Loop A HPI mass flows..... 198
252. Loop B HPI mass flows..... 198
253. Loop A cold-leg mass flows..... 199
254. Loop B cold-leg mass flows..... 199
255. Hot-leg mass flows..... 200
256. Downcomer liquid temperatures-vessel axial level 6 (all azimuthal sectors)..... 200
B-1. Pressurizer pressure..... 214
B-2. Downcomer liquid temperatures at vessel axial level 6 (all azimuthal sectors)..... 215

B-3. Heat-transfer coefficients at vessel axial level 6 (all azimuthal sectors)..... 216
B-4. Pressurizer pressure histories for Case 5 (Case 5A-base; Case 5B-parametric 1; Case 5C-parametric 2)..... 217
B-5. Pressurizer pressure histories for Case 6 (Case 6A-base; Case 6B-parametric 1; Case 6C-parametric 2)..... 217
B-6. Downcomer liquid temperatures at vessel axial level 6 (all azimuthal sectors) for Case 5A..... 218
B-7. Downcomer liquid temperatures at vessel axial level 6 (all azimuthal sectors) for Case 5B..... 218
B-8. Downcomer liquid temperatures at vessel axial level 6 (all azimuthal sectors) for Case 5C..... 219
B-9. Downcomer liquid temperatures at vessel axial level 6 (all azimuthal sectors) for Case 6A..... 219
B-10. Downcomer liquid temperatures at vessel axial level 6 (all azimuthal sectors) for Case 6B..... 220
B-11. Downcomer liquid temperatures at vessel axial level 6 (all azimuthal sectors) for Case 6C..... 220
B-12. Heat-transfer coefficients at vessel axial level 6 (all azimuthal sectors) for Case 5A..... 221
B-13. Heat-transfer coefficients at vessel axial level 6 (all azimuthal sectors) for Case 5B..... 221
B-14. Heat-transfer coefficients at vessel axial level 6 (all azimuthal sectors) for Case 5C..... 222
B-15. Heat-transfer coefficients at vessel axial level 6 (all azimuthal sectors) for Case 6A..... 222
B-16. Heat-transfer coefficients at vessel axial level 6 (all azimuthal sectors) for Case 6B..... 223
B-17. Heat-transfer coefficients at vessel axial level 6 (all azimuthal sectors) for Case 6C..... 223
B-18. PORV LOCA extrapolated system pressure..... 226
B-19. PORV LOCA extrapolated downcomer liquid temperature..... 226
B-20. PORV LOCA extrapolated downcomer heat-transfer coefficient..... 227
B-21. 4-in-diam. SBLOCA extrapolated system pressure..... 227
B-22. 4-in-diam. SBLOCA extrapolated downcomer liquid temperature..... 228
B-23. 4-in-diam. SBLOCA extrapolated downcomer heat-transfer coefficient..... 228
B-24. 4-in-diam. SBLOCA extrapolated system pressure..... 231
B-25. 4-in-diam. SBLOCA extrapolated downcomer liquid temperature..... 231
B-26. 4-in-diam. SBLOCA extrapolated downcomer heat-transfer coefficient..... 232
B-27. Rancho-Seco type transient extrapolated system pressure..... 232
B-28. Rancho-Seco type transient extrapolated downcomer liquid temperature..... 233
B-29. Rancho-Seco type transient extraplated downcomer heat-transfer coefficients..... 233

LIST OF TABLES

I. LOS ALAMOS OCONEE-1 PTS OVERCOOLING TRANSIENT CALCULATIONS..... 3
II. TRAC OCONEE-1 TRANSIENT RESULTS..... 5
III. SIMPLE TRIPS..... 16
IV. BTU-LIMITER CONTROL-BLOCK EQUATIONS..... 24
V. NEUTRON-POWER CROSS-LIMITER CONTROL-BLOCK EQUATIONS..... 26
VI. FEEDWATER-FLOW CONTROL-BLOCK EQUATIONS..... 27
VII. LEVEL-LIMITER CONTROL-BLOCK EQUATIONS..... 28
VIII. FEEDWATER-VALVE ADJUSTMENT CONTROL-BLOCK EQUATIONS..... 30
IX. MFW-PUMP-SPEED CONTROL-BLOCK EQUATIONS..... 32
X. PRIMARY-SIDE STEADY-STATE CONDITIONS..... 33
XI. SECONDARY-SIDE STEADY-STATE CONDITIONS..... 34
XII. INITIAL STEADY-STATE CONDITIONS..... 40
XIII. MAIN-STEAM-SAFETY AND TURBINE-BYPASS VALVE SETPOINTS..... 40
XIV. SEQUENCE OF EVENTS..... 41
XV. COMPARISON OF TRAC AND OCONEE-3 RESULTS..... 46
XVI. SEQUENCE OF EVENTS..... 49
XVII. MSLB (CASE 2) SEQUENCE OF EVENTS..... 74
XVIII. MSLB (CASE 4) SEQUENCE OF EVENTS..... 106
XIX. MSLB (CASE 3) SEQUENCE OF EVENTS..... 106
XX. PORV LOCA EVENT SEQUENCE..... 107
XXI. TBV EVENT SEQUENCE (BASE CASE)..... 123
XXII. TBV EVENT SEQUENCE PARAMETRIC CASE 1..... 137
XXIII. TBV EVENT SEQUENCE PARAMETRIC CASE 2..... 138
XXIV. TBV EVENT SEQUENCE BASE CASE..... 143
XXV. TBV EVENT SEQUENCE PARAMETRIC CASE 1..... 148
XXVI. TBV EVENT SEQUENCE PARAMETRIC CASE 2..... 157
XXVII. HOT-LEG BREAK LOCA - 2 IN. BREAK SEQUENCE OF EVENTS..... 160
XXVIII. HOT-LEG BREAK LOCA - 4 IN. BREAK EVENT SEQUENCE BASE CASE..... 182
XXIX. RANCHO-SECO TYPE TRANSIENT INITIAL CONDITIONS AND POSTULATED EVENT SEQUENCE..... 189
XXX. RANCHO-SECO TYPE TRANSIENT SEQUENCE OF EVENTS..... 190
B-I. EXTRAPOLATED RESULTS FOR TBV TRANSIENTS AT 7200 s..... 225
C-I. SYSTEMS AFFECTED BY UNCERTAINTIES..... 236

ACRONYMS

ANS	American Nuclear Society
BTU	British Thermal Unit
B&W	Babcock & Wilcox
ECCS	Emergency Core-Cooling System
EFW	Emergency Feedwater
EFWV	Emergency Feedwater Valve
FSAR	Final Safety Analysis Report
HPI	High-Pressure Injection
ICS	Integrated Control System
LOCA	Loss-of-Coolant Accident
LPI	Low-Pressure Injection
LPIS	Low-Pressure Injection System
MFCV	Main-Flow-Control Valve
MFW	Main Feedwater
MSLB	Main Steam-Line Break
MSSV	Main Steam Safety Valve
NDT	Nil-Ductility Temperature
NRC	Nuclear Regulatory Commission
ORNL	Oak Ridge National Laboratory
PORV	Power-Operated Relief Valve
PTS	Pressurized Thermal Shock
PWR	Pressurized Water Reactor
RCP	Reactor Coolant Pump
SG	Steam Generator
SUFCV	Start-Up Flow-Control Valve
TBV	Turbine-Bypass Valve
TRAC	Transient Reactor Analysis Code
TSV	Turbine-Stop Valve
USI	Unresolved Safety Issue

ACKNOWLEDGEMENTS

The authors wish to acknowledge the extraordinary efforts of word processors Jean Martinez and Cecilia Gonzales in the organization and processing of this document. Also, the efforts of Sylvia Lee in preparing the graphics for the calculations are greatly appreciated.

TRAC ANALYSES OF SEVERE OVERCOOLING TRANSIENTS FOR THE OCONEE-1 PWR*

by

B. Bassett, B. Boyack, M. Burkett
J. Ireland, J. Koenig, J. Lime, and R. Nelton

Compiled by

J. Ireland

ABSTRACT

This report describes the results of several TRAC-PF1 calculations of overcooling transients in a Babcock & Wilcox lowered-loop pressurized-water reactor (Oconee-1). The purpose of this study is to provide detailed thermal-hydraulic input to Oak Ridge National Laboratory for pressurized thermal-shock analyses. The transient calculations performed were plant specific in that details of the primary system, the secondary system, and the plant integrated control system of Oconee-1 were included in the TRAC input model. The results of the calculations indicate that the turbine-bypass valve failure transient was the most severe in terms of resulting in relatively cold liquid temperatures in the downcomer region of the vessel. The power-operated relief-valve LOCA transient was the least severe in terms of downcomer liquid temperatures because of vent-valve fluid mixing and near saturated conditions in the primary system. It is recommended that future calculations consider a wider range of operator actions to cover the spectra of overcooling transient sequences more completely.

---

*Work performed under the auspices of the United States Nuclear Regulatory Commission.

I. INTRODUCTION AND SUMMARY

Pressurized thermal shock (PTS) in pressurized water reactors (PWRs) has been identified by the Nuclear Regulatory Commission (NRC) as an unresolved safety issue (USI A-49). Because of this, the NRC has a major program distributed among several organizations to help resolve the PTS issue. The goal of this project is to determine the potential risk of older reactor vessels to severe overcooling transients that rapidly cool the primary system.

The Los Alamos contribution to this project is to use the multi-dimensional two-fluid, non-equilibrium numerical simulation code, TRAC-PF1[1], to provide accurate thermal-hydraulic conditions during postulated PTS accidents in selected PWRs. This report presents the results of several TRAC-PF1 thermal-hydraulic calculations performed for the Oconee-1 PWR. The Oconee-1 PWR is operated by Duke Power Company, and the nuclear steam-supply system was designed by the Babcock & Wilcox (B&W) Company. The main purpose of these calculations was to determine which of the overcooling transients specified by Oak Ridge National Laboratory (ORNL) was the most severe in terms of cold liquid temperatures in the downcomer region of the reactor vessel. These ORNL-specified transients are listed in Table I.

The concern over PTS arises because the material properties of the vessel wall change after several years of irradiation.[2] The vessel wall becomes embrittled and its nil-ductility temperature (NDT) increases. If during an accident, overcooling of the primary-system liquid cools the vessel wall below the NDT (the NDT for Oconee-1 is ~365 K) and the system subsequently repressurizes, the possibility exists that defects could be initiated or propagated in the vessel wall. Such overcooling of the primary-system liquid may result from the high-pressure injection (HPI) system or rapid cooling by the secondary system.

Because the risk of initiating or propagating flaws in the vessel wall depends on the coupling of the thermal stresses produced by overcooling with the mechanical stresses from repressurization, detailed system models are required. Modeling both the primary and secondary systems of the reactor plant is necessary to properly analyze the PTS phenomena. The steam-generator (SG) secondary-side inlet conditions directly affect primary temperature, pressure, and the emergency core-coolant injection. Secondary-side inlet conditions are highly dependent on main-feed pump and SG control-valve operations as well as the termination of the extracted steam supply to the feedwater heaters. Other important systems modeled in the TRAC input deck include a model of the B&W Integrated Control System (ICS) used at the Oconee-1 plant. The ICS monitors

TABLE I

LOS ALAMOS OCONEE-1 PTS OVERCOOLING TRANSIENT CALCULATIONS

Transient	Description
1. Oconee-3 turbine trip	Simulate actual plant transient that occurred on March 14, 1980.
2. Main-steam line break	34" steam-line break; all systems operate as designed; steam generators isolated at 10 min., unaffected steam generator refilled at 15 min.
3. Small-break LOCA (PORV stuck open)	Pressurizer relief valve sticks open; ICS fails to run back main feedwater; primary coolant pump trip.
4. Turbine-bypass valve failure (one bank of two valves) a. SG level control fails b. SG level control does not fail c. RCP restart; HPI throttled	One bank of TBVs fail to reseat after opening.
5. Turbine-bypass valve failure (two banks of two valves) a. SG level control fails b. SG level control does not fail c. RCP restart; HPI throttled	Two banks of TBVs fail to reseat after opening.
6. Small-break LOCA (2 in. hot-leg break)	Two-inch diameter hole in pressurizer surge line; RCP trip; all systems operate as designed.
7. Small-break LOCA (4 in. hot-leg break)	Four-inch diameter hole in pressurizer surge line; RCP trip; all systems operate as designed.
8. Rancho-Seco type transient	Initial loss of feedwater followed by run-away-emergency feedwater to both steam generators

the primary flows ad temperatures to determine the feedwater demand. It also regulates the main- and startup flow-control valves, the main-feedwater (MFW) pumps, and the turbine-bypass valves (TBVs). Details of the ICS are presented in Appendix A.

Several overcooling transients have been identified by ORNL,[3] and additional transients may be specified after these initial results are evaluated. The initial transients include a main steam-line break (MSLB) with a delay in isolating the affected steam generator, a small-break LOCA [full-open

failure of the power-operated relief valve (PORV)] with failure of the ICS to throttle main-feedwater flow and trip the reactor coolant pumps (RCPs), and turbine bypass-valve transients with steam-generator overfeed. An actual plant transient (Oconee-3 turbine trip) was also simulated by TRAC to compare with actual plant data to verify the code models of the primary side. In addition, two small hot-leg-break loss-of-coolant accidents (LOCAs) were analyzed to investigate the effects of vent-valve flows on downcomer fluid mixing.

Except for the small hot-leg-break cases, all calculations showed significant primary-system depressurization followed by repressurization if the HPI was not throttled. System repressurization did not occur for the small-break LOCA cases because the break sizes were too large. Some overcooling was obtained in all calculations as evidenced by highly subcooled liquid temperatures in the downcomer. The most severe transient in terms of overcooling was the TBV transient in which both banks of TBVs were assumed to fail open, and the least severe was the PORV-LOCA transient. Table II summarizes the key results calculated for these overcooling transients. Not all the transients were run to 7200 s because of computer-time limitations. Once the primary system had stabilized, the calculations were terminated, sometimes as early as ~1500 s. For these cases, the results were extrapolated to 7200 s using engineering judgment. The results of these extrapolations are presented in Appendix B. An assessment of the influence of uncertainties in the calculations is included in Appendix C.

It is recommended that other calculations be performed to fully address the Oconee-1 PTS issue. Specifically, other operator actions should be considered to fully cover all possible overcooling scenarios. Also, in the case of the small-break LOCAs, other break sizes and locations should be investigated.

II. TRAC INPUT MODEL DESCRIPTION AND STEADY-STATE RESULTS

At the time of these calculations, the Oconee-1 model developed for the PTS study represented the most comprehensive modeling of any nuclear-power plant assembled for use with the TRAC code. The model contains a primary side, a secondary side, and a complex control system consisting of both trips and controllers. This model operates at steady state over a pressure range from ~0.01 MPa (~1.5 psia) in the condenser of the secondary side to ~15.2 MPa (~2200 psi) in the primary side and over a temperature range from ~300-590 K (~80-600 ^{o}F).

TABLE II

TRAC OCONEE-1 TRANSIENT RESULTS

Transient	Minimum Downcomer Temp. (K)	Pressure[a] (MPa)	Minimum Cold-leg Temp. (K)	System Repressurization?
1. MSLB				
a. RCP restart; HPI throttled[b]	475	6.5	A-Loop 475 B-Loop 400	Yes
b. No RCP restart; HPI throttled[b]	450	8.5	A-Loop 435 B-Loop 445	Yes
c. Same as (1.a.) with EFW	405	3.5	A-Loop 402 B-Loop 422	Yes
2. SBLOCA (PORV LOCA with RCP trip)	528	11.5	A-Loop 518 B-Loop 525	Yes
3. TBV failure[c] (One Bank)				
a. SG level control fails	365	17.0	A-Loop 448 B-Loop 375	Yes
b. SG level control does not fail	440	17.0	A-Loop 477 B-Loop 430	Yes
c. RCP restart; HPI throttled	430	4.0	A-Loop 491 B-Loop 491	No
4. TBV failure[c] (Two Banks)				
a. SG level control fails	350	17.0	A-Loop 441 B-Loop 446	Yes
b. SG level control does not fail	465	17.0	A-Loop 463 B-Loop 465	Yes
c. RCP restart; HPI throttled	350	4.0	A-Loop 465 B-Loop 465	No
5. SBLOCA[c] (2 in. hot-leg)	425	1.0	A-Loop 370 B-Loop 410	No
6. SBLOCA[c] (4 in. hot-leg)	320[d]	0.5	A-Loop 430 B-Loop 425	No
7. Rancho-Seco type transient[c]	452	14.0	A-Loop 450 B-Loop 450	Yes

[a]This is the system pressure at the time of minimum downcomer temperature.
[b]For these MSLB calculations, the EFW system did not actuate because of input errors in the ICS and trip logic.
[c]These calculations were extrapolated to 7200 s and the temperatures, pressures shown represent estimated values.
[d]For this calculation, the minimum temperature corresponded to temperature "spiking" as a result of accumulator injection.

A. Primary Side

The primary side of the Oconee-1 model is similar to other TRAC models that have been used (Fig. 1). It consists of the three-dimensional vessel, two hot legs, two once-through steam generators, four cold legs, and some parts of the emergency core-cooling system (the low-pressure injection system was not modeled).

The volumes, elevations, and pipe lengths from the Oconee-1 plant are closely matched in the model. The wall areas and thicknesses of the primary piping are also modeled so that the thermal response of the piping is predicted. Heat transfer from the pipe walls to the environment is also allowed.

1. Vessel. The three-dimensional vessel is made up of 96 cells. These cells are arranged such that the vessel is divided into eight axial levels, two radial rings, and six azimuthal segments. The lower plenum is made up of one level; the core four levels; the upper plenum, two levels; and the upper head region contains one level. The two radial rings are divided so that the core region is bounded by the inner ring, and the downcomer annulus is modeled in the outer ring.

The vessel metal structures and wall masses are modeled by assi ing a representative thickness and area of a heat slab to each three-dimensional cell. Using these heat slabs, the stored energy of the vessel structure is approximated. The thermal conductivity for each heat slab is calculated by assigning five nodes across each slab thickness. These nodes are spaced so that they are closer together on the fluid side of the slab. There is no heat transfer through heat slabs between cells, that is, each cell's heat slab is isolated from any other cell's heat slab except through the fluid-dynamic coupling.

The six azimuthal divisions were chosen to allow for the angle and separation of the penetration of the hot and cold legs. Also, the accumulator injection ports were modeled close to their exact positions (both a..ially and azimuthally) in the vessel downcomer region.

With only one radial division for the inner portion of the vessel modeled, the circulation of hot water rising up from the core into the upper head, then back down and out the hot legs is lost. Without finer noding of the vessel, the upper head is effectively isolated from the rest of the vessel in many circumstances. To alleviate this problem, a connection is made between the upper head and the hot legs so that about one third of the normal steady-state flow passes through the upper head. This connection is called the upper-head tee.

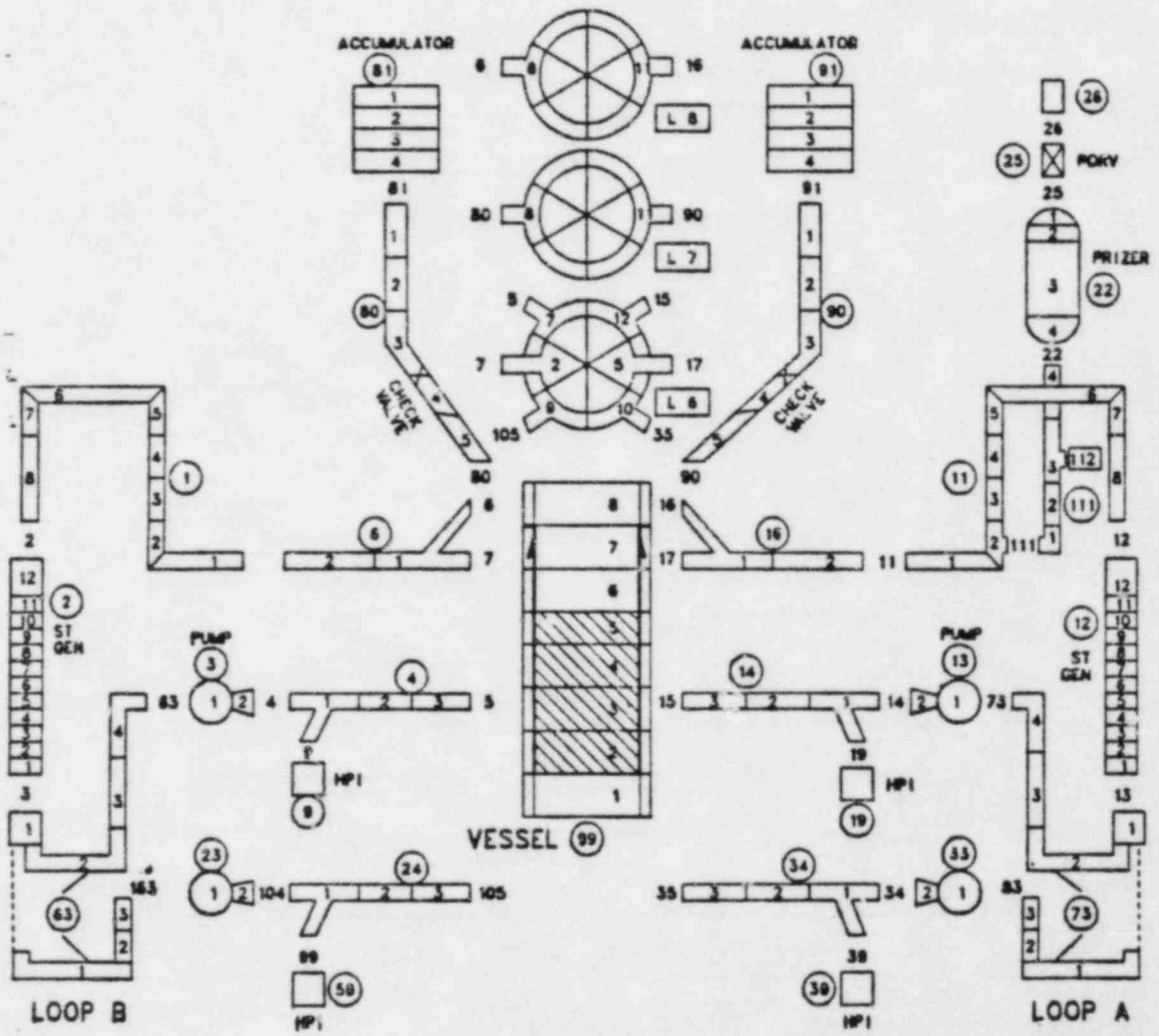

Fig. 1.
Primary-side model for Oconee-1.

The vessel includes vent valves that are modeled to allow flow from the upper plenum directly to the downcomer. This flow path is only available when the upper plenum pressure is higher than the downcomer pressure. A composite vent valve made up of one-sixth the total vent-valve area is modeled in each azimuthal cell of the inner radius of axial level 7. Figure 2 shows the vent-valve model used for these calculations. The vent valves are fully open when the pressure drop between the upper plenum and downcomer exceeds 0.12 psi.

2. Hot Legs. The loop-A and loop-B hot legs are modeled symmetrically except for the surge-line connection to the loop-A candy cane. The candy canes represent the highest elevation in the system. The surge line includes a "small-break", which is activated for the small hot-leg break transients.

The pressurizer is modeled with a very small cell at the bottom and two small cells at the top. This was necessary to allow correct fluid conditions to either enter or leave the pressurizer.

Pressure relief for the primary system is provided by a single PORV at the top of the pressurizer. This valve supplies adequate relief for the cases where secondary cooling is provided and the reactor has tripped (all cases in this study).

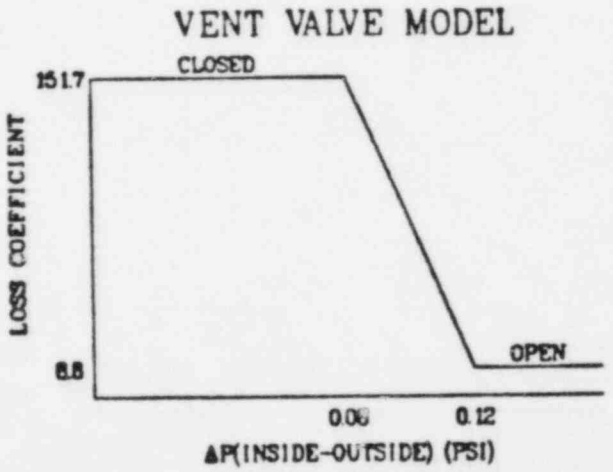

Fixed closed value allows leakage for $\Delta P < 0.08$
Fixed open value for $\Delta P > 0.12$

Closed value based on design leakage (W. Jensen, NRC)
Open value based on BAW-1628 table.

Fig. 2.
Vent-valve model.

3. Steam Generators. A complete model for B&W once-through steam generators was developed for this study. The primary side of the steam generator is made up of 12 cells whereas the secondary side uses 26. Heat transfer from the primary occurs through the steam-generator tubes to the secondary coolant. Cells 2-11 (Fig. 1) represent a composite of the volume inside and wall area of all tubes, and it is in these cells that heat transfer from the coolant to the walls of the tubes occurs. Cells 1 and 12 model the upper and lower plenums. The wall area and thickness of the plenums are modeled so that the heat capacitance and heat transfer of the external wall can be calculated.

The secondary of the steam generator is divided into four components (Fig. 3), two model the tube-bundle region, one models the downcomer, and the final one models the steam-outlet annulus. The tube-bundle region is made up of 10 cells (SG components 12-1 and 12-2, for loop A and 2-1 and 2-2 for loop B in Fig. 3). These cells model the total volume and the tube wall area for the region between all the steam-generator tubes, but model the heat-transfer characteristics of a unit cell of tubes. The top 4 of these 10 cells comprise the superheated-steam region of the model during normal full-power operation. The connection at the top cell of the tube-bundle region is for the emergency-feedwater (EFW) flow and the realigned main-feedwater flow. This connection closely models the correct plant geometry so that any flow from the "upper header" is correctly injected into the tube bundle.

The steam-generator downcomer consists of seven cells (SG Components 12-3 and 2-3 of Fig. 3), plus one cell for the main-feedwater injection and one cell for the aspirator port. During normal operation, the downcomer condenses enough superheated steam drawn through the aspirator port to heat the main feedwater to saturation temperature prior to entry into the tube-bundle region. The final six steam-generator secondary cells model the steam-exit annulus. The outlet from this annulus is near the midpoint of the steam generator, close to the actual location in the plant.

Because of insufficient information regarding pressure tap locations on the SG secondary side, the SG water levels were modeled using a collapsed liquid level calculation. This method is adequate for transients in which relatively slow changes in the secondary side occur, but may not be accurate for rapid changes such as in a MSLB transient. However, the response of a pressure transducer also may not be accurate for a violent secondary-side transient.

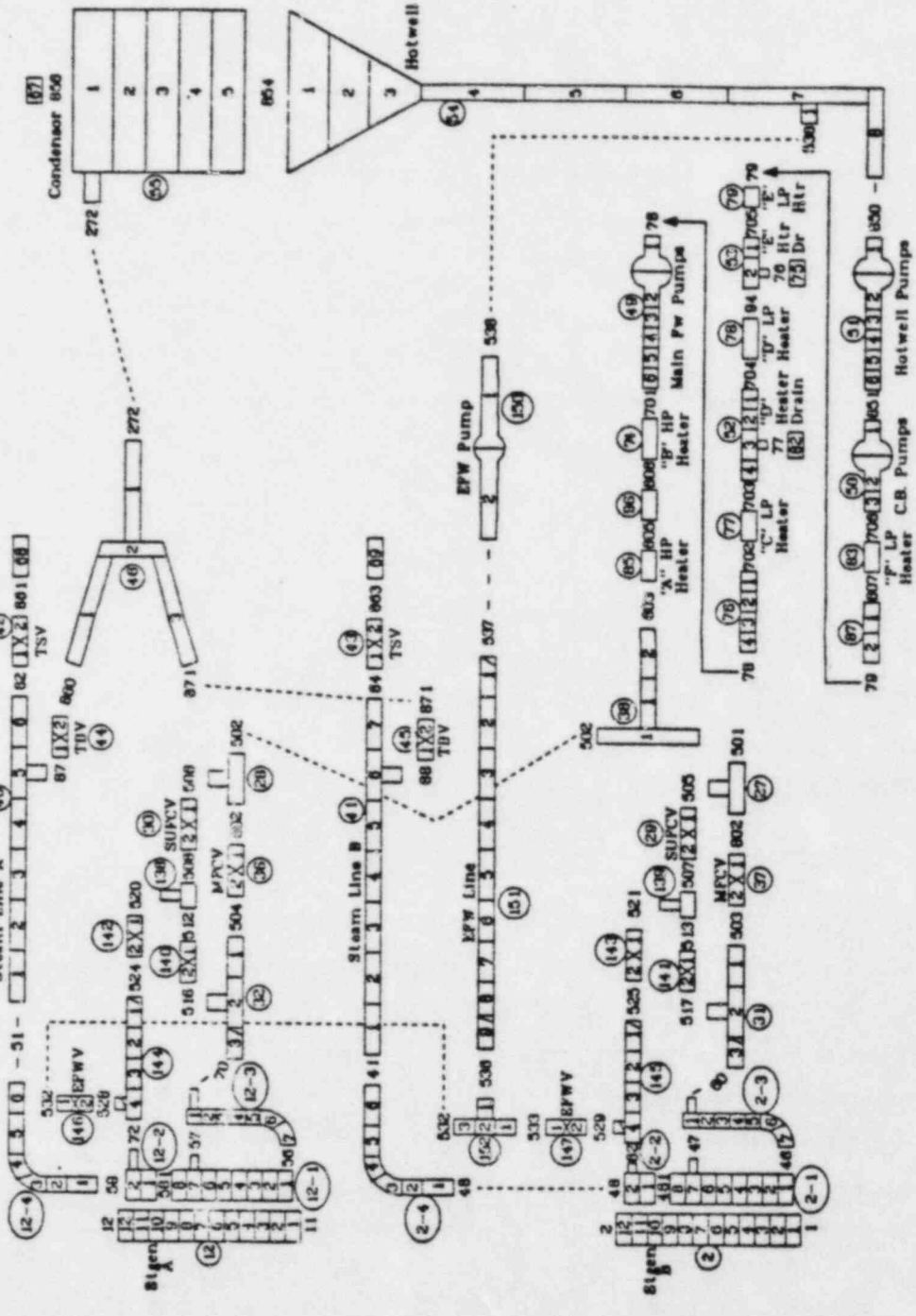

Fig. 3.
Secondary-side model for Oconee-1.

4. Cold Legs. All four cold legs of the plant are modeled. These legs each consist of a loop seal (lowest primary-loop point), a reactor coolant pump (RCP) and the HPI connection. The HPI nozzles are positioned closely to their correct height and distance from the vessel entrance. The RCPs are speed controlled during steady-state operation to obtain the required mass flow, but their steady-state speed is maintained fixed while they are running during a transient. During normal operation, the four cold legs of this model have symmetric flows.

5. Emergency Core-Cooling System (ECCS). Two major components of the ECCS were included in this model; the HPI system, and the accumulators (core flood tanks). If a transient were to be run that caused the primary pressure to fall below the low-pressure injection system (LPIS) setpoint, then the LPIS would also have to be added to the model.

The HPI system was modeled as four boundary conditions that can inject 283 K (50 °F) water into the primary through the four side nozzles of the cold legs. These nozzles are located so that they enter the main cold legs from the side at an elevation somewhat higher than the centerline of the cold/hot legs. The pressure-dependent flow rate of the two loop-B ports is identical, as is also the case for loop-A, but the loop-A capacity is greater than that of loop-B.

There is an accumulator tank for each loop that allows emergency coolant to flow directly into the downcomer region in axial level 7 of the vessel (Fig. 1). The accumulator flow is controlled by check valves such that when the primary pressure falls below the accumulator tank pressure, the check valves open. The initial accumulator pressure was ~4.2 MPa (~610 psia) with a coolant temperature of 305.4 K (90 °F).

B. Secondary Side

All major components of the secondary side are modeled except for the turbine-generator equipment and various valves that were not necessary for any transients of immediate interest. With the exception of the vessel, the secondary side required much more modeling detail than was previously necessary when only the primary system was modeled.

1. Feedwater Train. In this discussion, the feedwater train describes the secondary-side modeling from the condenser (component 55 in Fig. 3) to the tee where the feedwater is divided between the two steam generators (component 38 in Fig. 3). This section of the modeling takes the fluid discharge from the turbines and raises it to the temperature and pressure at which it is delivered to the steam generators.

The condenser is modeled as a large tank with a very large wall area. The thin walls have a high-thermal conductivity and a constant-temperature heat sink on the outside surface. This model fully condenses the incoming steam from either the turbine exhaust or the turbine-bypass system.

The hotwell is an even larger tank used for the collection and storage of the condensate. The lowest system pressure and temperature occur in this component. Cell 1 of the hotwell actually represents the volume and coolant inventory of the upper surge tank. It is included to reduce the complexity of the model while still providing an estimate of the available hotwell inventory. The coolant supplied to the emergency feedwater system is taken from the hotwell/upper surge tank combination.

The hotwell pump (component 51) includes the demineralizer/aerator section of the feedwater train. The model accounts for the effects of this section by including additional frictional losses and heat addition to the coolant.

Each feedwater heater is modeled to achieve a feedwater temperature rise close to the design value for that heater. In addition, the model includes a time-dependent estimate of the feedwater-heater heat capacitance. The heaters are modeled with four heat-conduction nodes (Fig. 4) such that the first two cross the metal wall and the outer two model the secondary-side steam/water mixture. The energy input from the extracted turbine steam is modeled by adding a volumetric heat source to the middle node of the steam/water mixture. This heat source is controlled by a trip so that it can be ramped off following a turbine trip.

The two parallel MFW pumps of the actual plant are combined into a single pump for this model. This is a variable speed pump with the speed determined by the ICS. This pump will also be tripped off if any of a variety of setpoints are reached as described in the control section of this report (Sec. II.C).

The coolant flow from the feedwater train splits to provide flow to the steam-generator control-valve section of each major loop. Because the loop-A and loop-B flow-control valves are identical, a discussion of the valves for only one loop is necessary.

2. Steam-Generator Control Valves. A schematic diagram of the control-valve arrangement is shown in Fig. 5. This schematic can be correlated to the two control-valve sections of the secondary-side noding diagram of Fig. 3. There are three check valves (valves 1, 2, and 3) in this arrangement to stop reverse coolant flow from the steam generator into any of the feedwater lines. The emergency-feedwater valve (EFWV) is closed during steady-state operation,

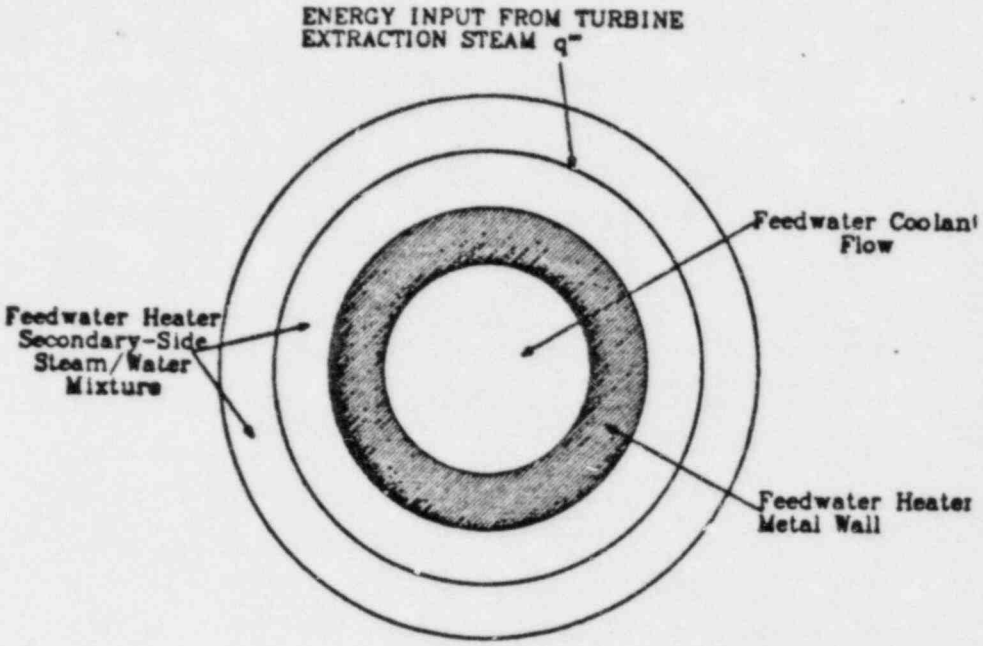

Fig. 4.
Detail of feedwater-heater model (cross-section).

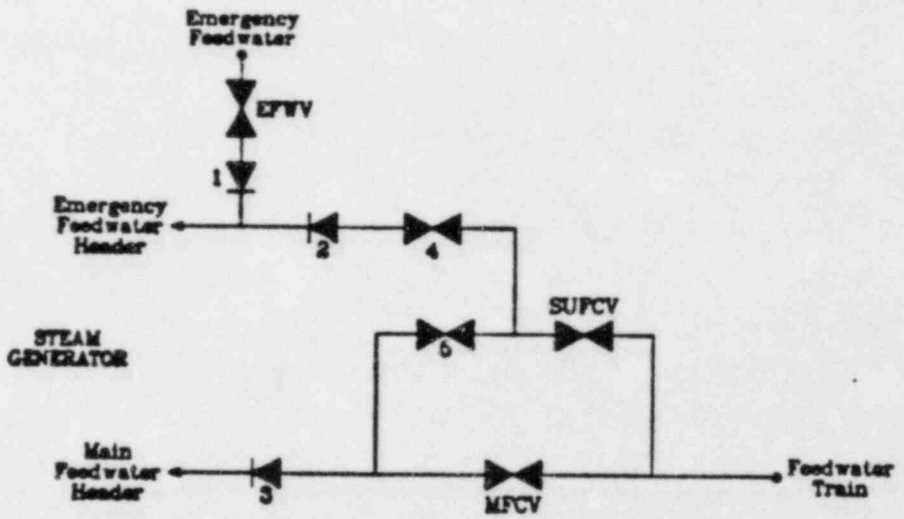

1: Emergency-Feedwater Check Valve
2: Realignment Check Valve
3: Main-Feedwater Check Valve
4, 5: Feedwater Realignment Valves
EFWV: Emergency-Feedwater Valve
SUFCV: Startup Flow-Control Valve
MFCV: Main Flow-Control Valve

Fig. 5.
Steam-generator control-valve schematic.

but opens and closes as necessary if EFW is demanded. (Refer to Section II.C.1 for further description of the EFWV.)

The remaining four valves in Fig. 5 provide the major control for the MFW flow. The valve area of the two flow-control valves is controlled by the ICS. During steady-state operation, the start-up flow-control valve (SUFCV) is 100% open and the main-flow-control valve (MFCV) is approximately 50% open. The action of these valves during a transient is generally difficult to predict because of the complexity of the ICS. In general, the MFCV closes following a reactor trip, and the SUFCV controls any feedwater flows below approximately 15% of the steady-state flow. The action of the flow-control valves may be overridden by signals from the trip system (refer to Section II.C.1).

When one of the two realignment valves, valves 4 and 5, is open, the other must be closed. During steady-state operation, or any time before the feedwater-realignment trip is hit, valve 4 is closed and valve 5 is open. Following the realignment, valve 4 opens and the MFCV and valve 5 close.

There are several different flow combinations that can occur. During steady-state operation, the flow splits along the parallel paths through the two flow-control valves, then rejoins to flow into the MFW header. The flow split is 85/15 with the larger flow through the MFCV. For flows less than 15% only a single path is open to the MFW header, and that is through the SUFCV, valve 5, and check-valve 3. If feedwater realignment occurs, the flow is from the feedwater train through the SUFCV, valve 4, check-valve 2, and into the EFW header. The EFW may also be running so that flows may be entering both SG headers, or the EFW may mix with the MFW flow before they enter the EFW header. If the steam generator is isolated, the MFCV, SUFCV, and EFWV are closed so that no flow can enter the steam generator.

3. Emergency Feedwater. The EFW system is modeled so that it takes water from the hotwell and delivers it to the EFWVs of both steam generators. The EFW pump is modeled as a composite of the turbine driven and motor driven pumps in the actual plant, and therefore has a large capacity. The EFW is delivered to a tee (component 152, Fig. 3) that splits the flow between the two steam generators. If both EFWVs are open, the EFW flow is symmetrically split as long as the secondary pressure of the two steam generators is equal. If only one EFWV is open, the full flow available is delivered to that steam generator. The EFW flow stops if the hotwell inventory has been depleted.

4. Steam Lines. The steam line for steam-generator B is longer than the steam-generator A steam line. Other than this difference, the steam lines and their valves are identical. A pressure boundary condition models the steam flow

exiting the secondary into the turbine inlet. During steady-state operation the steam-mass flow is modeled to reenter the secondary as boundary condition inlets to the condenser and the two heater drains. Following a turbine trip, the turbine-stop valves (TSVs) close the steam lines. If any pressure relief from the closed steam lines is necessary, steam is released through the turbine-bypass valves into the condenser. For a normal reactor/turbine-trip transient, the steam relief from the turbine-bypass valves is adequate so that modeling the main-steam safety valves is not necessary. Following a turbine trip, the secondary model is a closed loop unless a transient similar to a MSLB is modeled. For the MSLB, one of the turbine inlet boundary conditions is set to constant containment pressure and the corresponding turbine-stop valve is fixed open.

C. Control System

The control system for the various components of the TRAC input model is provided in two ways; with trips and with control blocks. Trips basically turn something on or off depending on certain conditions being met. In this model, control blocks use mathematical relations between system variables to adjust valve areas or pump speeds. The control blocks are used to model the B&W ICS.

1. Trips. Of the more than forty trips used in this model, only five are simple trips. Simple trips have only a system variable as input, and their output is only used to control some component action. A summary of the simple trips is presented in Table III. The TBVs are actually controlled by the ICS at the Oconee-1 plant, but because they have a single setpoint for the transients calculated for this study, simple trip modeling is adequate. The only noticeable difference with this modeling appears in the secondary-side pressure plots for transients with steam-line pressure relief for extended periods. In these cases, the plots appear somewhat saw-toothed because of the full opening or closing of the TBVs, whereas in the plant the ICS maintains a smoother pressure response by allowing partial valve openings.

The reactor trip system is presented in Fig. 6. As depicted, the signal output from the reactor trip is input to the TSVs, the condenser feed, the feedwater heaters, and the heater drains. Most of these trips actually occur following a turbine trip, but in this model the turbine and reactor trips occur together. For all of the transients calculated for this study, the reactor trip occurred immediately. If additional transients were to require the reactor trip to occur after other criteria had been met, this model would have to be modified. The delays and rates are not included in the information presented in Fig. 6, so these parameters will be discussed in the following paragraph.

TABLE III

SIMPLE TRIPS

Description	System Variable	Setpoint (MPa)/Action
TBV control-loops A and B	Steam-line pressure	7.064/opens 7.014/closes
Accumulator check-valves, both loops	Check-valve pressure drop	0.14/opens 0.05/closes
PORV control	Pressurizer pressure	16.99/opens 16.65/closes

The reactor trip is ~0.5 s from the beginning of the transient. To model the insertion of control rods into the core, a negative reactivity insertion of -0.0536 Δk is added ~1.0 s after the trip. The decay heat is calculated using the American Nuclear Society (ANS) decay-heat constants that are internal to the code. The turbine-stop valves start closing simultaneously with the reactor trip and take ~1.0 s to fully close (except in the MSLB transient where the loop-A TSV is fixed open). The condenser feed trip occurs ~1.0 s after the reactor trip and the feed decays to zero over 5.0 s. The volumetric heat sources used to model the feedwater heaters and the feedwater added to the train through the heater drains are tripped ~0.5 s after the reactor trip and also take 5.0 s to decay to zero.

Each box in Fig. 6 is divided into four sections. These sections are for the trip identification number, the trip description, trip input, and trip output. The trip output either goes to a component or to another trip as its input. The component numbers are enclosed in small circles and correspond to one of the components in Figs. 1 or 3. These trip system figures were developed as part of the TRAC-PF1 modeling work and are presented for clarity in understanding the interconnection between them. For further explanation of these figures, please refer to the trip system legend contained in Appendix A.

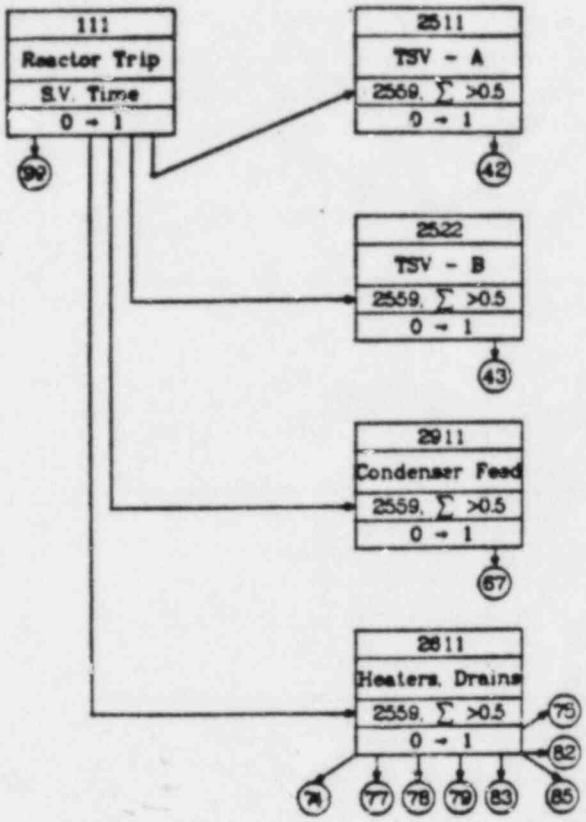

Fig. 6.
Reactor trip system.

Figure 7 presents the trip system that controls the HPI, the four RCPs, and the MFW realignment valves. HPI initiation occurs if the system pressure drops below 10.44 MPa, but is also cycled on and off to keep the least cooled hot leg at 42 ± 7 K subcooled (75 ± 12.5 °F). For some transients reported, the HPI subcooling monitor was not used. For those cases in which a particular trip is not wanted, it is left in the system but given a setpoint that cannot be reached. All four RCPs also use the HPI low-pressure setpoint, but have a 30.0 s delay from the time the setpoint is reached until the pumps trip. The A1 and B1 pumps are under separate trip control from the A2 and B2 pumps so that these pumps (A1 and B1) can be turned back on if the least cooled hot leg reaches 42 K subcooling. For some of these transients, the pump subcooling monitor is also disabled.

Following any RCP trip, the MFW is realigned to flow into the steam generators through the EFW header. This realignment occurs by taking control of the MFCVs away from the ICS and ramping them closed at a flow area fraction

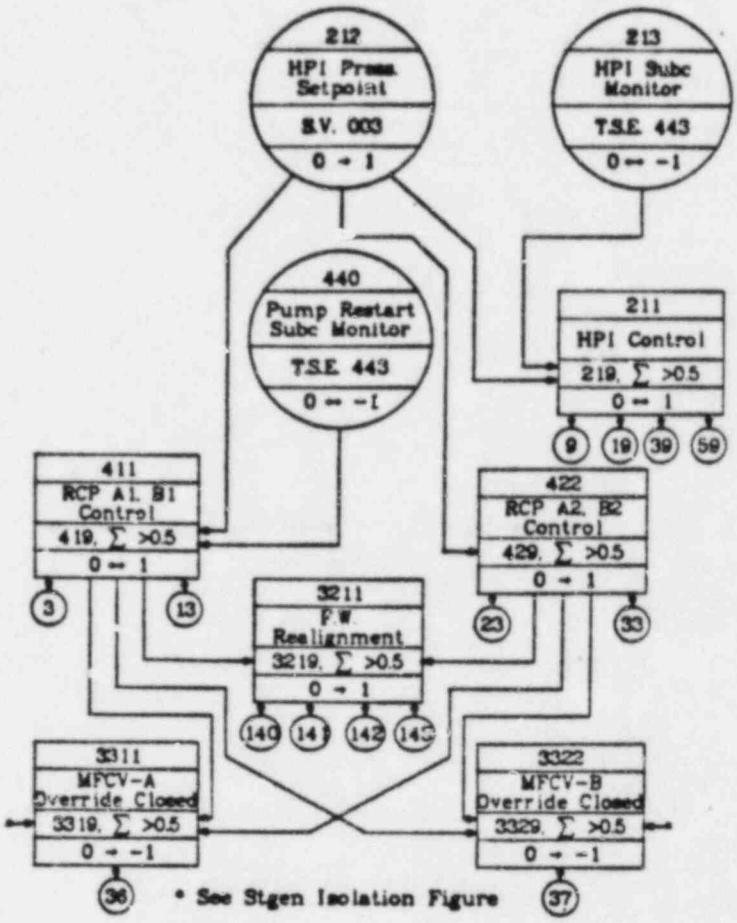

Fig. 7.
HPI, RCP, and MFW realignment trip system.

closing rate of 25% per s, and by opening or closing the appropriate realignment valves over a 5.0 s period. Further information on this valving arrangement is described in Section II.B.2 of this report.

The trip system for the three pumps of the feedwater train is presented in Fig. 8. The hotwell pump trips only if the hotwell level falls below 0.1524 m. If this pump trips, then the other two must also trip. The condensate booster pump trips if the hotwell pump has tripped, or if its suction pressure falls below 0.21 MPa. The MFW pump trips if any of the six trips feeding into it are actuated. These six trips include the two upstream pump trips, either SG level greater than 9.27 m, a suction pressure less than 1.72 MPa, or a discharge pressure greater than 8.89 MPa.

The SG isolation trip system for both loops is presented in Fig. 9. This system is designed to ensure that both flow-control valves and the EFW valve close if steam-generator isolation is required. The two reverse-value trips are necessary to make the three input values of the MFCV override trips compatible. If one of the SG isolation trips is turned back off, then EFW can be delivered to that steam generator if it is required, such as in the MSLB transient.

The controlling trips for the EFW system are presented in Fig. 10. The trip conditions that demand EFW are at the top of the figure, and the conditions to throttle EFW are at the bottom. EFW is demanded if the MFW discharge pressure drops below 5.271 MPa. The EFW demand opens the appropriate EFW valve at a fractional rate of 33% per s. If either EFW valve starts to open, the EFW pump comes up to full speed in 4 s. The EFW valves close if the SG water level goes above 6.2 m, but reopens when the level drops below 6.0 m. The EFW valves

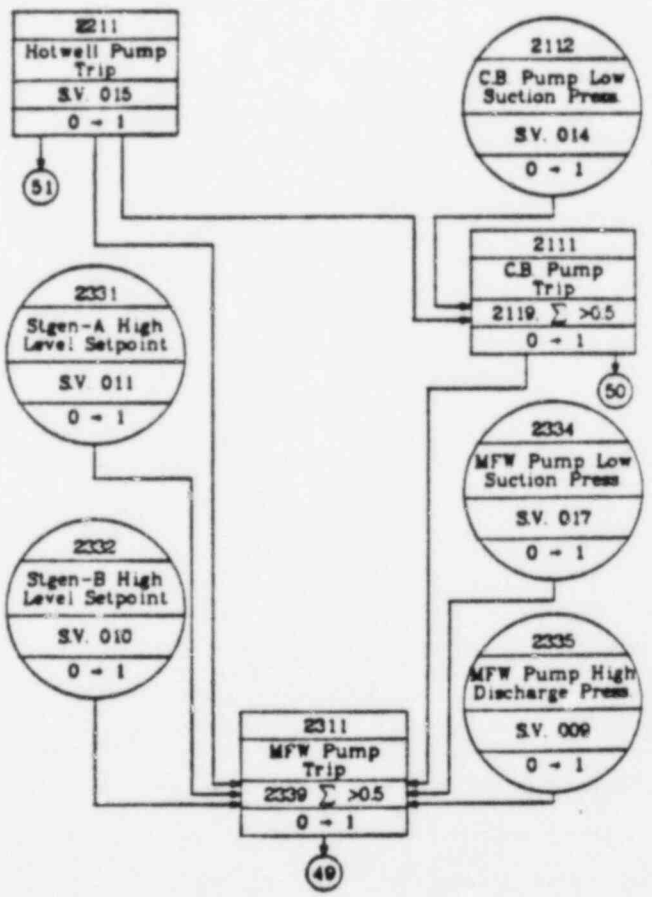

Fig. 8.
Hotwell, condensate-booster, and main feedwater pumps trip system.

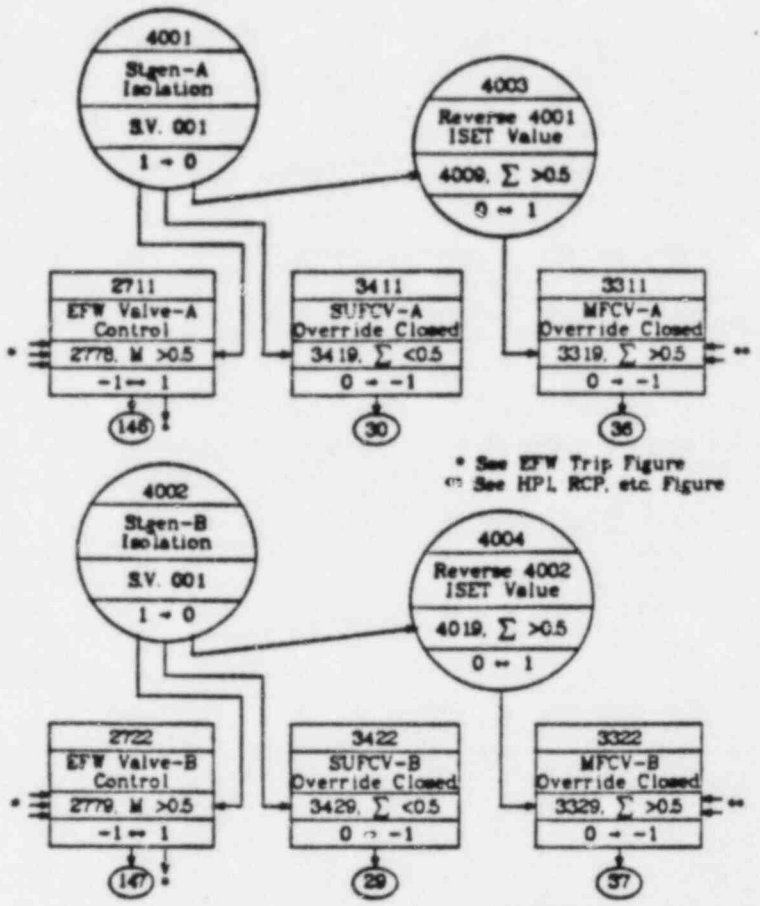

Fig. 9.
SG isolation trip system.

also close if the hotwell level is less than 0.0254 m. If both EFW valves close, the EFW pump trips off.

2. Integrated Control System. The B&W ICS matches the feedwater flow with the power demand and maintains a constant steam-line pressure and adequate superheat. The ICS can quickly respond to plant load demands while maintaining smooth plant operating parameters. The block diagram of Fig. 11 depicts how this control is accomplished. The ICS controls secondary pressure with the turbine valves, primary power with the control rods, and primary-to-secondary heat-transfer characteristics with the SG valves and MFW pump. Cross limits are sent back to the Integrated Master so that if some section is not performing adequately, the other parts of the ICS balance the response to prevent any power, pressure, or feedwater flow mismatches.

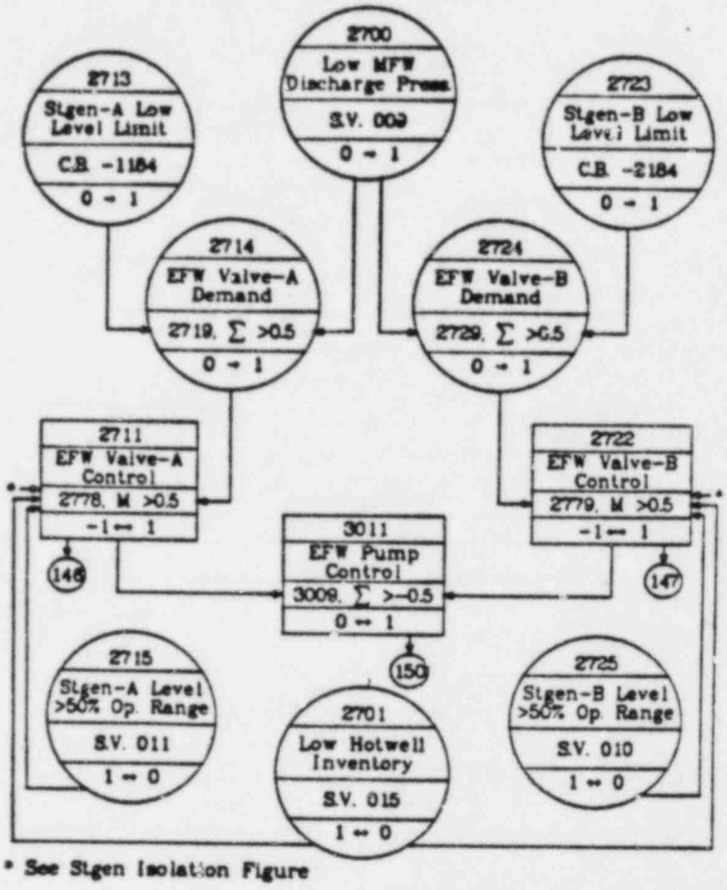

Fig. 10.
Emergency feedwater trip system.

The performance of the ICS must be taken into account for accurate simulation of most plant transients. In particular, the feedwater flow is under ICS control and does not have a simplistic response to most transient conditions.

The reactor is tripped instantly for all transients that were calculated in this study. This allows a great deal of simplification in modeling the ICS. As is shown in Fig. 11, the TBV section is modeled with simple trips (refer to Section II.C.1) and only the feedwater-control section needs to have detailed control-block modeling. If a transient were run with the reactor not tripped, ICS control of the TBVs would be necessary. Following a reactor/turbine trip, however, the turbine steam-flow control valves do not have to be modeled.

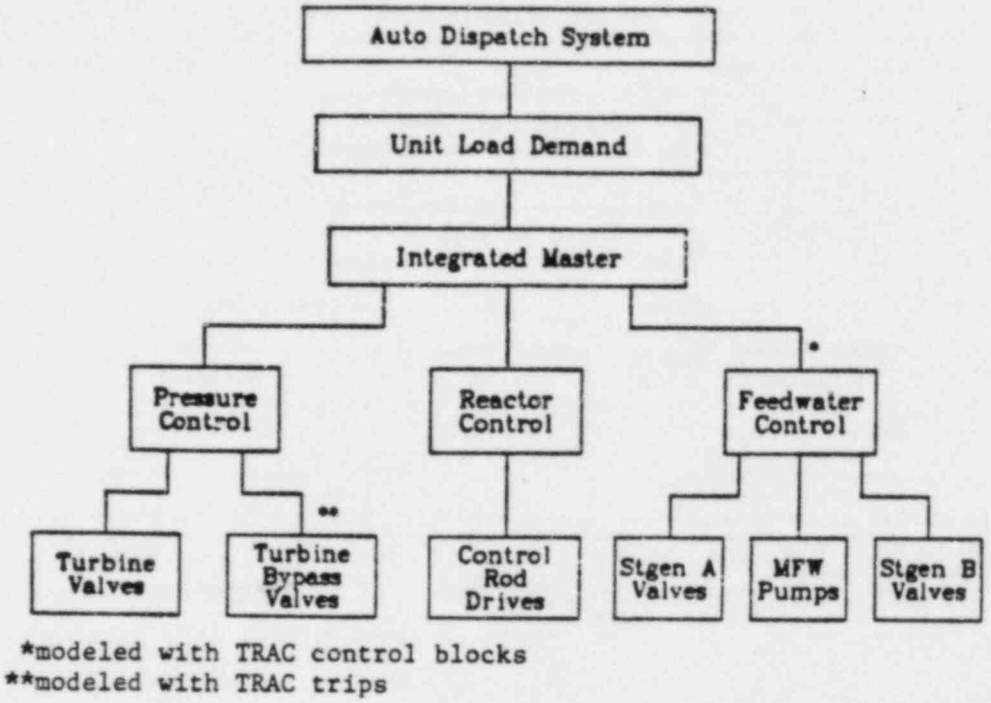

Fig. 11.
ICS organization.

The control-rod section of the ICS does not have to be modeled for these transients because of the early reactor trip nor is it needed for steady-state model operation because the reactor is at full power. If a transient were run where the rods were not inserted, this section of the ICS would have to be modified to allow correct reactor power control. Because of these simplifications, the only part of the Integrated Master modeled was the neutron-power cross-limiter.

Figure 12 presents a block diagram of the feedwater-control section of the ICS as it is modeled for this study. The British Thermal Unit (BTU) limiter monitors some primary and secondary parameters to determine if enough feedwater is flowing. This determination is compared against the reactor power to reduce the feedwater flow if the power is dropping. The requested feedwater flow is then compared with the actual feedwater flow to get a feedwater-flow error. This error value will then open or close the MFCV unless the SG level has reached either a high- or low-level limit. If limited, the valve action will then act to bring the level inside of the limit. The requested feedwater flow is also used along with the MFCV pressure drop to determine the MFW pump speed. Each of these blocks is separately discussed in the following paragraphs. This discussion is limited to just the information necessary to describe the loop-A

model. The loop-B model is similar except that it uses several of the signals generated for the loop-A side to avoid duplication of coding. A complete listing of the flow diagram and mathematical representation of the TRAC-PF1 ICS model is included in Appendix A.

A diagram of the BTU-limiter control blocks is given in Fig. 13. Each of the blocks represents one signal manipulation. As depicted in Fig. 13, there are four system parameters input and one signal output. The letters in each block represent a particular control-block output and identifies the mathematical representation of the control blocks as they appear in Table IV. Each of the block outputs is in volts and the limits are included with the equations where appropriate. The system parameters input are always in SI units. The steady-state output voltage for each of the blocks is given in the table. A BTU-limiter output value of 8 volts indicates the correct feedwater flow. For a value less than 8 volts, less flow is needed, and for a value greater than 8 volts, more flow is requested.

The neutron-power cross-limiter section of the TRAC-PF1 ICS model is presented in Fig. 14. This section has three input signals and one output voltage. Table V gives the equations and steady-state values that correspond to these control blocks. Blocks A1 and B1 set up a 20%-per-minute signal ramp

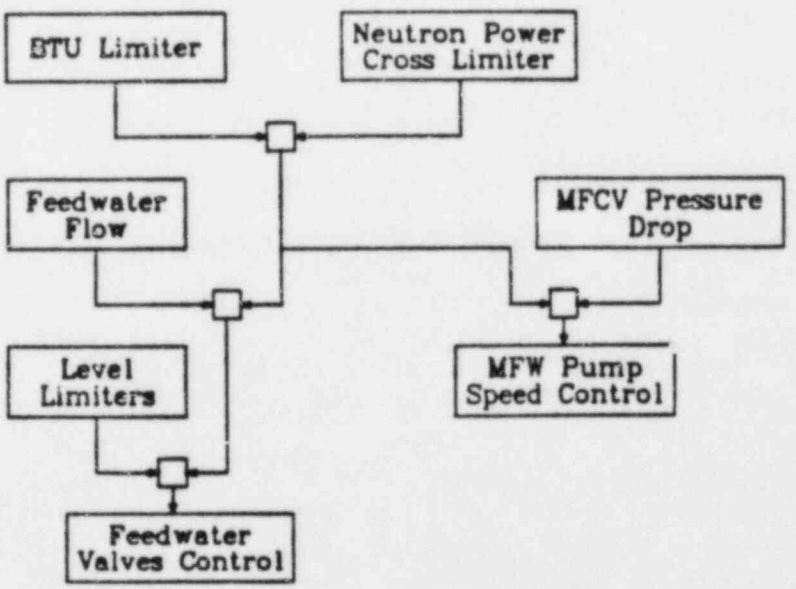

Fig. 12.
Feedwater-control section of the ICS.

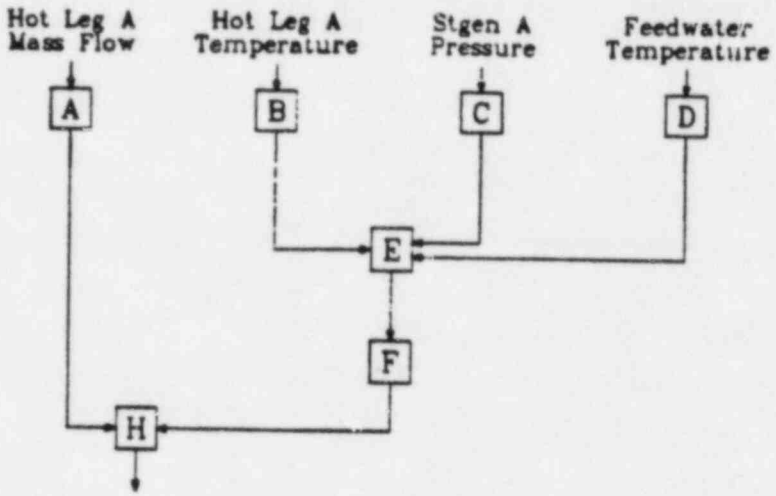

Fig. 13.
BTU-limiter control blocks.

TABLE IV

BTU-LIMITER CONTROL-BLOCK EQUATIONS

Equation	Steady-State Output Voltage
A = 0.00204083 * RCFLOWA	18.0
B = -605.4459 + 1.04092 * RCTEMPA , -10.0 < B < 9.080	8.0
C = 82.549 - (1.16958e-05) * SGPRESA , -1.0 < C < 9.080	8.0
D = -11.036 + 0.037260 * FWTEMP , -1.270 < D < 9.080	8.0
E = -16.0 + B + C + D , -10.0 < E < 12.0	8.0
F = 0.55555 + 0.055555 * E	1.0
H = -10.0 + A * F	8.0

after the reactor has tripped to ensure a feedwater runback of at least this rate. The control-block tables such as D1 and K1 use simple linear interpolation between points to complete the function values. All output block signals are in volts except for D1 (K) and J1 (watts). The DELT in block JL is

for time-step size. The final output from this section results in similar feedwater control as in the BTU-limiter section.

Figure 15 presents the feedwater-flow control blocks. The BTU-limiter voltage input comes from block H, and the neutron cross-limiter input from block SG. The blocks depict the selection of one limiter signal and the comparison of that signal with the current feedwater flow. The equations that make up this section of the ICS are presented in Table VI. All blocks in this table are output in volts except for block SL, which is in kg/s. A negative output from this section tends to close the feedwater-control valves; a positive value opens them, and a zero value indicates no change is requested.

The steam-generator level-limiter section of the TRAC-PF1 ICS model is presented in Fig. 16. This section passes the feedwater-flow comparison signal straight through unless the high-or low-level setpoints are reached. The

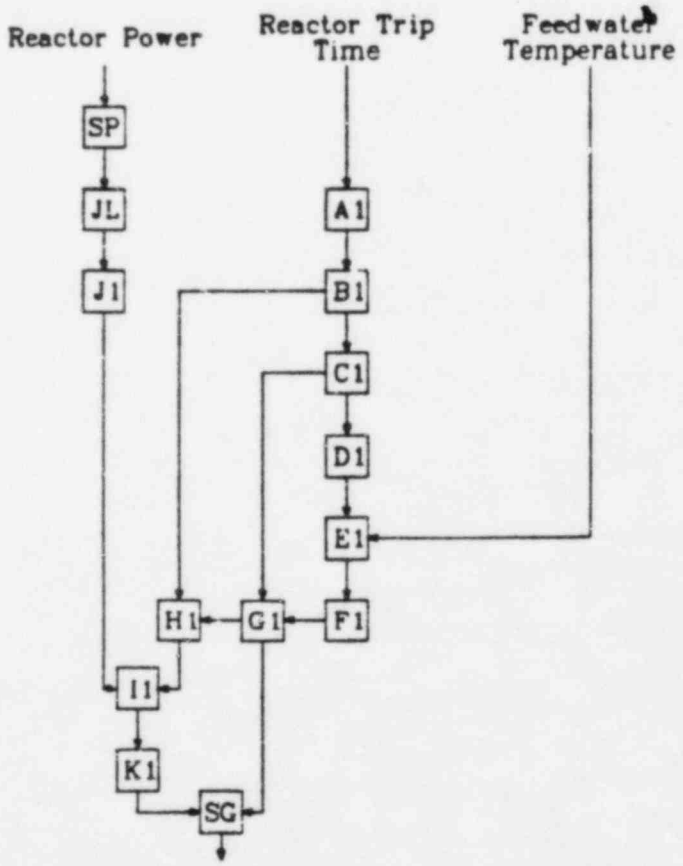

Fig. 14.
Neutron-power cross-limiter control blocks.

TABLE V

NEUTRON-POWER CROSS-LIMITER CONTROL-BLOCK EQUATIONS

Equation	Steady State
A1 = TIME - (TIME OF REACTOR TRIP)	0.0
B1 = 1.0 - (0.2/60.0) * A1 , 0.0 < B1	1.0
C1 = 18.0 * B1	18.0
D1 = f(C1) : C1: 0.0, 0.562, 3.6, 5.4, 9.36, 18.0, 21.42 / D1: 204.0, 240.0, 320.0, 356.0, 402.0, 460.0, 483.0	460.0
E1 = -460.0 - D1 + 1.8 * FWTEMP	0.2
F1 = 1.0 + 0.0013 * E1	1.0
G1 = F1 * C1	18.0
SP = POWER - 2568.0e6	0.0
First order lag of power with 4.5-s time constant	
JL = JL + ((SP - JL)/4.5) * DELT	0.0
J1 = 2568.0e6 - JL	2568.0×10^6
H1 = 1.6 + 14.4 * B1	16.0
I1 = -1.0 * (H1 - 6.23053e-9 * J1) , -10.0 < I1 < 10.0	0.0
K1 = f(I1) : I1: -10.5, - 0.5, 0.5, 10.5 / K1: -10.0, 0.0, 0.0, 10.0	0.0
SG = -10.0 + K1 + G1	8.0

high-level limit block (P1) is generally a large positive number until its setpoint is passed. As this setpoint is passed, P1 quickly becomes a large negative number that closes the feedwater-control valves. There are two low-level limit setpoints that can be used. The lower value (0.6096 m or 24 in.) is for normal operation. If a RCP trip has occurred, the higher value

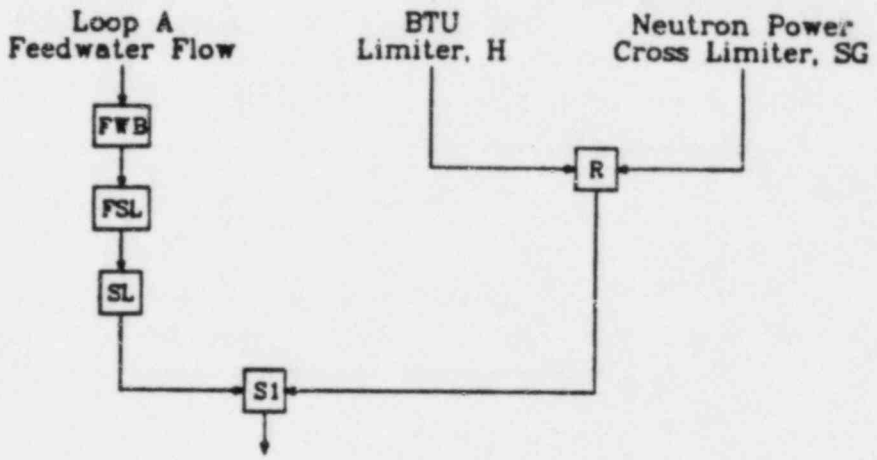

Fig. 15.
Feedwater-flow control blocks.

TABLE VI

FEEDWATER-FLOW CONTROL-BLOCK EQUATIONS

Equations	Steady-State Value
R = min(SG,H)	8.0
FWB = FWFLOWA - 680.4	0.0
First order lag of feedwater flow with 1.0-s time constant	
FSL = FSL + ((FWB - FSL)/1.0) * DELT	0.0
SL = FSL + 680.4	680.4
S1 = 10.0 + R - 0.026455 * SL	0.0

(6.096 m or 240 in.) is used to enhance natural circulation by maintaining a higher steam-generator level. When the low-level limit is reached, P2 changes from a large negative value to a positive value that is passed on to T1. T1 is the final feedwater-flow error used by the valve-control section of the ICS. Table VII gives the equations and steady-state values that correspond to these control blocks.

The ICS section that adjusts the flow-control-valve area is presented in Fig. 17. This section delivers a flow area to the two flow-control valves of this loop (Components 30 and 36) by using a proportional and integral controller in which the error signal is integrated and proportioned to determine the flow area. Two sets of constants are used for this controller depending on whether the ICS is low-level limited or not. The equations describing this action are given in Table VIII. If low-level limited, larger values for the controller are used to speed the opening valve action.

The MFW pump-speed control is determined by signals from both loops. The resulting voltage obtained from the comparison between the BTU-limiter output and the neutron cross-limiter output is used along with the minimum of the two MFCV pressure drops to obtain a pump speed. The control block diagram for this section of the ICS is presented in Fig. 18, and the corresponding equations in Table IX. There is a constraint on the rate of change of pump speed built into

TABLE VII

LEVEL-LIMITER CONTROL-BLOCK EQUATIONS

Equations	Steady-State Value
*operating level scale, 96 to 388 in (level in meters)	
HL1 = f(ALEV) : ALEV: 2.438, 9.855; HL1: -10.0, 10.0	-10.0
P1 = -2.0 * (HL1 - 7.0)	34.0
Q1 = min(S1,P1)	0.0
*startup level scale, 0.0 to 250 in	
LL1 = f(ALEV) : ALEV: 0.0, 6.350; LL1: -10.0, 10.0	-3.3
*pumps tripped: 240 in = 6.096 m = 9.2 V	
IF(PTRIP .EQ. 1) STP = 9.2	
pumps running: 24 in = 0.61 m = -8.08 V	
IF(PTRIP .NE. 1) STP = -8.08	-8.08
P2 = -2.0 * (LL1 - STP)	-9.6
T1 = max (P2,Q1)	0.0

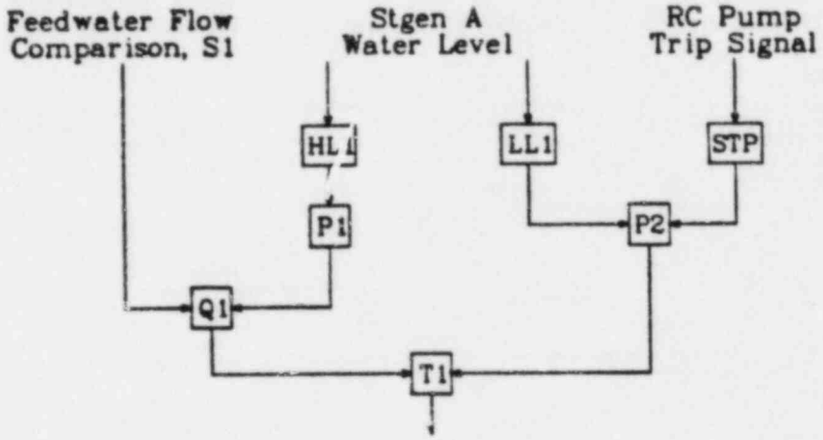

Fig. 16.
Level-limiter control blocks.

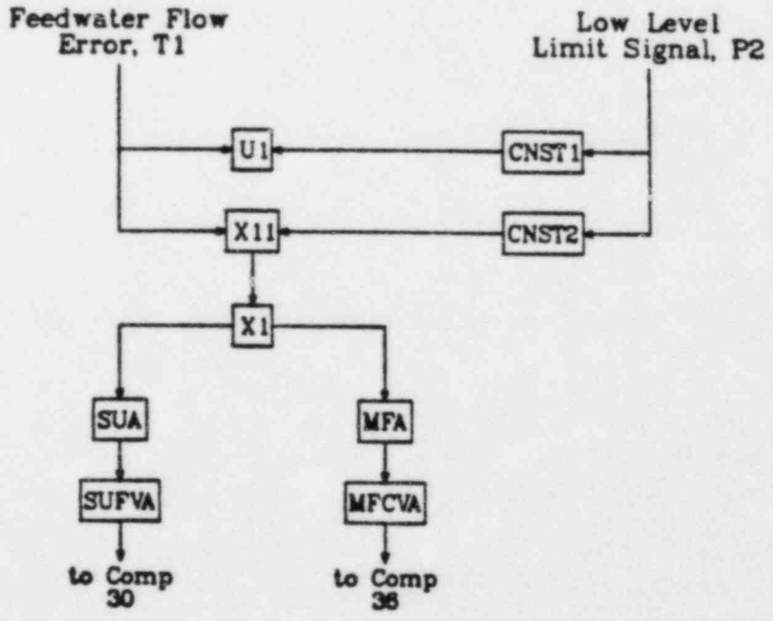

Fig. 17.
Feedwater-valve adjustment control block.

TABLE VIII

FEEDWATER-VALVE ADJUSTMENT CONTROL-BLOCK EQUATIONS

Equation	Steady-State Value
* if P2 < 0, low limit has not been hit	
IF(P2 .GE. 0.0) CNST1 = 0.12 IF(P2 .LT. 0.0) CNST1 = 0.1125	0.1125
IF(P2 .GE. 0.0) CNST2 = 2.4 IF(P2 .LT. 0.0) CNST2 = 0.9	0.9
*integrate, $T1_o$ is the last time-step value of signal T1	
U1 = U1 + CNST1 * (T1 + $T1_o$)/2.0 * DELT , -18.0 < U < 2.0	0.0
X11 = U1 + CNST2 * T1	0.0
X1 = X11 + 8.0 , -10.0 < X1 < 10.0	8.0
SUA = 64.1164 + 7.44164 * X1 , -10.0 < SUA < 10.0	10.0
SUFVA = 0.1 * SUA , 0.0 < SUFVA < 1.0	1.0
MFA = 0.5555 * X1 - 4.4444 , -10.0 < MFA < 10.0	0.0
MFCVA = 0.5 + 0.5 * MFA , 0.0 < MFCVA < 1.0	0.5

the TRAC-PF1 MFW pump model (27 rad/s/s) so that an additional constraint was not needed in the ICS model.

D. Steady-State Calculation

The primary-side steady-state operating conditions for the TRAC model are presented in Table X along with operating specifications from the Oconee-1 plant for comparison. The two primary-system loops and all four cold legs had symmetric flows. The mass flowrates through the reactor pumps were controlled during the steady state by adjusting the pump speed with control blocks. During the transient calculations, the calculated pump speeds were held constant as long as the pumps were running. All steady-state primary-loop values compared well with available data with only slight discrepancies in the core and vessel

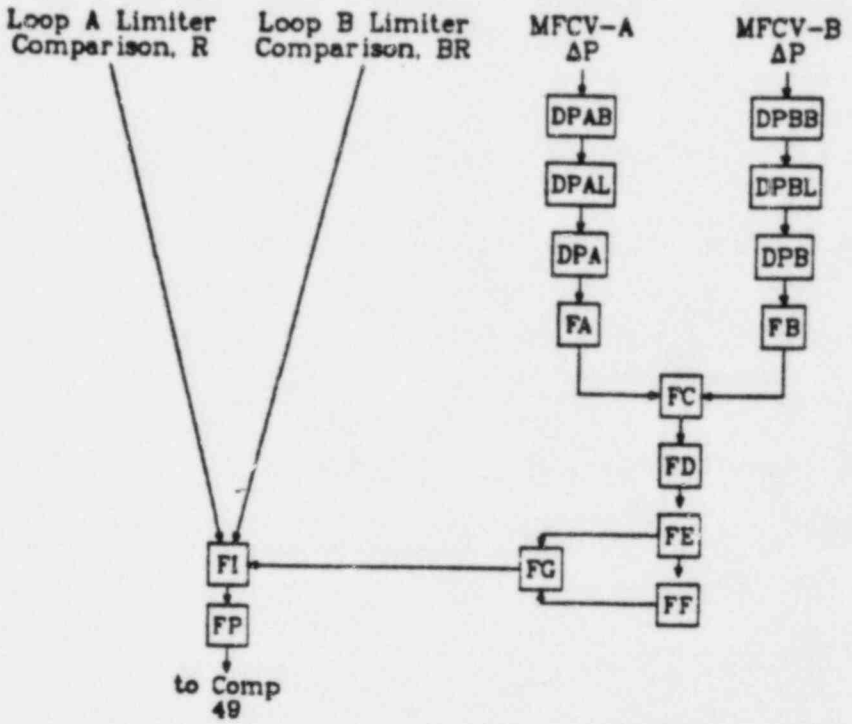

Fig. 18.
MFW-pump-speed control blocks.

pressure drops. In Table X, the coolant velocity and loop-flow lengths are added to show the relative time it takes coolant to travel through the loop from vessel exit to inlet.

Table XI presents a selection of secondary-side steady-state operating conditions for this model. In general, the comparison is very good with available Oconee-1 plant data. The feedwater flowrates for the two loops were independently controlled by the ICS through control of the MFW pump speed and MFCV areas. The steam outlet flowrate was approximately 2% higher than the feedwater flow so that the steam-generator inventory is slowly depleted with time. The approximate time it takes coolant to travel from the hotwell to a steam generator is estimated from the average velocity and pipe length to be over 11 min.

TABLE IX

MFW-PUMP-SPEED CONTROL BLOCK EQUATIONS

Equations	Steady-State Value
DPAB = DELPA - 3.55e5	0.0
First-order lag with a 1.0-s time constant *40 psi limit on both sides	
DPAL = DPAL + ((DPAB - DPAL)/1.0) * DELT , -2.4E5 < DPAL < 2.4E5	0.0
DPA = DPAL + 3.55E5	3 55E5
FA = 2.90074E-5 * DPA - 10.0	0.2975
*the loop-B pressure-drop equations are the same	
FC = min (FA,FB)	0.2975
FD = FC - 0.2975	0.0
FE = 0.2 * FD * ABS(FD), -10.0 < FE < 10.0	0.0
*integrate FE_o is last time-step value of signal FE	
FF = FF + 0.2333 * (FE + FE_o)/2.0 * DELT , -10.0 < FF < 10.0	0.0
FG = FF + FE , -10.0 < FG < 10.0	0.0
FI = 0.5 * (R + BR) - FG	8.0
FP = f(FI)	523.6

FI	FP rad/s
-2.0	370.4
0.0	392.8
6.0	460.0
10.0	586.43

TABLE X

PRIMARY-SIDE STEADY-STATE CONDITIONS

Parameter	TRAC Model	Oconee-1 Nuclear Station
Power (MW)	2568.0	2568.0
Coolant flowrate, total (kg/s)	17640.0	17640.0
Hot-leg temperature (K)*	589.56/589.33	589.3
Cold-leg temperature (K)	563.81/563.81/ 563.61/563.61	563.5
Primary pressure (MPa)~ (3 m below top of hot leg)	14.96/14.96	14.96
Core pressure drop (MPa)	0.117	0.11
Vessel pressure drop (MPa)	0.378	0.41
Pressurizer water level (m)	5.63	5.59
HPI coolant temperature (K)	283.2	305.4
Accumulator coolant temperature (K)	305.4	305.4
Hot-leg coolant velocity (m/s)	~19.5	-
Coolant flow path length (m) (external to vessel)	63.5	-

*loop A/loop B, or cold-leg A1/A2/B1/B2

TABLE XI

SECONDARY-SIDE STEADY-STATE CONDITIONS

	TRAC Model	Oconee-1 Nuclear Station
Feedwater flow, loop A/loop B (kg/s)	679.04/678.38	680.4
Feedwater temperature (K)	511.19	511.0
Steam outlet flow, loop A/loop B (kg/s)	693.8/692.5	680.4
Steam outlet superheat (K)	17.7/17.03	33.3
Steam outlet pressure (MPa)	6.37/6.37	6.38
Steam pressure at turbine inlet (MPa)	6.2/6.2	6.2
Steam-generator secondary inventory (kg)	1.711E4/1.715E4	~1.77E4
Aspirator steam flow (kg/s)	95.4/95.3	-
MFW pump inlet pressure (MPa)	2.77	2.68
temperature (K)	461.0	462.0
Condensate booster-pump inlet pressure (MPa)	8.0	6.9
temperature (K)	308.3	309.0
Hotwell pressure (MPa)	0.015	0.01
temperature (K)	305.6	305.9
inventory (kg)	5.31E5	5.31E5
Upper surge-tank inventory (kg)	2.69E5	2.98E5
Feedwater train average coolant velocity (m/s)	~1.5	-
Hotwell to SG flow length (m)	1004.3	-
MFCV area fraction (%)	48.60/48.15	50
Loop flow fraction (%)	85/85	85

III. TRAC TRANSIENT CALCULATIONS

A. Oconee-3 Turbine Trip

1. Introduction. As a benchmark case for the Oconee-1 PTS study the Oconee-3 turbine-trip and steam-generator-overfeed transient of March 14, 1980 was simulated. The actual transient is documented in Ref. 4, and measured data is available for the first three minutes of the transient.* The data available include primary- and secondary-system pressures, hot- and cold-leg temperatures, pressurizer and steam-generator water levels, and main-feedwater flow rates and supply temperatures.

In this transient, the plant was operating at 100% power when the Electro-Hydraulic Control system caused a turbine trip and subsequent reactor trip. After the reactor trip, the ICS malfunctioned and caused an overfeed to the steam generators, resulting in an overcooling of the primary system. The steam-generator water levels increased above the expected levels until the main-feedwater pumps tripped on a steam-generator high-water-level signal.

The transient was modeled using the TRAC-PF1 code and the basic TRAC model of the Oconee-1 PWR (Fig. 1), with modifications to the steam lines to add main-steam safety valves (MSSVs). The TBVs were also modeled. The condensate-heater feedwater-train modeling and the ICS modeling was not included for this transient because these systems were not necessary. Instead, the measured main-feedwater flow rates and feedwater supply temperature given in Ref. 4 were specified as boundary input in the TRAC calculation.

The TRAC-calculated results compared very well with the Oconee-3 data and general trends and major peaks and dips in the data were predicted. The actual transient had slightly more overcooling than the TRAC calculation. The calculated primary pressure, hot- and cold-leg temperatures, and pressurizer water level were slightly higher than the measured data. The major differences between calculated and measured results were in the steam-generator secondary pressures and in the steam-generator B water level. The calculated secondary pressures cycled between the TBV open and close setpoints, whereas the measured secondary pressures dropped and remained below the TBV setpoints for the transient period modeled.

The measured secondary-side water level of steam generator B was found to be inconsistent with the measured main-feedwater flow rate. The steam generator refilled at a much faster rate than could be accounted by just the main-

*Data not shown in this report because it is proprietary.

feedwater flow, which indicates that auxiliary feedwater might have been inadvertently delivered to steam generator B during the transient. This inconsistency was not mentioned in Ref. 4 nor was auxiliary-feedwater flow data given.

A more accurate transient might be calculated if additional information can be obtained about actual auxiliary-feedwater flow rates, TBV setpoints and operating characteristics, decay power, and HPI flow distribution.

2. Model Description and Assumptions. The basic TRAC model of the Oconee-1 PWR, Fig. 1, was used to model the Oconee-3 transient. The steam lines were modified to add the steam safety valves as shown in Fig. 19. Neither the condensate-heater feedwater train nor the ICS was modeled. Instead, the measured feedwater flow rates, Fig. 20, and the feedwater temperature were specified as boundary input in the TRAC calculation. The standard ANS decay power, Fig. 21, was used and is automatically calculated by TRAC. The Oconee-3 measured reactor power is also shown in Fig. 21. The Oconee-3 power curve was used in a second TRAC calculation to determine the effect of reduced decay power, even though it did not include gamma-ray heating.

Table XII presents calculated and measured steady-state conditions. There is excellent agreement in the steady-state values except for a small difference in primary system pressure. Table XIII presents the MSSV and TBV setpoints used in the TRAC calculation. These are Final Safety Analysis Report (FSAR) values, as actual Oconee-3 setpoints were not available.

Table XIV shows the sequence of events that occurred in the Oconee-3 transient. The primary-coolant pumps did not trip in this transient. No auxiliary-feedwater flow was assumed in either steam generator. The HPI flow was assumed to be divided evenly among all four cold legs.

3. Transient Calculation. The TRAC-calculated transient compared very well with the actual plant transient. The actual transient had slightly more overcooling than the TRAC calculation. The calculated primary pressure, pressurizer water level, and hot- and cold-leg temperatures were slightly higher than the measured values. In general, differences between calculated and measured values were consistent throughout the transient.

Figures 22 and 23 compare the calculated and measured primary pressure and pressurizer water level, respectively. The TRAC calculation showed a decrease in pressure to a minimum of 12.97 MPa (1881 psia) whereas the actual transient decreased to a slightly lower minimum. The calculated pressurizer water level dropped about 3.04 m (10 ft).

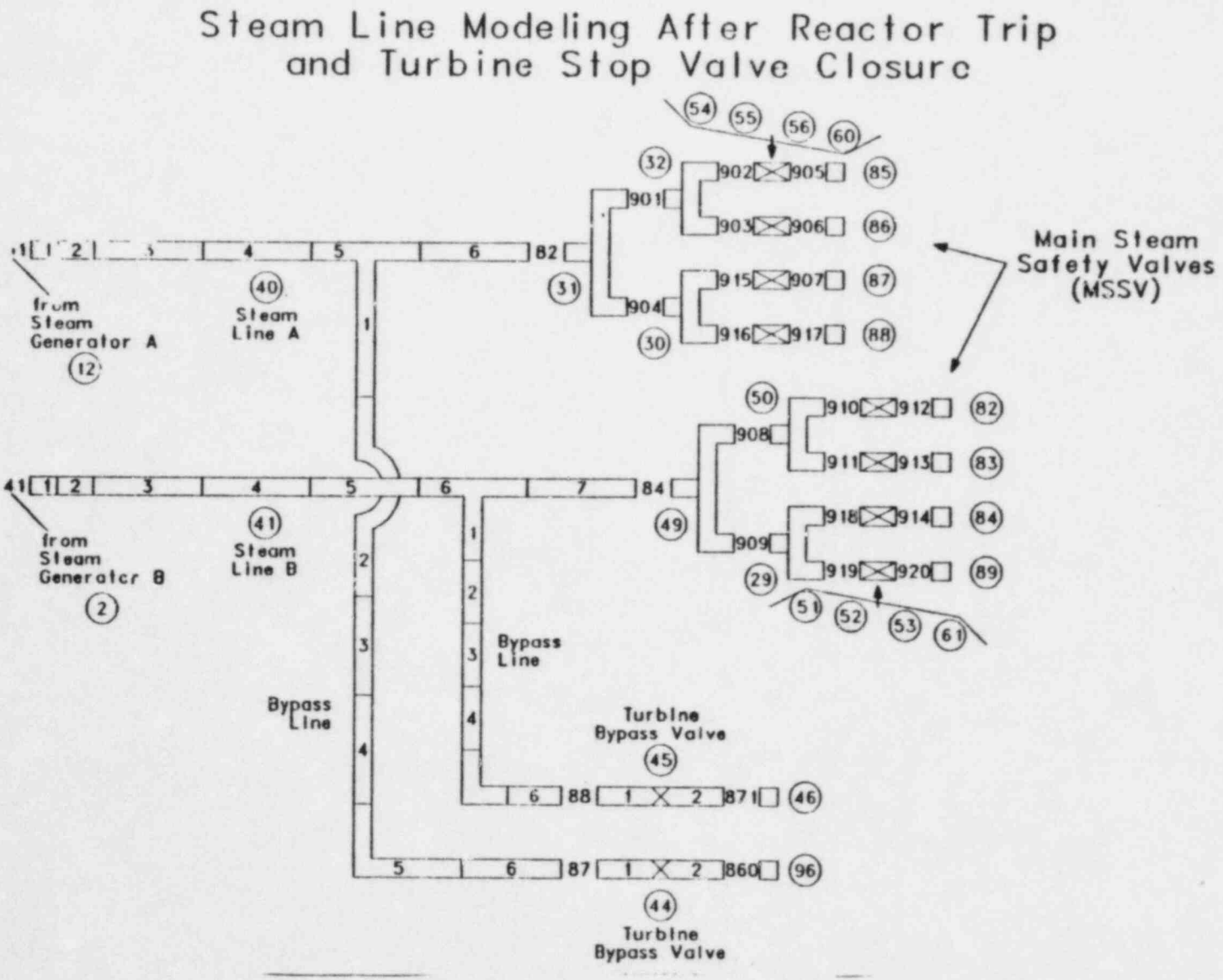

Fig. 19.
Main-steam safety-valve modeling for Oconee-3 transient.

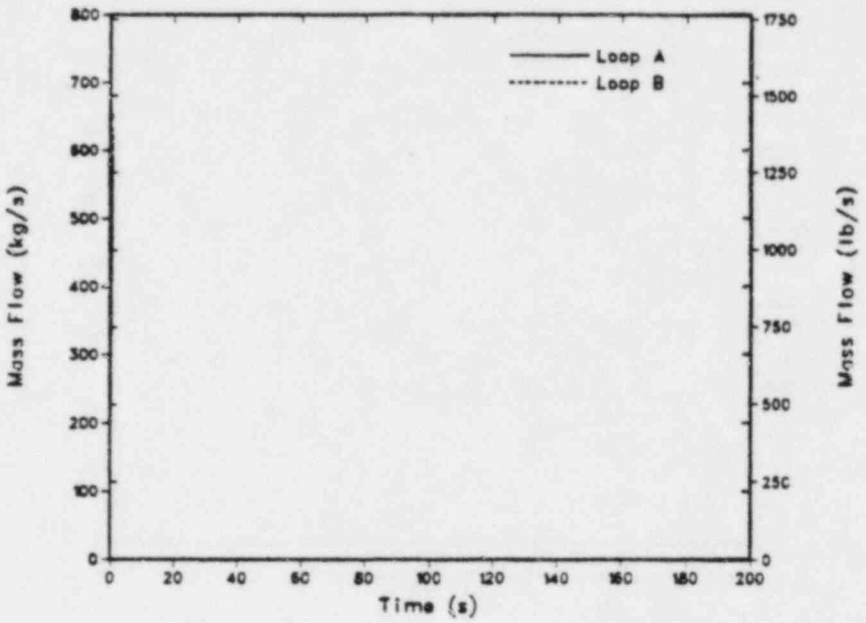

Fig. 20.
Measured main-feedwater flow rates.

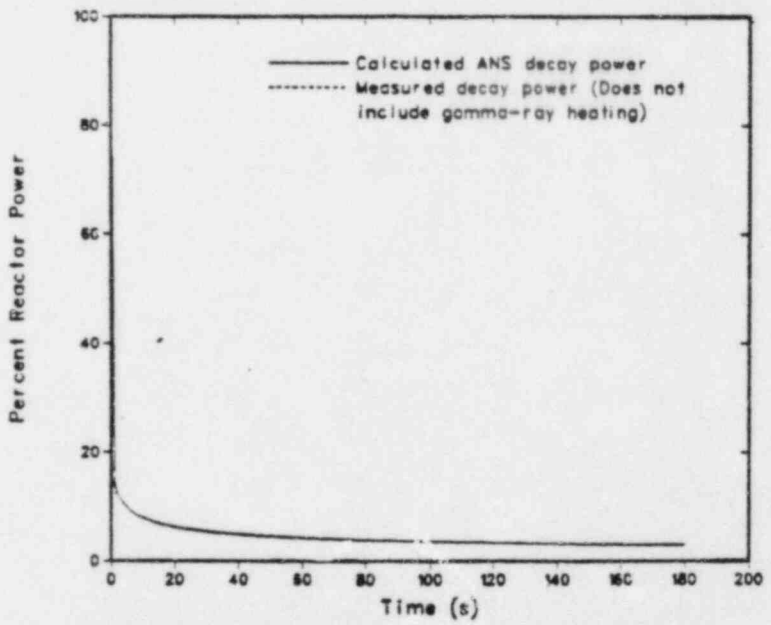

Fig. 21.
TRAC-calculated decay power and Oconee-3 measured thermal power.

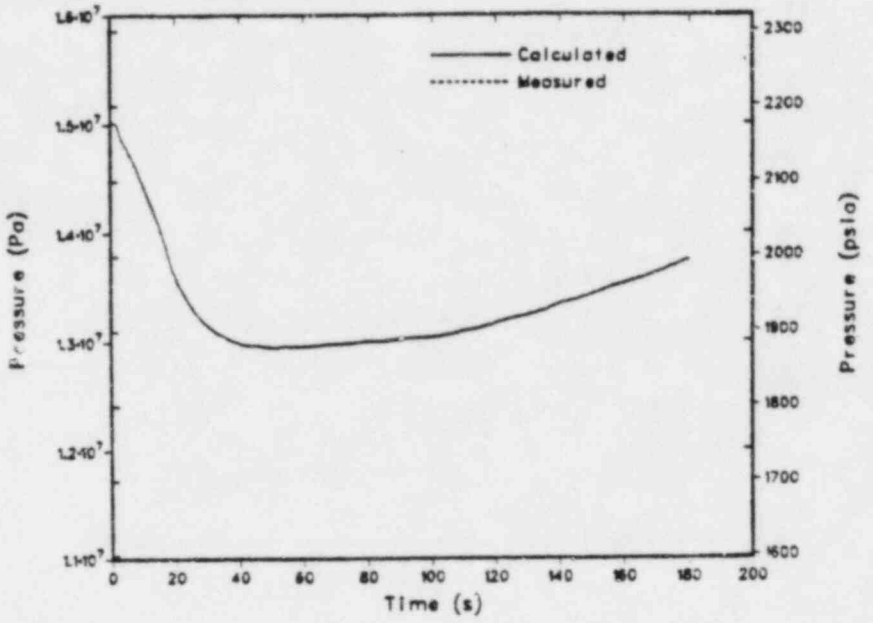

Fig. 22.
Calculated and measured primary pressures.

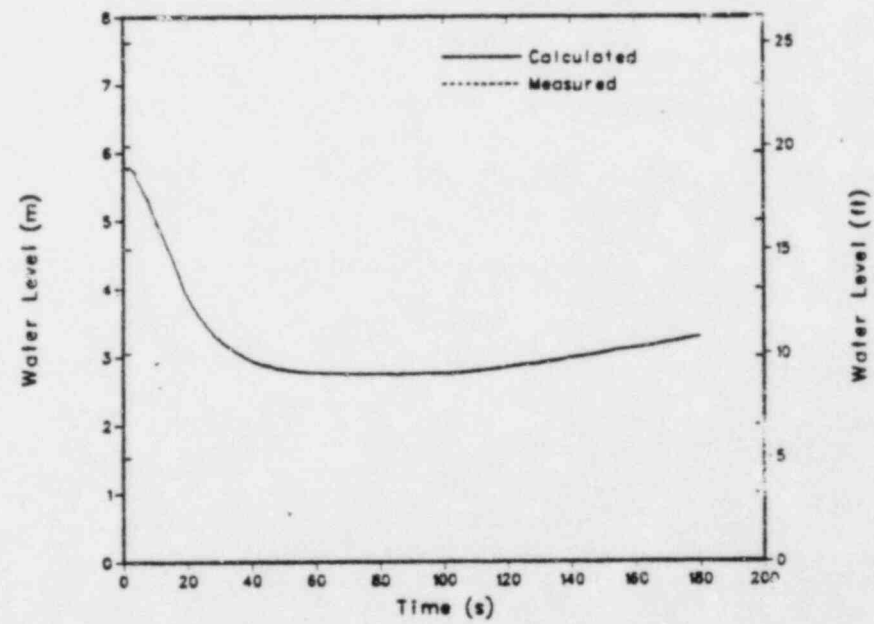

Fig. 23.
Calculated and measured pressurizer water levels.

TABLE XII

INITIAL STEADY-STATE CONDITIONS

Parameter	TRAC	Oconee-3
Reactor power (100% power)	2568 MW	
Cold-leg temperature	563.0 K (554 °F)	
Hot-leg temperature	588.9 K (600 °F)	
Primary-mass flow (each loop)	8820 kg/s (19445 lb/s)	
Primary pressure	15.03 MPa (2180 psia)	
Steam generator (each loop): Secondary Pressure	6.29 MPa (913 psia)	
Main-feedwater flow	680.0 kg/s (1500 lb/s)	
Feedwater temperature	510.9 K (460 °F)	

TABLE XIII

MAIN-STEAM-SAFETY AND TURBINE-BYPASS VALVE SETPOINTS

The following setpoints are FSAR values and were those used in the TRAC calculation. Actual Oconee-3 setpoints were not available.

1. Main-Steam-Safety Valve Setpoints

	Pressure (MPa)		Pressure (psig)	
	Open	Close	Open	Close
Bank 1	7.34	6.96	1050	995
Bank 2	7.408	7.029	1060	1005
Bank 3	7.512	7.133	1075	1020
Bank 4	7.615	7.236	1090	1035

2. Turbine Bypass-Valve Setpoints

Pressure (MPa)		Pressure (psig)	
Open	Close	Open	Close
7.067	6.998	1010	1000

TABLE XIV

SEQUENCE OF EVENTS

The following times are actual transient times and are the event times used in the TRAC calculation.

Event	Time (s)
1. Turbine trip and reactor trip occurred.	0
2. Operator assumed manual control of ICS to reduce main feedwater.	8
3. HPI pump A started to assist pump B to maintain pressurizer water level.	30
4. Main feedwater pumps tripped.	103
5. End of plant data and calculation.	180

Figures 24 and 25 show the hot- and cold-leg temperatures of loop A and loop B, respectively. Temperatures in loop A were slightly lower than in loop B because of a higher main-feedwater flow rate in the loop A steam generator. The initial increase in cold-leg temperatures in the first 10 s of the transient resulted from the sudden reduction in steam-generator heat removal caused by turbine stop-valve closure. Thereafter, the reduced reactor-thermal power allowed the cold-leg temperatures to decrease.

Figures 26 and 27 compare actual and calculated secondary pressures for loop A and loop B, respectively. The pressure peaks at about 6 s were also caused by turbine stop-valve closure. TRAC calculated lower peak pressures because of a modeling error in the location of the turbine-bypass valves. They were mistakenly located at the end of the turbine-bypass line rather than at the beginning. As a result, the calculated pressure peaks were lower because of the added volume of the turbine-bypass lines. Later in the transient, after about 40 s, the calculated secondary pressures were higher than the measured pressures. The calculated pressures cycled between the TBV open and close setpoints. The actual pressures decreased below the TBV setpoints and remained below the setpoints for the duration of the transient. The reason for this difference is not clear. Possibly the Oconee-3 plant had different TBV setpoints and rate characteristics from those modeled in the calculation.

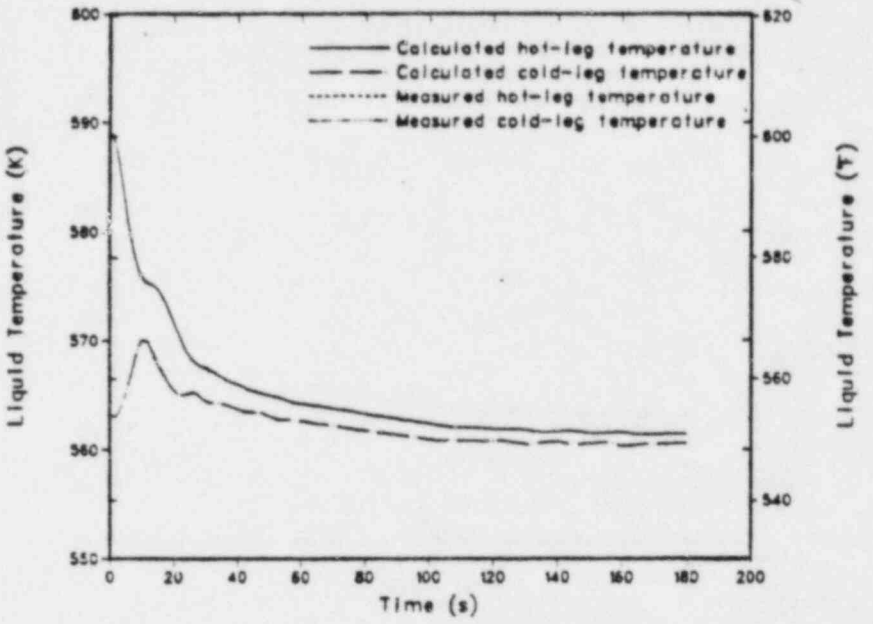

Fig. 24.
Calculated and measured hot- and cold-leg temperatures for loop A.

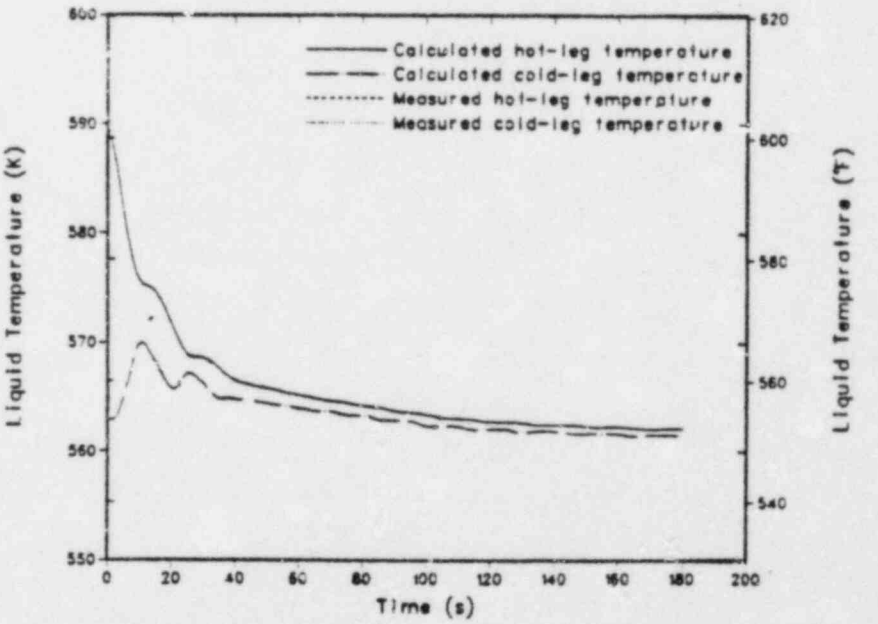

Fig. 25.
Calculated and measured hot- and cold-leg temperatures for loop B.

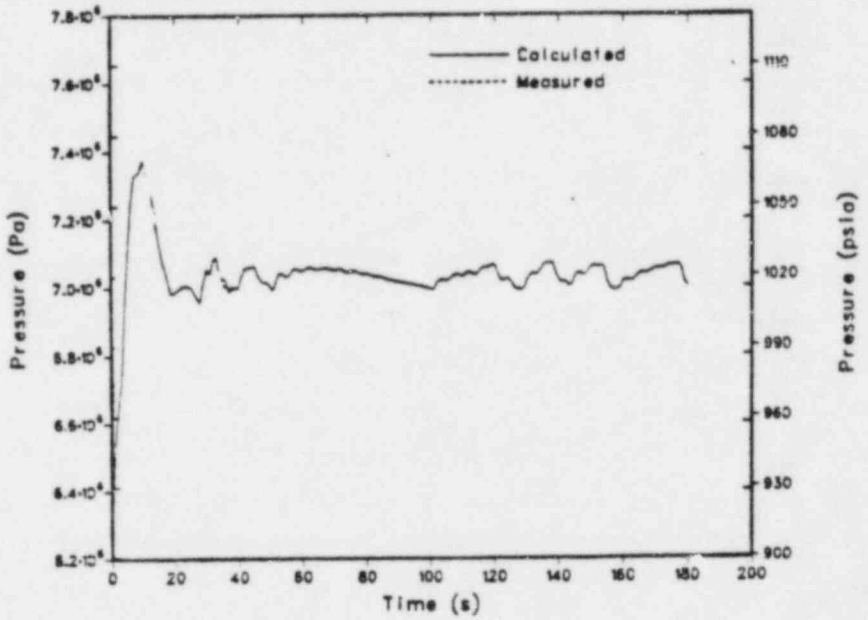

Fig. 26.
Calculated and measured steam-generator A secondary pressures.

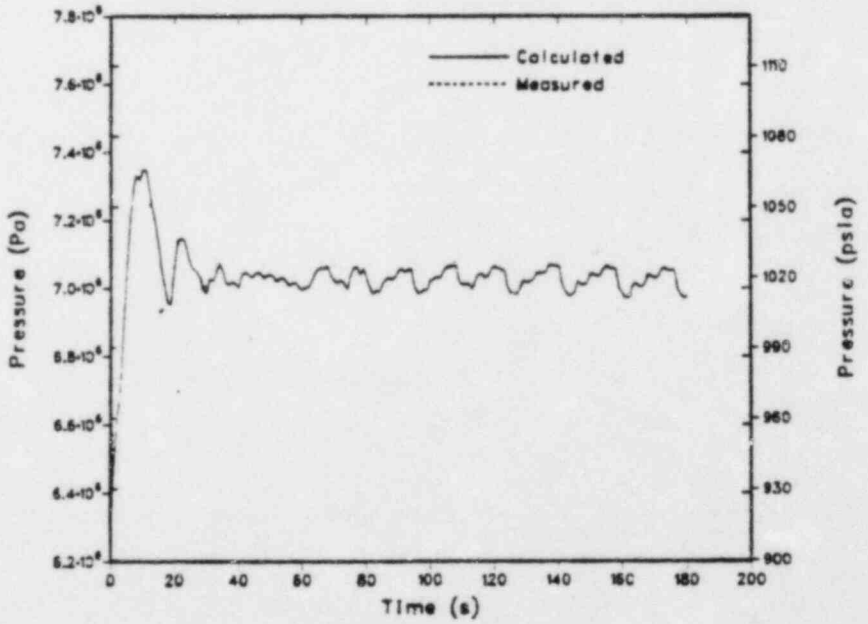

Fig. 27.
Calculated and measured steam-generator B secondary pressures.

Figures 28 and 29 show the secondary-side water levels for steam-generators A and B, respectively. There was excellent agreement between calculated and measured water levels in steam-generator A, but considerable difference in steam-generator B. Subsequently it was found that the measured water level and main-feedwater flow in steam-generator B were inconsistent. The steam generator was refilling at a much faster rate than could be accounted for by just the main-feedwater flow. This indicates that auxiliary feedwater may have been inadvertently delivered to steam-generator B. This inconsistency was not mentioned in Ref. 4 nor was auxiliary-feedwater flow data given.

Table XV compares the calculated and measured minimum pressures, temperatures, and pressurizer water level reached in the transient. Additional minimum-value results are presented for another TRAC calculation in which it was assumed the measured Oconee-3 thermal power (Fig. 21) to be the decay power.

The Oconee-3 measured thermal power did not include gamma-ray heating. The results do show the sensitivity of the transient to decay power.

4. Summary. The Oconee-3 turbine-trip and steam-generator-overfeed transient of March 14, 1980 was modeled using the TRAC-PF1 code. The calculational results compared very well with the measured data. Differences between calculated and measured results were minor and consistent throughout the transient. The actual transient had slightly more overcooling than the TRAC calculation. The calculated pressures, loop temperatures, and pressurizer water level were slightly higher than the measured values.

An inconsistency in the measured data given for steam-generator B was found. The steam generator was refilling at a much faster rate than could be accounted for by just the main-feedwater flow. This indicates that auxiliary-feedwater flow may have been inadvertently delivered to steam-generator B in the actual transient. If it was assumed in the TRAC calculation that auxiliary feedwater was delivered to steam-generator B, the calculation would have agreed better with the data. Other factors that could affect the degree of overcooling are decay power, HPI flow, TBV setpoints, and valve-rate characteristics.

B. Main Steam-Line Break

1. Introduction and Summary. For this transient, the overcooling of the primary side of the plant is caused by a severe depressurization of the secondary side. The secondary-side depressurization is caused by a full double-ended steam-line break in one of the steam generators (SG A). The accident sequence begins with the break of a 34-in. steam line coincident with reactor and turbine trip from full reactor power. The main forcing function for the overcooling of the primary side is the delay by the operator in isolating

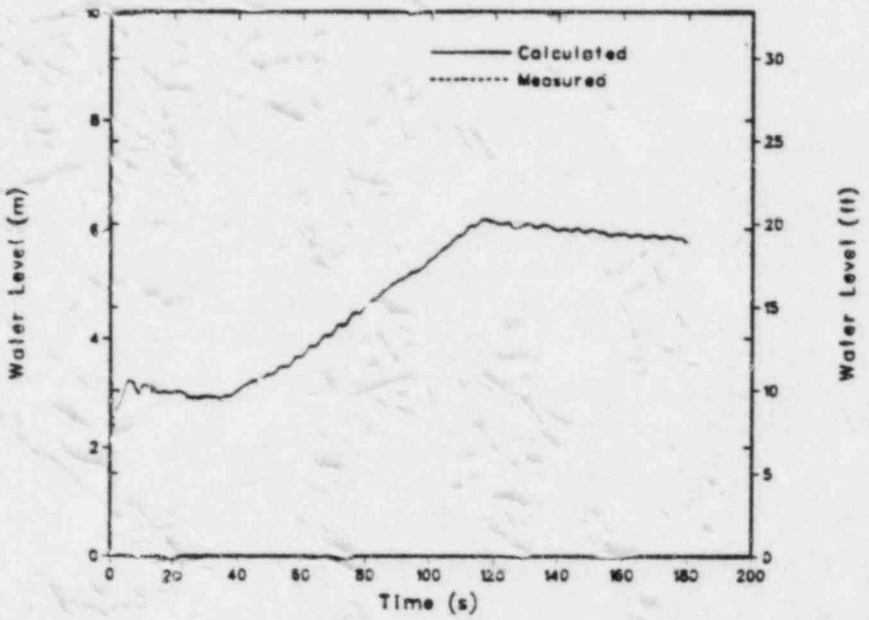

Fig. 28.
Calculated and measured water levels in steam-generator A.

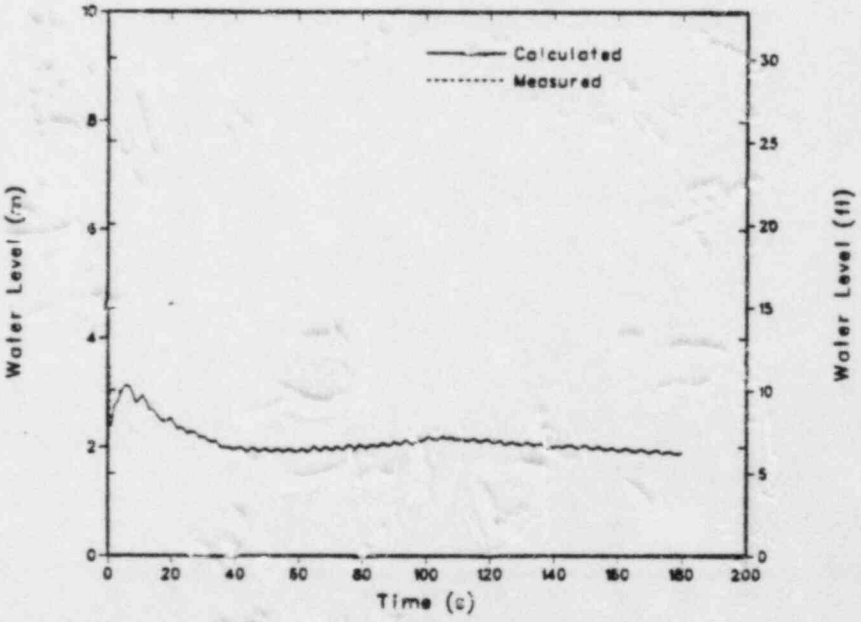

Fig. 29.
Calculated and measured water levels in steam-generator B.

TABLE XV

COMPARISON OF TRAC AND OCONEE-3 RESULTS

1. With ANS Decay Power in TRAC Calculation

	TRAC	Oconee-3
Minimum primary pressure	12.97 MPa (1881 psia)	
Minimum pressurizer water level	2.75 m (9.02 ft)	
Minimum hot-leg temperature (Loop A)	561.5 K (551 °F)	
Minimum cold-leg temperature (Loop A)	560.6 K (549 °F)	

2. With Reduced Decay Power in TRAC Calculation

A TRAC calculation was performed using the Oconee-3 measured reactor power as a decay-power curve input to TRAC. The Oconee-3 reactor-power curve did not include gamma-ray heating. These results are presented to show the sensitivity of the transient to decay power.

Minimum primary pressure	12.50 MPa (1813 psia)
Minimum pressurizer water level	2.12 m (6.96 ft)
Minimum hot-leg temperature (Loop A)	557.8 K (544 °F)
Minimum cold-leg temperature (Loop A)	558.0 K (545 °F)

the MFW and EFW to the affected steam generator, coupled with a delay in throttling the HPI flow and restarting one RCP in each loop following attainment of adequate fluid subcooling in the primary system.

The base case analyzed (Case 1) had all of the ICS, protection, and emergency systems operate as designed. In Case 1, the operator is assumed to isolate all feedwater to both steam generators 600 s into the transient and then restores the unaffected steam generator at 900 s. Also, the operator restarts one RCP in each loop after attaining 42 K subcooling, and throttles the HPI to maintain 42 ± 12.5 K fluid subcooling.

Three parametric cases were analyzed in addition to the base case. Case 2 was identical to the base case except the EFW system did not actuate as designed because of a modeling error in the input deck. In Case 3, in addition to the EFW system failing to actuate as designed, the RCPs never restarted after the subcooling margin was reached because of input deck errors. In Case 4, the MFW pump was tripped at 0.5 s and the subcooling monitor for restarting the RCPs was moved from the hot leg to the top of the core. Although these parametric cases were not specified by ORNL, they are still useful calculations because they give other possible scenarios that possibly could occur during a MSLB transient.

In terms of downcomer fluid temperatures and primary system repressurization considerations, the MSLB base case was one of the most severe of all the specified ORNL transients. A relatively cold downcomer liquid temperature of ~405 K and hence a small margin against the NDT limit was calculated for the base-case MSLB transient. Repressurization of the primary system to the PORV setpoint (~16.9 MPa) was also calculated for the base case.

2. Model Description. The TRAC-PF1 input model for the Oconee-1 plant is described in Section II of this report, and the primary and secondary noding diagrams are shown in Figs. 1 and 3 respectively. For the MSLB calculations, the steam-line break was modeled in the SG A steam-line shown in Fig. 3 (component 68). The TSV (component 42) was fixed open, and all of the steam from SG A passed through the TSV to atmospheric pressure. In the unaffected steam-line (SG B) the TSV was closed, and the TBV system operated as designed. All of the other systems also operated as designed except for the parametric cases. The significant features and initial conditions for the MSLB calculations were:

1. Full reactor power.
2. Nominal temperatures and pressures in primary/secondary.
3. Decay heat - 1.0 times ANS standard.
4. Reactor and turbine trips coincident with MSLB.
5. Operator fails to isolate feedwater to both SGs until 600 s.
6. Operator restores unaffected SG (SG B) at 900 s.
7. RCPs restarted after 42 K subcooling reached.
8. HPI throttled to maintain 42 ± 12.5 K subcooling.

3. Results.

a. Base Case (Case 1). Key events calculated during the transient for Case 1 are presented in Table XVI. The calculation was run long enough (7200 s) to determine whether or not the operators could recover the plant following the steam-line break. Figures 30 through 66 show plots of key system parameters calculated for the transient. Both short (0-900 s) and long (0-7200 s) time-scale plots are presented to give a complete description of the system thermal-hydraulics.

The transient was initiated by fixing the TSV in loop A open and modeling a break in the steam line downstream from the TSV (component 68 - Fig. 3). The TSV in loop B was closed at transient initiation and terminated condenser feed from the turbine. The turbine and reactor were then tripped followed by a feedwater - heater flow/drain trip. At ~5 s the TBV in loop B opened after the TBV setpoint (7.06 MPa) was reached. The TBV in loop B continued to open and close until ~40 s, after which time the TBV remained closed until late in the transient (~5462 s). HPI initiation occurred at ~21 s after the primary system pressure had decreased to 10.44 MPa. At ~29 s the ICS detected a low-level limit in SG A and the EFW pump was started. The EFW valve to SG A was opened, and EFW flow was initiated. At ~47 s the MFW pump tripped on low-suction pressure. The ICS detected a low water level in SG B at ~48 s, and EFW flow was initiated after the EFW valve in loop B opened. At ~51 s, the RCPs were tripped (30 s after HPI initiation), and the feedwater realignment trip occurred (all feedwater directed through the EFW header). At ~53 s, the condensate-booster pump tripped on low-suction pressure. The SG B water level reached 50% (operating range) at ~346 s, and the EFW valve to SG B was shut. All of the EFW flow was then directed to SG A. The 42 K liquid subcooling margin in all primary system loops was reached at ~526 s, and HPI was throttled. Also, RCPs A1 and B1 were restarted at this time because the subcooling margin was sufficient. At ~530 s the primary system had depressurized to the accumulator tank setpoint (4.17 MPa), and the check valves downstream from the accumulators opened. At ~538 s the accumulator check valves closed. Per the transient specifications[3], the steam-generator secondary sides were isolated at 600 s. Because of reverse heat transfer in SG B (heat transfer from secondary to primary side), condensation caused the water level to increase to the high-level limit (90% operating range) at ~655 s. At 900 s, SG B was restored to allow the EFW and TBV systems to operate if needed. However, because the SG B level was at the 90% limit and the secondary pressure was low, these systems did not actuate until much later in the transient. Following isolation of the steam

TABLE XVI

SEQUENCE OF EVENTS

	EVENT	TIME(s)
1.	MSLB - loop A steam line	0.0
2.	Turbine and reactor trip; TSV loop B closes	0.5
3.	TBV loop B opens (setpoint 7.063 MPa)	5.0
4.	HPI initiation (setpoint 10.44 MPa)	21.2
5.	SG A low level limit reached; EFW pump starts; loop A SG EFW flow initiated	29.4
6.	TBV loop B closes	39.9
7.	MFW pump trip on low suction pressure	47.8
8.	SG B low-level limit reached; loop B EFW flow initiated	48.7
9.	RCPs trip (30 s after HPI initiation)	51.2
10.	Condensate booster pump trip (low suction pressure)	53.9
11.	SG B level at 50%; loop B EFW Valve closed	346.7
12.	RCPs (A1, B1) restart (42 K subcooling reached); HPI throttled	526.0
13.	Loop A, B accumulator setpoints reached (setpoint 4.17 MPa)	530.9
14.	Loop A, B accumulators off	537.9
15.	SG A, B isolated; EFW pump and hotwell pump tripped off	600.0
16.	SG B restored	900.0
17.	PORV setpoint reached (setpoint 16.9 MPa) -- PORV opens and closes for remainder of calculation	4678-7200.0
18.	TBV loop B opens (setpoint 7.063 MPa) - TBV opens and closes for remainder of calculation to maintain setpoint pressure	5462-7200.0
19.	SG B level drops below 50% operating range; EFW initiated - EFW pump on/off for remainder of calculation to maintain level at 50%	6121-7200.0
20.	Calculation terminated	7200.0

generators, the primary system began to repressurize. At ~4678 s, the PORV setpoint was reached (16.9 MPa), and the PORV cycled opened and closed for the remainder of the transient. The secondary side of SG B repressurized to the TBV setpoint (7.06 MPa) at ~5462 s, and the TBV opened and closed for the remainder of the transient to maintain the setpoint pressure. At ~6121 s, the SG B water level dropped below 50% (operating range), and the EFW system was activated to

maintain the level at 50%. The calculation was terminated at 7200 s, and the primary system was full of liquid. At this time, the decay power produced in the core was being removed through the unaffected steam generator (SG B).

The pressurizer pressure history is shown in Figs. 30 and 31. Initially, the primary-system pressure decreased rapidly because of the rapid secondary-side blowdown in SG A following the MSLB. The depressurization was terminated by ~100 s when natural circulation flows were established following pump coastdown and RCP trip at ~51 s. The primary system then began to repressurize slightly until the RCPs were restarted at ~526 s. The enhanced heat transfer through the steam generators, condensation of the steam in the loop B candy cane, and throttling of the HPI after the RCPs were restarted caused the primary-system pressure to decrease to the minimum value for the transient (~3.5 MPa). After the steam generators were isolated at 600 s, the primary system repressurized to the PORV setpoint (16.9 MPa) at ~4678 s. The PORV then cycled for the remainder of the transient to maintain the primary-system pressure at or below the PORV setpoint.

The pressurizer water level is shown in Figs. 32 and 33. The pressurizer completely emptied by ~40 s because of liquid contraction resulting from the severe overcooling of the primary system. After the HPI had been on for some time, the pressurizer began to slowly refill until the RCPs were restarted, and the HPI was throttled at ~526 s. Again, the resulting overcooling of the primary system caused the liquid to contract further, thus the pressurizer again emptied. After the steam generators were isolated at 600 s, the primary system liquid expanded because of fluid heat-up and the pressurizer slowly refilled.

Downcomer liquid temperatures for the base case are presented in Figs. 34 and 35 at the top axial downcomer level just below the cold-leg inlet nozzles. Because of the severe overcooling in the affected loop (loop A), asymmetrical liquid temperatures are calculated in the vessel downcomer. The fluid temperatures in the downcomer cells associated with the loop-A cold legs were calculated to be ~20 K colder than the cells on the loop-B side (Fig. 34). The minimum downcomer fluid temperature calculated was ~405 K at ~526 s when the RCPs were restarted. While the RCPs were tripped off, the downcomer fluid temperatures were affected by the vent-valve flow shown in Fig. 36. The warmer upper-plenum fluid mixed with the colder downcomer fluid during the time the RCPs were tripped. During the time the RCPs were operating, the vent-valves did not open because the pressure gradient was reversed.

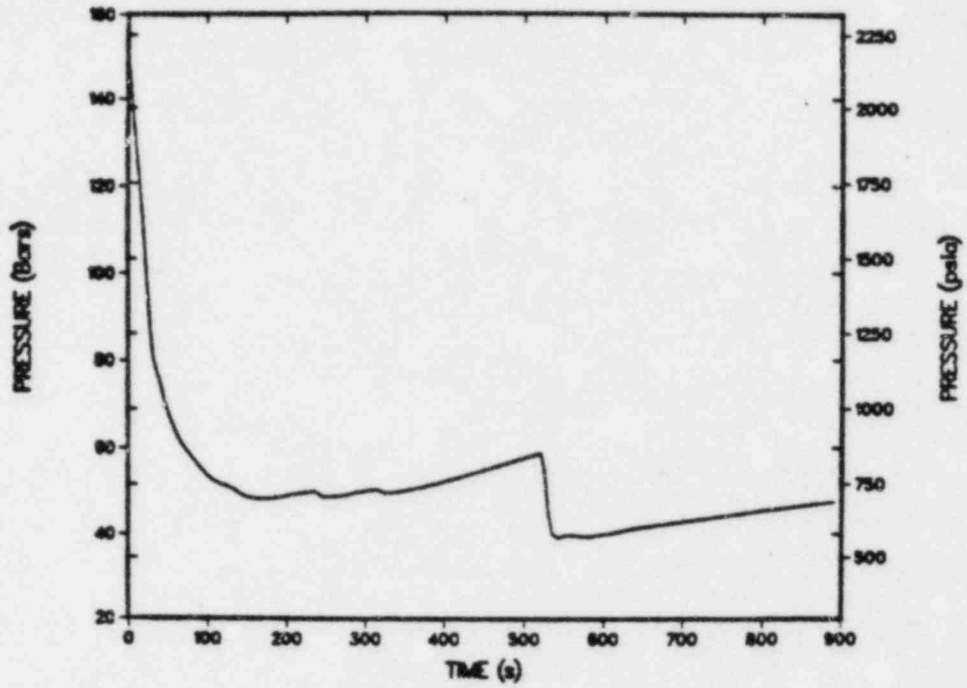

Fig. 30.
Pressurizer pressure (0-900 s) - base case.

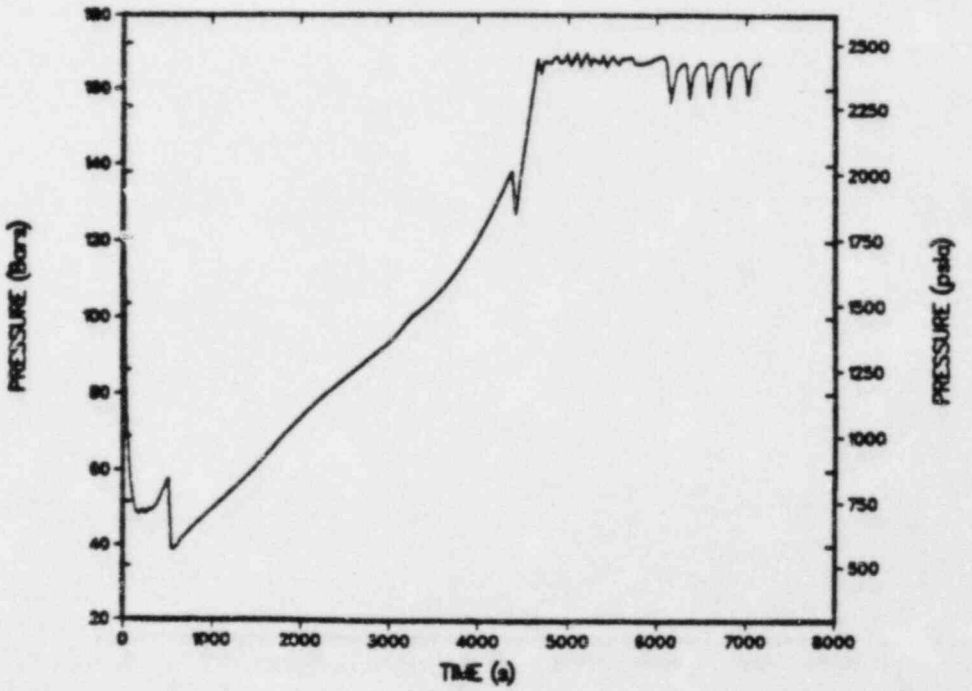

Fig. 31.
Pressurizer pressure (0-7200 s) - base case.

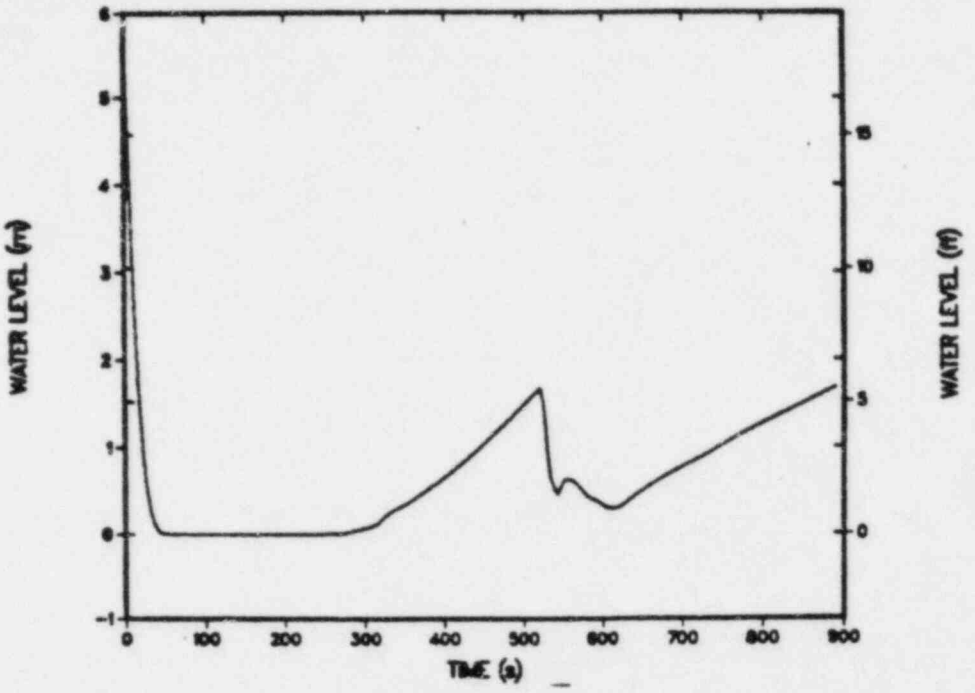

Fig. 32.
Pressurizer water level (0-900 s) - base case.

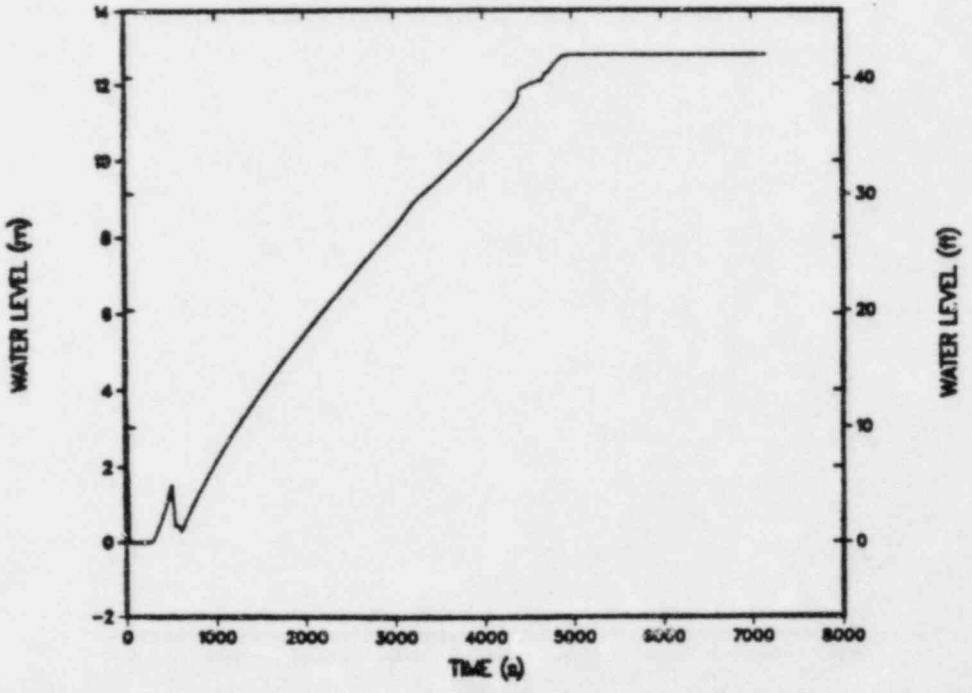

Fig. 33.
Pressurizer water level (0-7200 s) - base case.

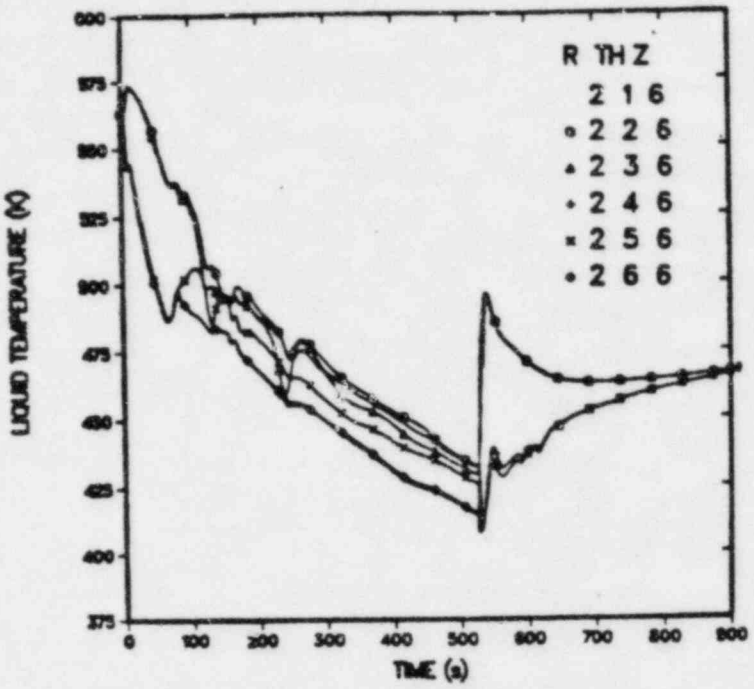

Fig. 34.
Downcomer liquid temperatures (0-900 s) at vessel axial level 6 (all azimuthal sectors) - base case.

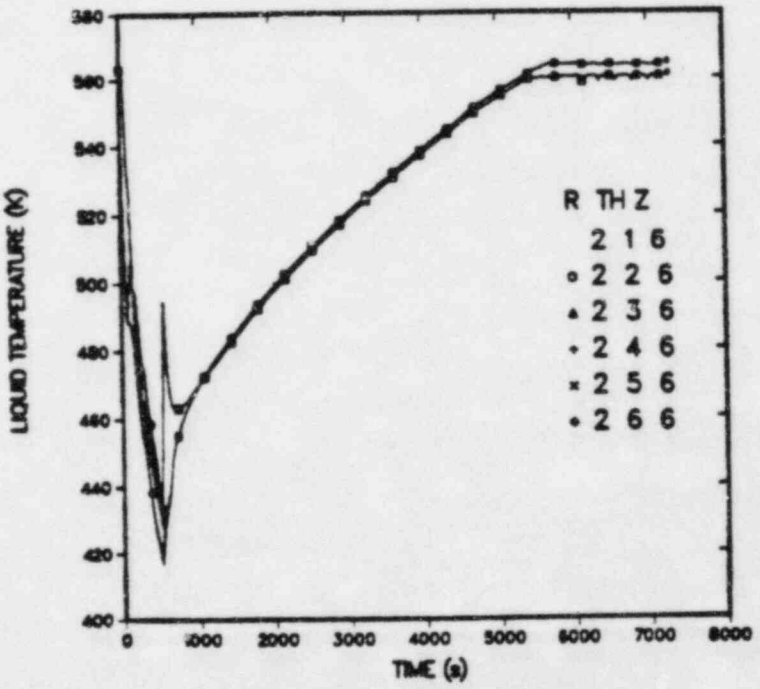

Fig. 35.
Downcomer liquid temperatures (0-7200 s) at vessel axial level 6 (all azimuthal sectors) - base case.

The hot-leg liquid subcooling in each hot leg is shown in Figs. 37 and 38. Figures 39 and 40 show the hot-leg mass flows and Fig. 41 shows the candy-cane void fractions. The subcooling margin calculated in loop A is significantly larger than in loop B for much of the transient because of the MSLB in loop A and the resulting enhanced heat transfer in the affected steam generator. The enhanced heat transfer caused higher natural-circulation flows in loop A compared to loop B (Figs. 39 and 40) from ~150 s to the time the RCPs (A1 and B1) were restarted (~526 s). The 42-K subcooling margin was reached in loop A at ~275 s, but the RCPs could not be restarted until this margin was reached in all loops. The flow in loop B stagnated at ~150 s because the candy-cane in this loop reached saturation and voided (Fig. 41). The subcooling margin in loop B was not reached until ~526 s at which time the RCPs were restarted. After the RCPs were restarted, the void in the loop-B candy cane condensed and was swept out (Fig. 41) and the subcooling margin in both loops equalized. It should be noted that at the time the subcooling margin was reached in all loops (~526 s) and the RCPs were restarted, the HPI was also throttled. The subcooling margin never decreased below 42 K for the remainder of the transient, thus the HPI was never turned back on nor were the RCPs tripped again.

As discussed in the preceding paragraph, the loop-B candy cane voided at ~150 s (Fig. 41) and the void was swept out after the RCPs were restarted. Even though the candy cane in loop B voided, which is the highest point in the primary system, the vessel did not void as shown in Fig. 42. Figure 42 shows the volume fraction of the upper-plenum liquid, which is the region above the reactor core. From Fig. 42 it is seen that the vessel remained completely full of liquid for the entire transient.

Figures 43 through 46 show mass flows and liquid temperatures in the cold legs. Figures 43 and 45 show the cold-leg mass flows for loop A and loop B respectively. As discussed previously, before the RCPs were restarted significant natural-circulation flows were calculated in loop A because of enhanced heat transfer in the affected steam generator. The loop-B flows prior to RCP restart were essentially stagnant as shown in Fig. 45 because the loop-B candy cane voided. When the RCPs (A1, B1) were restarted at ~526 s, essentially steady-state flows were calculated in cold legs A1 and B1, but the flows in cold legs A2 and B2 reversed (flow out from vessel) as shown in Figs. 43 and 45. For the remainder of the transient, the cold-leg flow directions and magnitudes remained essentially the same as shown in Figs. 43 and 45 after ~526 s. The cold-leg fluid temperatures are shown in Figs. 44 and 46 for loops A and B

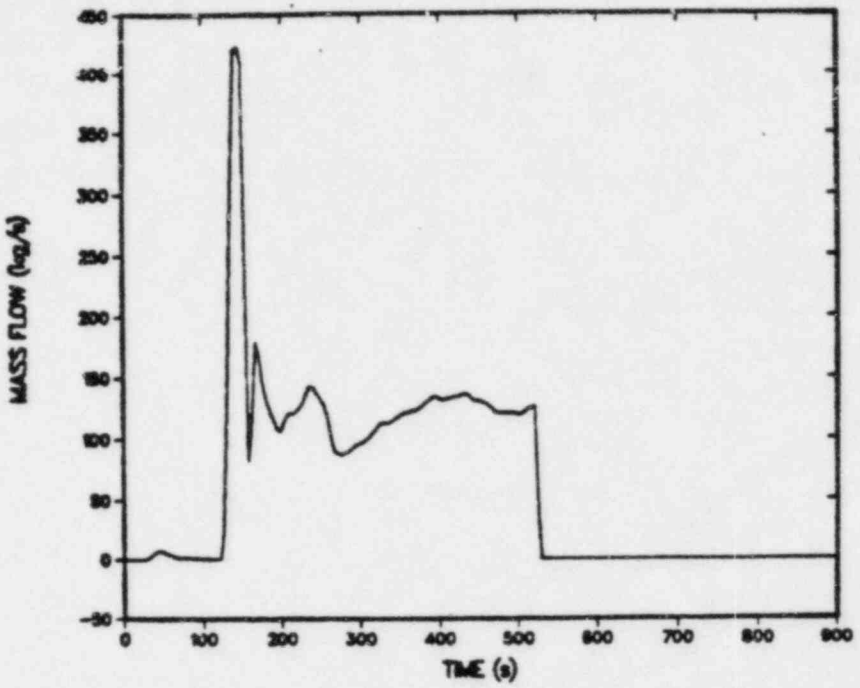

Fig. 36.
Total vent-valve flow into downcomer - base case.

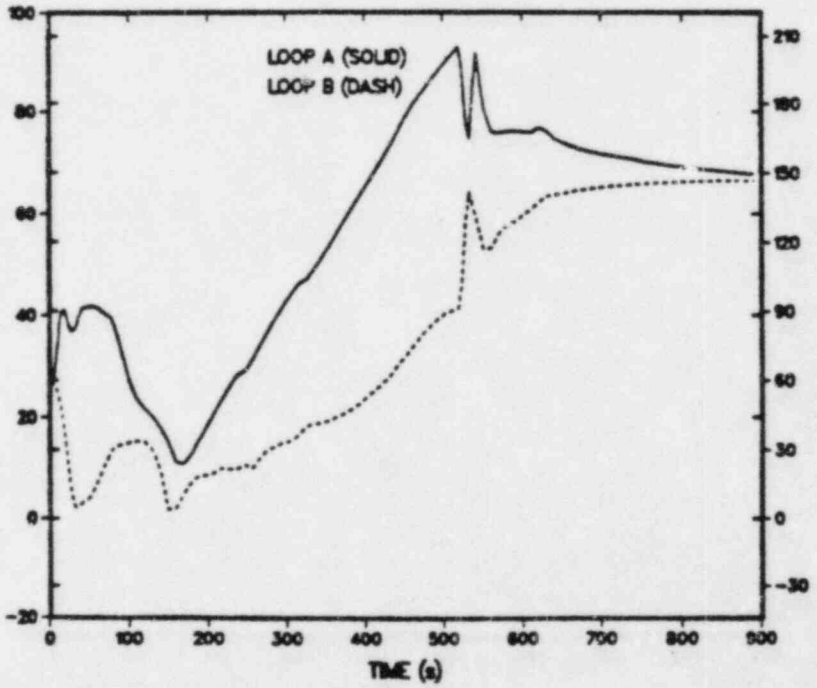

Fig. 37.
Hot-leg liquid subcooling (0-900 s) - base case.

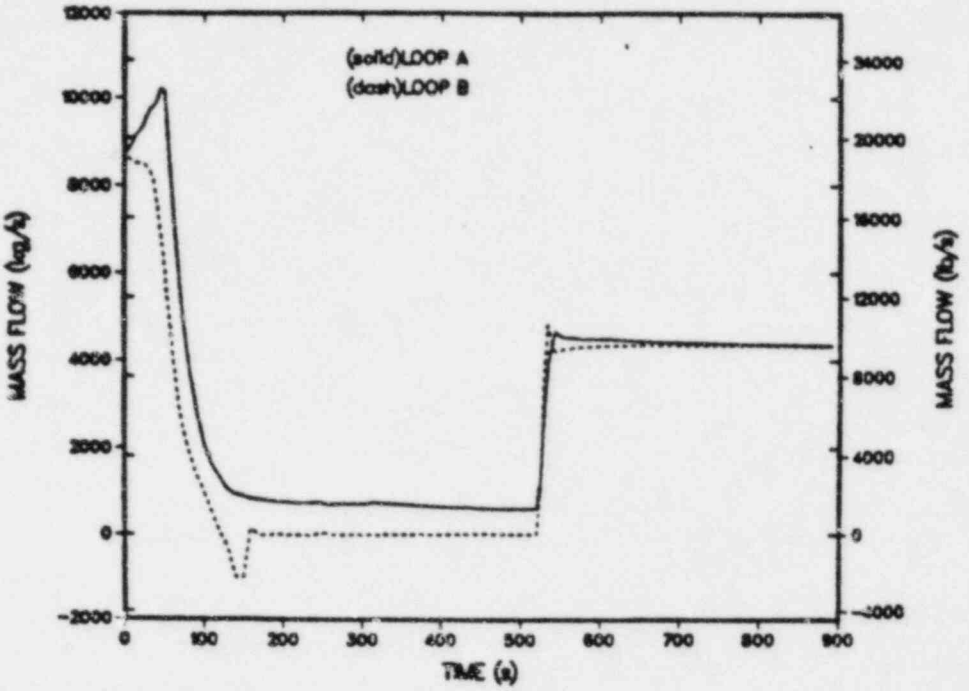

Fig. 38.
Hot-leg liquid subcooling (0-7200 s) - base case.

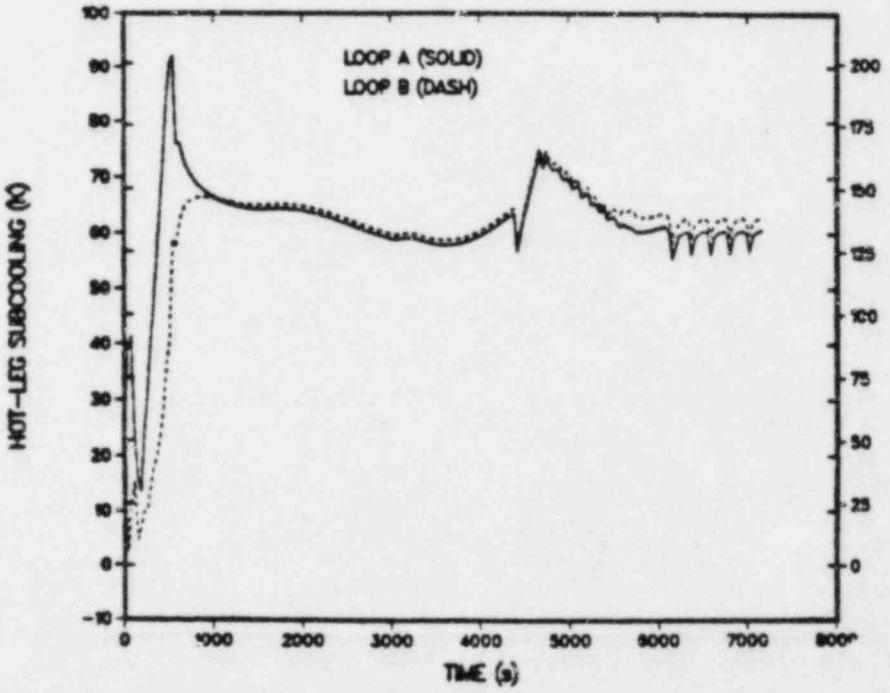

Fig. 39.
Hot-leg mass flows (0-900 s) - base case.

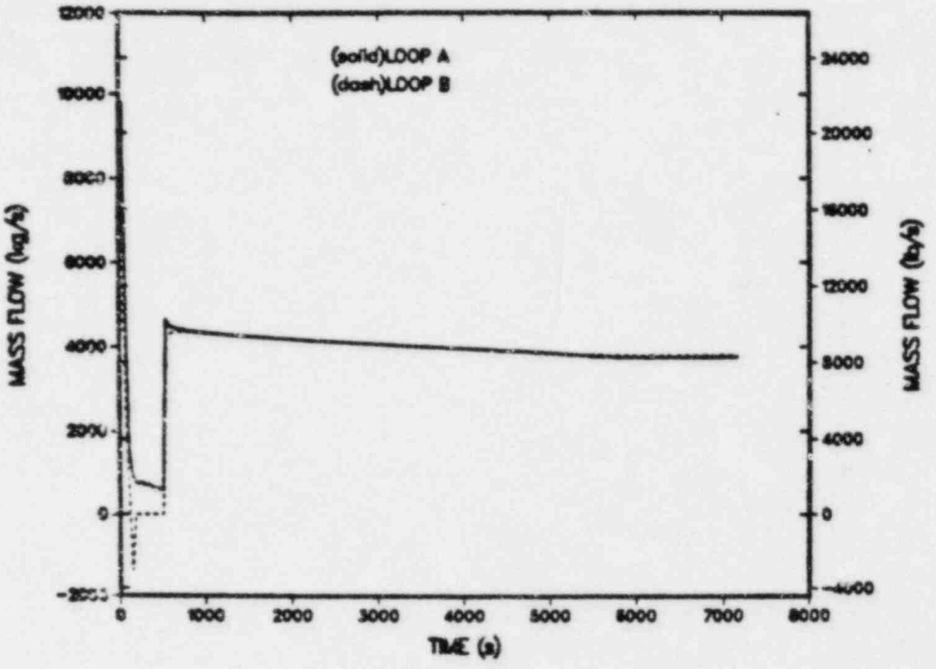

Fig. 40.
Hot-leg mass flows (0-7200 s) - base case.

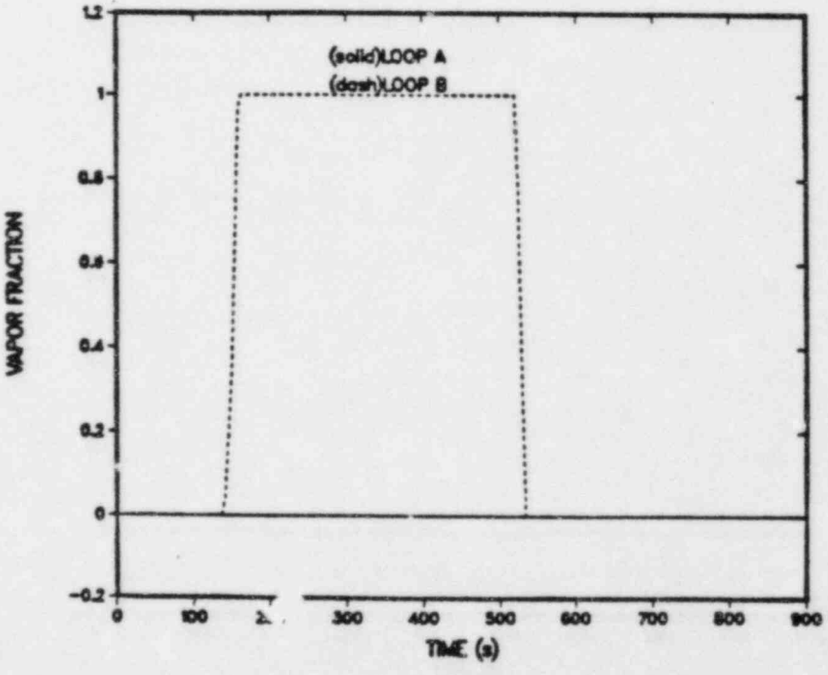

Fig. 41.
Candy-cane void fractions - base case.

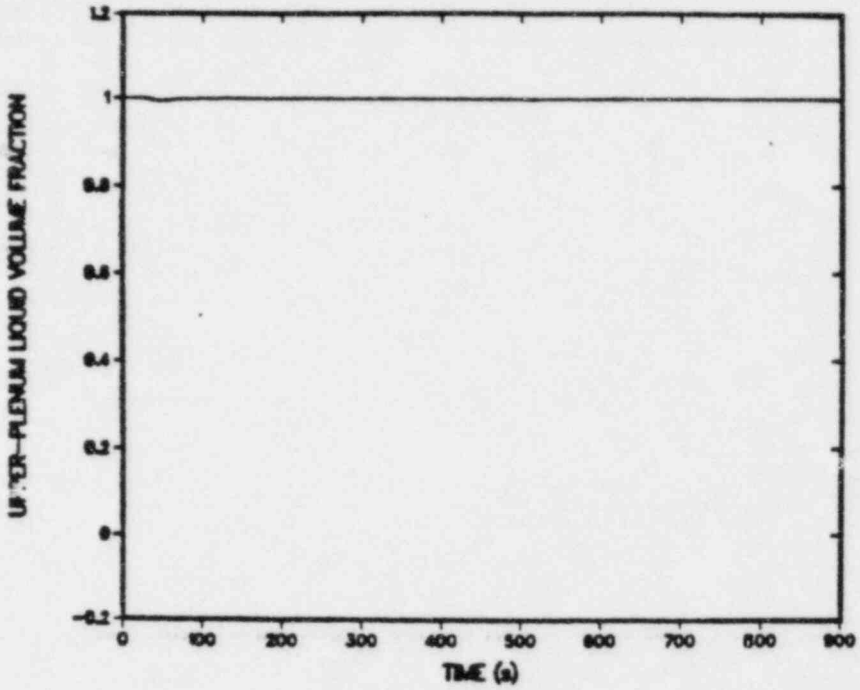

Fig. 42.
Upper-plenum liquid volume fraction - base case.

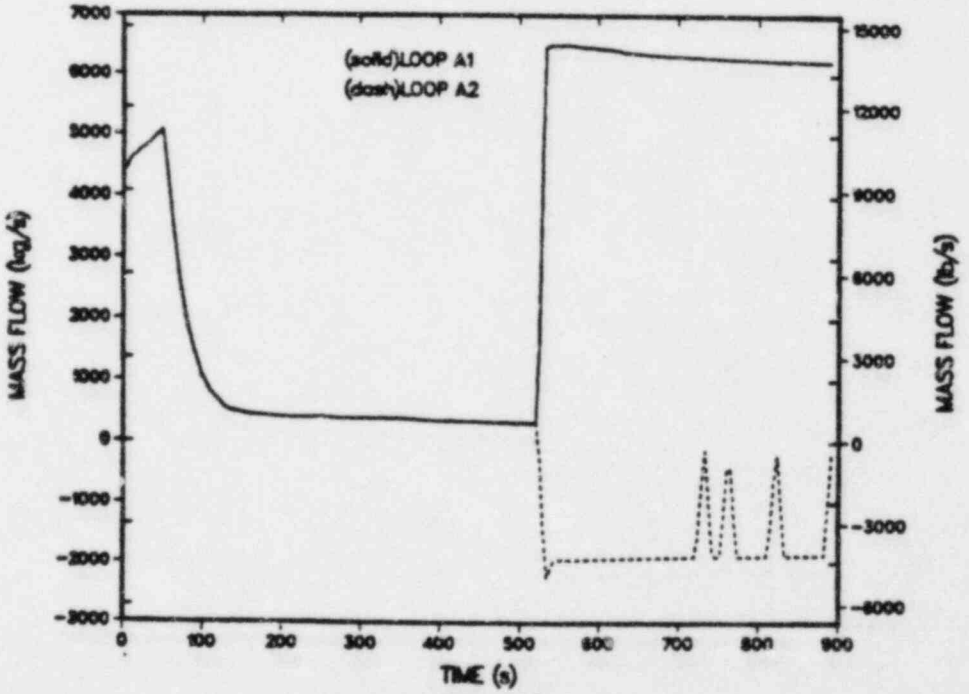

Fig. 43.
Loop-A cold-leg mass flows - base case.

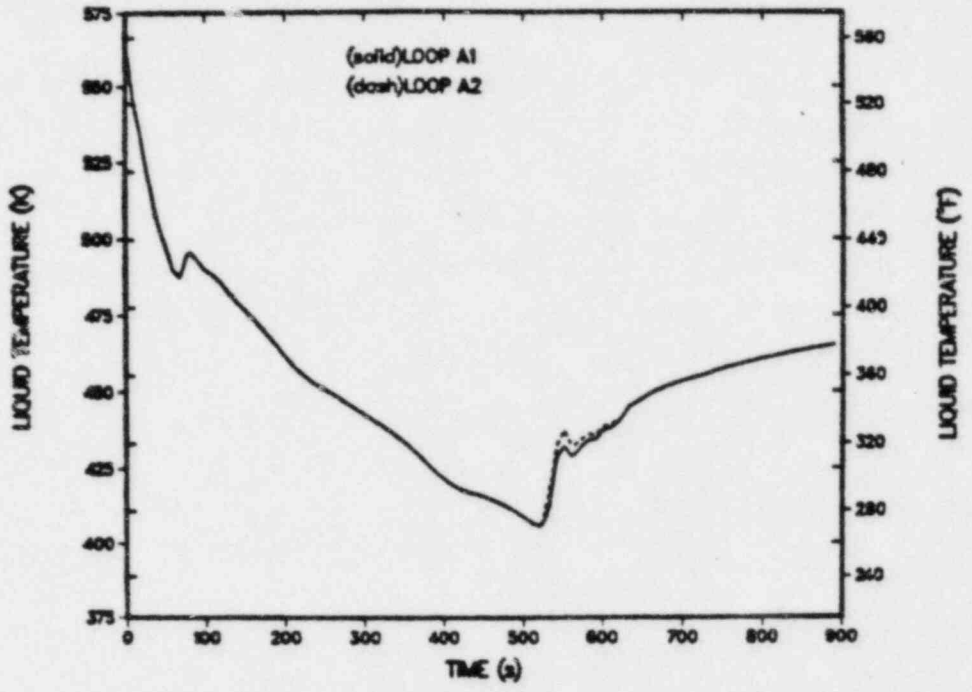

Fig. 44.
Loop-A cold-leg liquid temperatures - base case.

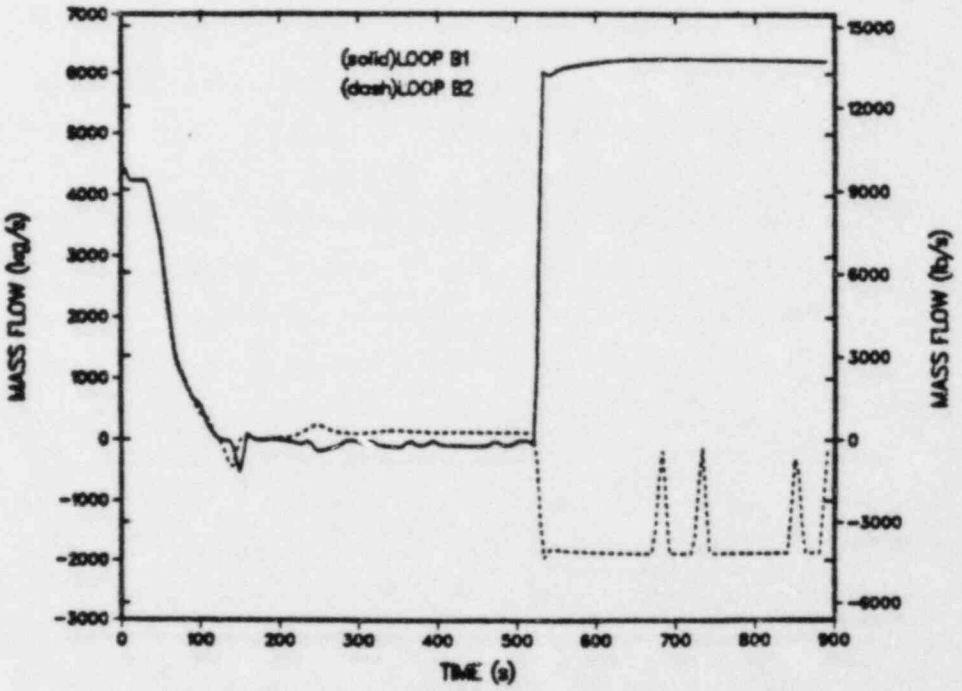

Fig. 45.
Loop-B cold-leg mass flows - base case.

respectively. It is seen that the loop-A fluid temperatures were significantly colder than loop B during the time the RCPs were tripped (~50-526 s).

Detailed results of key system parameters in the steam generator are shown in Figs. 47 through 54. Figures 47 through 50 show details for the affected steam generator (SG A), and Figs. 51 through 54 show details for the unaffected steam generator (SG B). Figure 47 shows the secondary-side water mass in SG A, and Fig. 48 shows the secondary-side pressure history. The secondary side depressurized to essentially atmospheric pressure by ~85 s, and this time corresponded to the minimum water mass inventory. Figure 49 shows the resulting flow out the broken steam line during the course of the transient. After the secondary side of SG A had depressurized sufficiently (~100 s), the EFW penetration increased, and the water inventory began increasing (Fig. 47) as less EFW was bypassed out the broken steam line.

Figure 50 presents some detailed plots to help explain the EFW penetration phenomena. The top plot in Fig. 50 compares the TRAC-calculated vapor velocity at the EFW injection point to the complete flooding curve predicted by the Wallis-Kutateladze correlation (K = 3.2) for various pressures in the SG A secondary side. This plot shows that EFW penetration will not occur until the vapor velocity is less than ~8 m/s, and this velocity is not reached in the TRAC calculation until the secondary side had depressurized to ~0.5 MPa. The bottom plot in Fig. 50 gives the TRAC calculated liquid-vapor velocity correlation at the EFW injection point location. This plot shows that EFW penetration as calculated by TRAC did not occur until the vapor velocity decreased to ~7.5 m/s, which closely agrees with the Wallis-Kutateladze correlation.

Figure 47 shows that the secondary-side water inventory remained relatively constant (~1000 kg) after EFW penetration occurred at ~85 s and did not change significantly until ~350 s. As will be discussed later, the reason for the increasing inventory after ~350 s was because the EFW to SG B was terminated and all EFW was directed to SG A. The inventory decreased following RCP restart at ~526 s because of the enhanced heat transfer from forced convection on the primary side. Then, at 600 s the steam generators were isolated, and EFW was terminated. The water inventory in SG A then decreased to zero and remained empty for the remainder of the transient.

Figures 51 through 54 show some key parameter plots for SG B. Figures 51 and 52 show the secondary-side water inventory calculated for SG B. At ~48 s, the low-level limit was reached following TBV operation in SG B, and EFW was initiated. The water level continued to increase to the 50% operating range at which time the EFW valve to loop B was shut (~350 s). The SG B level remained

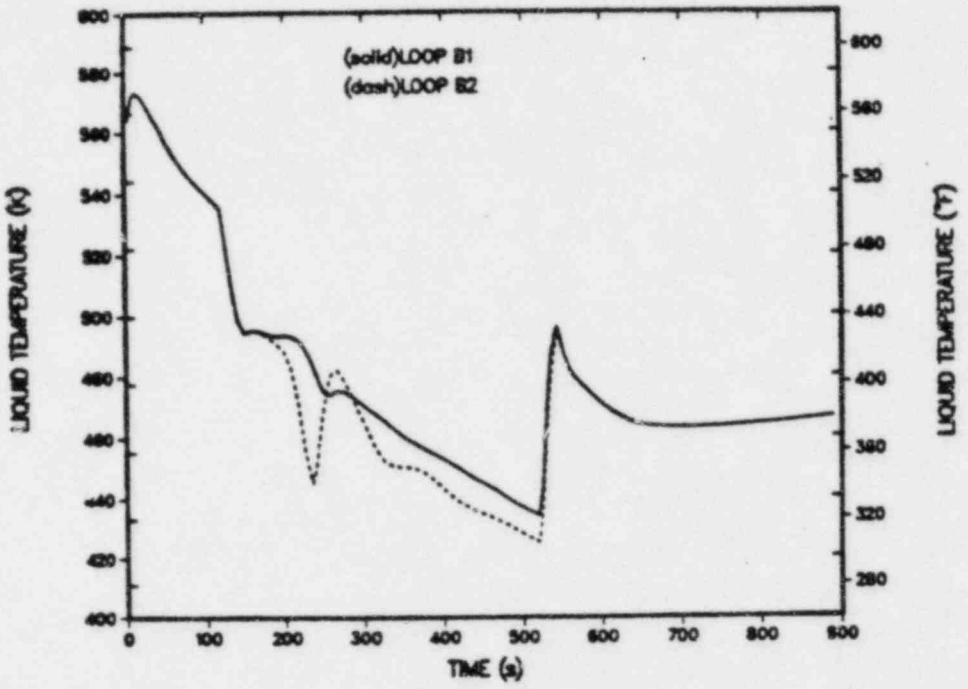

Fig. 46.
Loop-B cold-leg liquid temperatures - base case.

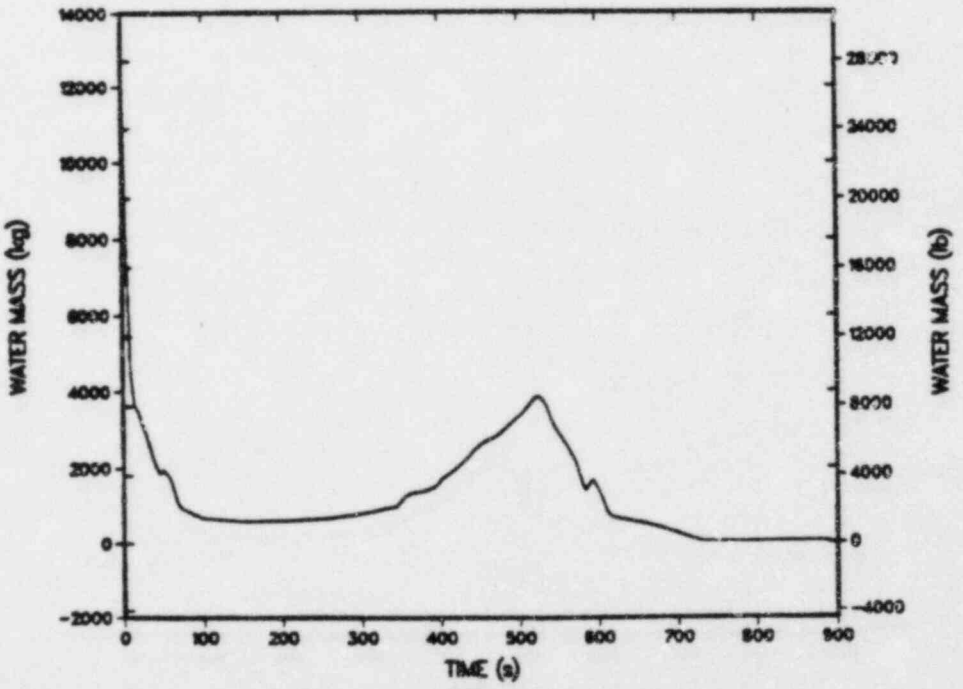

Fig. 47.
SG A secondary-side water inventory - base case.

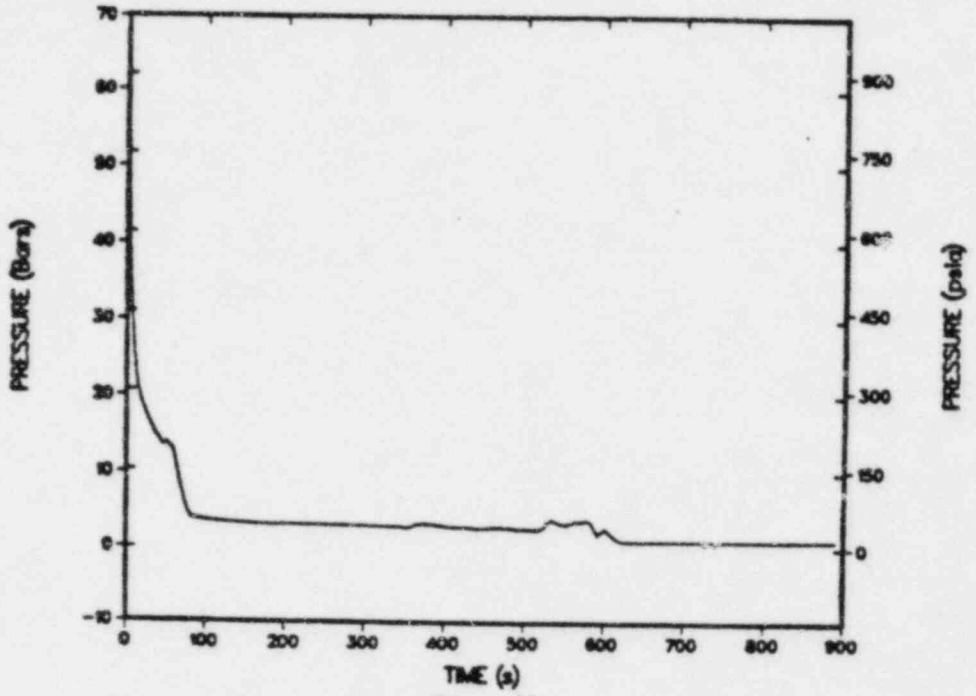

Fig. 48.
SG A secondary-side pressure - base case.

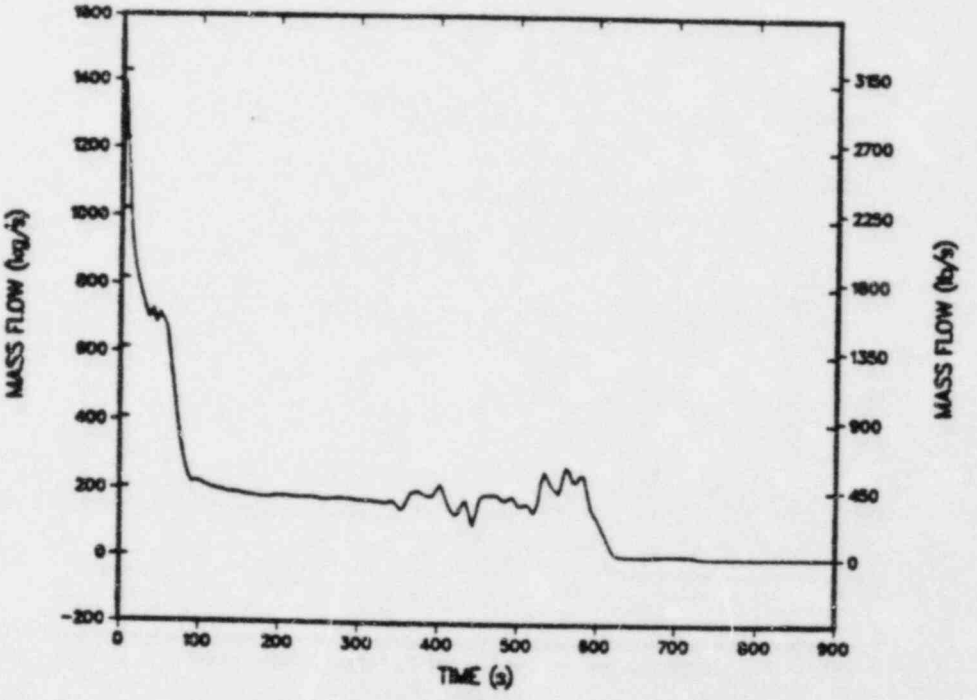

Fig. 49.
SG A steam-line flow - base case.

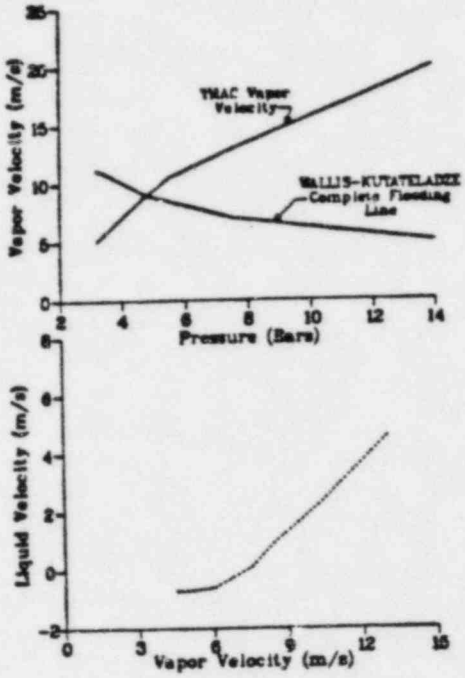

Fig. 50.
CCFL phenomena in affected steam generator (SG A) - base case.

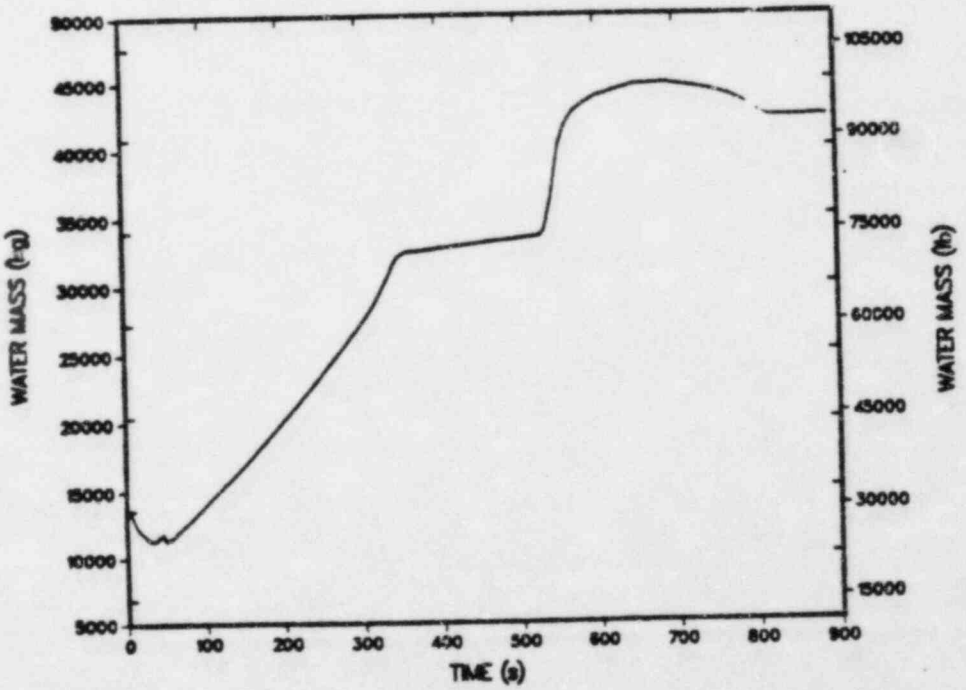

Fig. 51.
SG B secondary-side water inventory (0-900 s) - base case.

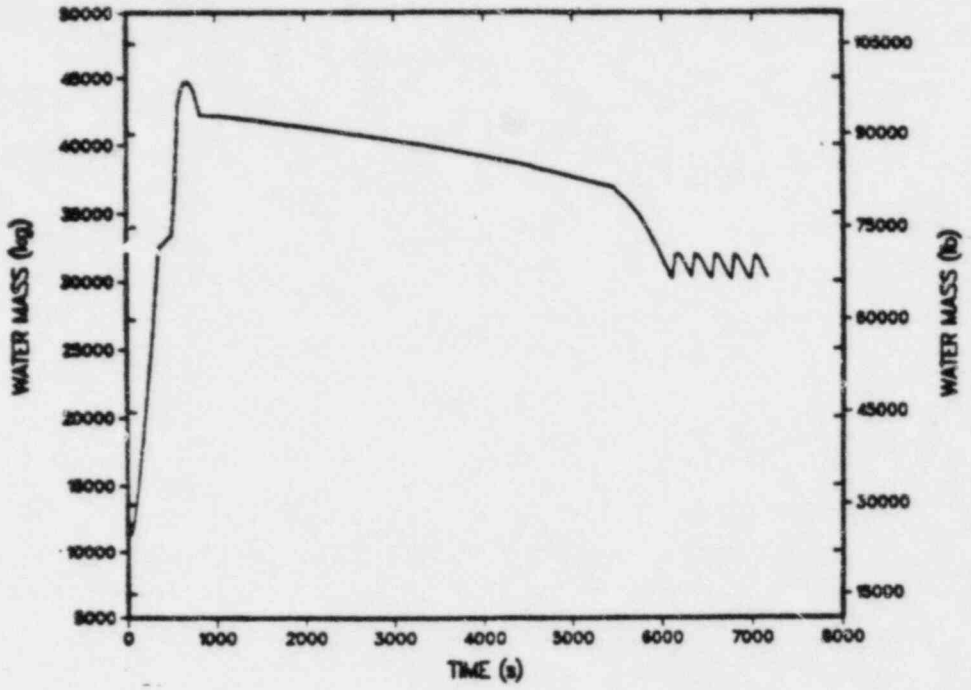

Fig. 52.
SG B secondary-side water inventory (0-7200 s) - base case.

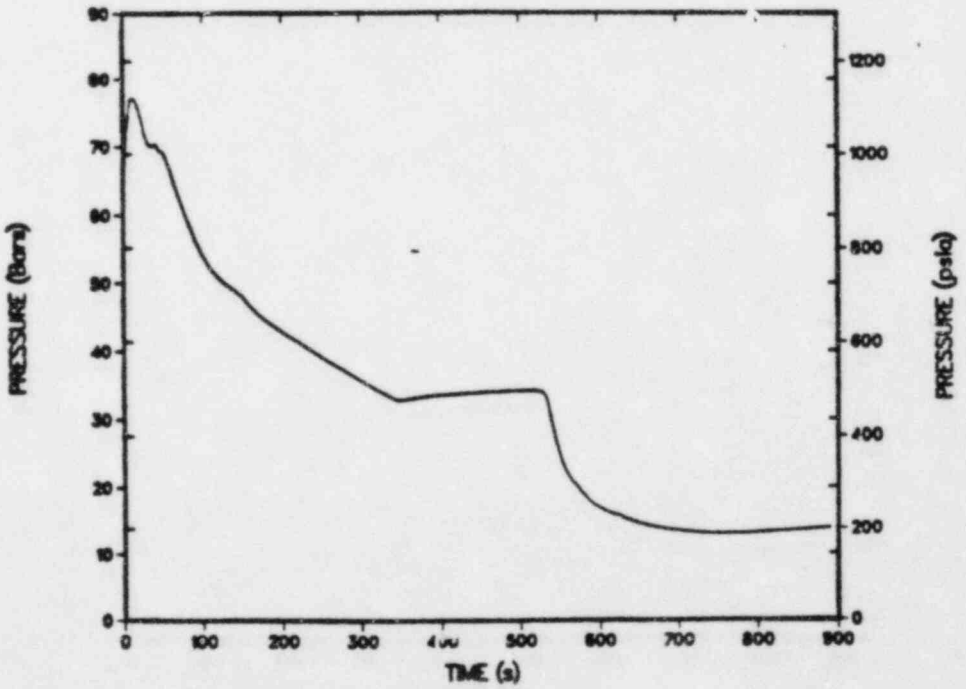

Fig. 53.
SG B secondary-side pressure (0-900 s) - base case.

essentially constant at the 50% level until the RCPs were restarted at ~526 s. After the RCPs were restarted, the SG B primary-side liquid temperatures decreased below the secondary-side temperatures and secondary-to-primary heat transfer occurred. The steam in the top regions of the secondary side began to condense on the SG tubes, and the liquid level began to rise (Fig. 51). The level rose until the SGs were isolated at 600 s. The secondary-side liquid level then remained at approximately 90% of the operating range until SG B was restored at 900 s. After 900 s, the water inventory slowly decreased (Fig. 52) because all of the primary-system energy removal occurred through SG B after this time (no EFW to SG A after 600 s). At ~6121 s the SG B secondary-side level decreased to 50% of the operating range, and EFW was initiated. For the remainder of the transient, the EFW was controlled to maintain the 50% operating-range level.

The SG B secondary-side pressure history is shown in Figs. 53 and 54. Initially the pressure was controlled at the TBV setpoint (7.063 MPa) following closure of the TSV in the loop-B steam line. The pressure then began to decrease after EFW was initiated following the low-level limit trip at ~50 s. The pressure continued to decrease because of condensation from the cold EFW until the 50% operating-range level was reached at ~350 s and EFW was terminated. The pressure remained essentially constant at ~3.5 MPa until the RCPs were restarted at ~526 s. After this time, as discussed previously, condensation of the steam in the secondary side on the SG tubes because of secondary-to-primary heat transfer caused the pressure to decrease further to ~1.5 MPa. The pressure remained at ~1.5 MPa until ~900 s. After SG B was restored at 900 s, the secondary-side pressure increased slowly (Fig. 54) until the TBV setpoint was reached at ~5462 s. The TBV system maintained the TBV setpoint pressure for the remainder of the transient.

Figures 55 through 61 show some details in other important components in the secondary side. The MFW pump speed is shown in Fig. 55 and the MFW liquid temperatures are shown in Fig. 51. The MFW pump tripped on low-suction pressure at ~48 s. The loop-A MFW liquid temperature (Fig. 56) essentially followed the saturation temperature corresponding to the SG A secondary-side pressure; thus this temperature was much cooler than for SG B. Figure 57 shows the MFW mass flows into each SG. It is seen that the MFW flow to SG A was much higher than to SG B because of the lower back pressure in SG A. The EFW flows to each SG are shown in Fig. 58. EFW was started at ~30 s to SG A and at ~50 s to SG B. Again, because of the low secondary pressure in SG A, more EFW flow was directed to that steam generator. At ~350 s, the EFW valve to SG B was shut (50% level

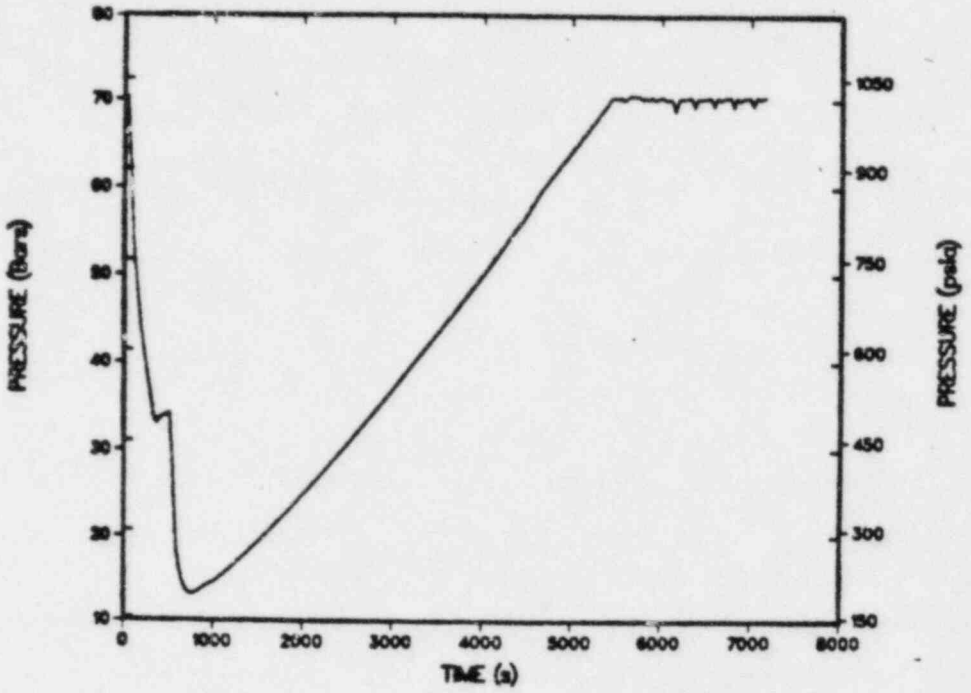

Fig. 54.
SG B secondary-side pressure (0-7200 s) - base case.

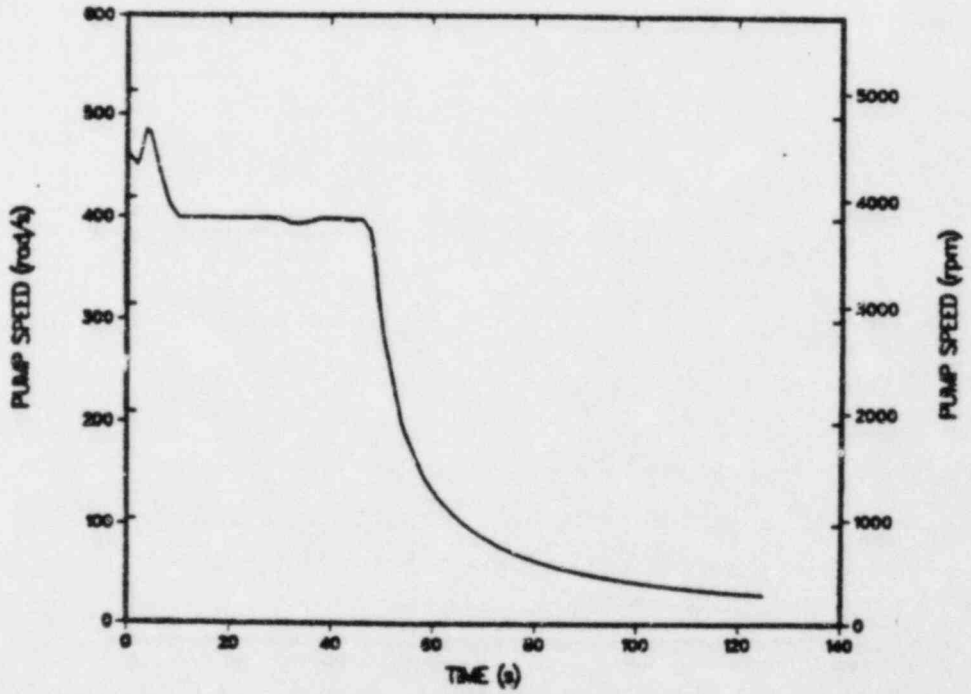

Fig. 55.
MFW pump speed - base case.

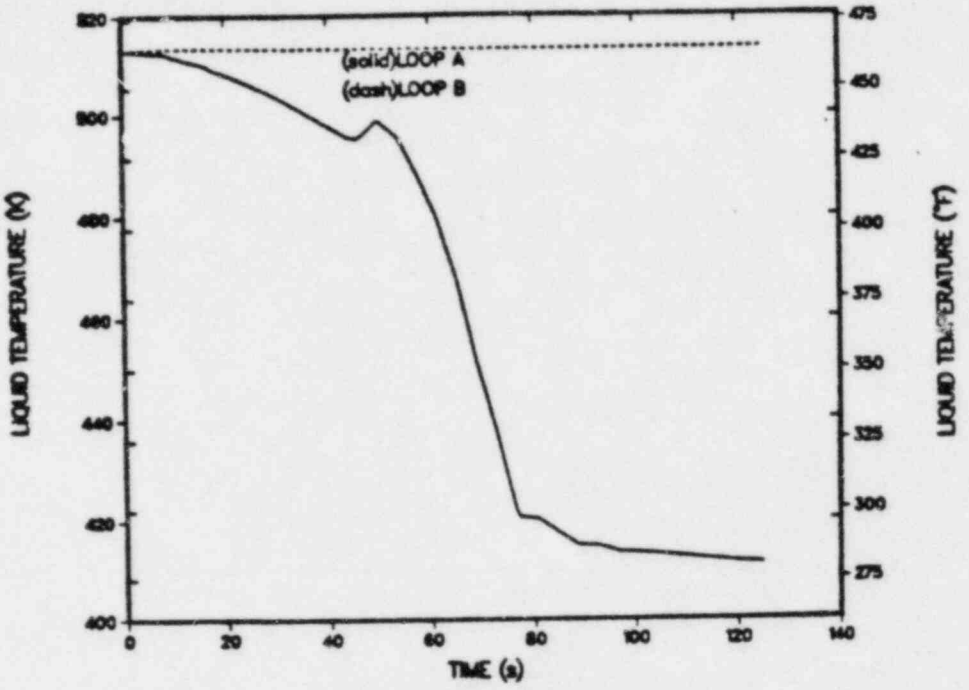

Fig. 56.
MFW liquid temperature - base case.

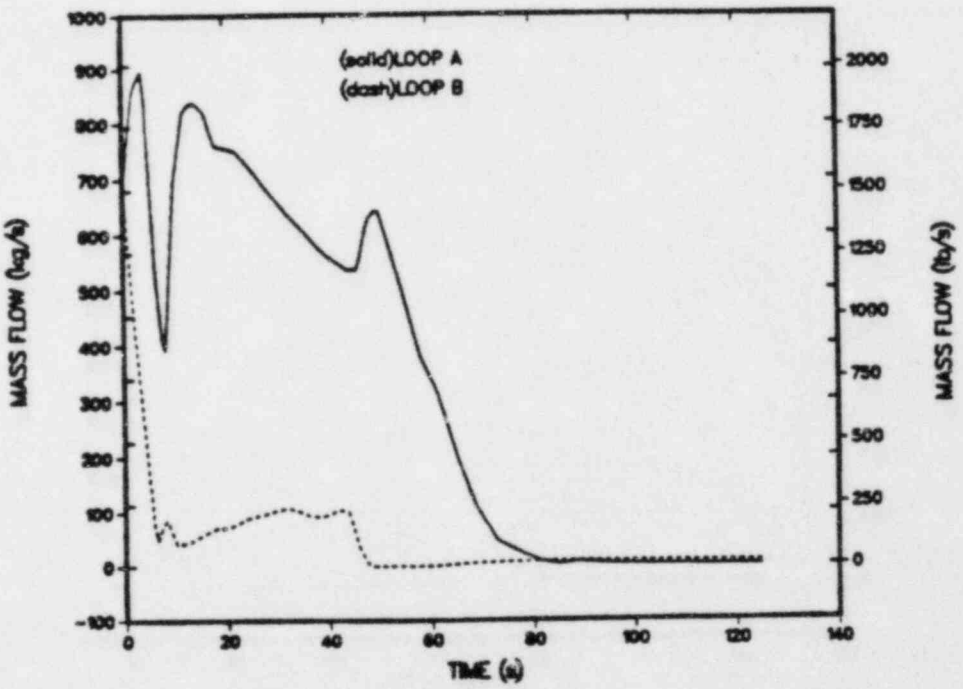

Fig. 57.
MFW mass flows - base case.

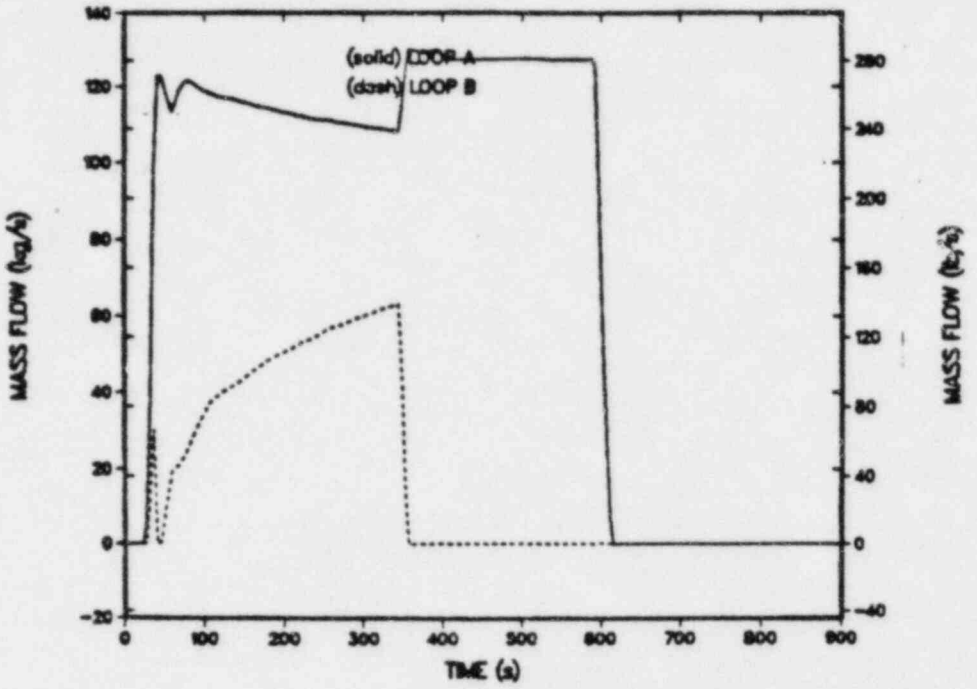

Fig. 58.
EFW mass flows (0-900 s) - base case.

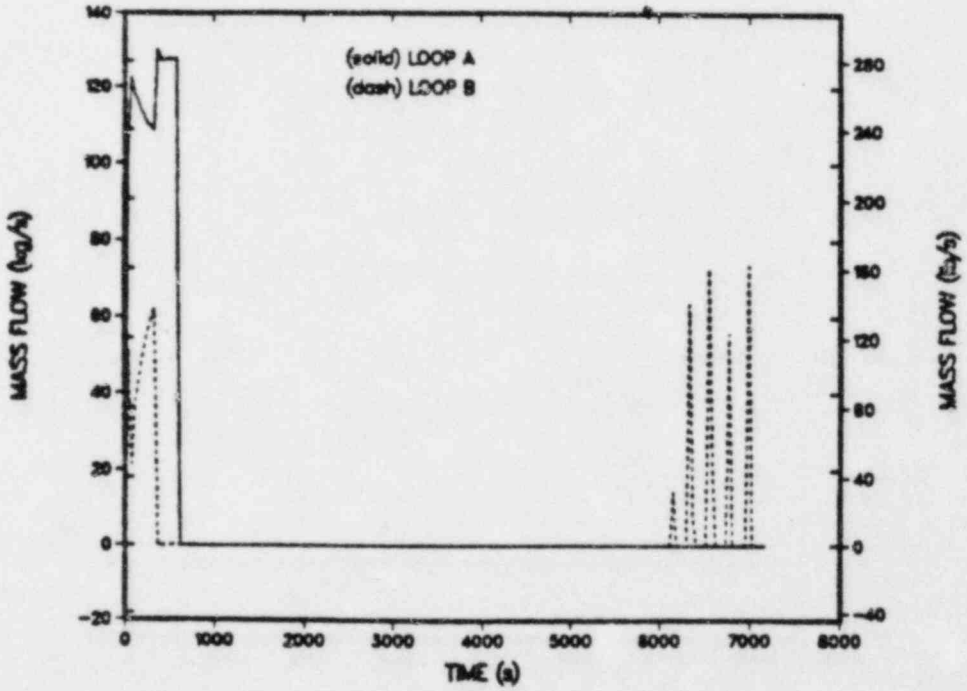

Fig. 59.
EFW mass flows (0-7200 s) - base case.

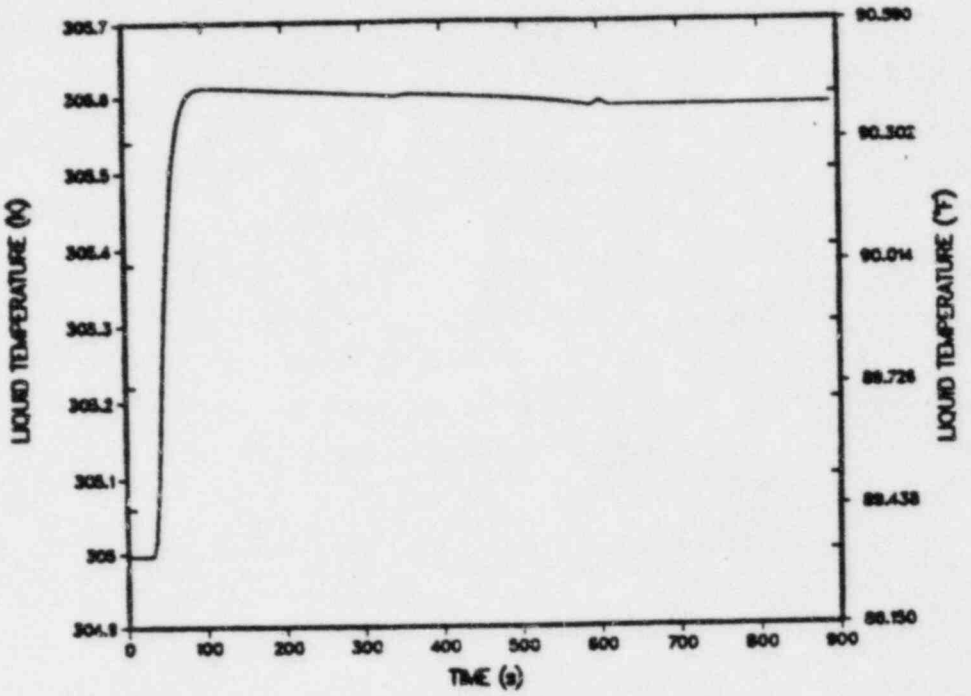

Fig. 60.
EFW liquid temperature at pump discharge - base case.

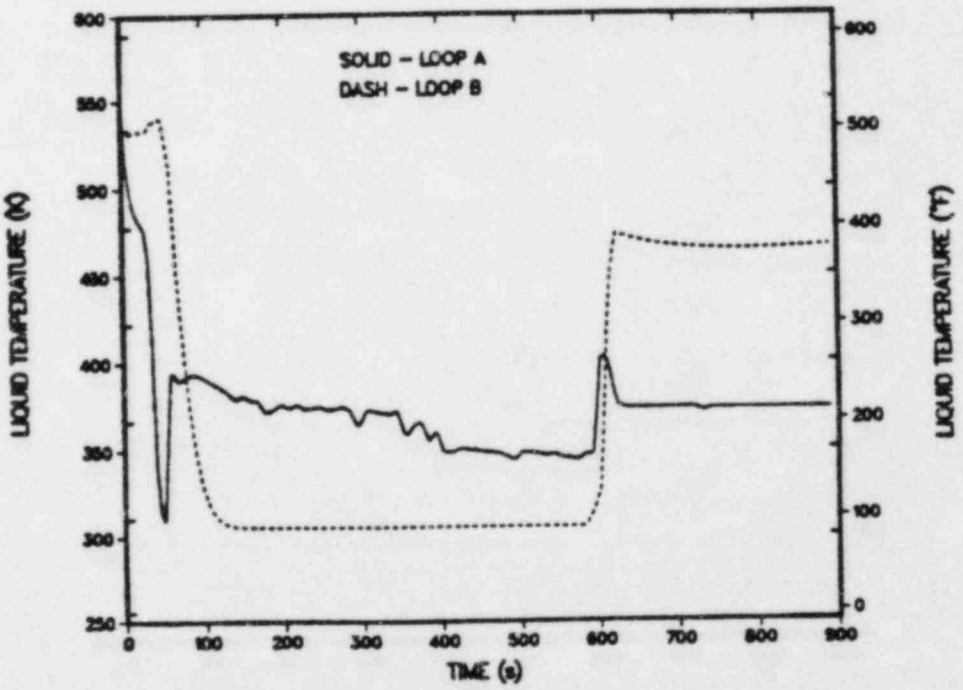

Fig. 61.
EFW liquid temperatures at injection locations - base case.

in SG B reached), and all of the EFW was directed to SG A. At 600 s the SGs were isolated, and the EFW pump was tripped off. Figure 59 shows that at ~6121 s, EFW was initiated again to SG B after the level had dropped below 50% of the operating range. The EFW temperature at the pump discharge is shown in Fig. 60, and the EFW temperatures at each injection point are shown in Fig. 61.

Other key system parameters are shown in Figs 62 through 66. The HPI flows are shown in Figs. 62 and 63 for loops A and B respectively. HPI was initiated at ~21 s and was terminated at ~526 s after the subcooling margin in the primary system was reached. Figures 64 and 65 show the accumulator water levels and fluid volumes discharged into the primary system. The accumulator pressure setpoint of 4.17 MPa was reached at ~530 s and the accumulators operated for ~8 s. Approximately 2 m^3 of accumulator liquid was discharged into the primary system. Figure 66 shows the PORV mass-flow history. The PORV setpoint of 16.9 MPa was not reached until ~4678 s, and the PORV then cycled for the remainder of the transient to maintain the primary-system pressure at or below the setpoint.

b. Parametric case - Case 2. This case was identical to the base case (Case 1) except the EFW system did not actuate as intended because of input modeling errors. All of the other systems functioned as designed in Case 2 including the subcooling-monitoring system. The sequence of events calculated for Case 2 is given in Table XVII. The events that occurred during the first 54 s were approximately the same as those calculated for the base case (except that the EFW system did not actuate). At ~400 s, the RCPs were restarted after the 42 K subcooling margin was reached. Also at this time, the HPI was throttled. At 600 s the SGs were isolated, and at 900 s the calculation was terminated.

The primary-system pressure is shown in Fig. 67. The pressurizer water level is shown in Fig. 68. The minimum pressure calculated was ~5.0 MPa and occurred at ~175 s. After natural-circulation flows were established (~150 s), the primary system began to repressurize (Fig. 68), and the repressurization continued for the remainder of the transient. The slope of the pressure curve changed after the RCPs were restarted at ~400 s because of forced circulation and enhanced heat transfer through the unaffected steam generator (SG B). The pressurizer completely emptied by ~40 s and began to refill after the primary system began to heat up because of fluid expansion. After the HPI was throttled at ~400 s, the pressurizer water level rise was terminated (Fig. 68). After the SGs were isolated at 600 s, the pressurizer water level began to increase again because of fluid expansion.

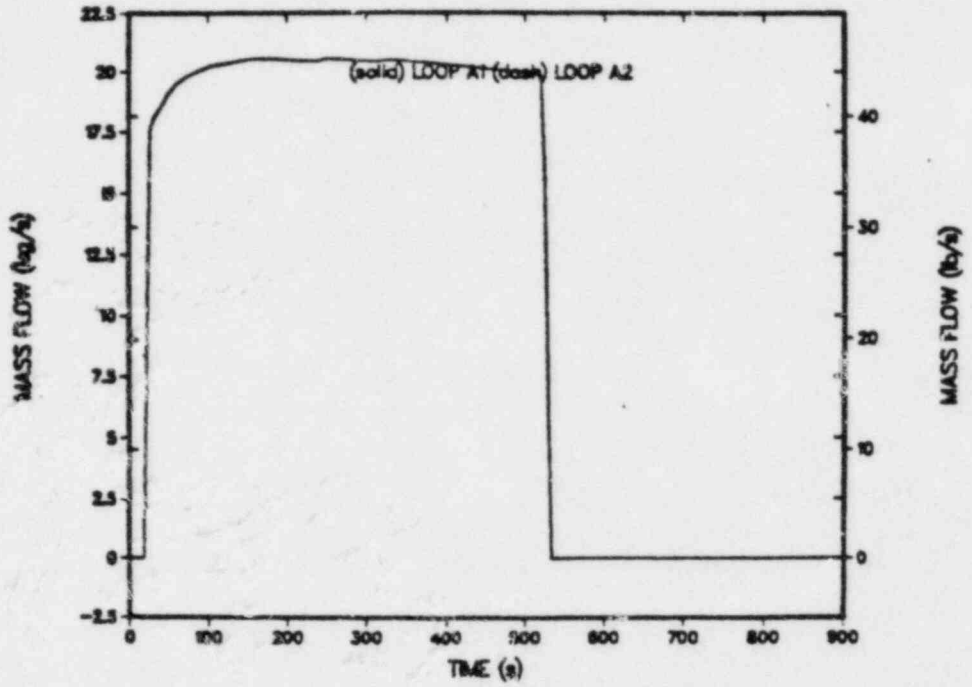

Fig. 62.
Loop-A HPI flows - base case.

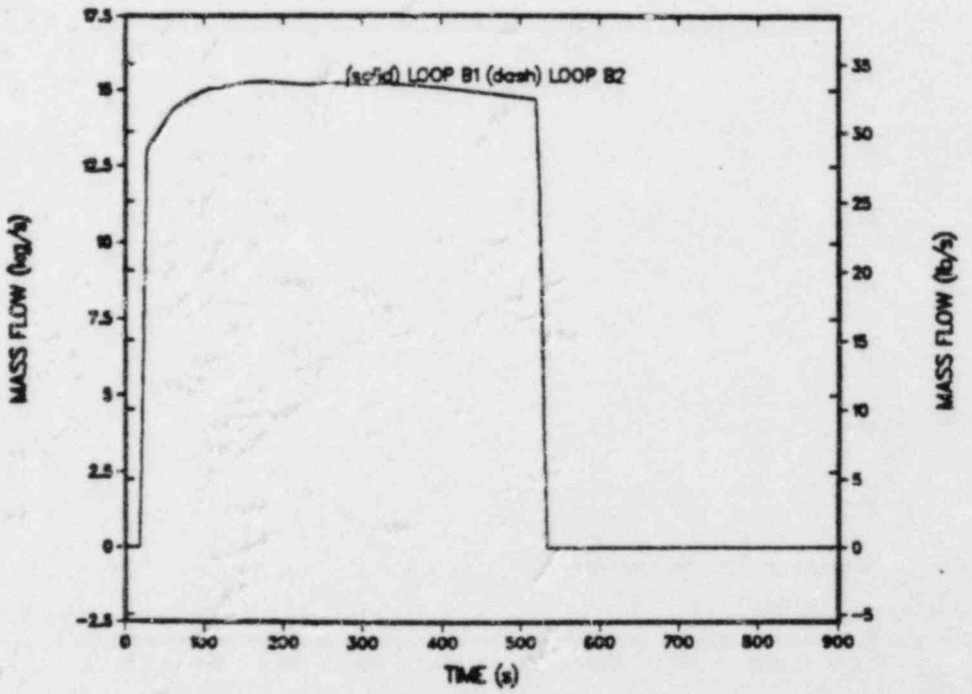

Fig. 63.
Loop-B HPI flows - base case.

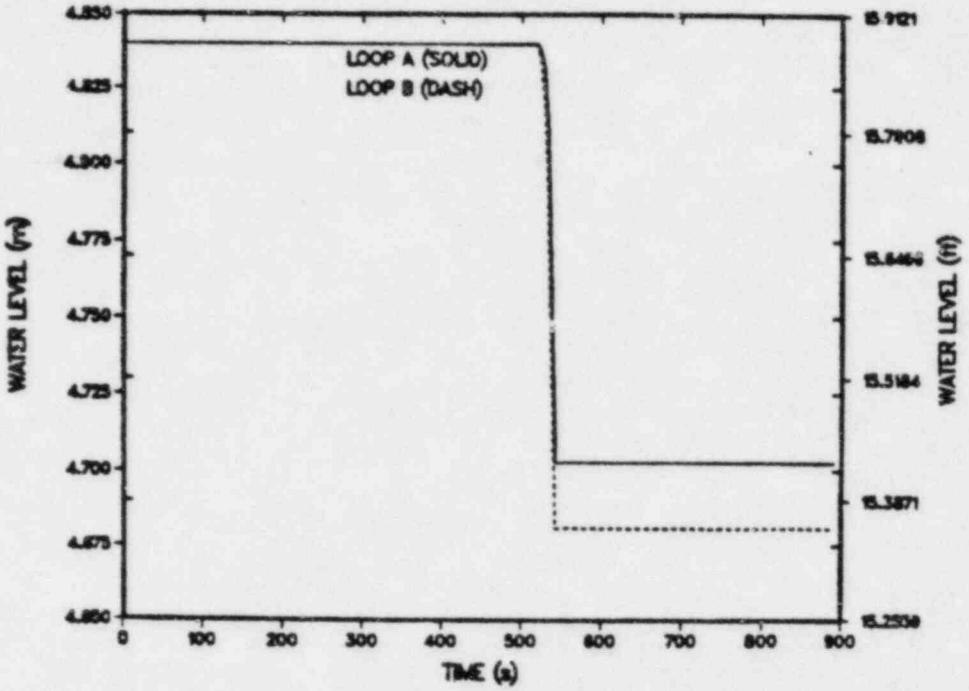

Fig. 64.
Accumulator water levels - base case.

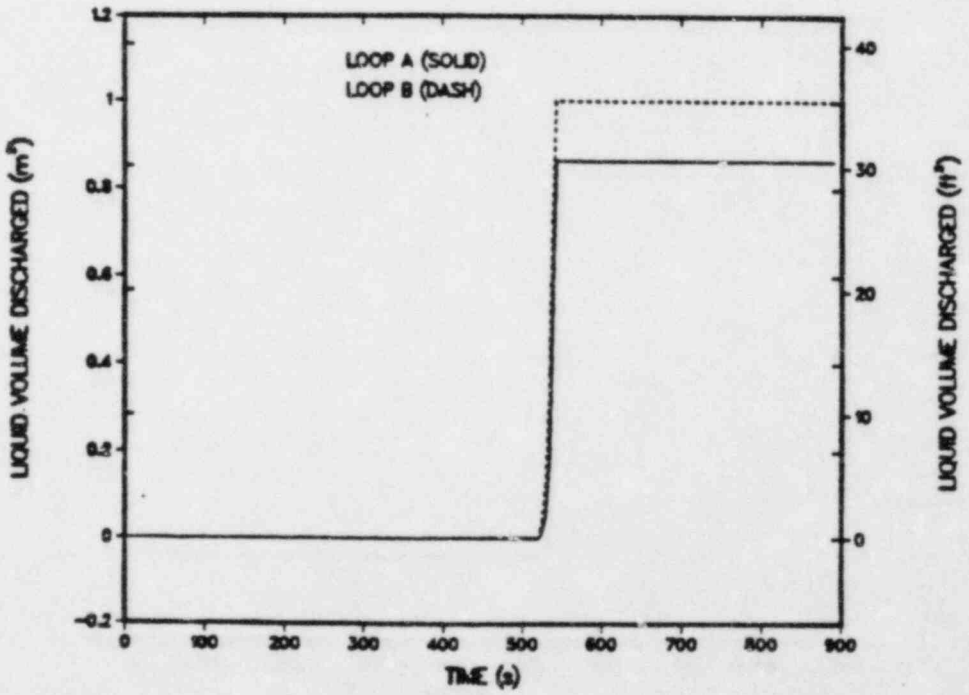

Fig. 65.
Accumulator liquid volume discharged - base case.

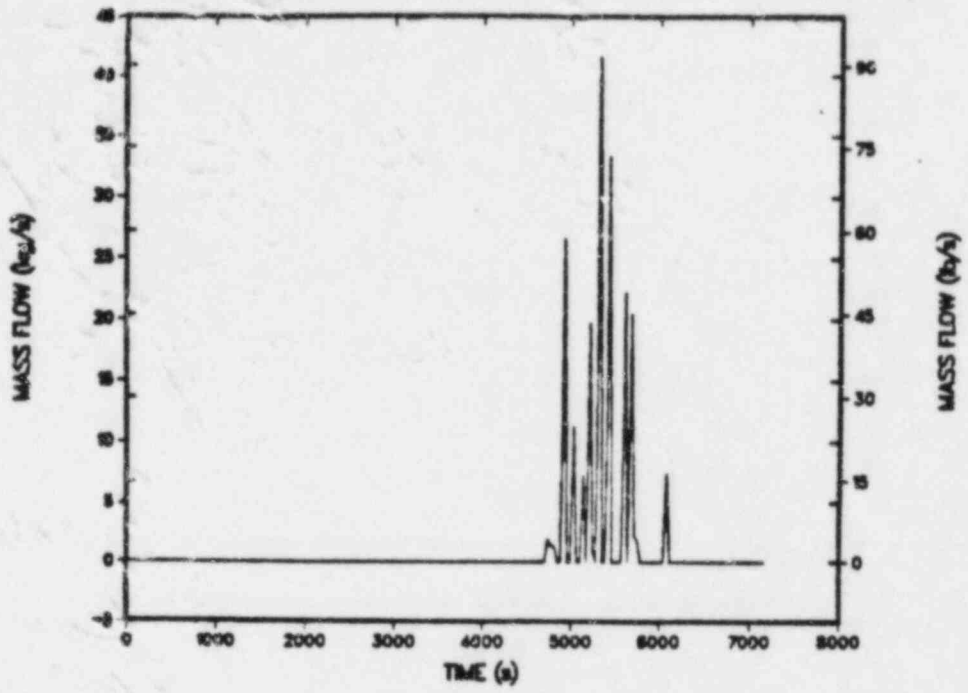

Fig. 66.
PORV mass flow - base case.

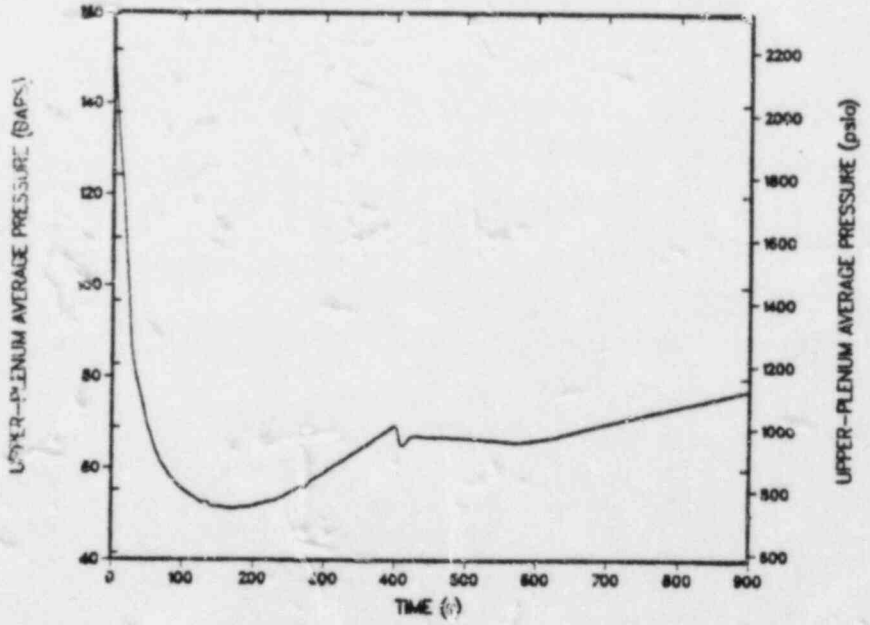

Fig. 67.
Pressurizer pressure - Case 2.

TABLE XVII

MSLB[a] (Case 2)
SEQUENCE OF EVENTS

EVENT		TIME(s)
1-14.	Approximately same as base case	0-53.9
15.	RCP's (A1, B1) restart (42 K subcooling reached); HPI throttled	400.6
16.	SG A, B isolated	600.0
17.	Calculation terminated	900.0

[a]EFW pump never started

Figure 69 shows the downcomer fluid temperatures near the cold-leg connections in the vessel. The minimum downcomer fluid temperature calculated was ~475 K and occurred when the RCPs were restarted at ~400 s. Asymmetrical fluid temperatures in the downcomer were calculated in Case 2 similar to the base case with the colder temperatures calculated for the loop-A side of the downcomer.

Figure 70 shows the hot-leg mass flows for Case 2 and Fig. 71 shows the candy-cane void fractions. Natural-circulation flows were calculated after the RCPs coasted down at ~150 s. The natural-circulation flow in loop A was much higher than in loop B because of the enhanced heat transfer through the affected steam generator. At ~400 s the RCPs (A1, B1) were restarted and forced circulation through the primary system was calculated. Figure 71 shows that the loop-B candy cane voided soon after loss of forced circulation in loop B (~150 s). The candy cane remained voided until the RCPs were restarted. The loop-A candy cane voided for a brief period after the SGs were isolated at ~600 s (Fig. 71).

The cold-leg loop flows for loops A and B are shown in Figs. 72 and 73 respectively. These flows were similar to those calculated for the base case, except that the loop-A flows were somewhat higher in the base case. The cold-leg temperatures in each cold leg are shown in Figs. 74 and 75. The minimum liquid temperature calculated in loop A was ~475 K, and the minimum temperature in loop B was ~400 K. It is interesting to note that in Case 2 the

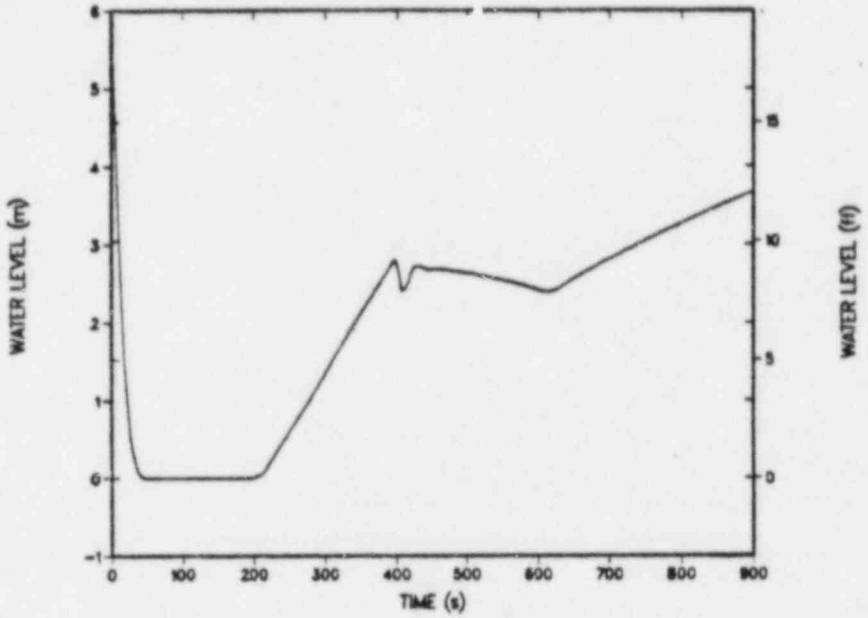

Fig. 68.
Pressurizer water level - Case 2.

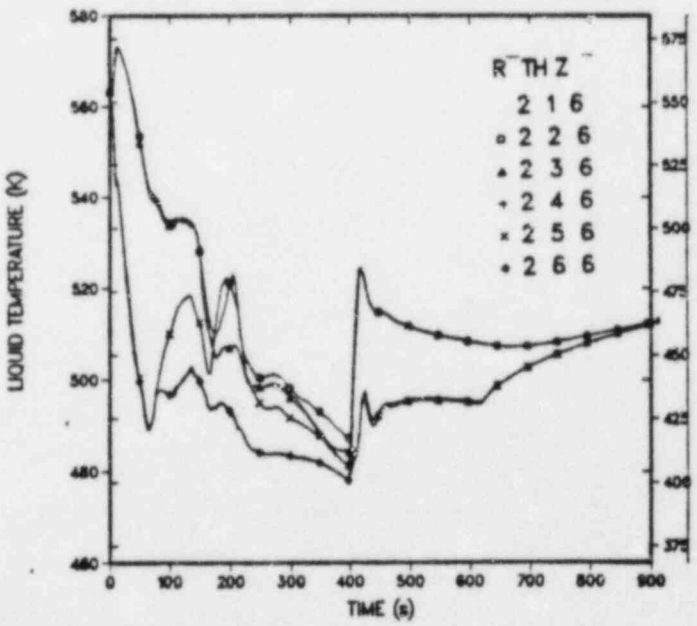

Fig. 69.
Downcomer liquid temperatures at vessel axial level 6 (all azimuthal sectors) - Case 2.

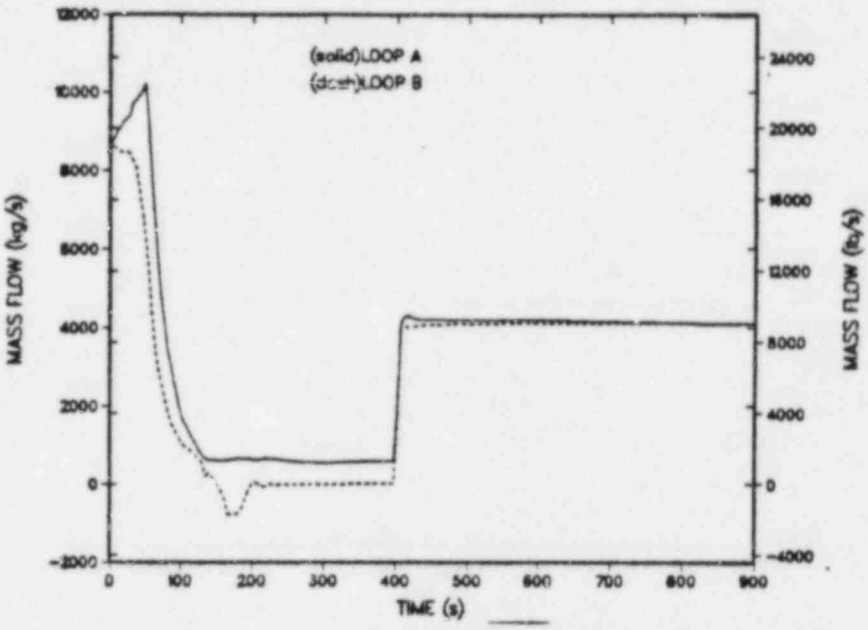

Fig. 70.
Hot-leg mass flows - Case 2.

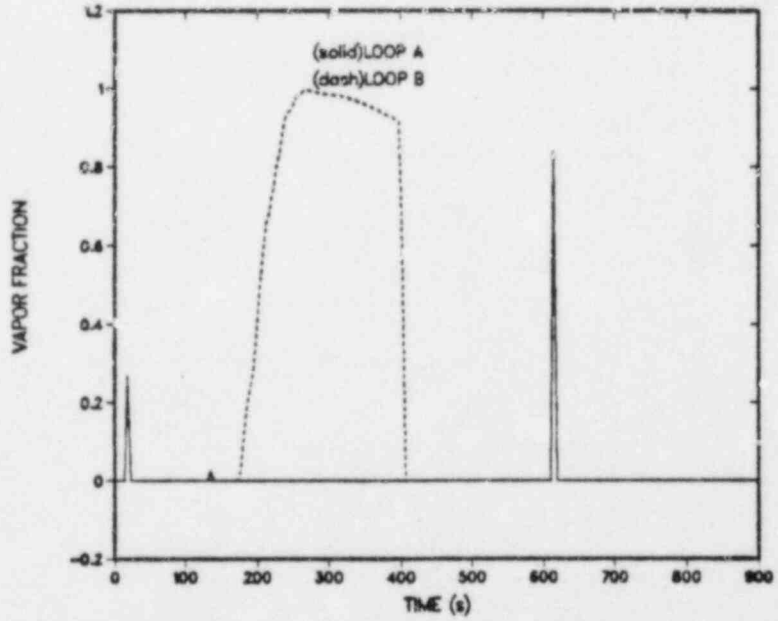

Fig. 71.
Candy-cane void fractions - Case 2.

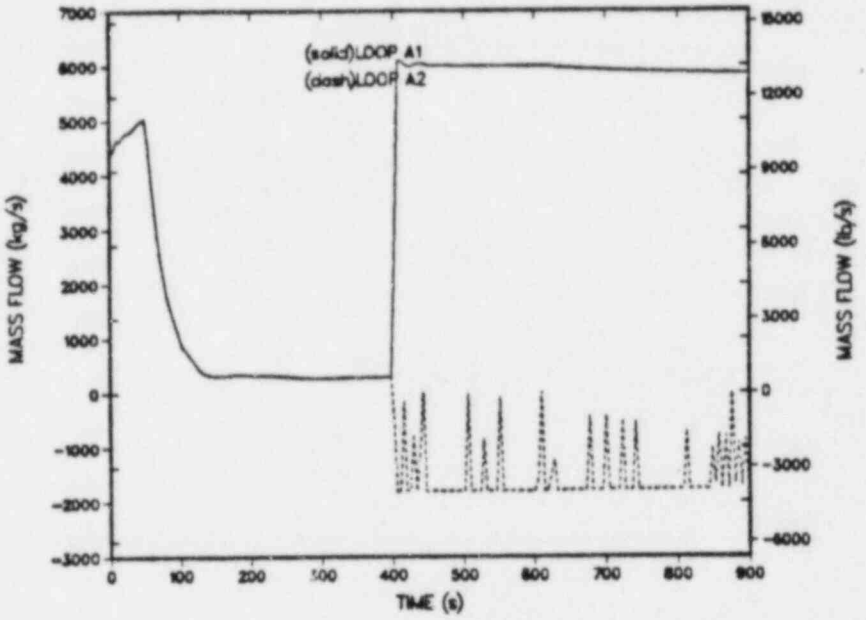

Fig. 72.
Loop-A cold-leg mass flows - Case 2.

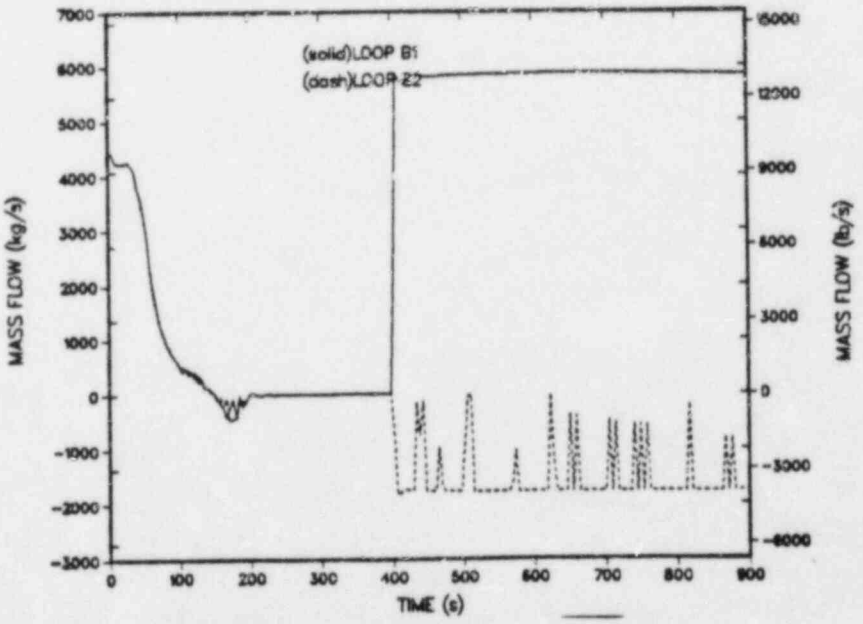

Fig. 73.
Loop-B cold-leg mass flows - Case 2.

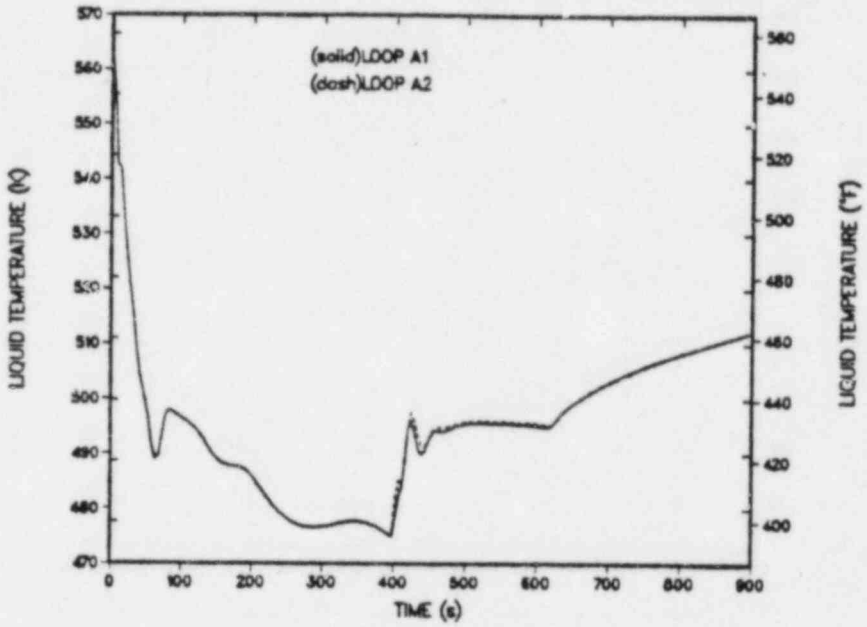

Fig. 74.
Loop-A cold-leg liquid temperatures - Case 2.

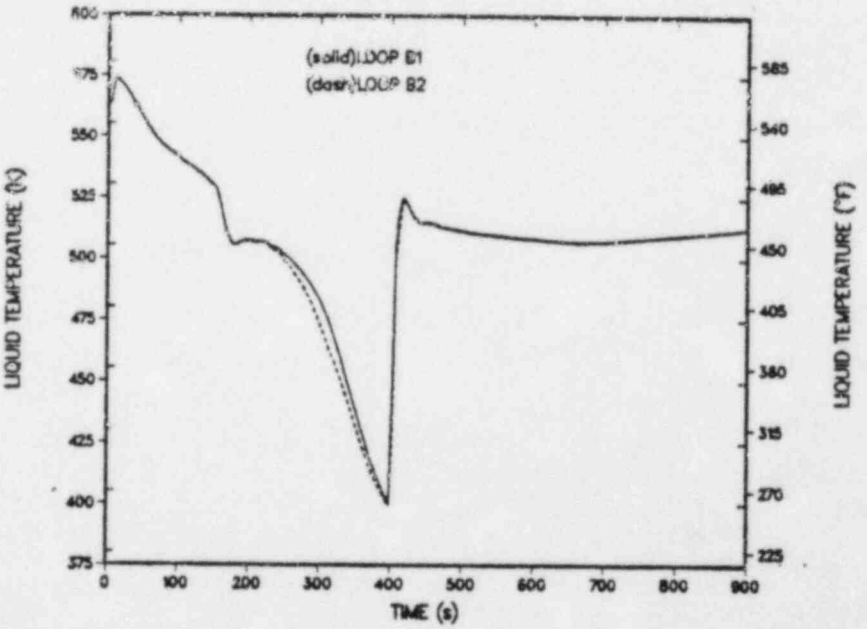

Fig. 75.
Loop-B cold-leg liquid temperatures - Case 2.

loop-B cold-leg temperatures were colder than loop A; however this was not true in the base case. The reason for this is because the EFW system was operational in the base case and caused the loop-A cold-leg temperatures to be less than loop B.

Details of key steam-generator parameters are shown in Figs. 76 through 80. Figure 76 shows the secondary-side water inventory for SG A. Because the EFW system did not work and because the MFW pump tripped at ~50 s, the inventory in SG A was depleted by ~100 s and never recovered. The associated secondary-side pressure in SG A is shown in Fig. 77. By ~85 s, SG A had depressurized to essentially atmospheric pressure. The steam-line flow out the broken steam line is shown in Fig. 78. Figure 79 shows the SG B secondary-side water inventory, and Fig. 80 shows the secondary-side pressure in SG B. Because of secondary-to-primary side heat transfer in SG B, condensation of the steam caused the SG B water inventory to increase and the pressure to decrease. The condensation effect increased after the RCPs were restarted at ~400 s because the heat-transfer rate from the secondary to the primary increased.

Other system parameters are shown in Figs. 81 and 82. The MFW pump was tripped at ~50 s on low-suction pressure, and the feedwater flow decayed to zero by ~150 s. Figure 82 shows the HPI flows into each cold leg. At ~400 s the HPI was throttled after adequate subcooling was reached in the loops.

c. Parametric case - Case 3. Parametric Case 3 was identical to Case 2 except that the RCPs did not restart as intended because of input errors. Another significant difference between Case 3 and Case 2 is that the MFW pump did not trip until ~330 s in Case 3 because of errors in the ICS modeling. Because the MFW pump did not trip until late in the transient, this calculation can be considered as a MSLB with run-away main feedwater. The sequence of events calculated for Case 3 is given in Table XVIII. The events that occurred during the first 54 s were approximately the same as the base case except that the EFW system did not actuate, and the MFW pump did not trip until much later. At ~330 s, the MFW pump was tripped because of a high water level in SG B. At ~356 s the HPI was throttled after the 42 K subcooling margin was reached. The RCPs failed to restart at this time. At ~465 s the HPI was turned back on again because the 42 K subcooling margin was lost. At 600 s the SGs were isolated, and at ~693 s the HPI was again throttled. The calculation was terminated at 1260 s.

The primary-system pressure is shown in Fig. 83, and the pressurizer water level is shown in Fig. 84. The minimum pressure calculated was ~5.5 MPa and occurred at ~125 s. After natural-circulation flows were established (~150 s),

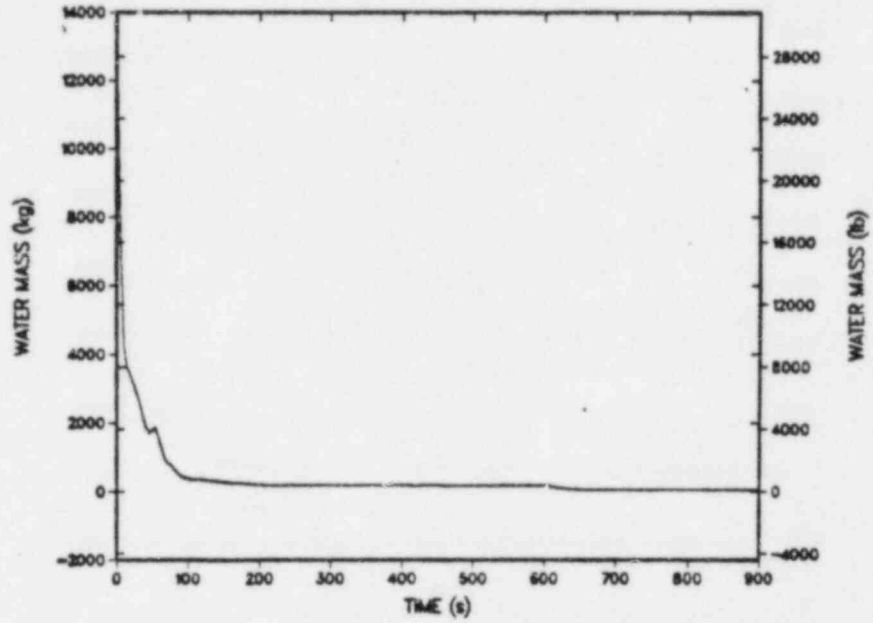

Fig. 76.
SG A secondary-side water inventory - Case 2.

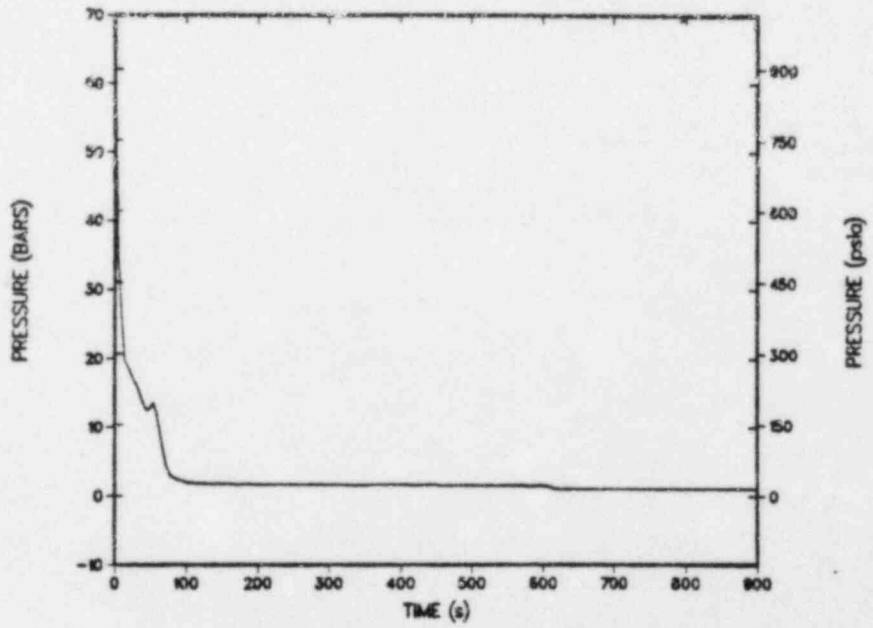

Fig. 77.
SG A secondary-side pressure - Case 2.

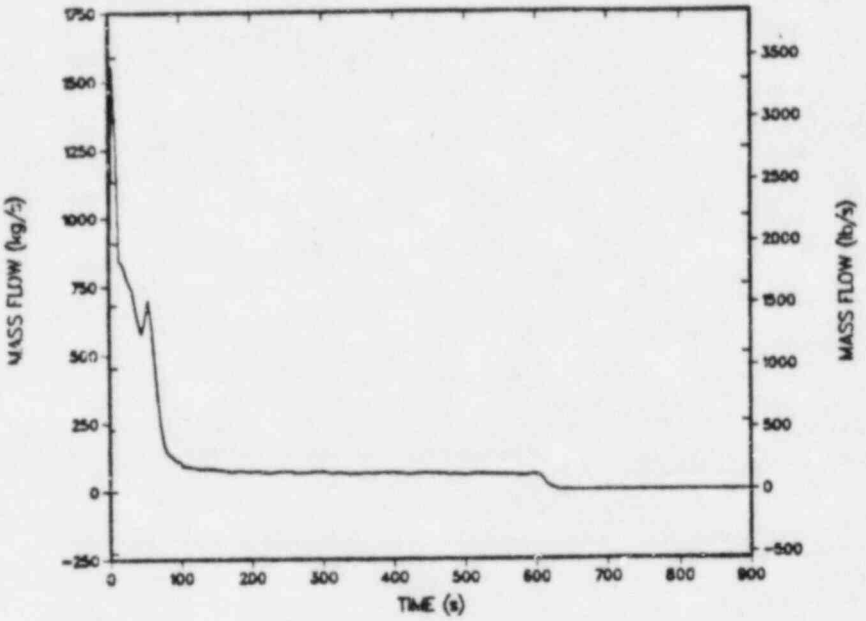

Fig. 78.
SG A steam-line flow - Case 2.

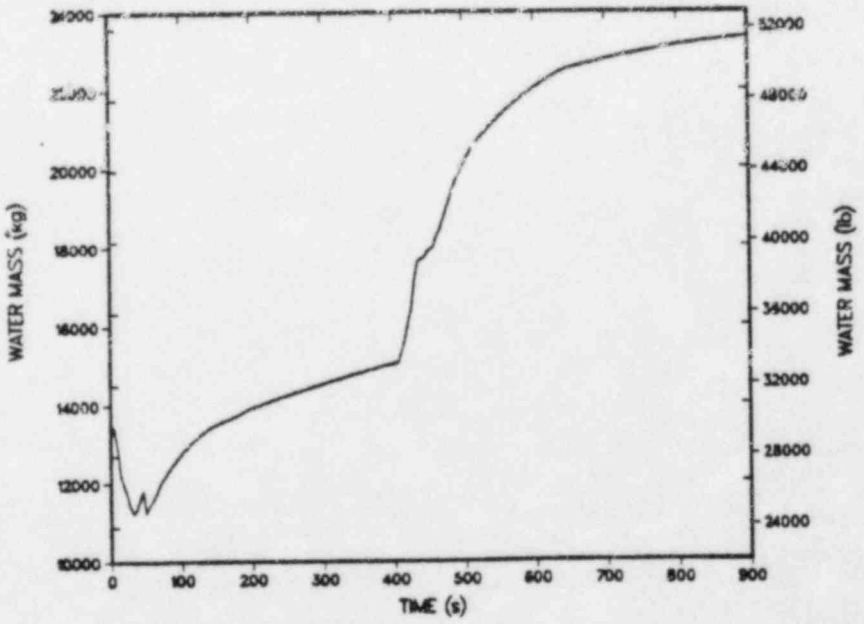

Fig. 79.
SG B secondary-side water inventory - Case 2.

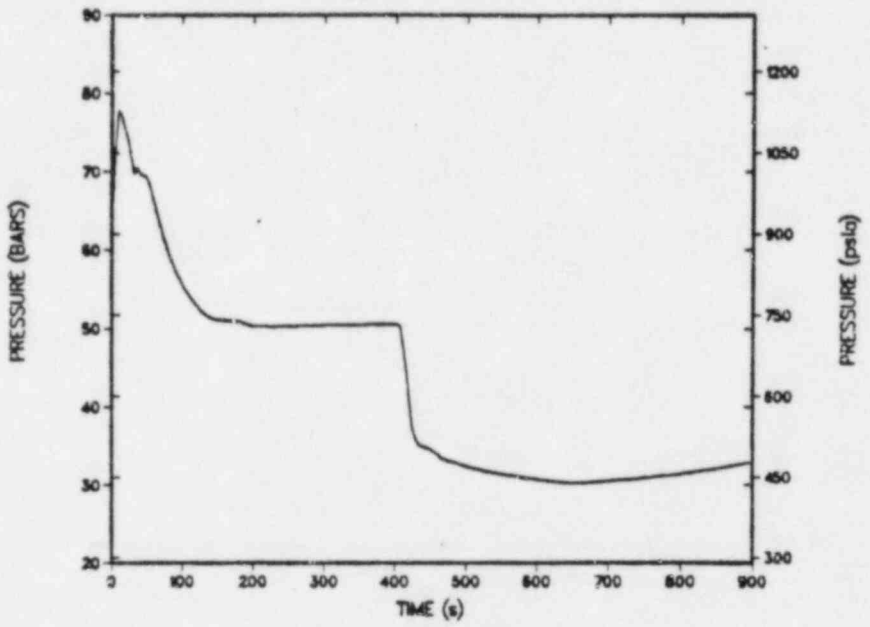

Fig. 80.
SG B secondary-side pressure - Case 2.

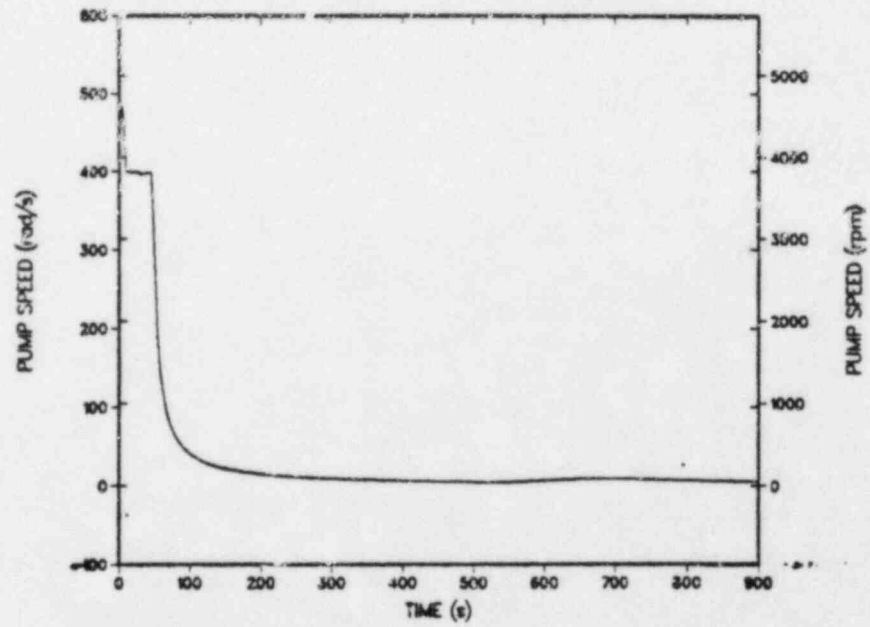

Fig. 81.
MFW pump speed - Case 2.

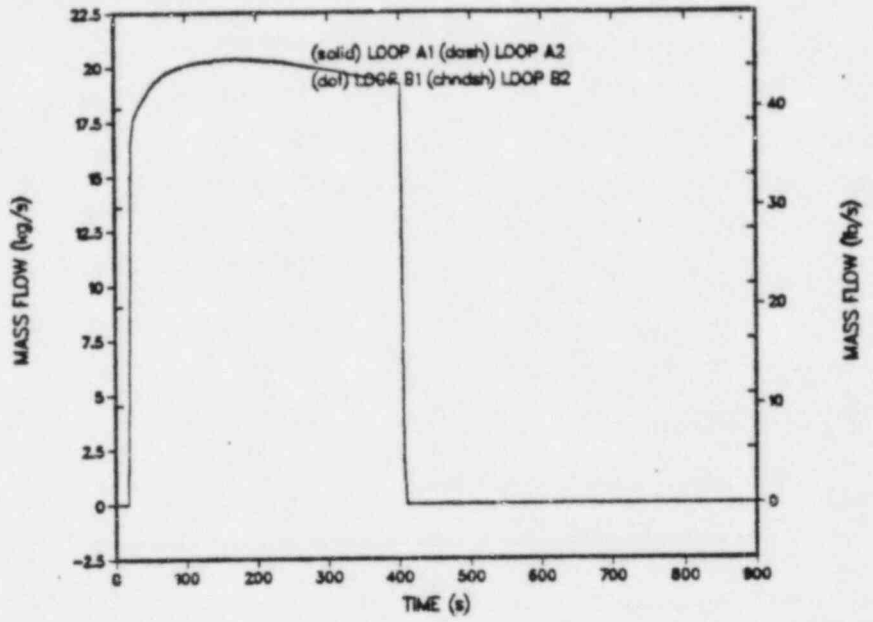

Fig. 82.
HPI flows - Case 2.

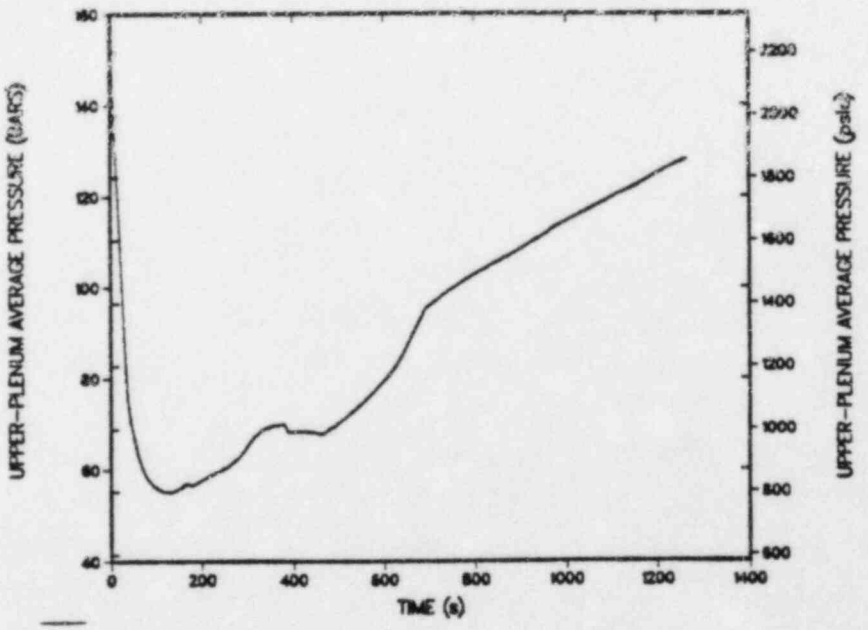

Fig. 83.
Pressurizer pressure - Case 3.

the primary system began to repressurize (Fig. 83), and the repressurization continued for the remainder of the transient. The slope of the pressure curve changed dramatically at ~470 s and again at ~700 s because the HPI was turned on at ~465 s and throttled again at ~693 s (Table XVIII). The primary system repressurized more than in Case 2 because the RCPs were not restarted, and natural-circulation flows existed for most of the transient. The pressurizer completely emptied by ~30 s and began to refill at ~175 s after the primary system began to repressurize. The pressurizer water level decrease at ~350 s and subsequent increase at ~460 s can be attributed to HPI throttling (Table XVIII). The change in slope in pressurizer water level at ~700 s can also be attributed to HPI throttling.

Figure 85 shows the downcomer fluid temperatures for Case 3. The minimum downcomer fluid temperature calculated was ~450 K and occurred at ~650 s. The downcomer temperatures for Case 3 were colder than for Case 2 because of the run-away MFW flow. Asymmetrical temperatures were also calculated similar to the base case. The downcomer fluid temperatures increased after ~650 s because the steam generators were isolated at 600 s.

Figure 86 shows the hot-leg mass flows for Case 3 and Fig. 87 shows the candy-cane void fractions. Natural-circulation flows were calculated in both loops after the RCPs coasted down at ~150 s. As in Case 2 and the base case, the natural-circulation flow in loop A was higher than in loop B. Natural-circulation flows continued for the remainder of the transient because the RCPs never restarted. Figure 87 shows that the candy canes in both loops never voided. The reason the candy canes never voided in Case 3 was because the MFW provided enough cooling to the loop-B SG to prevent any secondary-to-primary heat transfer as occurred in the base case and Case 2.

The cold-leg loop flows for loops A and B are shown in Figs. 88 and 89, respectively. These flows are similar to Case 2 and the base case except that the RCPs were not restarted in Case 3. Figure 88 shows that the loop-A cold legs had natural-circulation flows up until the time the SGs were isolated. These flows then decayed to approximately zero because of significant loss of heat transfer through the steam generators. The temperatures in each cold leg are shown in Figs. 90 and 91. The minimum fluid temperature calculated in loop A was ~435 K, and the minimum fluid temperature in loop B was ~445 K.

Details of important SG parameters are shown in Figs. 92 through 97. The pressures, inventories, and steam-line flows for SG A were similar to Case 2 and will not be discussed further. However, the SG A secondary-side pressures (Fig. 93) and steam-line flows (Fig. 94) for Case 3 were higher than Case 2

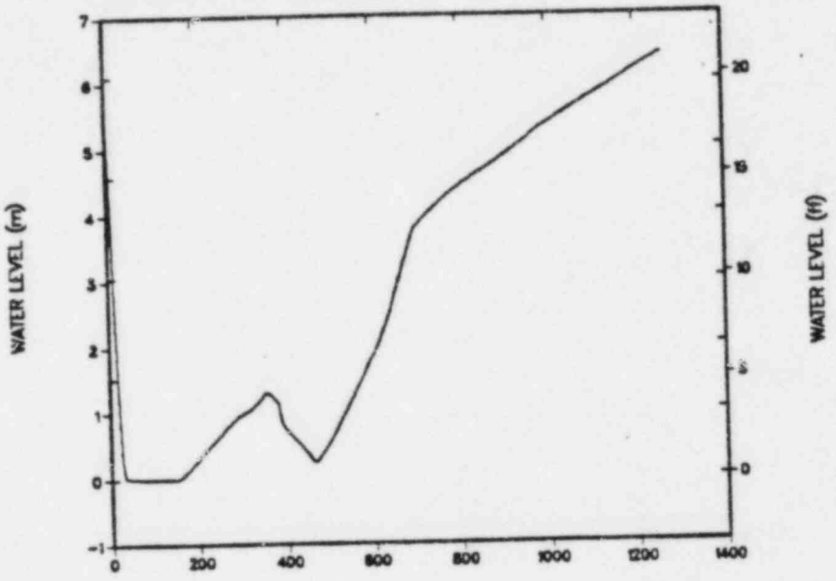

Fig. 84.
Pressurizer water level - Case 3.

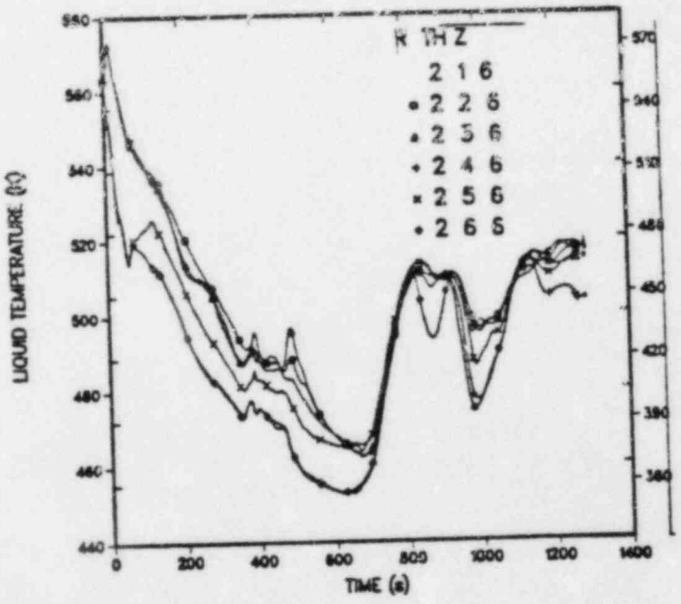

Fig. 85.
Downcomer liquid temperatures at vessel axial level 6 (azimuthal sectors) - Case 3.

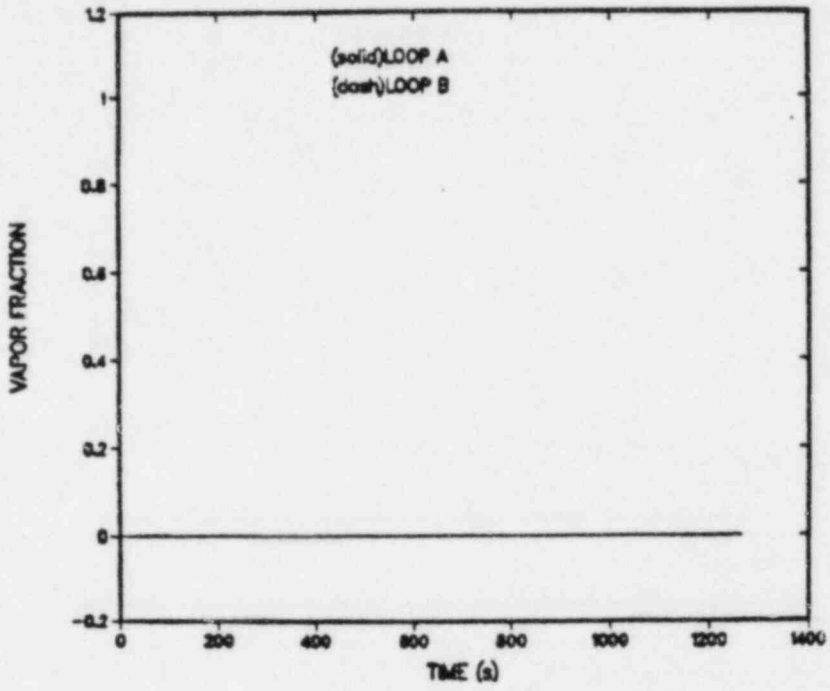

Fig. 86.
Hot-leg mass flows - Case 3.

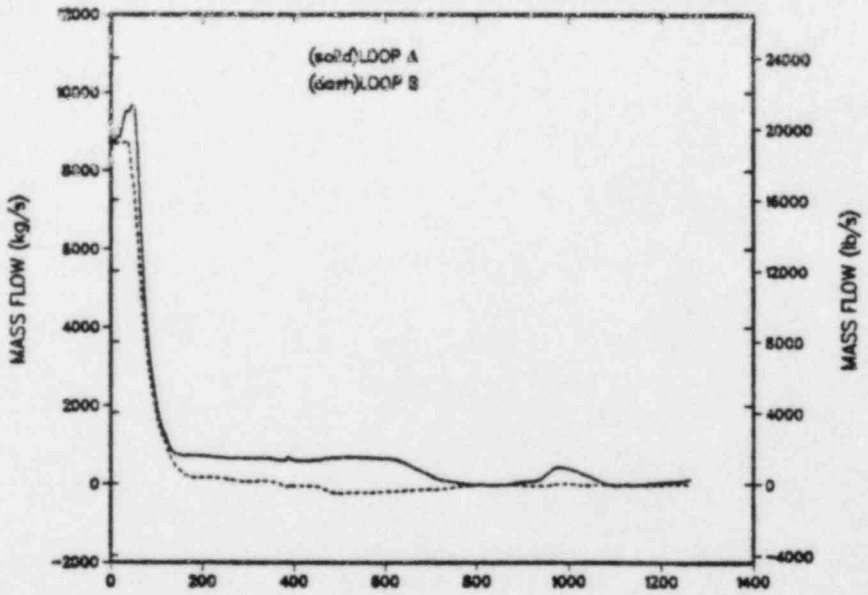

Fig. 87.
Candy-cane void fractions - Case 3.

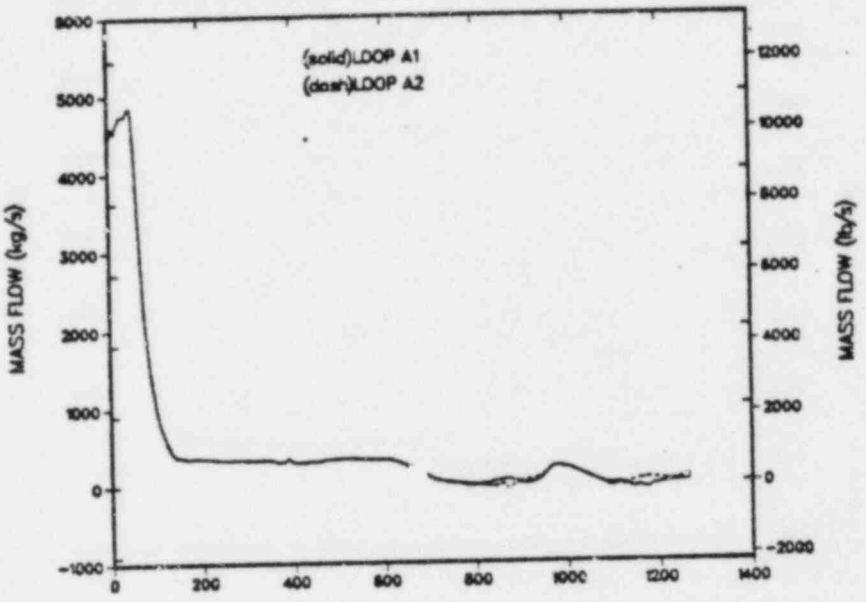

Fig. 88.
Loop-A cold-leg mass flows - Case 3.

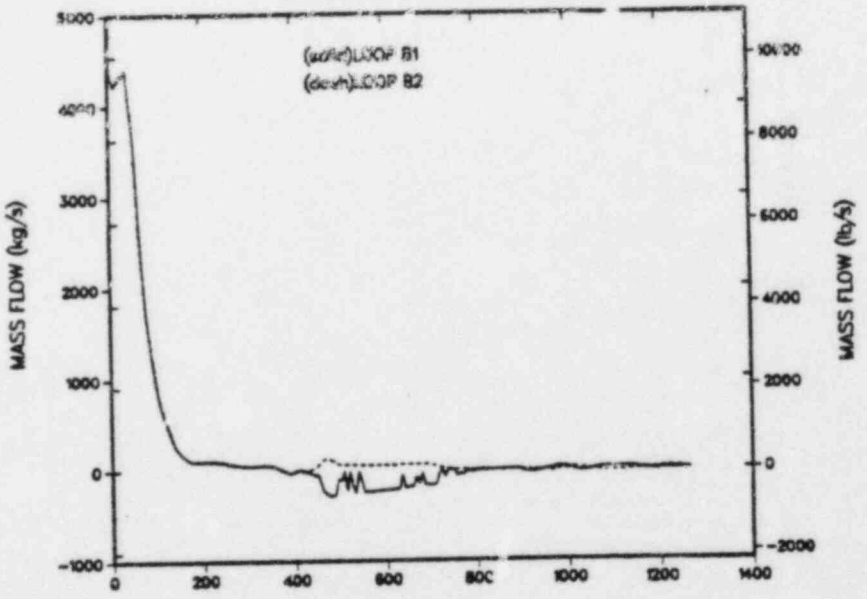

Fig. 89.
Loop-B cold-leg mass flows - Case 3.

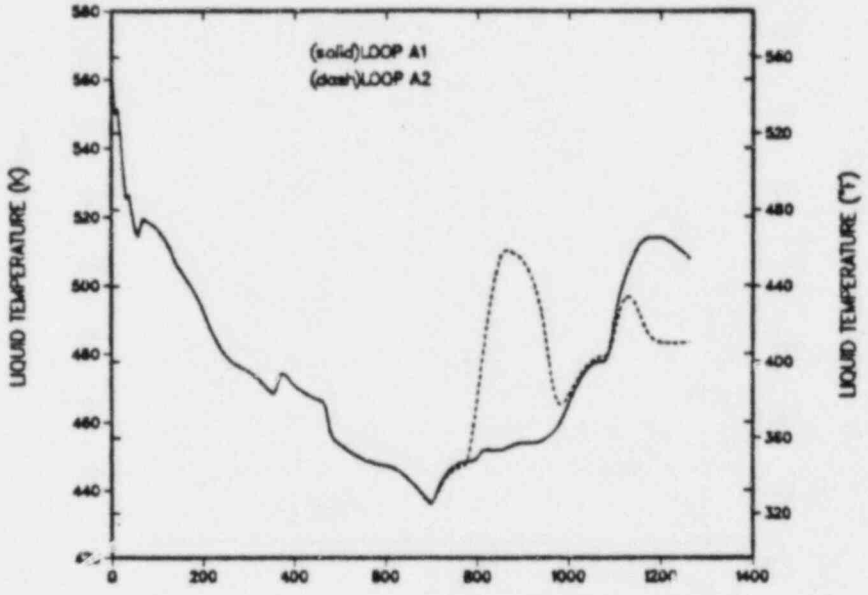

Fig. 90.
Loop-A cold-leg liquid temperatures - Case 3.

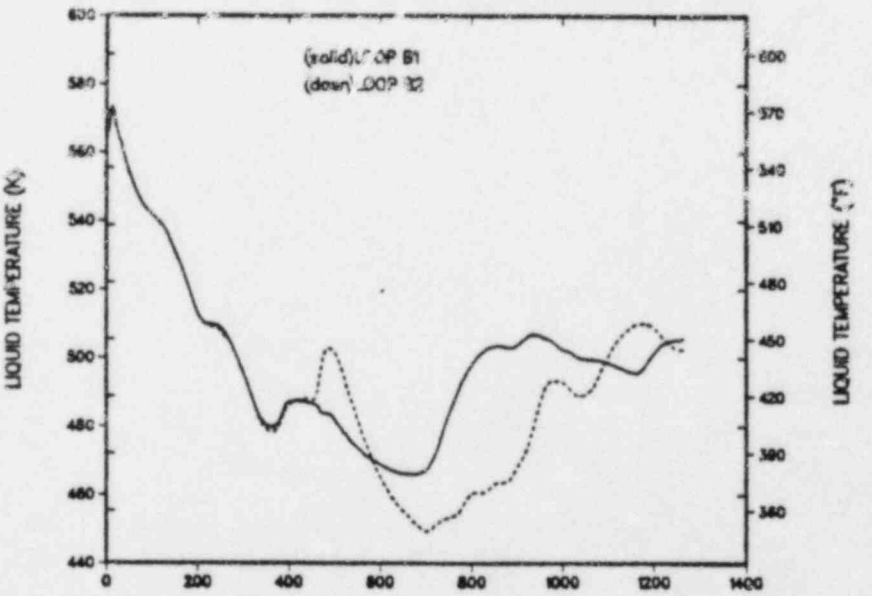

Fig. 91.
Loop-B cold-leg liquid temperatures - Case 3.

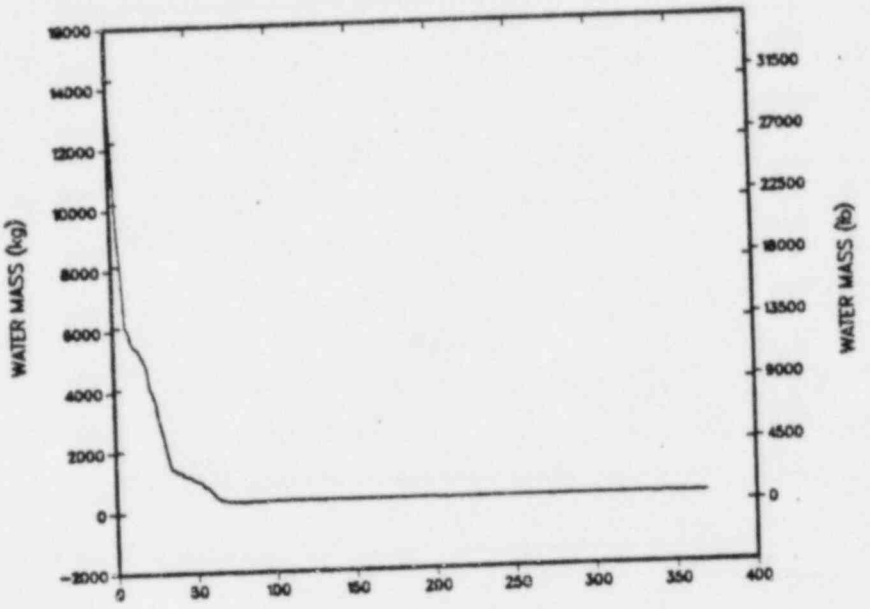

Fig. 92.
SG A secondary-side water inventory - Case 3.

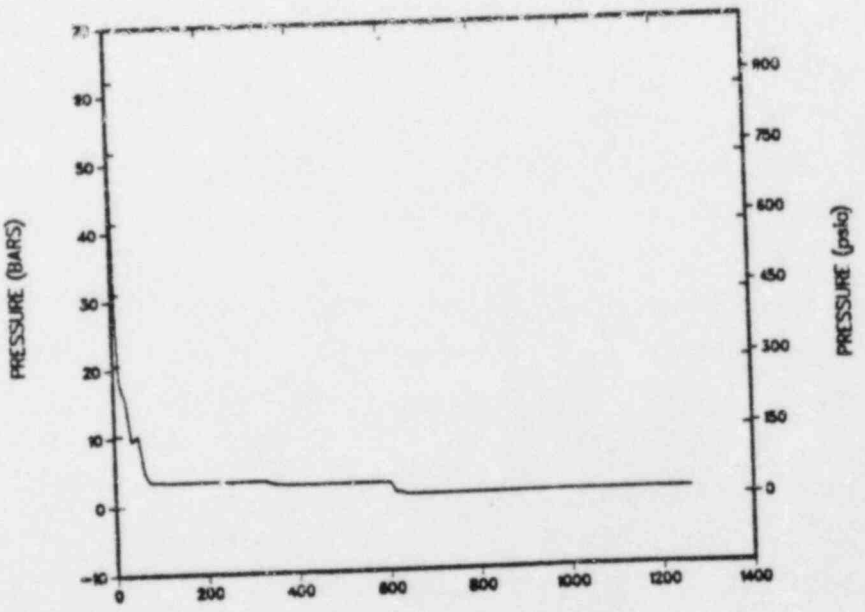

Fig. 93.
SG A secondary-side pressure - Case 3.

before 600 s because of the run-away MFW flow. Figure 95 shows the secondary-side water inventory calculated in SG B, and Fig. 96 shows the SG B secondary-side pressure. The run-away MFW filled SG B to the 90% operating range, and then the MFW pump was tripped (Fig. 97). The level then remained essentially constant for the remainder of the transient. The secondary-side pressure in SG B (Fig. 96) decreased because of condensation from the MFW until the MFW pump was tripped at ~330 s. After SG B was isolated at 600 s, the secondary pressure decreased further because of secondary-to-primary side heat transfer.

d. Parametric case-Case 4.

In parametric Case 4, the base case was recalculated to 2100 s with boundary condition and modeling changes. After the base case was run, information was provided by Duke Power that resulted in several clarifications in the location and operation of various instruments. This information resulted in the following changes to the model:

1. The MFW pumps automatically trip at 0.5 s instead of 47 s (based on RELAP-5 calculation Ref. 5). This is because of uncertainties in the measurement of the steam-generator liquid level during transient conditions (ΔP versus collapsed level).
2. The HPI throttling is based on subcooling at the exit of the core instead of the hot leg when the RCPs are not operating. HPI throttling is based on subcooling in the hot leg only when the RCPs are operating.
3. The correct instrument location for measuring subcooling for RCP restart is located 3.0 m below the top of the candy-cane centerline instead of the horizontal part of the hot leg.

These changes did not dramatically affect the minimum downcomer liquid temperature; it reached a minimum of ~420 K as opposed to ~405 K in the base case.

The major events of the transient are presented in Table XIX. The transient was initiated by a double-ended guillotine break in the loop-A steamline. Both steam generators blew down momentarily, but the TSV quickly isolated the loop-B generator. At the same time, the reactor tripped, the MFW pumps were tripped, and the feedwater-heater drain tank flow was ramped to zero. Closure of the TSV pressurized the loop-B steam generator and the TBV began cycling open and close to relieve the pressure. This lasted only ~40 s because the EFW flow into the steam space at the top of the generator lowered the pressure in SG B. EFW flow began at ~11.5 s because of low liquid level in SG A.

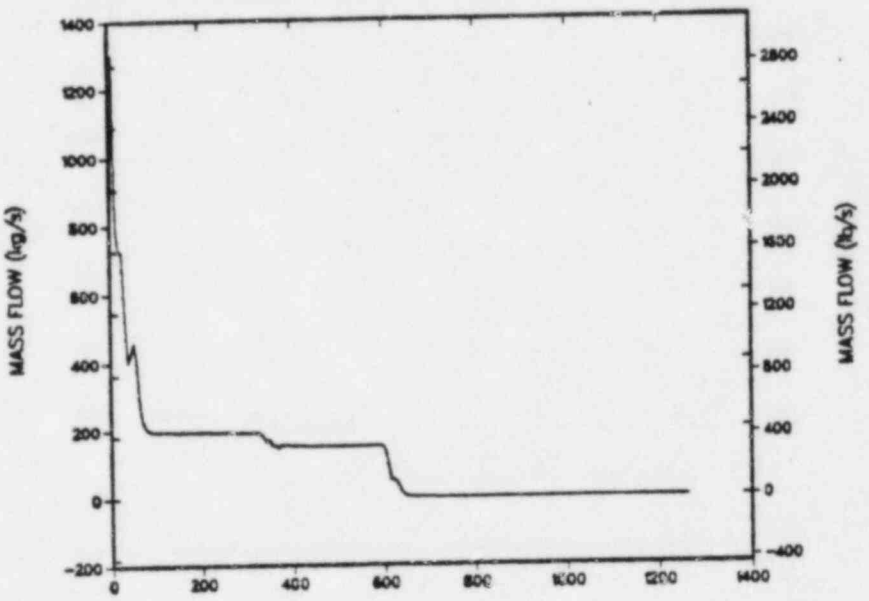

Fig. 94.
SG A steam-line flow - Case 3.

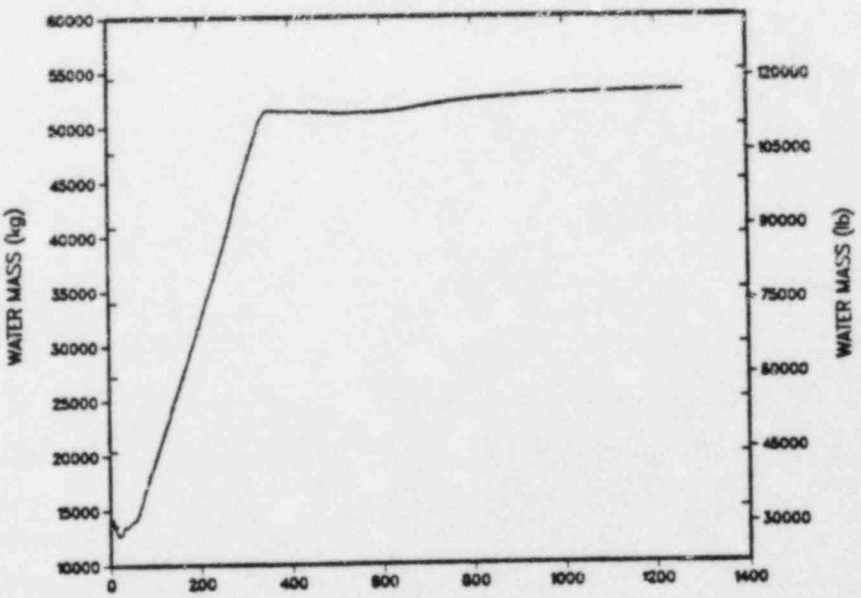

Fig. 95.
SG B secondary-side water inventory - Case 3.

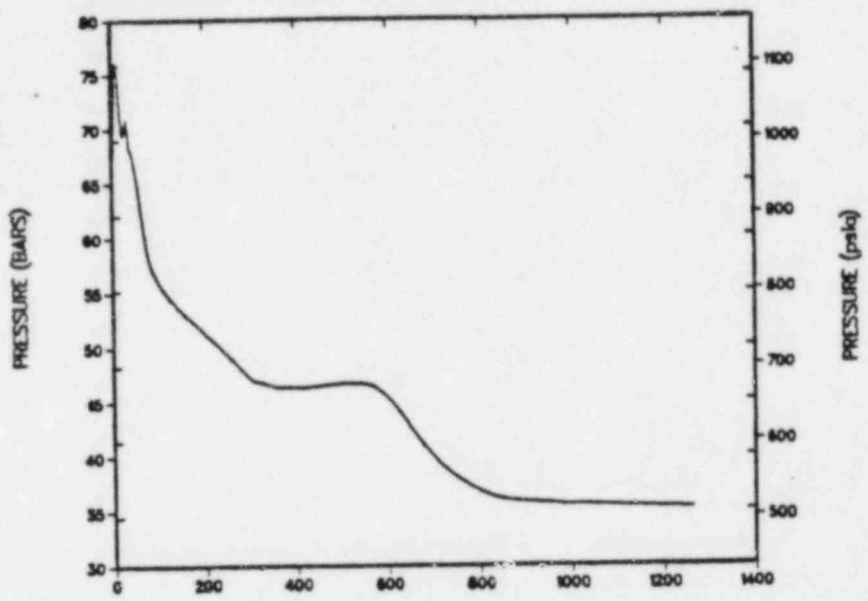

Fig. 96.
SG B secondary-side pressure - Case 3.

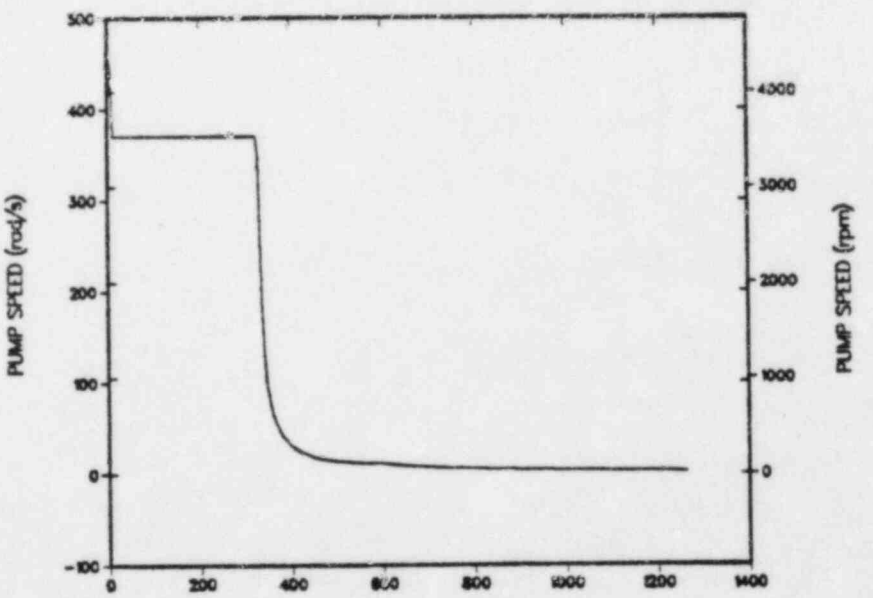

Fig. 97.
MFW pump speed - Case 3.

The steamline break initially caused rapid overcooling and depressurization of the primary side. At ~22.4 s, low primary-system pressure actuated the HPI system and thirty seconds later, the RCPs tripped. The candy-cane in loop B voided after loss of forced circulation; thus, there was no natural circulation in loop B during the transient. Because the RCPs were tripped, instruments at the core exit were used to determine subcooling for HPI throttling; conditions were met at ~302 s. Adequate subcooling for the restart of the RCPs was never met because the loop-B candy-cane was voided. At ~311 s, the liquid level in SG B reached 50% of the operating range and the EFW flow was rerouted to SG A.

At 600 s, all feedwater to SG A was terminated as specified by the ORNL event sequence. At this point, the overcooling transient was essentially over. The decay heat began to repressurize and heat the primary side. SG A boiled dry

TABLE XVIII

MSLB (CASE 4) SEQUENCE OF EVENTS

Event	Time (s)
MSLB-loop A steamline	0.0
Turbine and reactor trip; MFW pump trip; TSV B closure	0.5
TBV B cycling	5.4-40.0
EFW to both SGs	11.5
HPI initiated	22.4
RCPs trip	52.4
Loop-B candy-cane voided	140
HPI throttled	302
EFW B terminated	311
SG A isolated	602
SG B restored	900
Calculation terminated	2100

at about 1875 s. The calculation was terminated at 2100 s because no significant differences from the base case were obtained including the minimum downcomer liquid temperature.

Plots comparing the system pressures and downcomer liquid temperatures for Case 4 and the base case are shown in Figs. 98-99. Differences in the system pressure cannot be seen until ~302 s when the HPI was throttled in Case 4; the system was no longer refilling in this case.

The repressurization rate was slower in Case 4 because the RCPs were not operating. In Case 4, flow stagnated in loop B and remained stagnant, and thus little energy was deposited from the secondary-side. In the base case, restart of the RCPs lead to significant secondary-to-primary heat transfer and a faster repressurization rate. The downcomer liquid temperatures differ slightly for the two cases; the warming effect of terminating HPI flow ~225 s earlier in Case 4 is compensated by the cooling effect of not restarting the RCPs.

Plots illustrating key events on the secondary side are shown in Fig. 100-107. The break flow and SG-A pressure history (Figs. 100,101) indicate the rapid blowdown of SG A; by 80 s, the generator had almost depressurized to atmospheric pressure. After blowdown, the break flow leveled off at ~250 kg/s until all feedwater flow was terminated at 600 s. Figure 102 gives the pressure for the secondary side of SG B. When the TSV closed, there was an initial pressurization, and the TBV cycled to relieve the pressure. EFW began at ~11.5 s and the cold EFW caused the pressure to decrease as a result of condensation on the secondary side of SG B.

The EFW flows to both generators are shown in Fig. 103. When EFW to SG B was terminated, flow was rerouted to SG A. ORNL specified that EFW be terminated at 600 s; the total feedwater delivered to the generators is shown in Fig. 104 and 105. Even with the MFW pumps tripped at 0.5 s, MFW was still delivered by the condensate-booster and hotwell pumps.

The mass inventory in the tube-bundle region is shown in Figs. 106 and 107. After SG A blows down, the feedwater flow equaled the break flow until the EFW to SG B was terminated. At this point, the mass in SG A increased until feedwater termination at 600 s; the generator boiled dry at ~1875 s. In SG B, the EFW and MFW filled the generator until ~400 s.

On the primary side, Figs. 108-113 depict the mass flows and temperatures in loops A and B. The RCPs operated for ~52.4 s and then coasted down. The initial overcooling of loop A increased the mass flow because of enhanced heat transfer through SG A. Reverse heat transfer in SG B caused the flow directions to reverse for ~30 s before the loop-B flow stagnated. In the loop-A cold legs

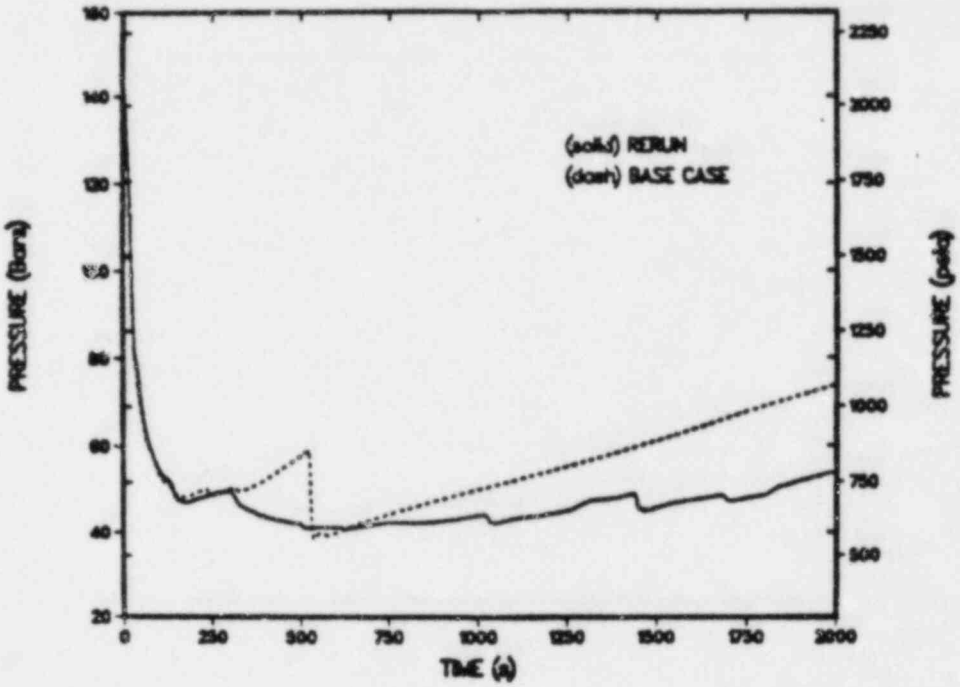

Fig. 98.
System pressure for Case 4 and base case.

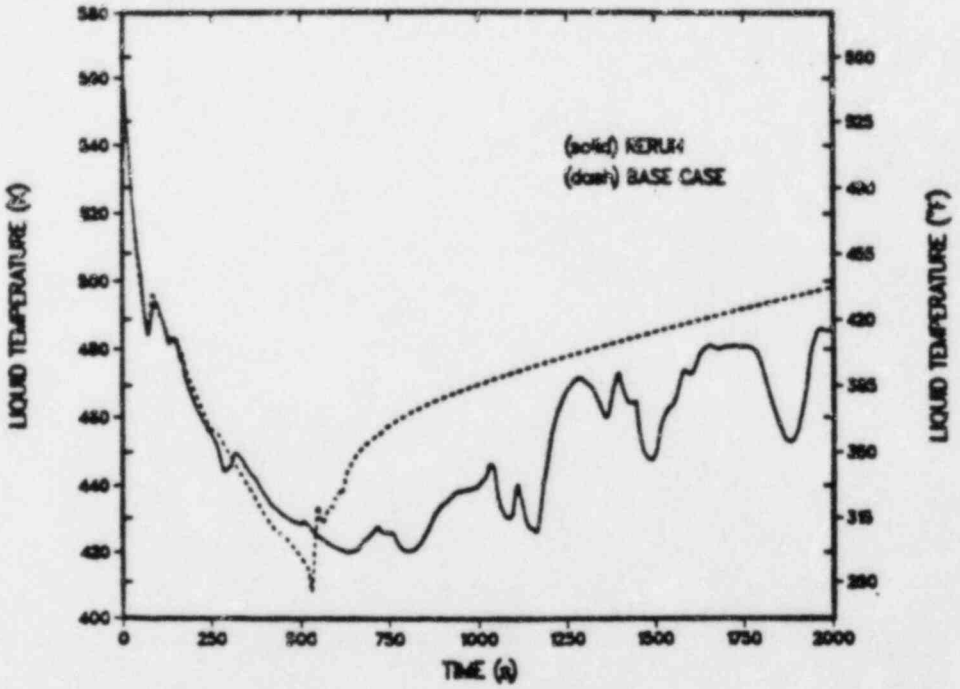

Fig. 99.
Downcomer liquid temperatures at vessel axial level 6 for Case 4 and base case.

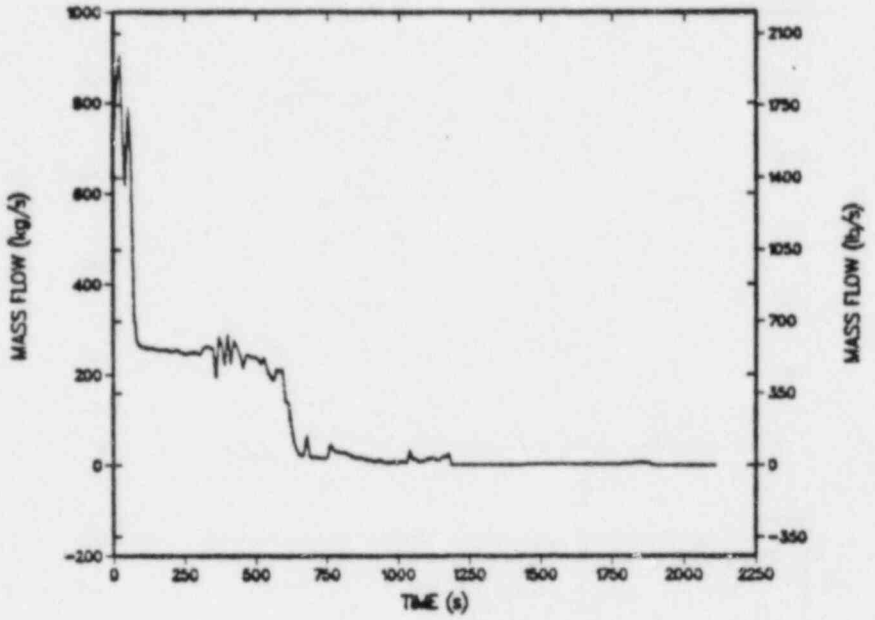

Fig. 100.
Break flow for Case 4.

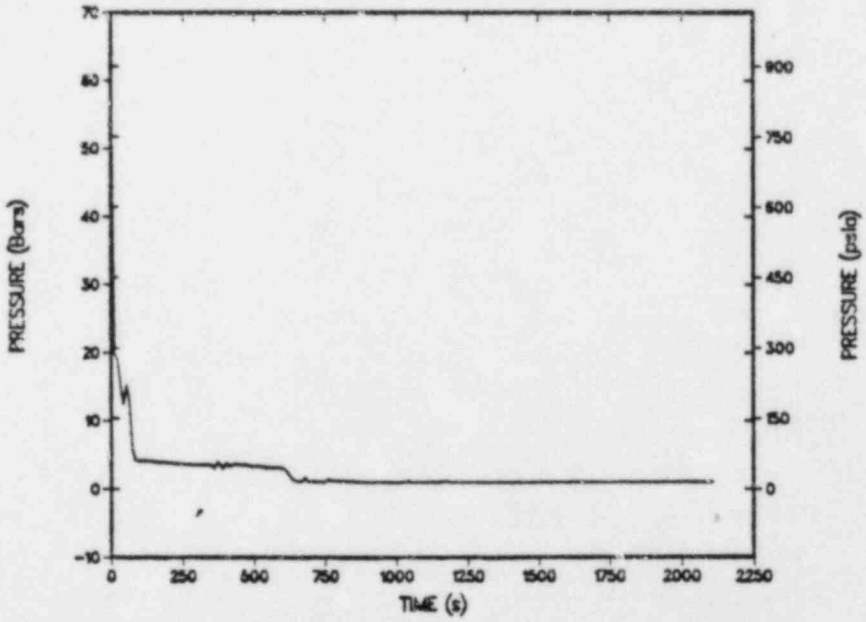

Fig. 101.
SG-A secondary pressure for Case 4.

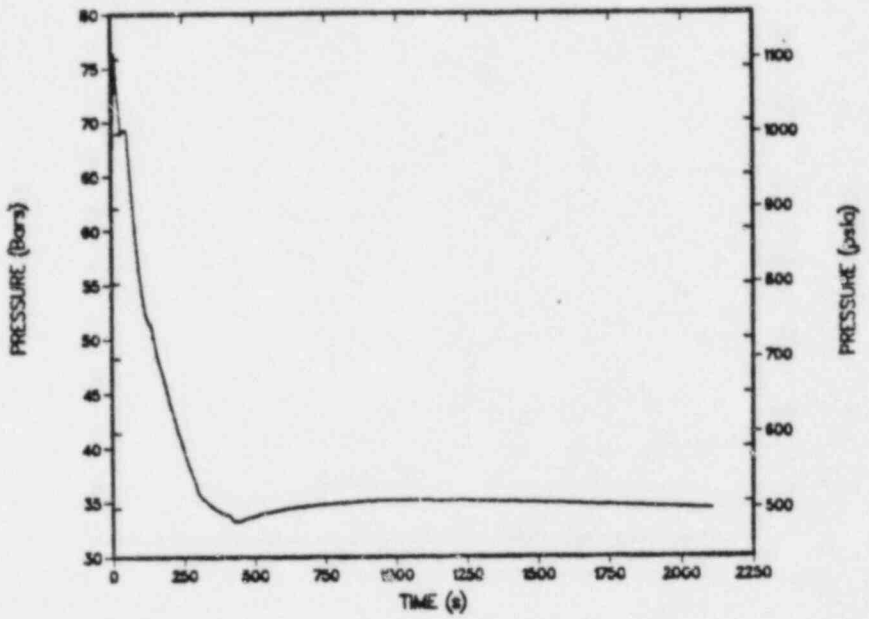

Fig. 102.
SG-B secondary pressure for Case 4.

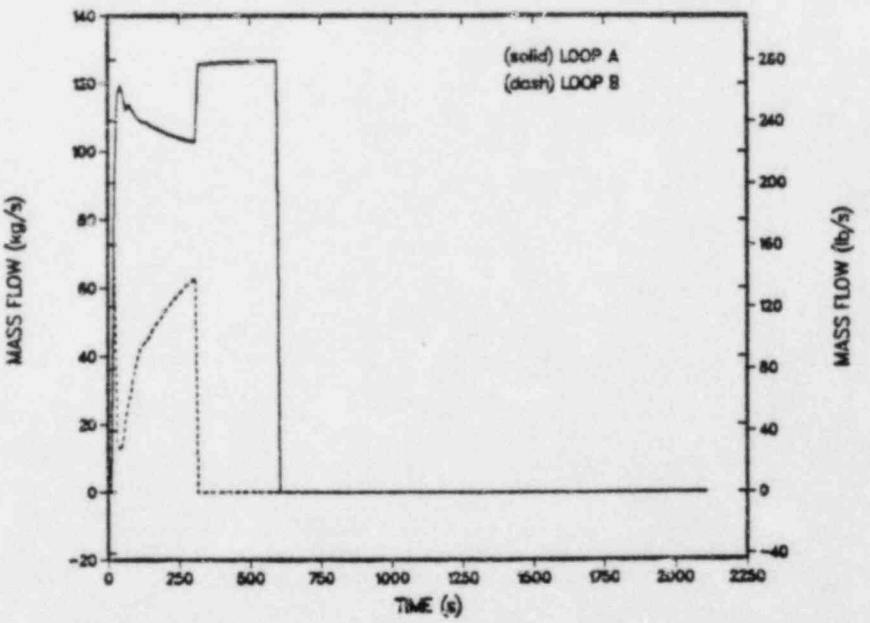

Fig. 103.
EFW flow (SG A and SG B) for Case 4.

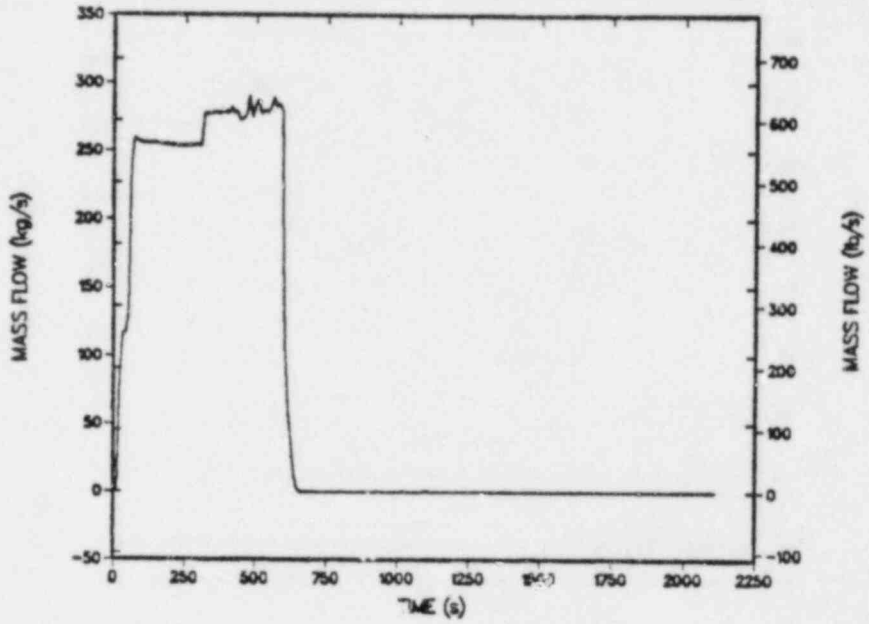

Fig. 104.
SG A total feedwater flow for Case 4.

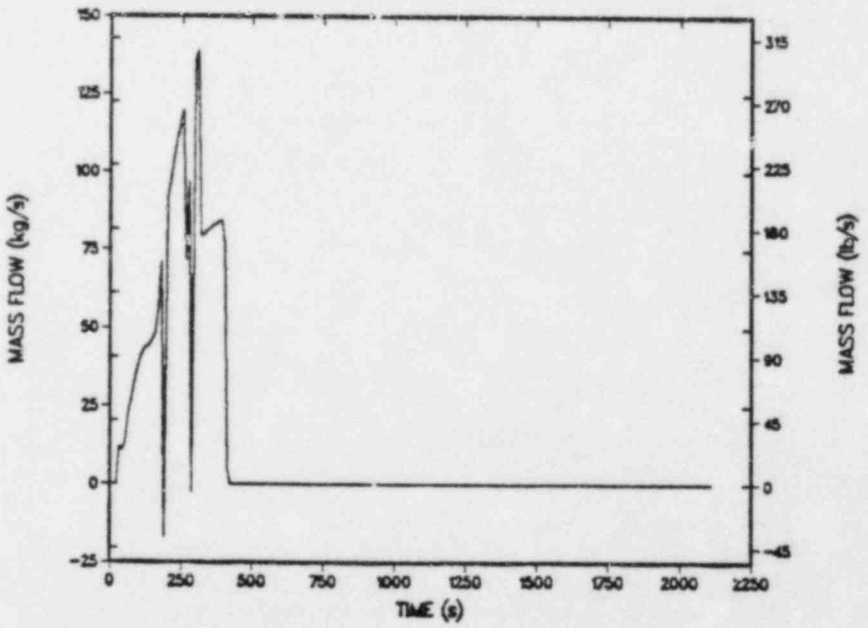

Fig. 105.
SG B total feedwater flow for Case 4.

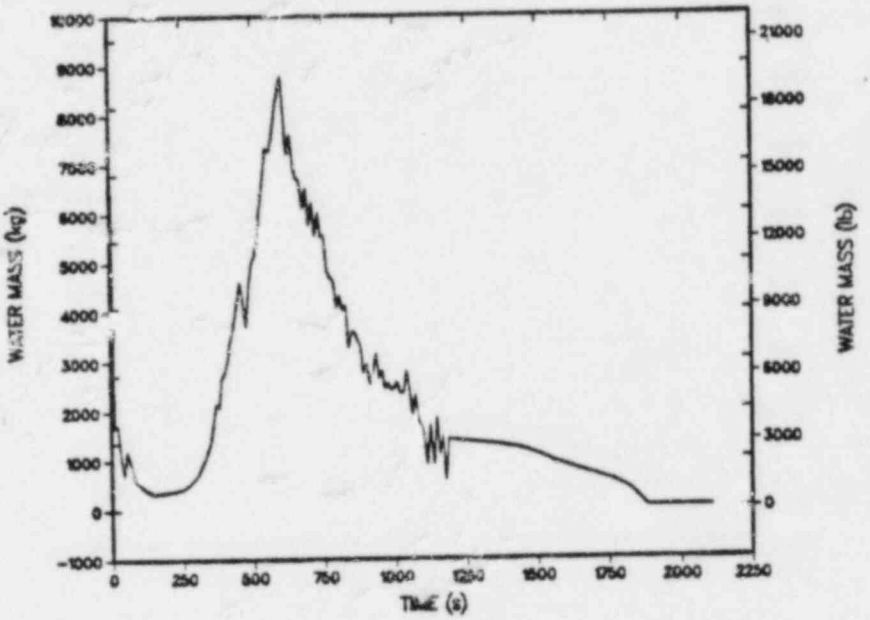

Fig. 106.
SG-A tube-bundle-region mass inventory for Case 4.

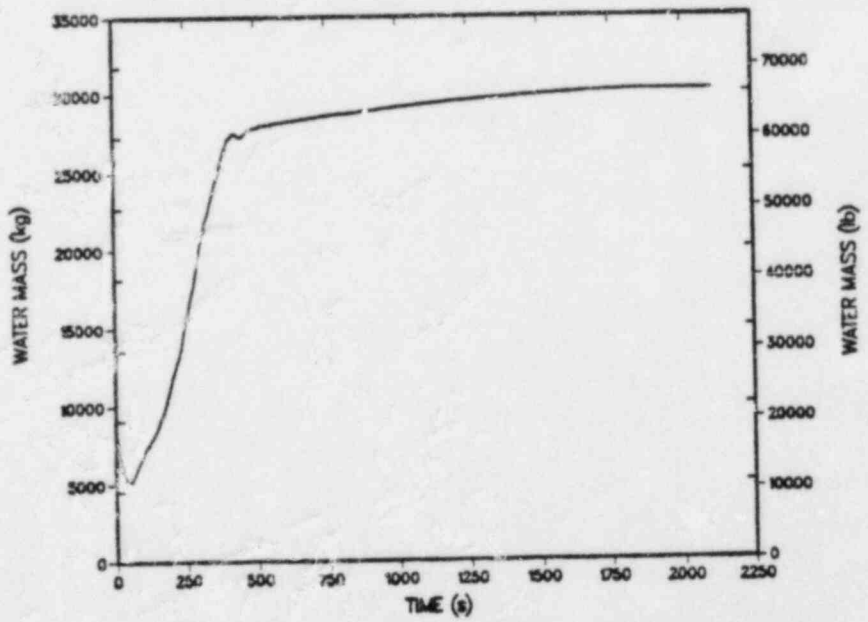

Fig. 107.
SG-B tube-bundle-region mass inventory for Case 4.

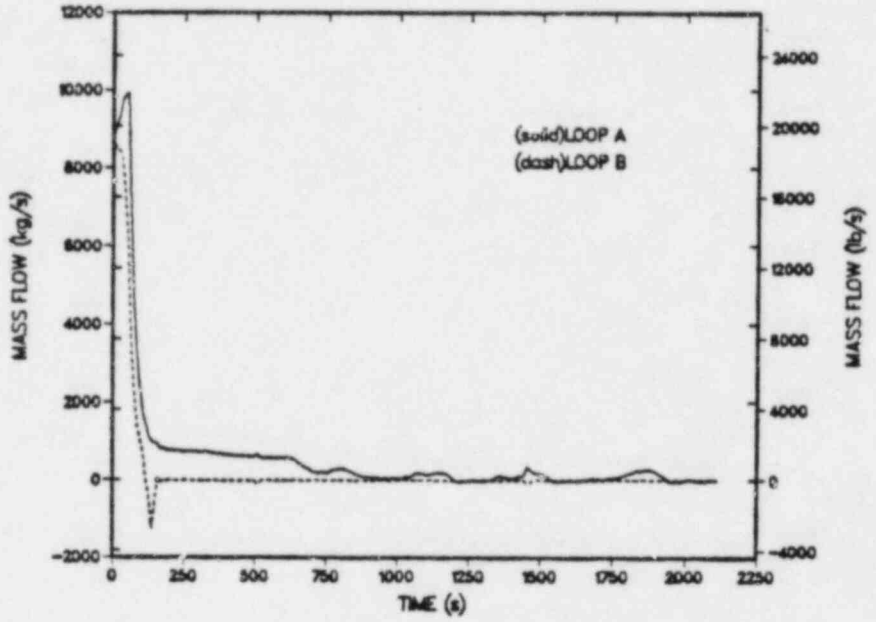

Fig. 108.
Hot-leg A and B mass flows for Case 4.

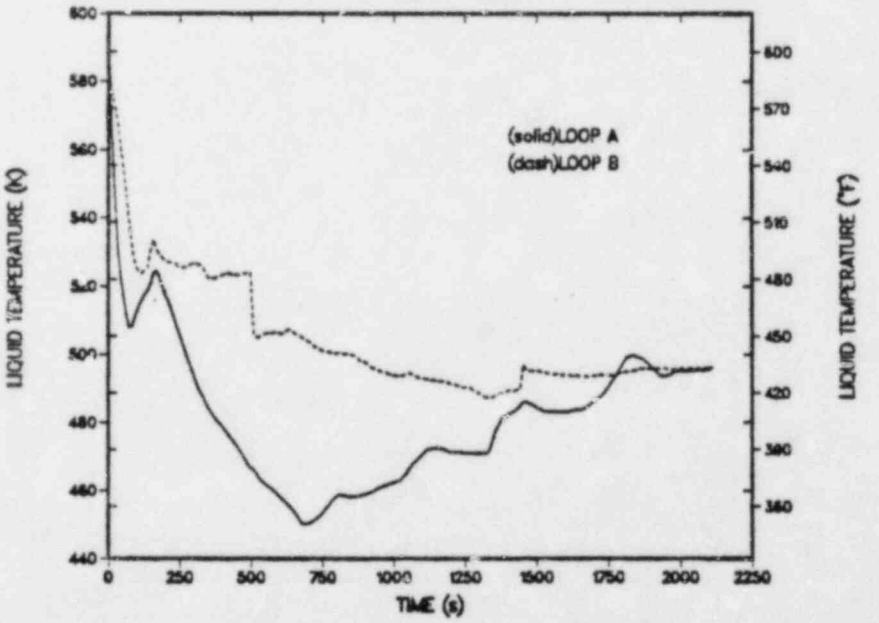

Fig. 109.
Hot-leg A and B liquid temperatures for Case 4.

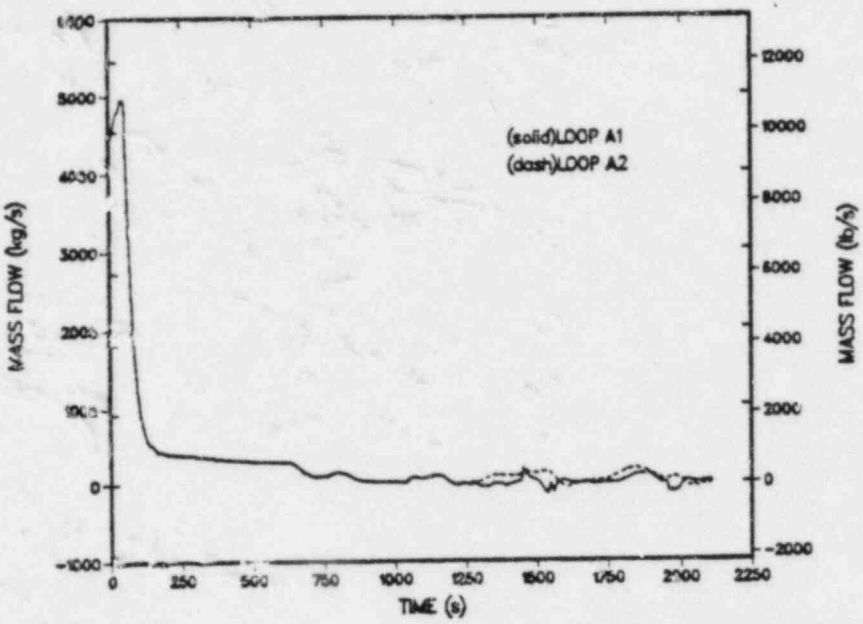

Fig. 110.
Loop A cold-leg mass flows for Case 4.

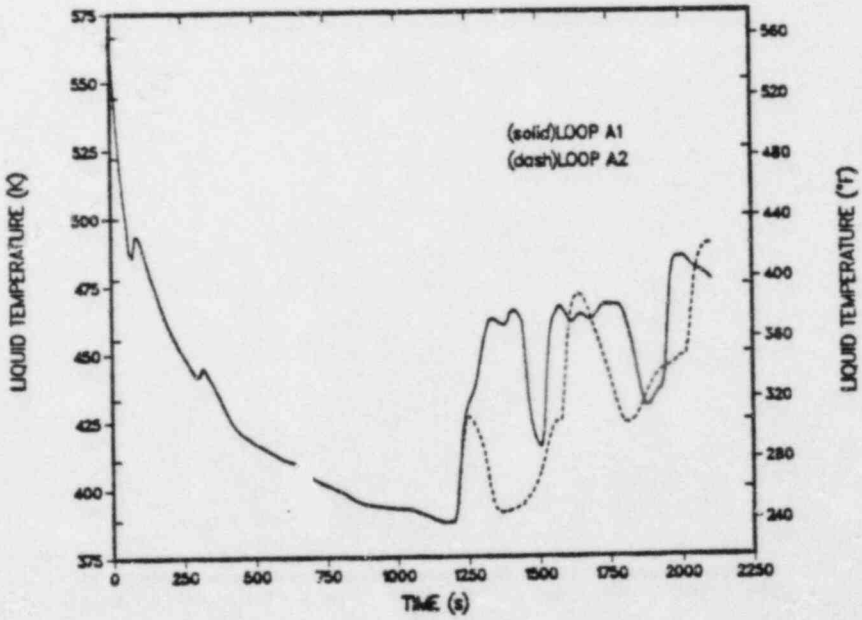

Fig. 111.
Loop A cold-leg liquid temperatures for Case 4.

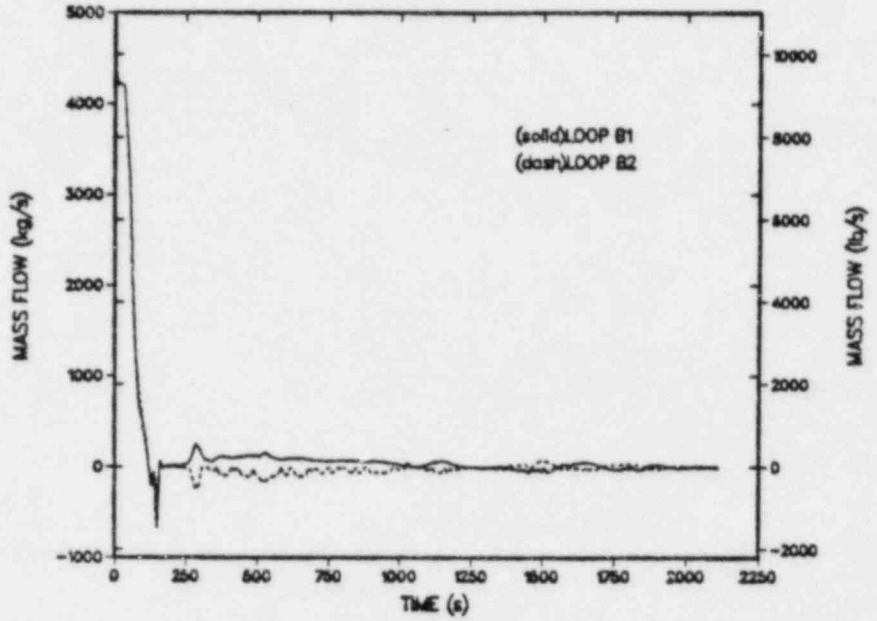

Fig. 112.
Loop B cold-leg mass flows for Case 4.

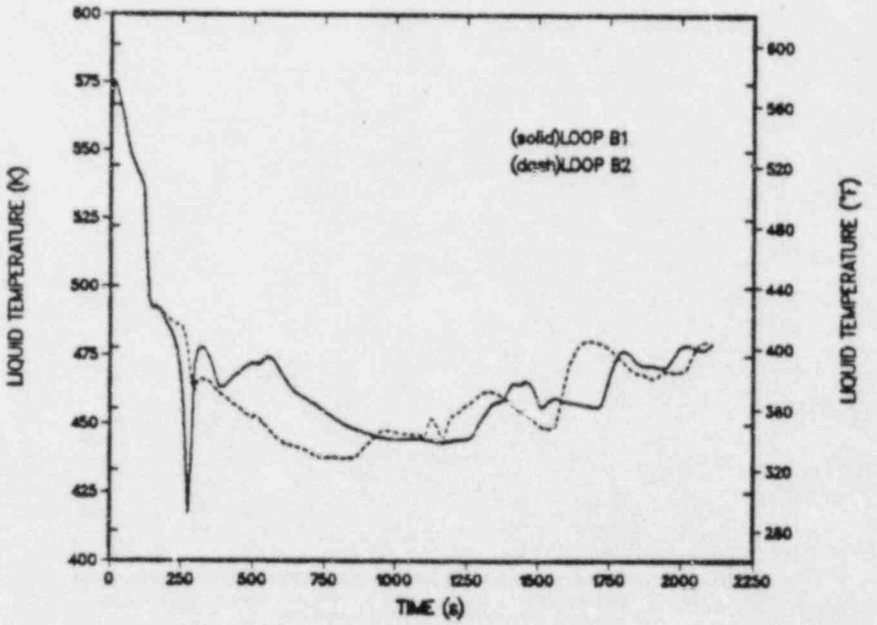

Fig. 113.
Loop B cold-leg liquid temperatures for Case 4.

high natural-circulation flows kept the fluid mixed and the temperatures uniform. In the loop-B cold legs there was a small circular flow pattern. Figure 114 indicates the total HPI flow for the transient; the flow was decreased to zero when adequate subcooling was reached at the core exit.

Figures 115 - 116 show the total vent-valve flow and the average upper-plenum liquid temperature. The vent valves make a significant contribution to warming the downcomer liquid. The total vent-valve flow for Case 4 is similar to that calculated for the base case (Fig. 36) except that the vent valves were always operating in Case 4 (no RCP restart).

In conclusion, Case 4 gives a minimum downcomer liquid temperature of approximately 420 K and indicates the system will repressurize similar to the base case. The changes made to the base-case calculation for Case 4 gave a more accurate prediction of the postulated accident at Oconee-1 and still indicate that this transient could pose a threat of PTS to the reactor vessel. However, these changes made no significant impact with regard to the overall conclusions stated for the base case, and the minimum downcomer fluid temperature remained approximately the same (~405 K - base case, ~420 K - Case 4).

4. Conclusions. The overcooling of the primary side of the Oconee-1 plant caused by a full double-ended steam-line break in one of the steam lines was simulated with TRAC-PF1. The main forcing function for the overcooling was a delay by the operator in isolating the affected steam generator coupled with a delay in throttling the HPI flow. The base case analyzed had all plant protection and control systems operate as designed. The minimum downcomer fluid temperature calculated for the base case was ~405 K. Repressurization of the primary system to the PORV setpoint was calculated for the base case following an initial depressurization to ~3.5 MPa.

Three parametric cases were analyzed in addition to the base case. In the first two parametric cases (Cases 2 and 3), input and modeling errors prevented the EFW system from operating as designed. Case 3 had an additional input error that prevented the RCPs from restarting once adequate subcooling was achieved. For these parametric cases, the downcomer fluid temperatures were considerably higher than the base case (Case 2 - ~475 K; Case 3 - ~450 K); thus greater margins against PTS were calculated.

In the last parametric case (Case 4) other changes were made to the model to reflect information provided by Duke Power after the base case was run. In this case, the subcooling monitor was corrected and the MFW pump was tripped at 0.5 s. This case was run to 2100 s, and the minimum downcomer fluid temperature

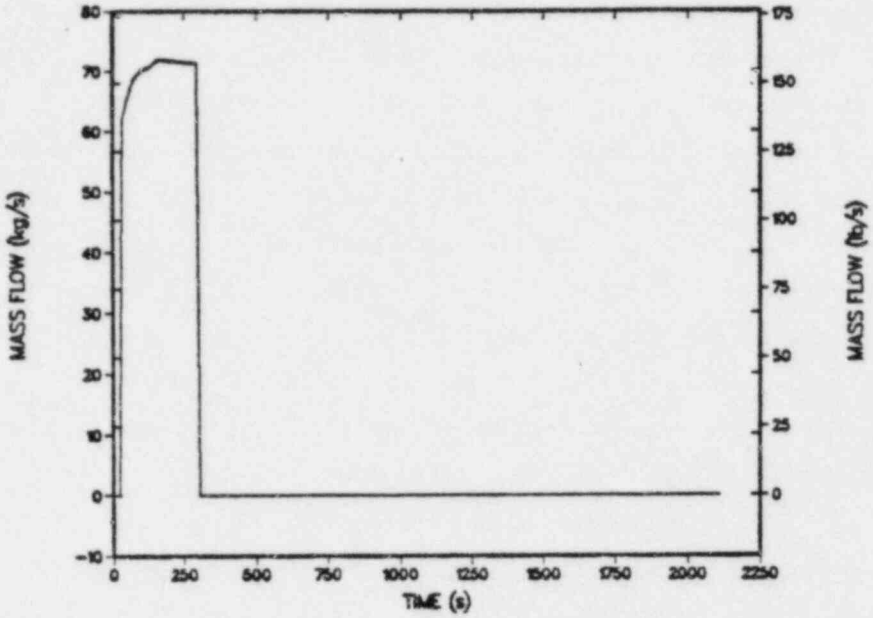

Fig. 114.
Total HPI flow for Case 4.

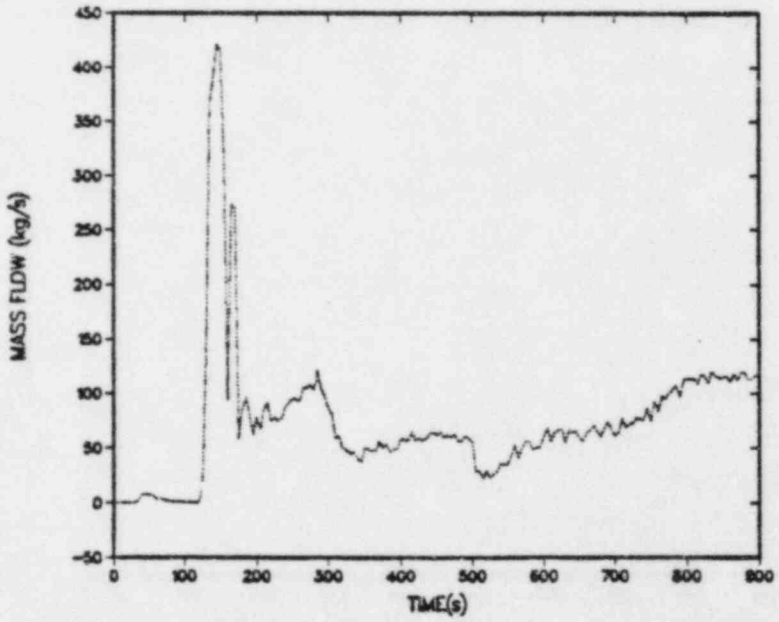

Fig. 115.
Total mass flow through vent valves for Case 4.

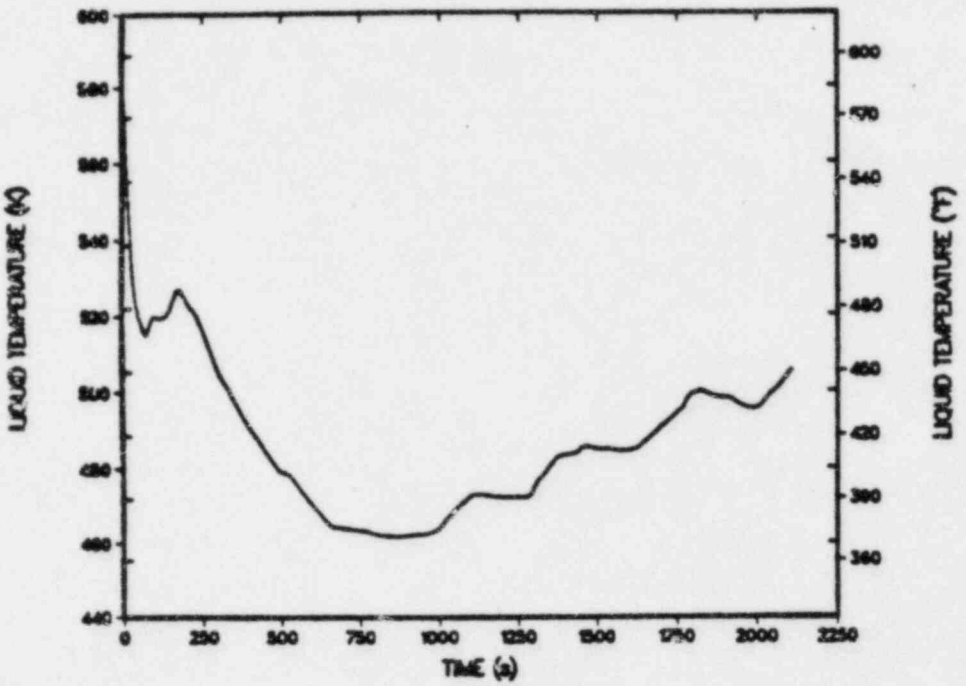

Fig. 116.
Upper plenum liquid temperature for Case 4.

was ~420 K. None of the changes incorporated into Case 4 resulted in significant differences from the base case.

C. PORV LOCA

1. Introduction and Summary. This section of the report presents the Oconee-1 plant response to a small primary-system break (the failure of the PORV in the full-open position). The PORV was assumed to open at transient initiation and remain stuck-open for the remainder of the accident sequence. This event was followed by the reactor and turbine trips from full power. In addition to the PORV failure, the ICS failed to run back the main feedwater. As a result, the steam generators continued to fill until the MFW pumps were tripped on a high SG level signal. The PORV failure and the ICS failure were the only assumed system-related failures. The RCPs tripped 30 s after HPI initiation, and this was the only specified operator action.

TRAC calculated a minimum vessel downcomer liquid temperature of ~528 °K between 600 s and 700 s into the transient. The primary system was calculated to repressurize to ~11.5 MPa after 800 s.

2. Model Description and Assumptions. A complete description of the primary-side, secondary-side, and ICS modeling can be found in Section II. The steady-state operating conditions are also presented in that section.

TABLE XIX

MSLB[a] (CASE 3)

SEQUENCE OF EVENTS

	Event	Time (s)
1-14.	Approximately same as base case except no MFW pump trip at 47.8 s	0-53.9
15.	SG B level at 50%	197.0
16.	SG B level at 90%; MFW pump trip[b] on high SG B level	331.0
17.	HPI throttled after 42 K subcooling reached; RCPs (A1, B1) fail to restart	356.0
18.	HPI on (42 K subcooling margin lost)	465.0
19.	SG A, B isolated	600.0
20.	HPI off	693.0
21.	Calculation terminated	1260.0

[a]EFW pump never started; RCPs never restarted
[b]Because of signal-variable errors in the ICS modeling the MFW pump did not trip until 331.0 s. This pump should have tripped on low-suction pressure similar to the base case.

The PORV LOCA specification containing the initial conditions, event sequence, and assumed failures is presented in Ref. 3. The TRAC transient event sequence for the PORV LOCA is presented in Table XX. To ensure a MFW pump trip on a high SG level signal, the low-suction and high-discharge pressure trips that could prematurely trip the MFW pump were overridden. Also, the MFW pump speed was increased to its rated maximum speed (595.8 rad/s) whereas the loop-A and -B MFCV flow areas were maintained at their steady-state operating values until the MFCV overriding trip at ~100 s. At this point, the SUFCVs were opened by the ICS to continue filling the SGs. The MFW pump maintained the maximum speed setting until the trip on high SG level.

3. Transient Calculation. Figures 117 and 118 present the secondary-side pressures for loops A and B, respectively. Immediately following the reactor and turbine trips, the TSV closures produced an increase in secondary-side pressure. The TBVs for both loops were repeatedly activated between ~4 s and ~100 s to relieve increases in secondary pressure. The differences in the pressure distributions between ~150 and ~250 s can be attributed to differences in MFW mass flows to each SG. After the RCPs were tripped, the MFCV override trip closed the MFCVs, and the MFW was realigned to the upper header of the SGs. The SUFCVs were opened fully by the ICS to continue the feed to the SG upper headers. The MFW mass flow and liquid temperatures for loops A and B are shown in Figs. 119 and 120, respectively. Figures 121 and 122 show the MFW (realignment) mass flows supplied to the SG upper header of both loops. The additional mass flow to the loop-A SG produced the lower loop-A secondary-side pressure by condensing a portion of the steam located in the upper levels of the SG, and caused the larger loop-A secondary-side inventory. The SG inventories for loops A and B are presented in Figs. 123 and 124. The EFW pumps were not activated because the MFW pump was able to attain the high SG level.

TABLE XX

PORV LOCA EVENT SEQUENCE

	Event	Time (s)
1.	PORV opens	0.0
2.	Turbine and Reactor trip	0.5
3.	Turbine-stop valves close	0.5
4.	Secondary-side heater and heater-drain trip	1.1
5.	Condenser feed from turbine trip	1.6
6.	TBV-loop A opens for first time	4.4
7.	TBV-loop B opens for first time	4.7
8.	Condensate-booster pump trip on low-suction pressure	11.0
9.	TBV-loops A and B open/close	16.2
10.	HPI actuation on low primary-system pressure	70.3
11.	TBV-loops A and B open/close	71.1
12.	RCPs trip 30 s after HPI actuation	100.3
13.	MFW realigned to SG upper headers	100.3
14.	MFCV override trip	100.3
15.	MFW pump trip on high SG level (loop A)	250.3
16.	TBV-loop B opens for last time	330.0
17.	Minimum primary pressure (~7.2 MPa) attained	550.0
18.	Pressurizer water-solid	600.0
19.	Maximum primary repressurization (~11.5 MPa)	850.0
20.	End of calculation	1000.0

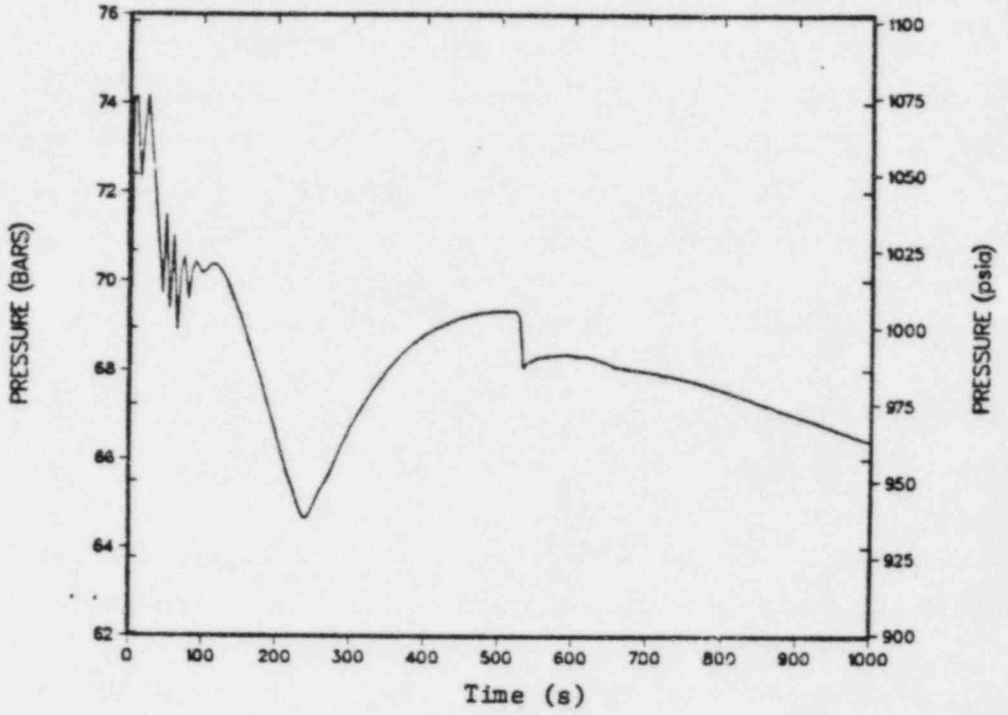

Fig. 117.
SG A secondary pressure.

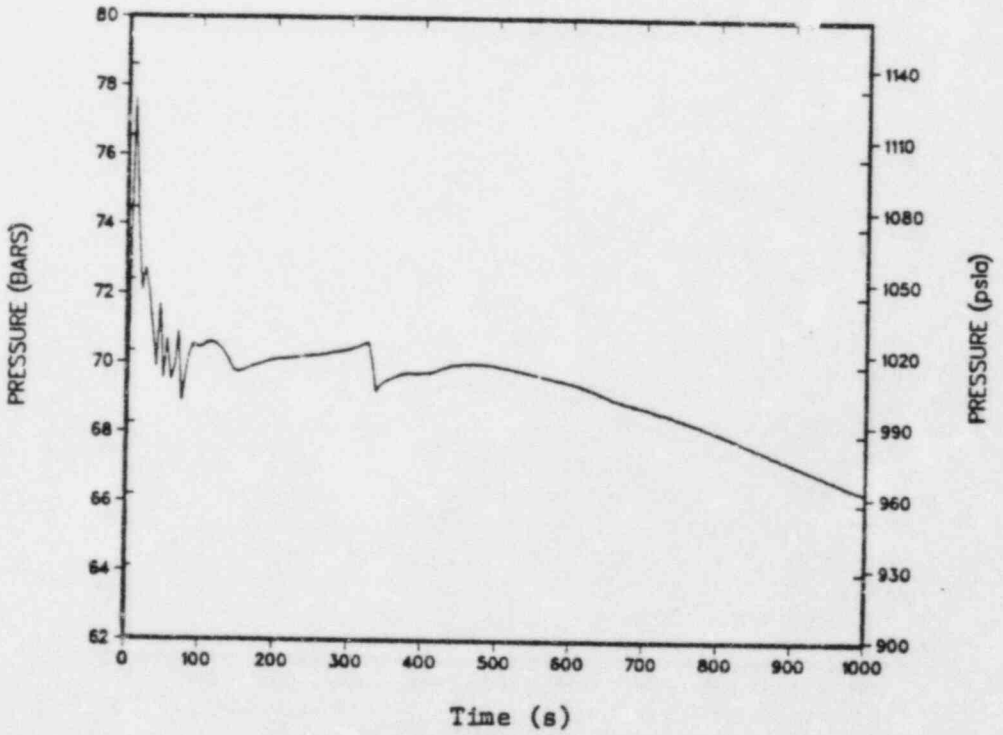

Fig. 118.
SG B secondary pressure.

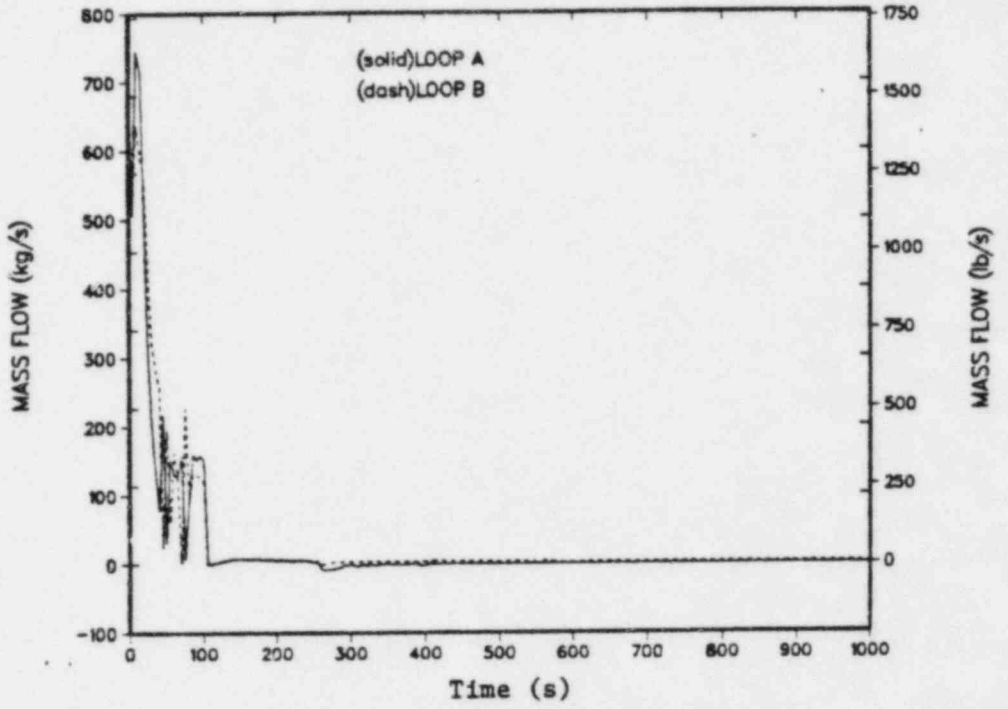

Fig. 119.
Main-feedwater flow - loops A and B.

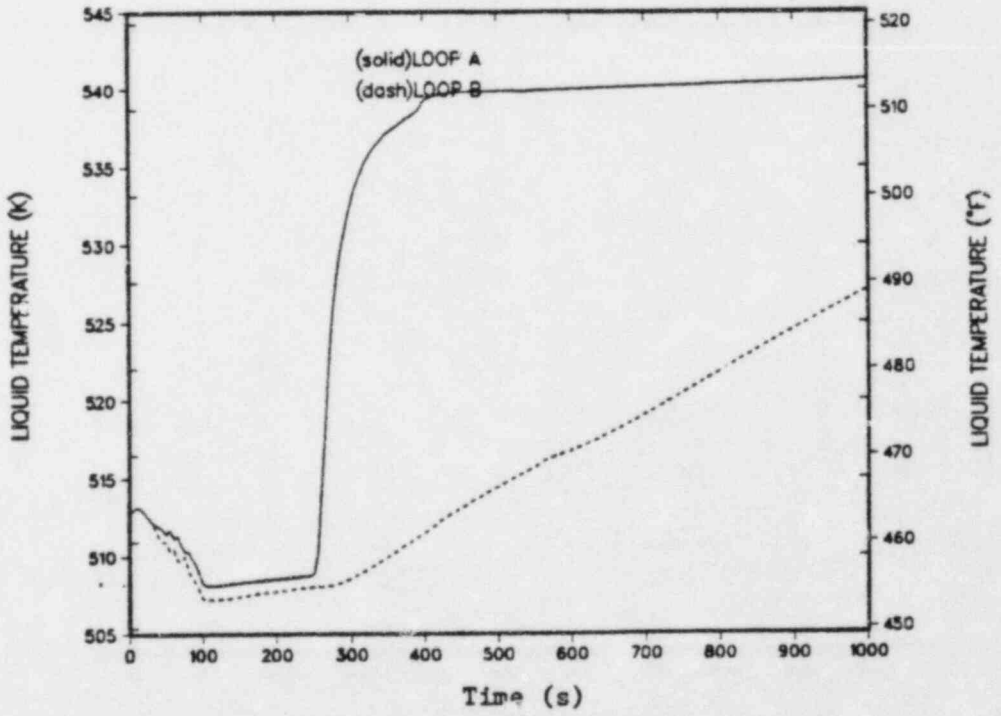

Fig. 120.
Main-feedwater liquid temperature - loops A and B.

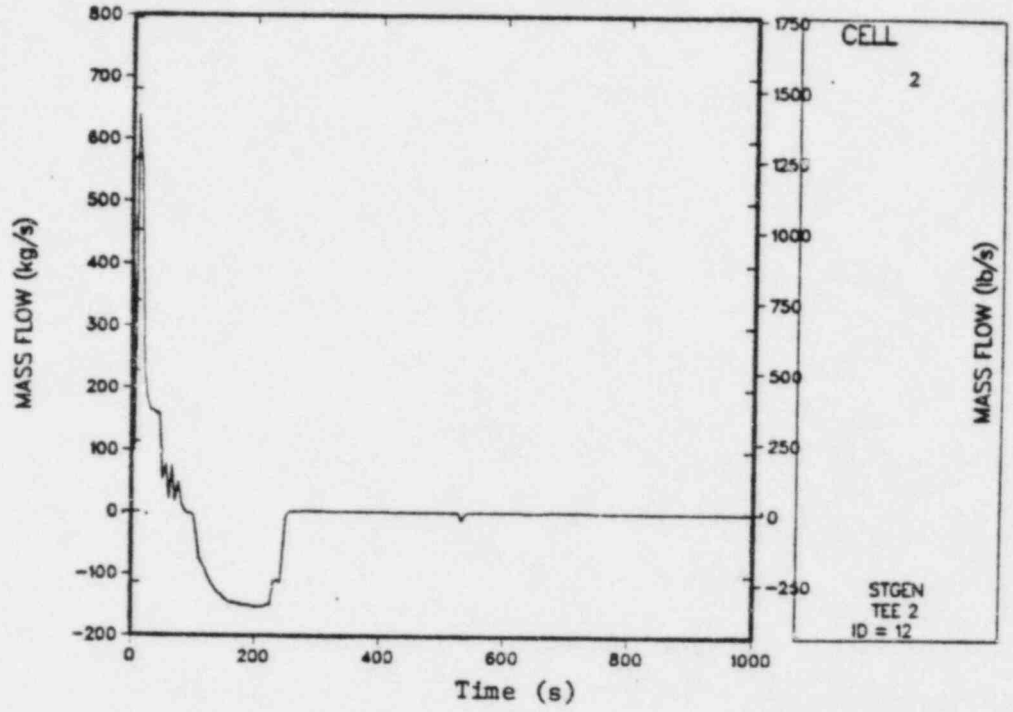

Fig. 121.
Realignment mass flow - loop A (negative flow is into SG).

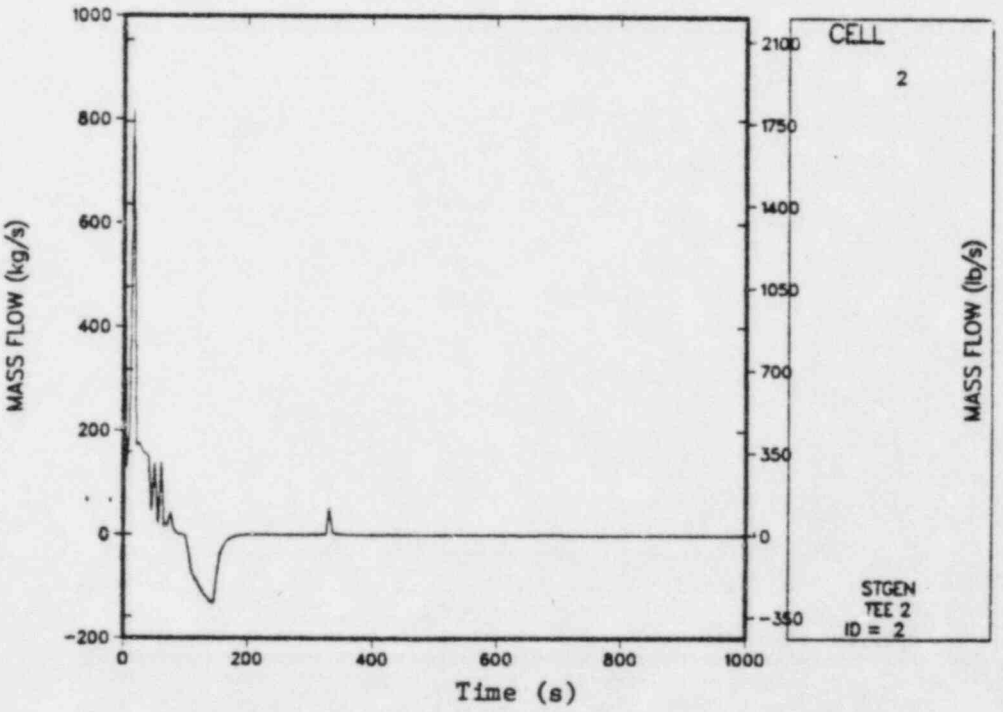

Fig. 122.
Realignment mass flow - loop B (negative flow is into SG).

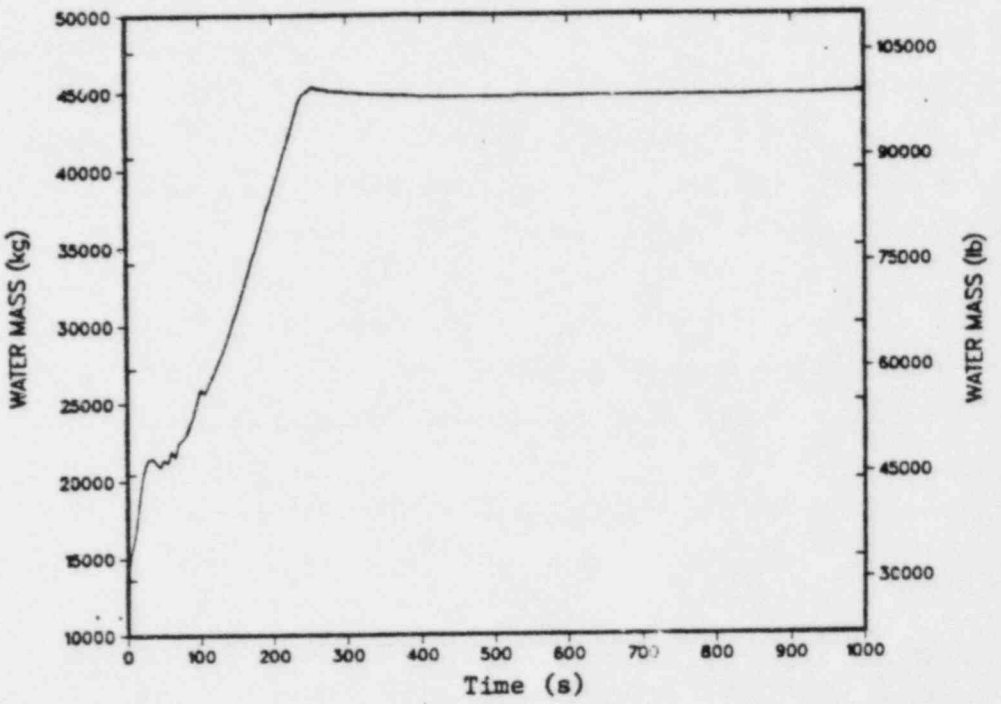

Fig. 123.
Steam-generator secondary inventory - loop A.

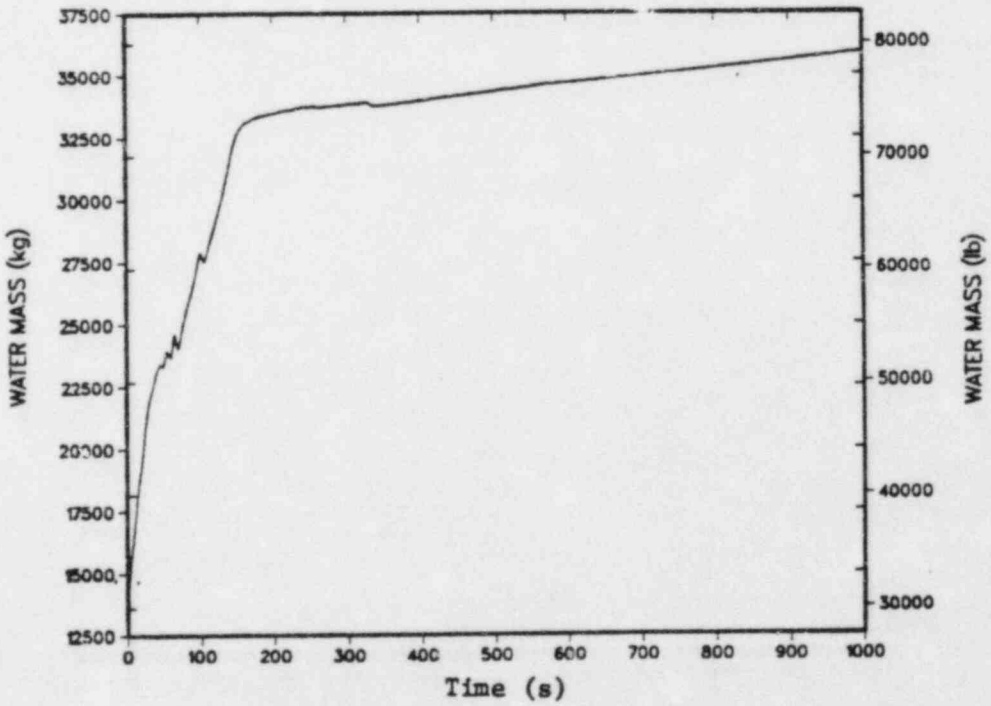

Fig. 124.
Steam-generator secondary inventory - loop B.

Pressurizer pressure and water level are shown in Figs. 125 and 126, respectively. The primary-system pressure fell sharply until the HPI was activated on low primary-system pressure at ~70 s. The primary system continued to depressurize and reached a minimum pressure of ~7.2 MPa at ~550 s. At this time, the primary system began to repressurize, and by ~850 s reached ~11.5 MPa. As soon as the HPI was initiated, the pressurizer began to refill because the HPI mass flow was sufficiently larger than the break mass flow. The break (PORV) mass flow and vapor fraction are shown in Figs. 127 and 128. The pressurizer remained voided until it refilled at ~500 s. Following this time, the pressurizer vapor fraction decreased rapidly and correspondingly the PORV mass flow increased. By ~1000 s the primary-system pressure was in equilibrium.

Mass flow rates and liquid temperatures for the loop-A and -B hot legs are shown in Figs. 129 and 130, respectively. The primary-system flows decreased following the RCP trip at ~100 s, and natural-circulation flows were soon established. TRAC calculated a minimum hot-leg temperature of ~552 K for both loops (Fig. 130). Loop-A and -B cold-leg mass flows are presented in Figs. 131 and 132. The cold legs exhibited trends similar to the hot legs. The corresponding cold-leg liquid temperatures are presented in Figs. 133 and 134. Minimum cold-leg temperatures were calculated to be ~518 K at ~550 s for loops A1 and A2, and ~525 K at ~625 s for loops B1 and B2.

The void fractions for the loop-A and -B candy-canes and the upper plenum (level 8) of the vessel are shown in Figs. 135 and 136, respectively. No voiding occurred in the candy canes; however, the upper plenum voided slightly between ~400 s and ~650 s.

Figure 137 shows the downcomer liquid temperatures at the top axial level just below the cold-leg inlet nozzles. TRAC calculated a minimum downcomer liquid temperature of ~528 K. The system pressure at this minimum downcomer liquid temperature was calculated to be ~7.2 MPa.

4. Summary. The Oconee-1 plant response to a small primary-system break (failure of the PORV in the full-open position) was calculated with TRAC-PF1. In addition to the failure of the PORV, the ICS failed to run-back the MFW, which resulted in a MFW-pump trip on a high SG level. The only specified operator actions included a RCP trip 30 s after HPI actuation. TRAC calculated a minimum downcomer liquid temperature of ~528 K at ~600 s into the transient. The primary system was calculated to repressurize to ~11.5 MPa after ~800 s.

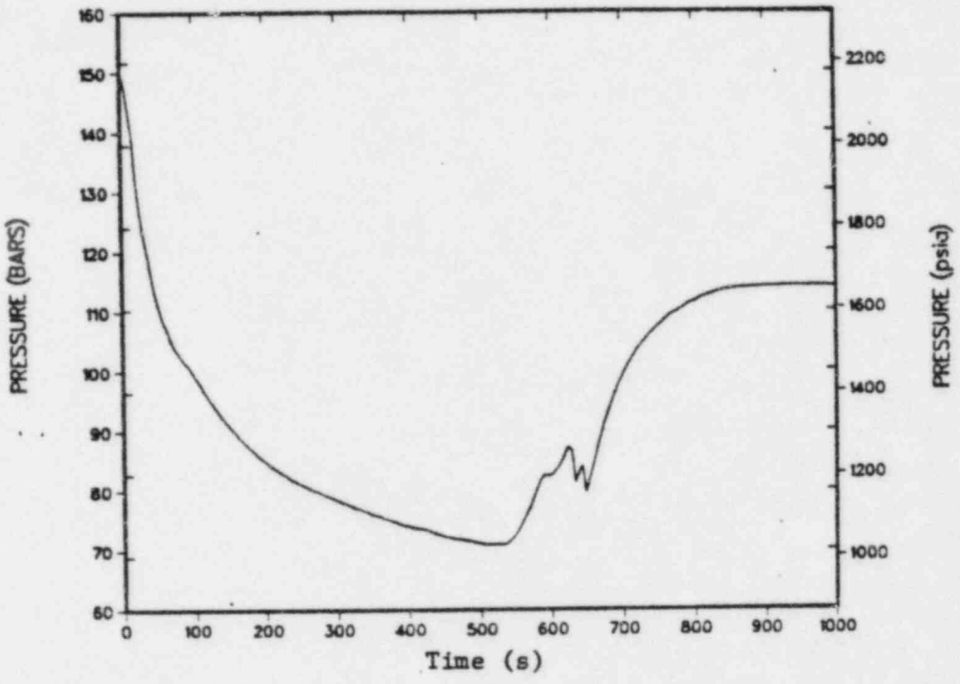

Fig. 125.
Pressurizer pressure.

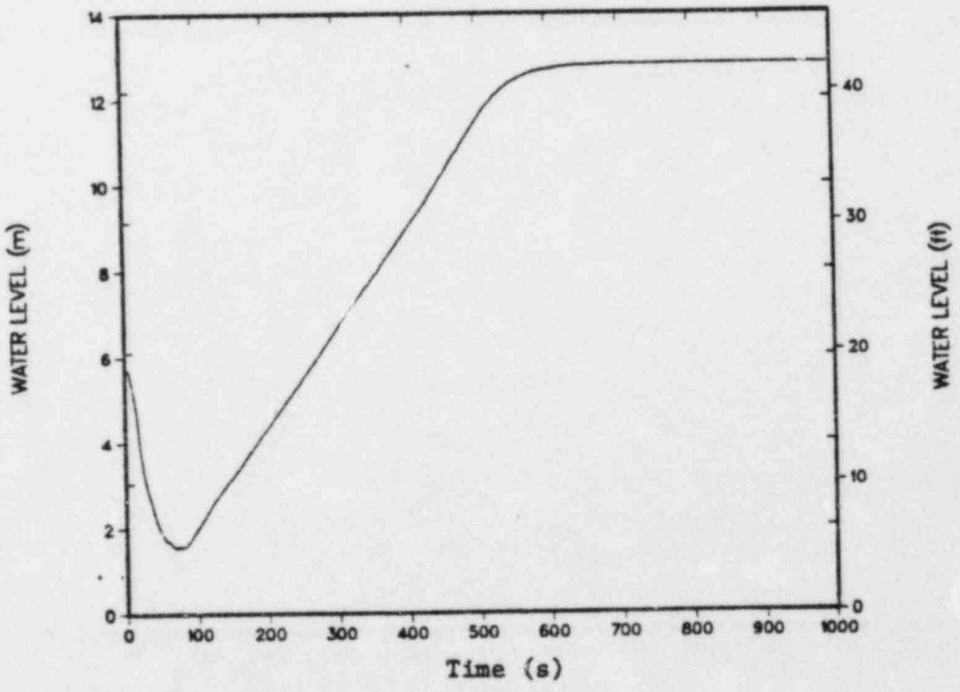

Fig. 126.
Pressurizer water level.

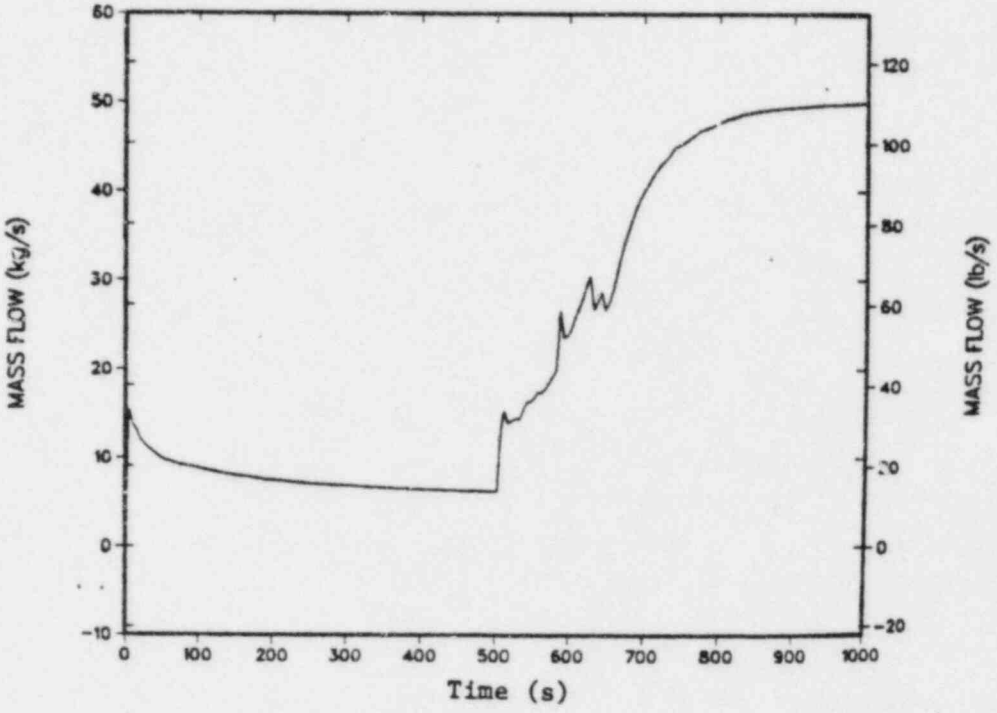

Fig. 127.
PORV mass flow.

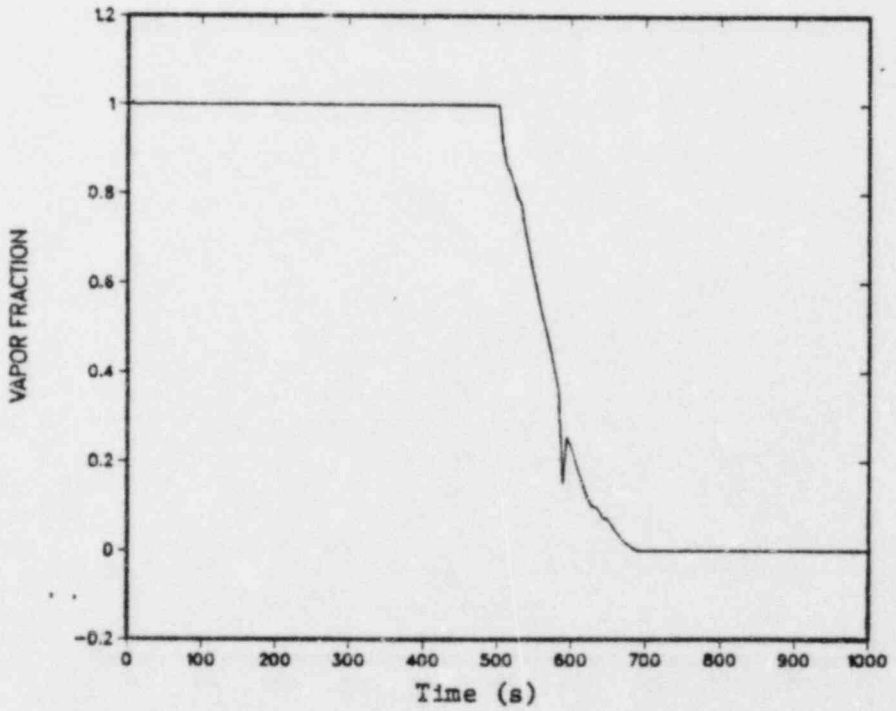

Fig. 128.
PORV vapor fraction.

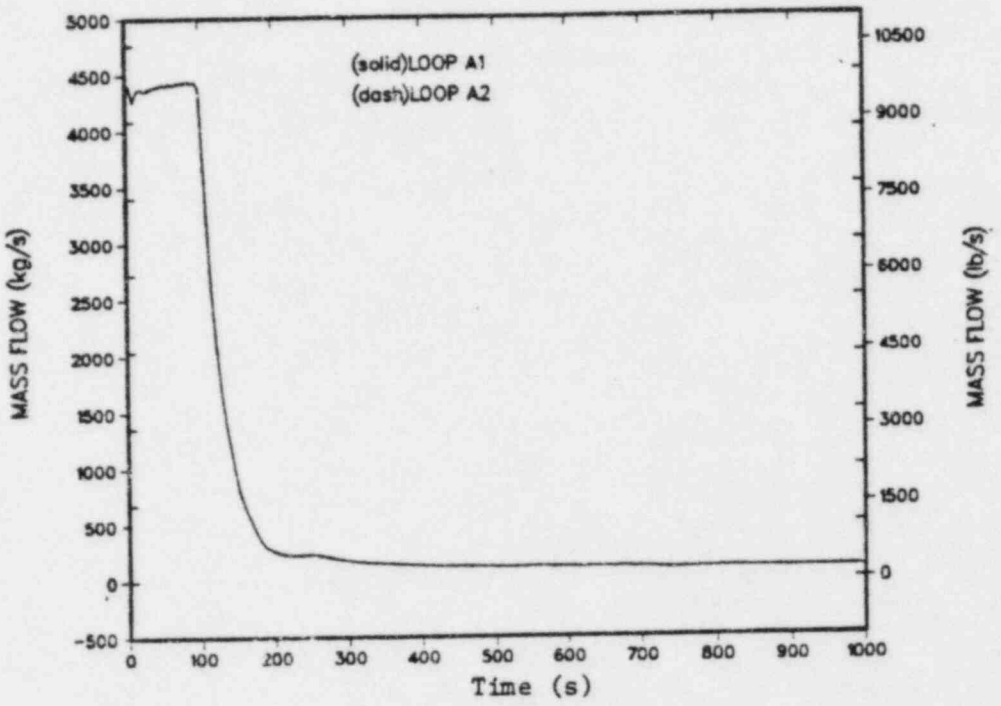

Fig. 129.
Hot-leg mass flows - loops A and B.

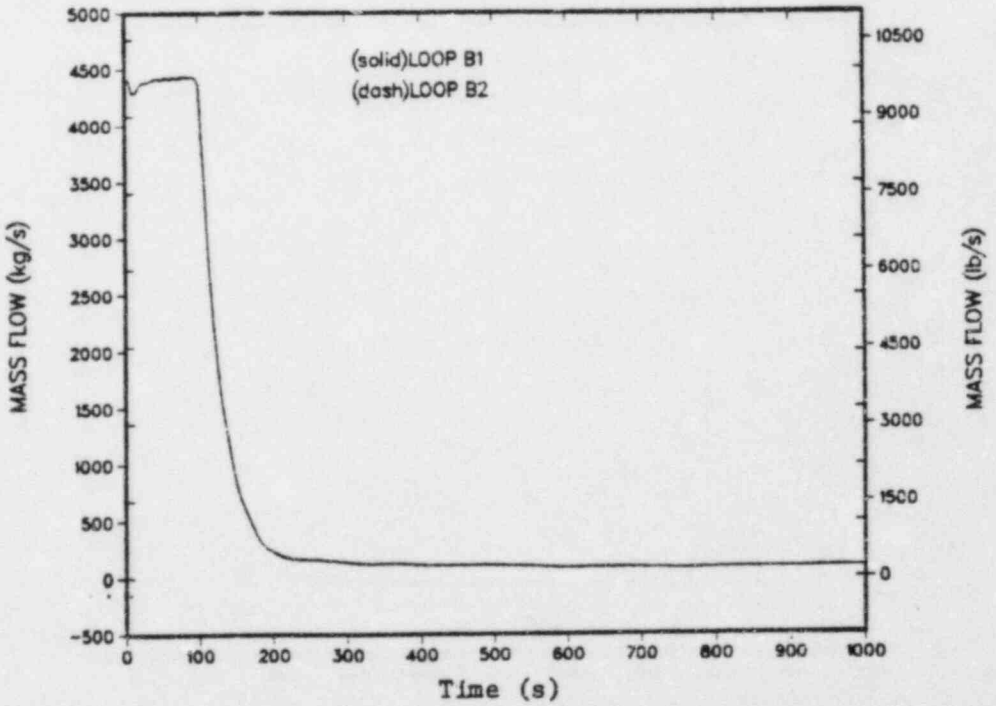

Fig. 130.
Hot-leg liquid temperatures - loops A and B.

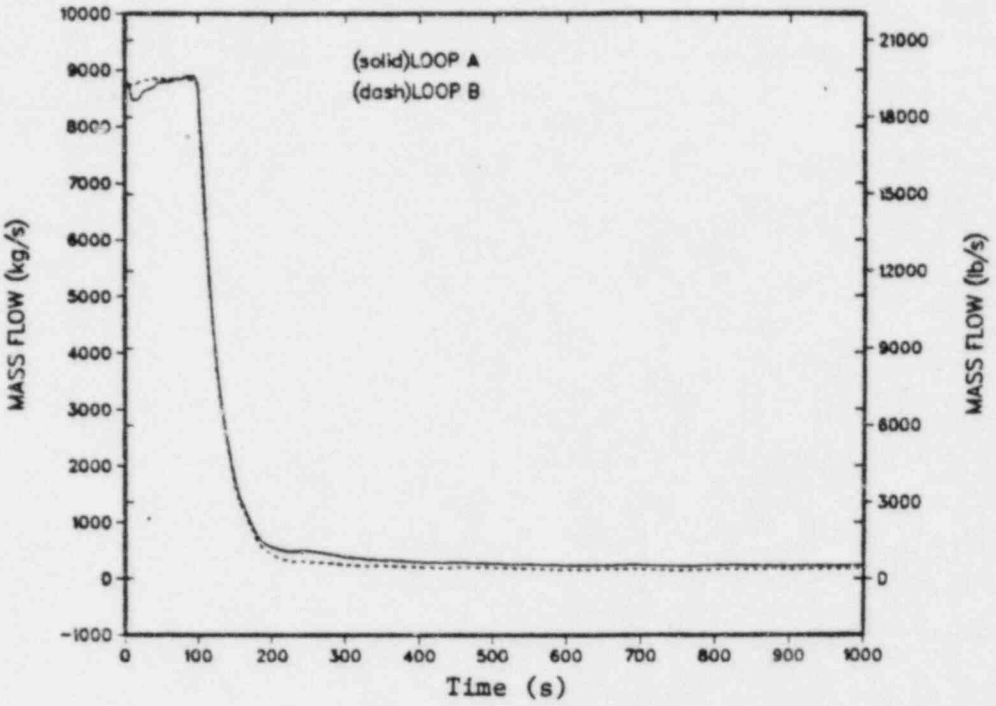

Fig. 131.
Cold-leg mass flows - loops A1 and A2.

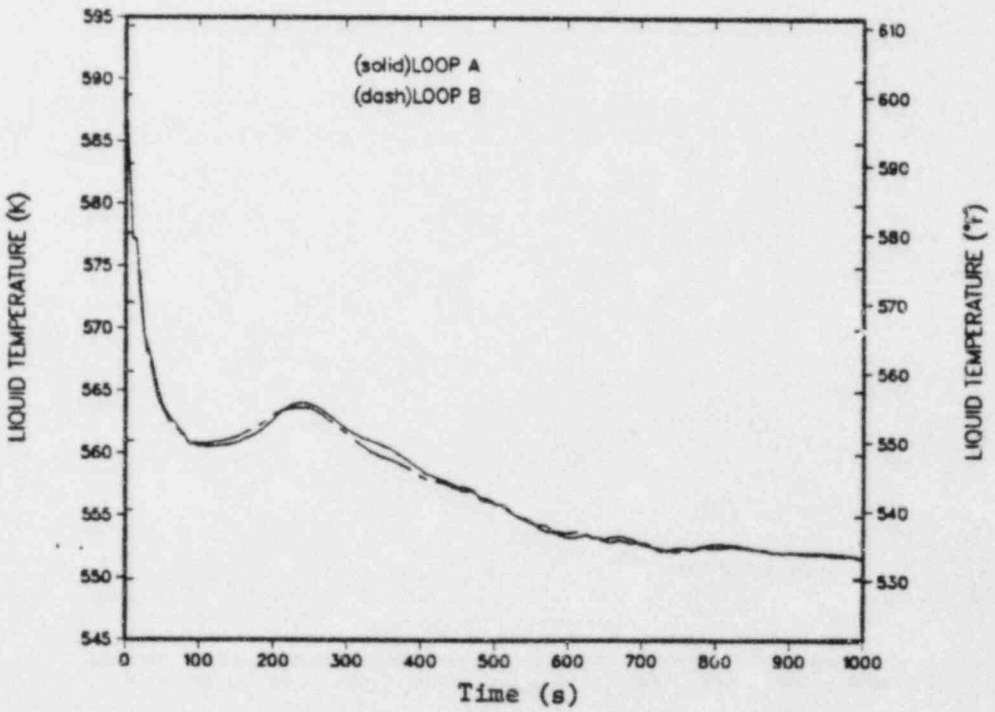

Fig. 132.
Cold-leg mass flows - loops B1 and B2.

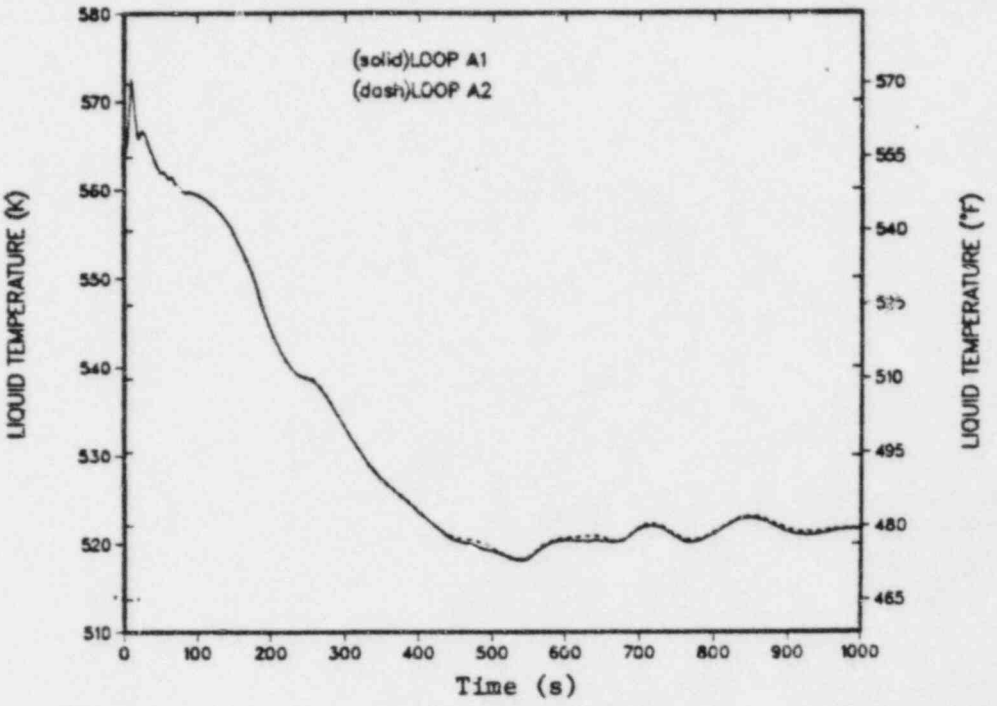

Fig. 133.
Cold-leg liquid temperatures - loops A1 and A2.

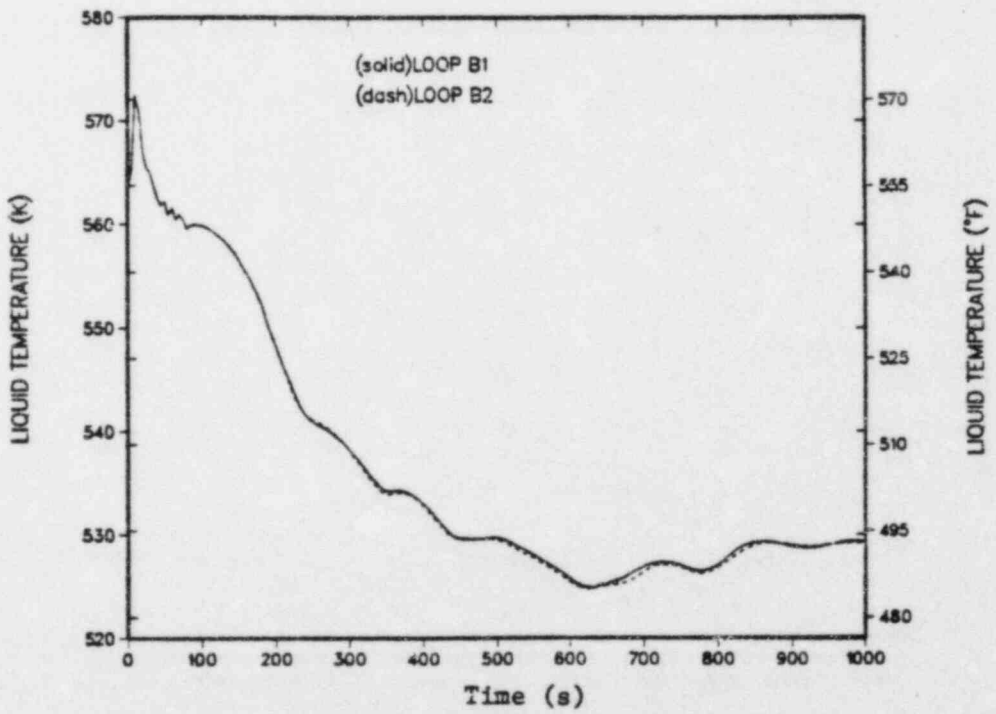

Fig. 134.
Cold-leg liquid temperatures - loops B1 and B2.

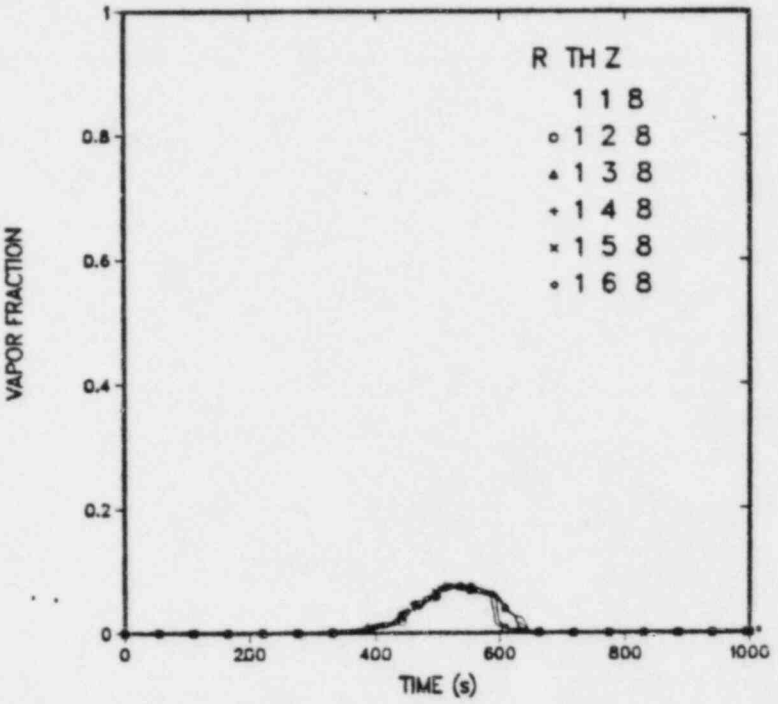

Fig. 135.
Candy-cane void fractions - loops A and B.

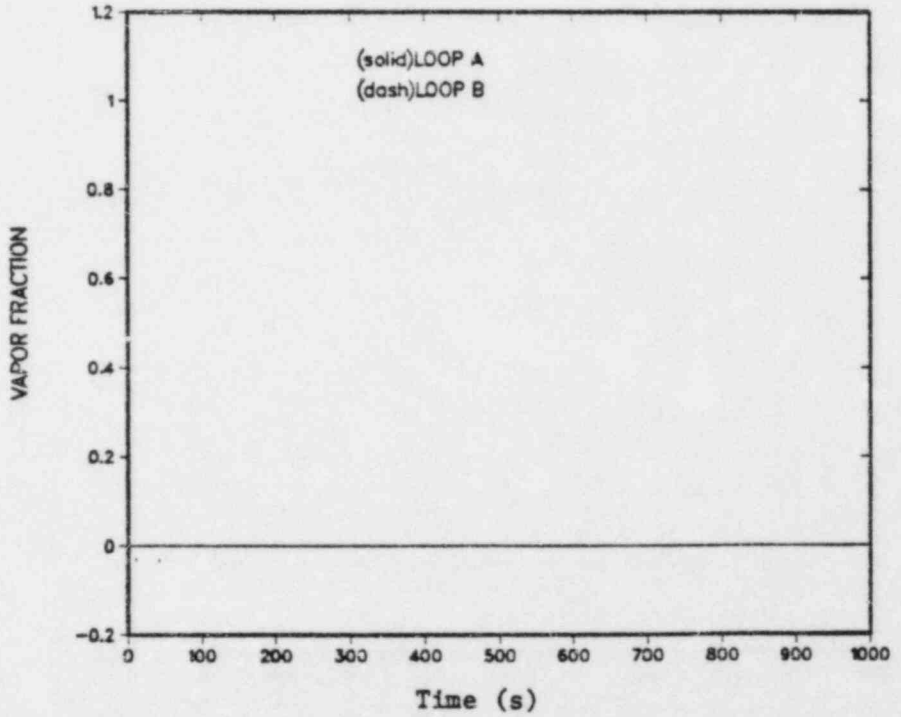

Fig. 136.
Vessel upper-plenum void fractions - all azimuthal cells.

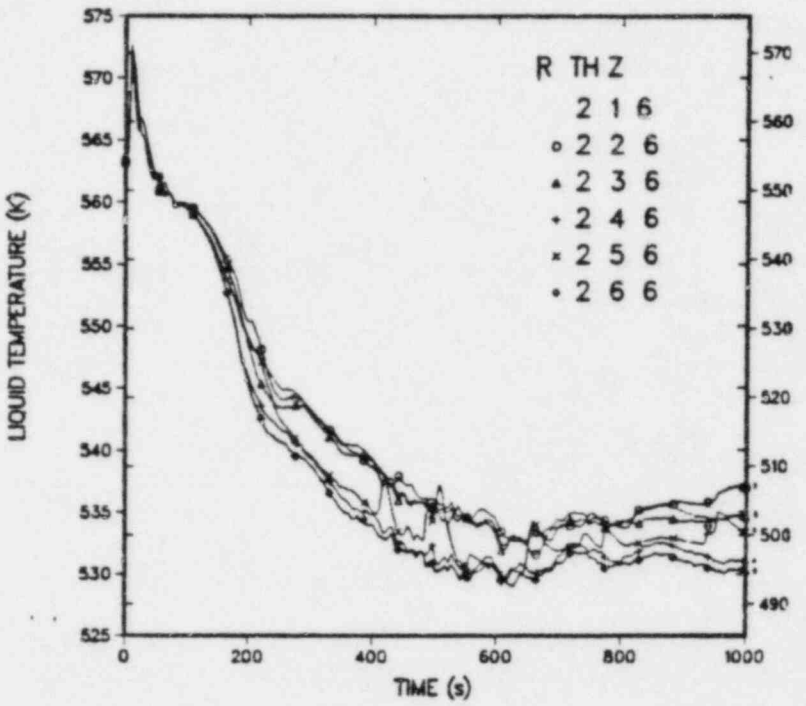

Fig. 137.
Downcomer liquid temperatures at vessel axial level 6 (all azimuthal sectors).

D. Turbine Bypass-Valve Failures

1. One Bank of Two TBVs

a. Introduction and Summary. For this study, the performance of the Oconee-1 plant following a secondary-side depressurization was predicted. The base case analyzed was the failure of one bank of TBVs to reseat after initially opening following reactor and turbine trips from full power. Additional failures assumed for the base case were failure of the level control in the affected steam generator, failure of the operator to restart the RCPs, and failure of the operator to throttle the HPI system. The lowest downcomer liquid temperature (~458 K) and hence the smallest margin against the NDT limit was calculated for the base case. Repressurization of the primary system to the PORV setpoint was also predicted for the base case. In additional parametric cases that examined a reduced number of failures, a greater margin against the NDT limit was calculated.

b. Model Description. The primary-system model used for the TBV transients is shown in Fig. 1. On the secondary side, the main-steam lines from each steam generator to the TSVs are modeled. The turbine bypass lines lead to the condenser, which is input as a pipe with a constant-temperature heat sink. The condensate collects in the hotwell. The hotwell and condensate-booster

pumps deliver the condensate to the feedwater heaters. The main-feed pumps then pump the feedwater to the steam generators.

The significant features of the TBV failure transient are (one bank of two TBVs):

1. Reactor and turbine trips cause the TBVs to open.
2. Failure of one bank of TBVs to close causes a secondary-side depressurization through the affected loop.
3. Failure of the SG liquid-level control in the affected loop follows initiation of EFW.
4. The operator does not restart the RCPs.
5. The operator does not throttle the HPI.

Two parametric cases were also calculated. The steam-generator liquid-level control in the affected loop operates correctly in Case 1. The steam generator liquid-level control also operates correctly in Case 2. In addition, operator actions to restart the RCPs and throttle the HPI are permitted if the primary system subcooling-monitor trip points are exceeded.

c. Results.

i. Base Case. Table XXI presents the calculated event times for the base case. Following the reactor and turbine trips, the TSVs closed (0.5 s), secondary pressures rose, and the TBVs opened for the first time at ~4 s. The secondary pressure peaked and then decreased permitting the loop-B TBV to reseat at ~45 s. However, the loop-A TBV failed to reseat causing the secondary to depressurize at a faster rate than loop B.

The pressurizer pressure is presented in Fig. 138. The PORV opened at ~1037 s when its pressure setpoint of 16.99 MPa was exceeded. The PORV then cycled for the remainder of the calculated transient to maintain the primary system pressure at or below the PORV setpoint.

The loop-A (affected loop) and loop-B secondary pressures are shown in Figs. 139 and 140, respectively. The stuck-open TBV in loop A caused that loop to depressurize both more rapidly than loop A and to a lower level. MFW flows for both loops A and B are shown in Figs. 141 and 142, respectively. Per the problem specifications[3] the ICS failed to run back MFW to the loop-A SG and thus the flow did not decrease until the MFW trip on high liquid level in the loop-A SG occurred at ~61 s. The ICS ran back MFW flow to loop B by shutting the MCFV and allowing MFW flow only through the SUFCV. The small oscillatory flow in loop A was related to variations in the loop-A SG secondary-side liquid

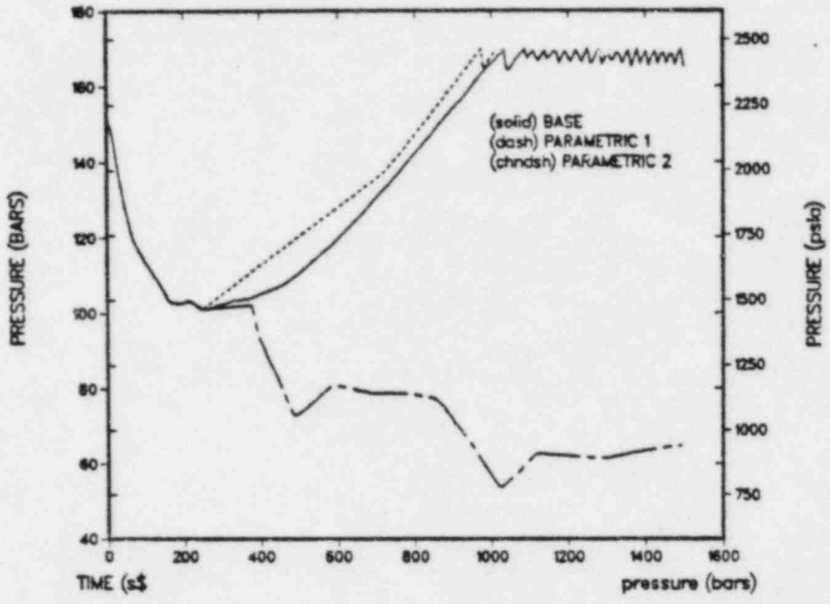

Fig. 138.
Pressurizer pressure.

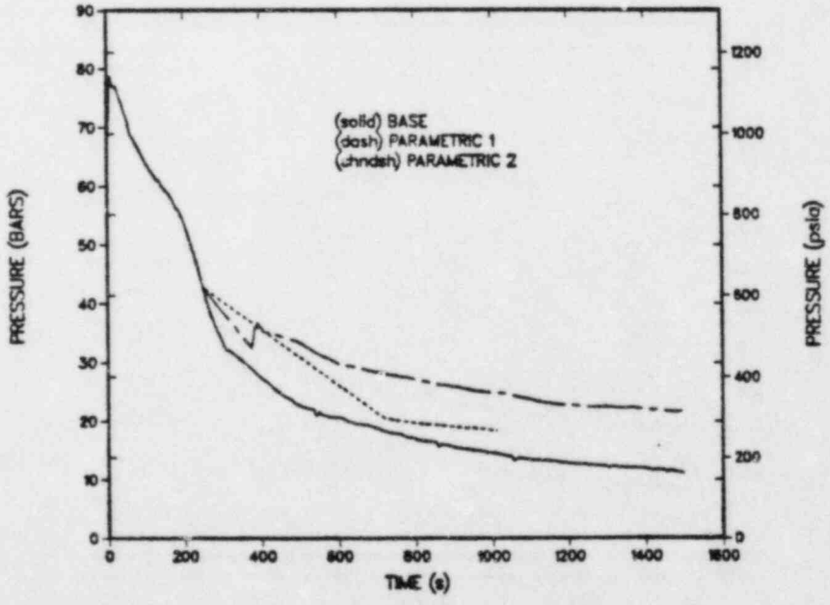

Fig. 139.
Steam-generator-secondary pressure - Loop A.

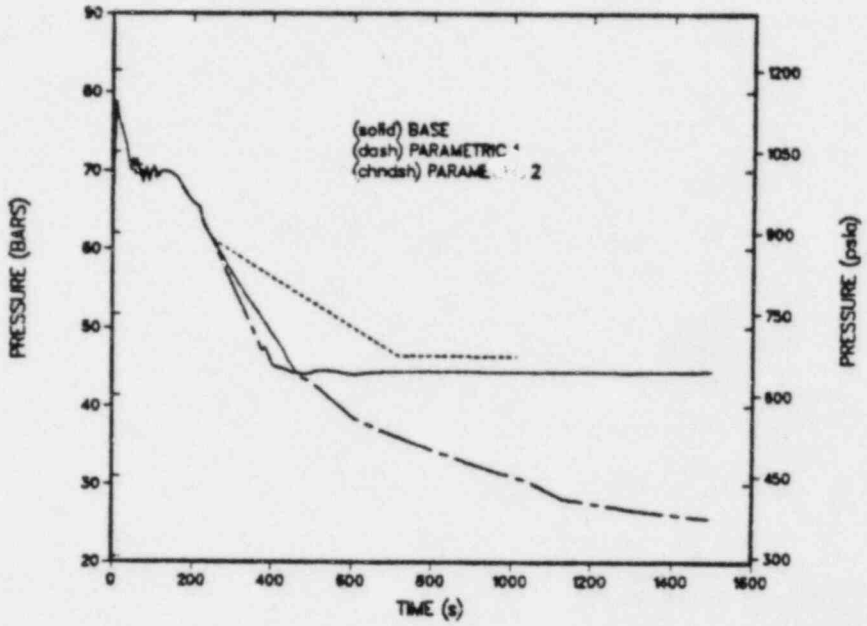

Fig. 140.
Steam-generator-secondary pressure - loop B.

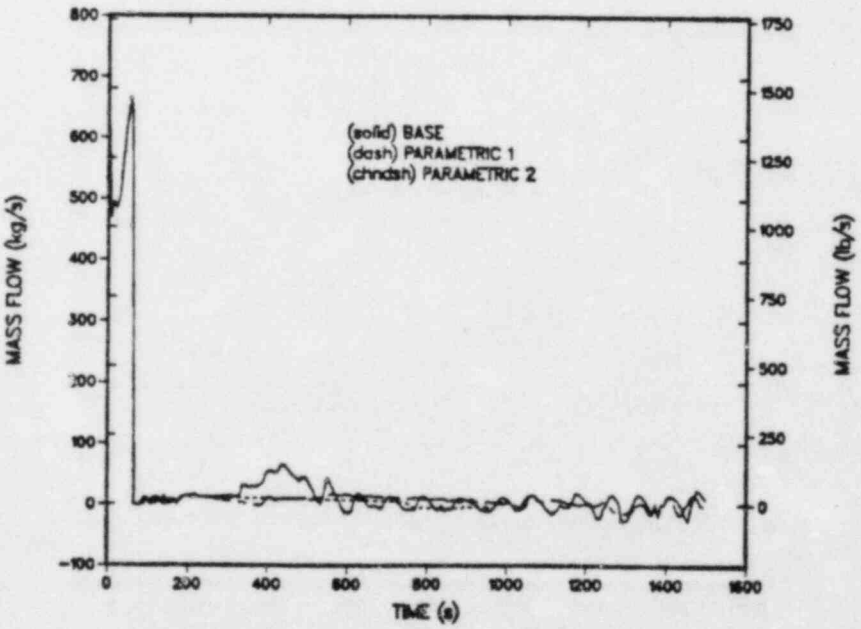

Fig. 141.
Main-feedwater flow - loop A.

TABLE XXI

TBV EVENT SEQUENCE

Base Case

	Event	Time (s)
1.	Turbine and reactor trip	0.5
2.	Turbine-stop valves close	0.5
3.	TBV loop A opens (fails to reseat thereafter)	4.1
4.	TBV loop B opens	4.3
5.	MFW pump trip on high SG A liquid level	60.7
6.	HPI started following trip on low pressure	153.1
7.	RCPs trip on 30 s delay after HPI actuation	183.0
8.	Feedwater realignment trip	183.0
9.	Main-flow control valves overriding trips	183.0
10.	EFW pump on	209.1
11.	Loop-B EFW valve shut on high SG liquid level	460.8
12.	PORV opens	1036.7

level. Loop-A and -B MFW liquid temperatures are presented in Fig. 143 and 144, respectively. An increase in the loop-B temperature followed the feedwater realignment trip at ~183 s. The temperature stabilized at the saturation temperature after the SG secondary was isolated at ~460 s.

EFW flows through loops A and B are shown in Figs. 145 and 146, respectively. The loop-B flow decreased sharply at ~460 s when the loop-B EFW valve shut as the SG-B liquid level exceeded 6.2 m (240 in). A residual flow continued through the loop-B SUFCV until it shut under ICS action at ~600 s. A higher flow through loop A was predicted because TBV A was open producing a larger pressure drop potential for flow through loop A. Loop-A and -B EFW liquid temperatures are presented in Figs. 147 and 148, respectively. A rapid rise in the loop-B fluid temperature followed closure of the EFW-B valve. A small flow of hotter fluid through the SUFCV produced the temperature rise.

The water inventories in the loop-A and -B SG secondaries are shown in Figs. 149 and 150, respectively. The inventory in the loop-A SG rose before ~60 s because the ICS failed to run back the MFW. The MFW trip occurred at

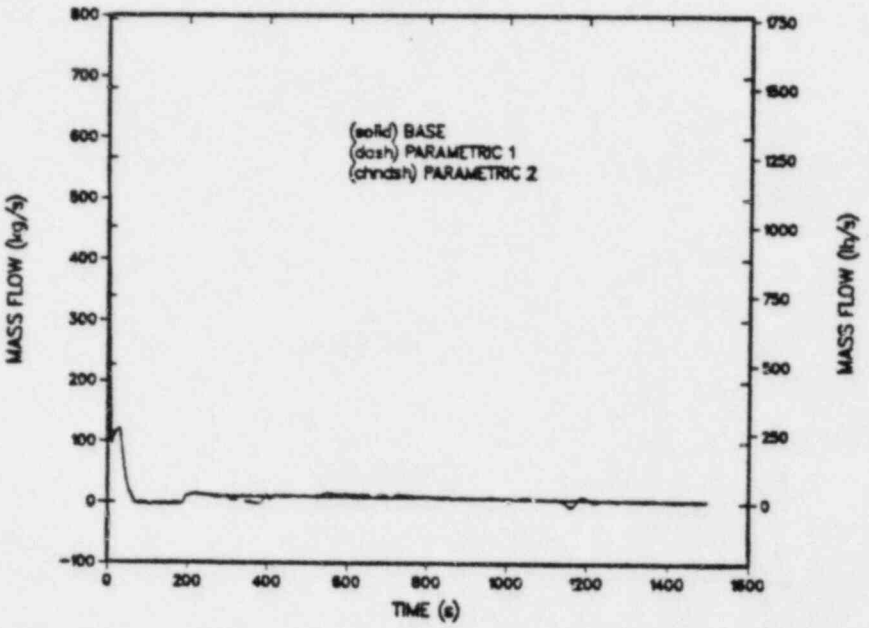

Fig. 142.
Main-feedwater flow - loop B.

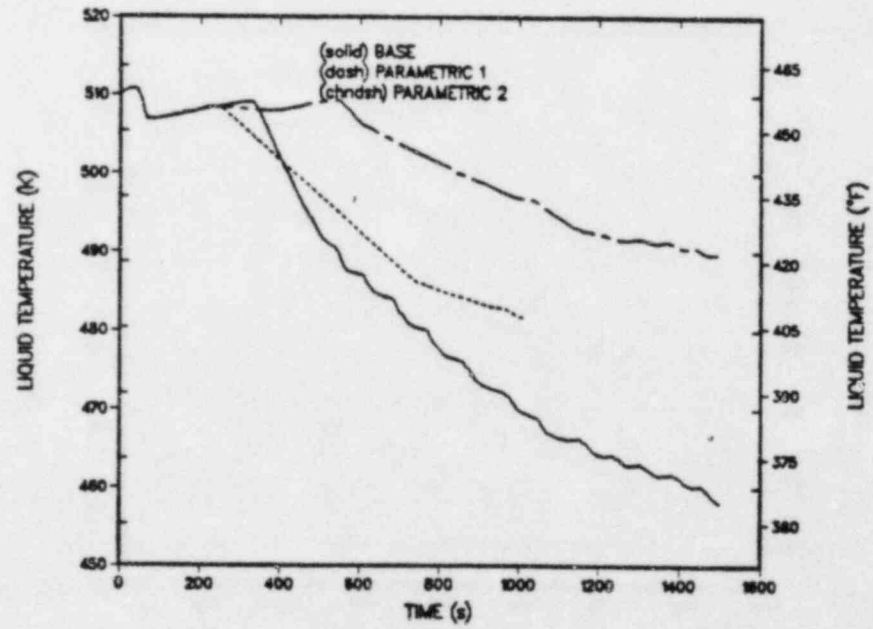

Fig. 143.
Main-feedwater liquid temperatures - loop A.

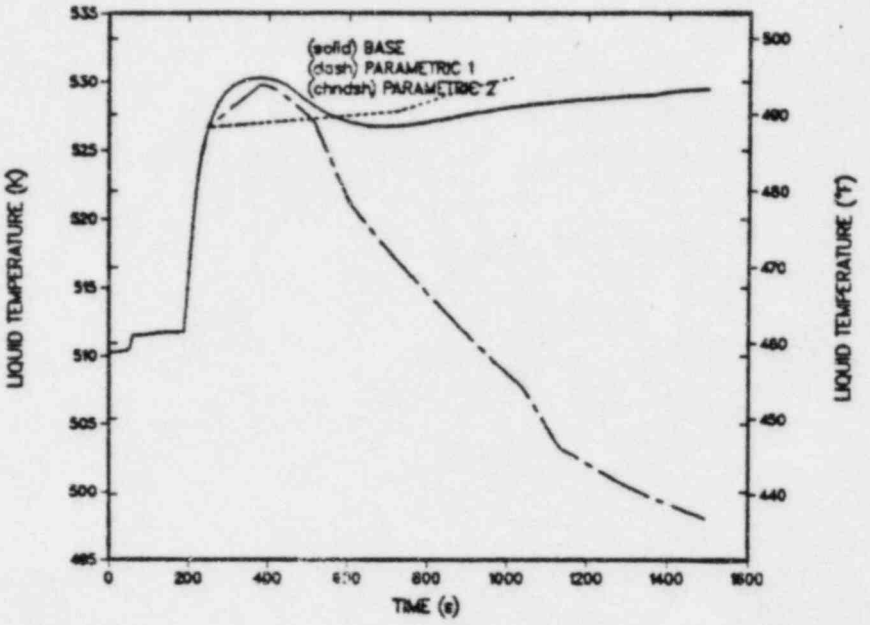

Fig. 144.
Main-feedwater liquid temperatures - loop B.

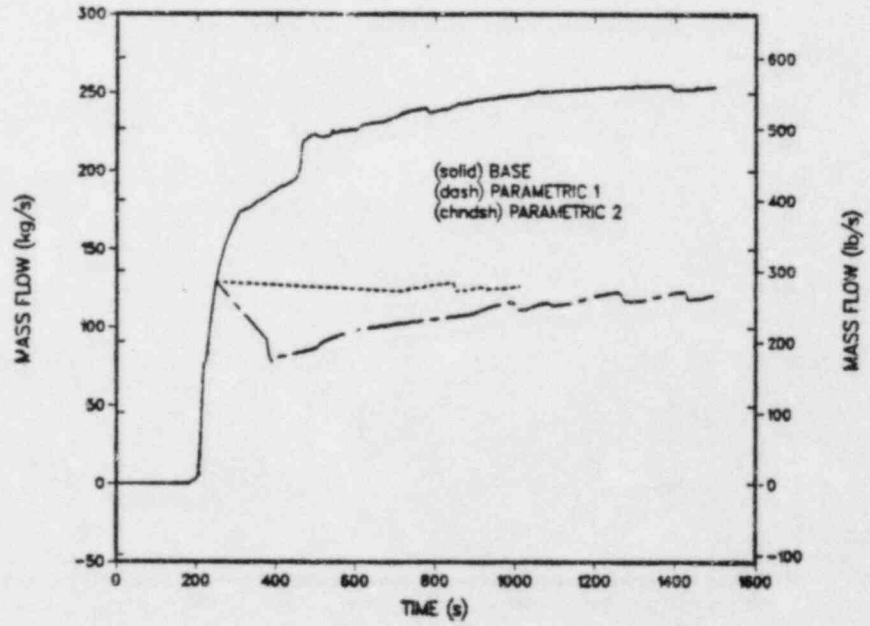

Fig. 145.
Flow through emergency-feedwater header - loop A.

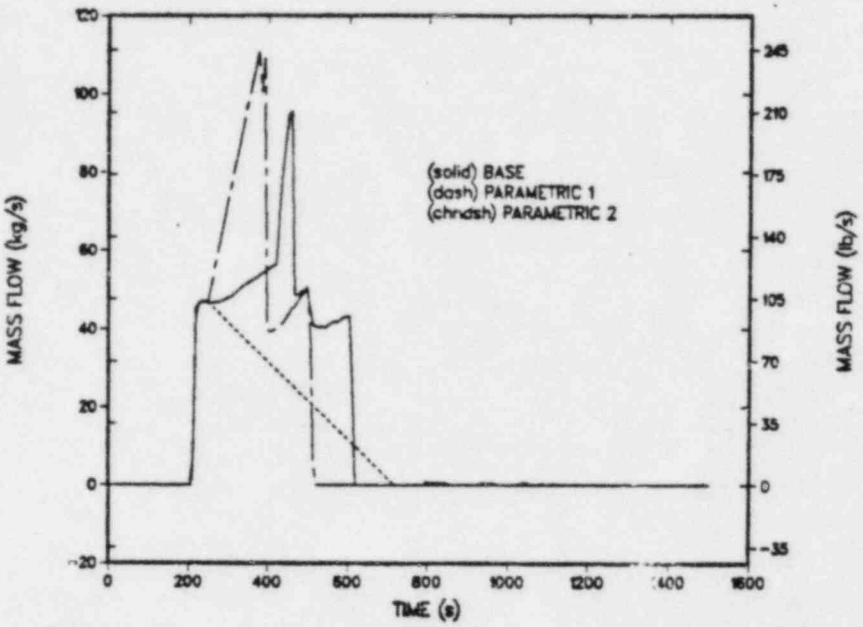

Fig. 146.
Flow through emergency-feedwater header - loop B.

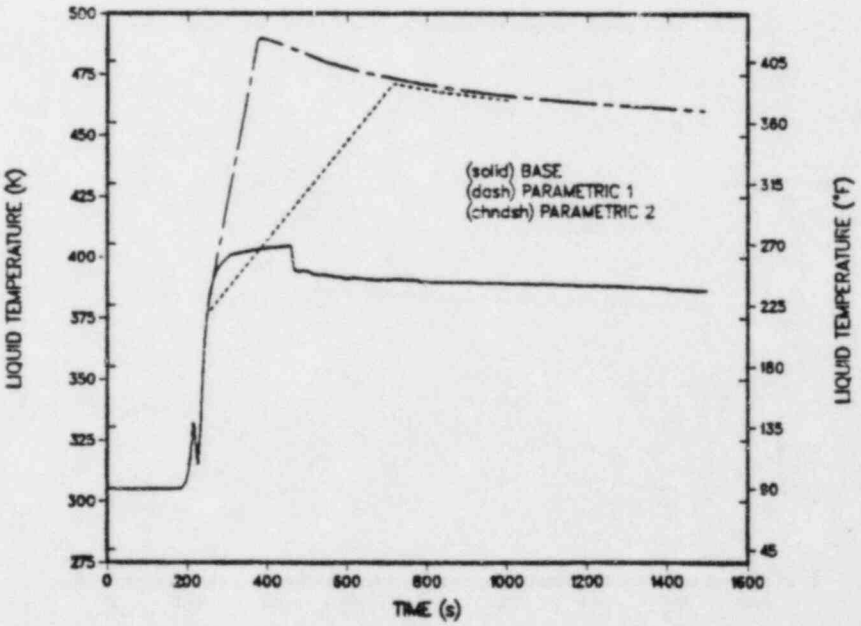

Fig. 147.
Liquid temperatures in the emergency-feedwater header - loop A.

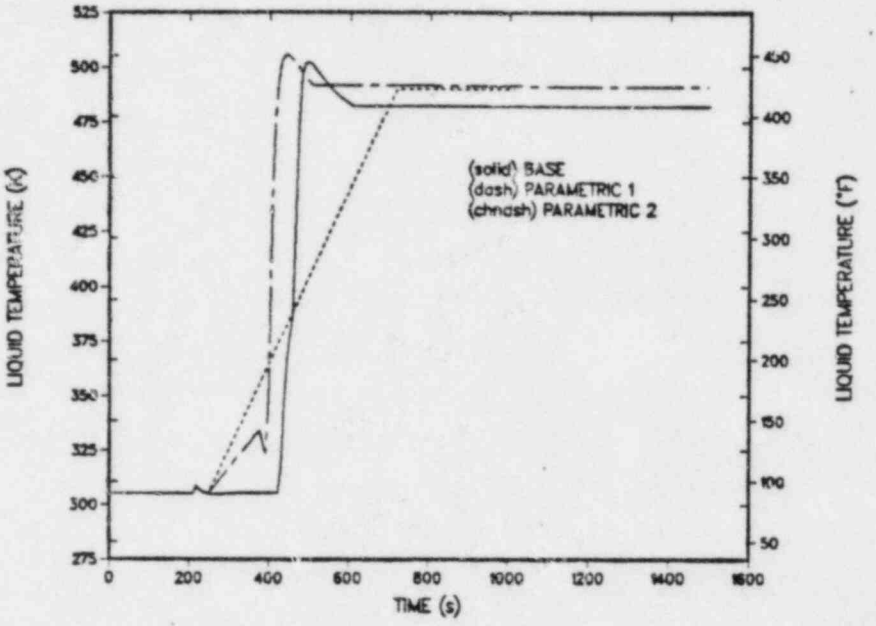

Fig. 148.
Liquid temperatures in the emergency-feedwater header - loop B.

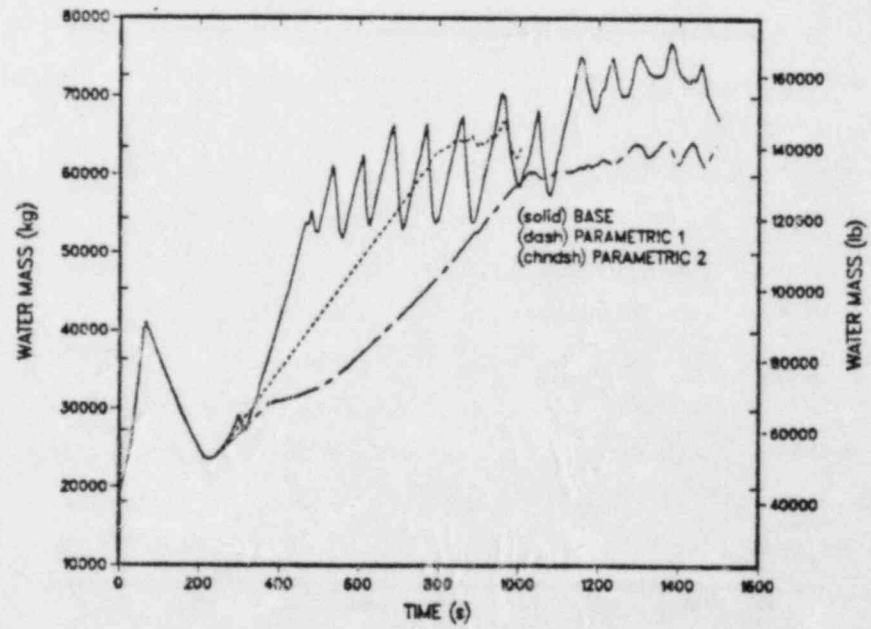

Fig. 149.
Steam-generator-secondary inventory - loop A.

~60 s, and the liquid inventory boiled off until the EFW pump actuated at ~210 s. With no liquid-level control, the steam-generator secondary continued to fill and oscillations developed as the liquid level reached ~12.4 m. The transient history of the loop-B SG was very different. There was no initial increase in SG inventory because the ICS reduced flow. Closure of the loop-B SUFCV by ICS action at ~600 s was evident.

Mass flows through the primary-loop hot legs are shown in Figs. 151 and 152, respectively. Following the RCP trips at ~183 s, the flows coasted down and natural circulation was established. A higher flow rate was established in loop A because of the higher SG temperature difference resulting from the failure of TBV A to reseat. Similar phenomena were observed in the cold legs as shown in Figs. 153 through 156, respectively. The corresponding cold-leg temperatures are presented in Figs. 157 through 160, respectively. Vapor fractions in the loop-A and -B candy-cane sections are shown in Figs. 161 and 162, and it can be seen that no voiding occurred during the transient. The pressurizer water level is presented in Fig. 163.

Downcomer liquid temperatures for the base case are presented in Fig. 164 at the top axial downcomer level (just below the cold-leg nozzles). At the end of the calculated transient (1500 s), the minimum temperature was ~458 K.

ii. Parametric Case 1. A single specification was changed for this parametric study. The loop-A SG level control following EFW activation was assumed to operate to maintain the secondary-liquid level at or below 6.2 m. It was assumed that the operator does not restart the RCPs and does not throttle the HPI. The event sequence for this case is presented in Table XXII. The event sequence was identical to the base case through event 10. At ~290 s the loop-A EFW valve shut on high SG-A secondary-liquid level. The loop-B EFW valve shut on high SG-B secondary-liquid level as in the base case. However, the PORV opened ~60 s early in Case 1 because of reduced heat transfer to SG A.

Results for Case 1 are presented in Figs. 138 through 163 and may be compared directly to the base case. The general trends of Case 1 were similar to the base case. The major differences appeared in the secondary side of loop A, and were caused by shutting the loop-A EFW valve on high SG liquid level at ~290 s. The reduced EFW flow affected the primary side also. Compared to the base case, the pressurizer pressure increased more rapidly to the PORV setpoint as shown in Fig. 138. This was caused by reduced primary-to-secondary heat transfer associated with the reduced loop A steam-generator-secondary water inventory (Fig. 149). The steam-generator-secondary pressure histories for loops A and B (Figs. 139 and 140) were similar because the level control

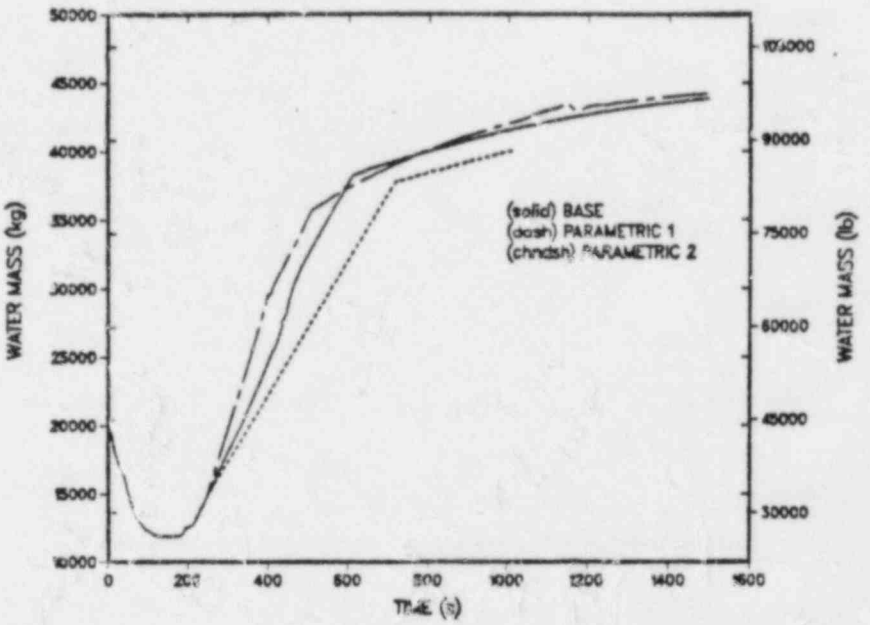

Fig. 150.
Steam-generator-secondary inventory - loop B.

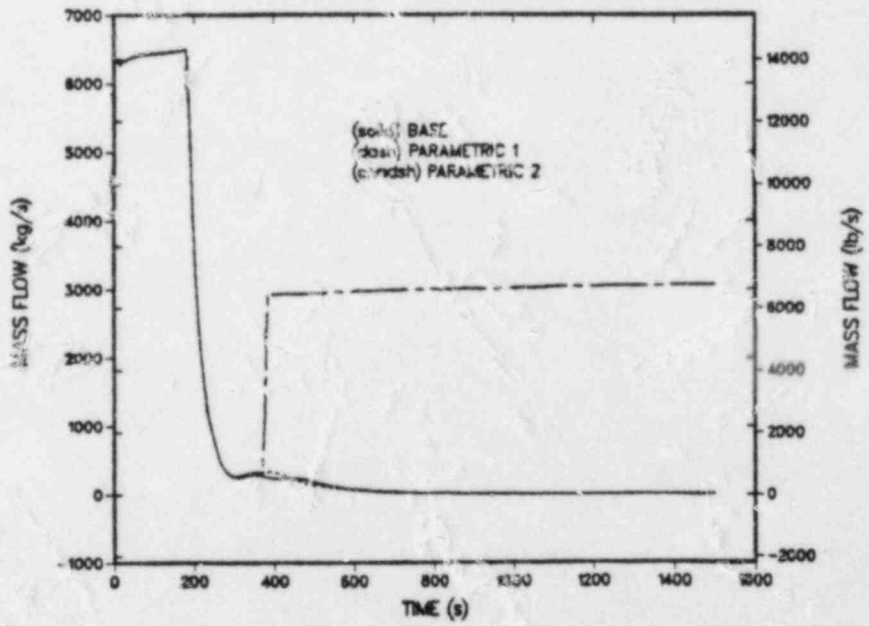

Fig. 151.
Hot-leg flow - loop A.

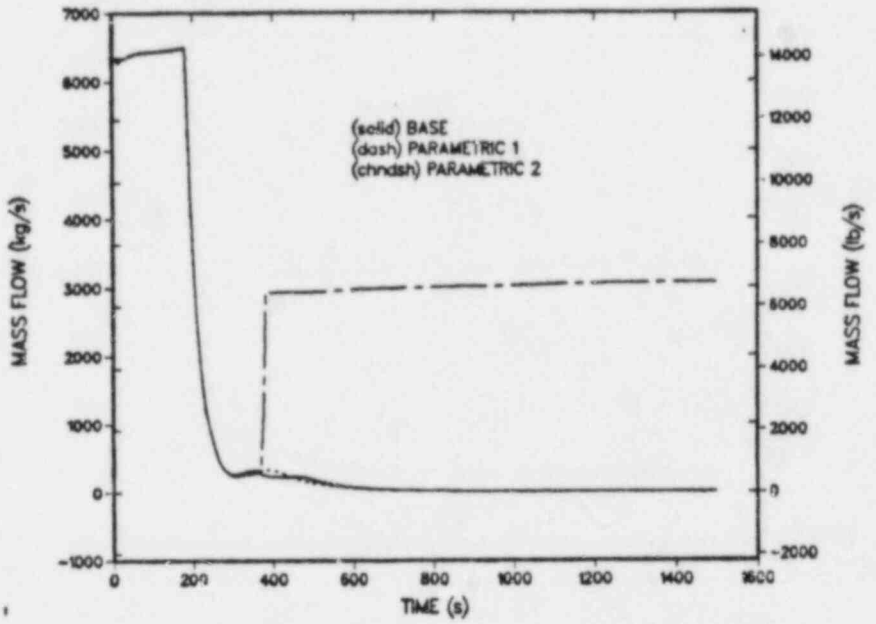

Fig. 152.
Hot-leg flow - loop B.

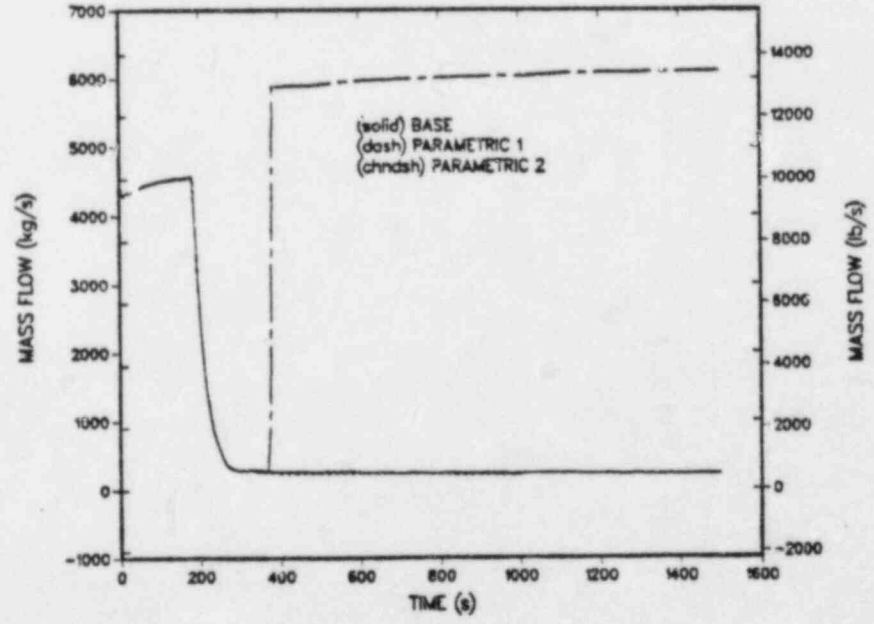

Fig. 153.
Cold-leg flow - loop A1.

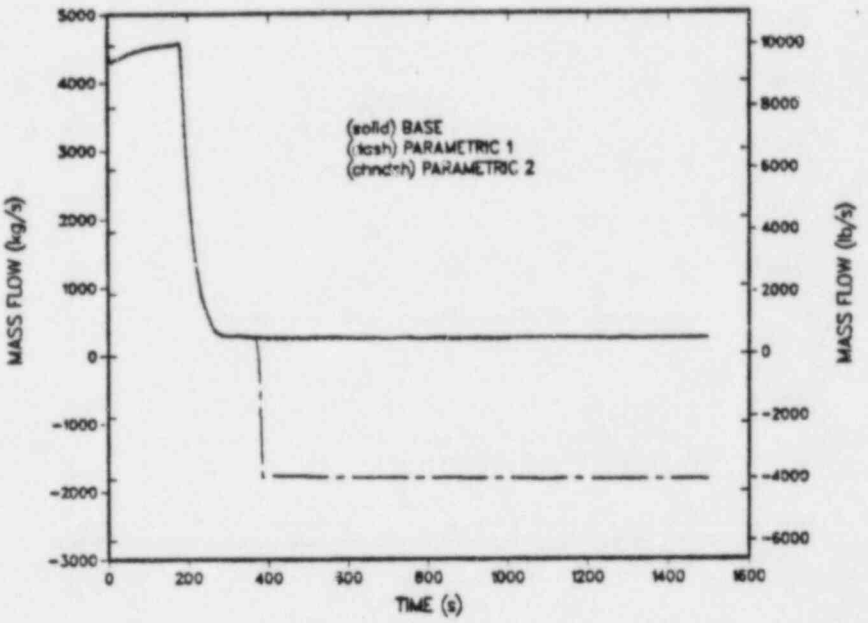

Fig. 154.
Cold-leg flow - loop A2.

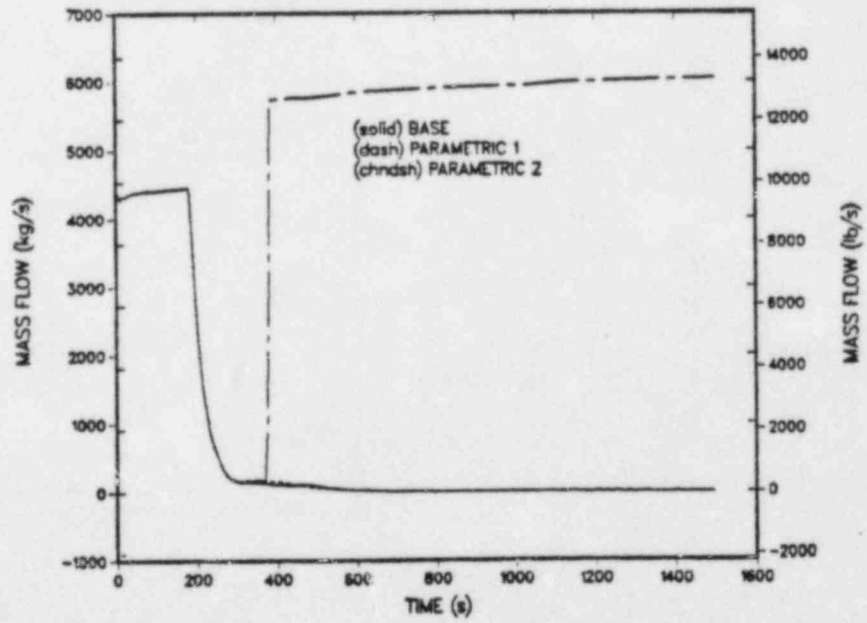

Fig. 155.
Cold-leg flow - loop B1.

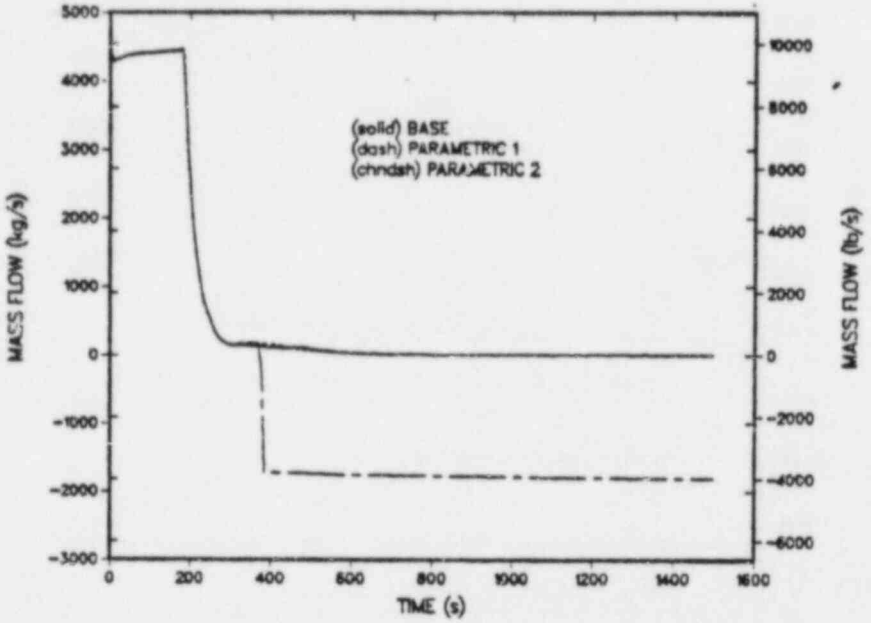

Fig. 156.
Cold-leg flow - loop B2.

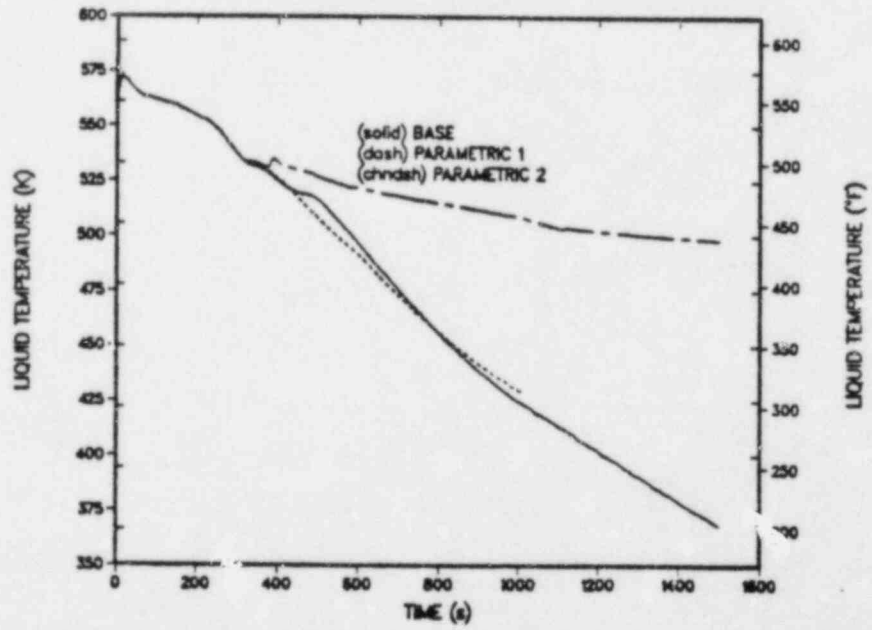

Fig. 157.
Cold-leg liquid temperatures - loop B1.

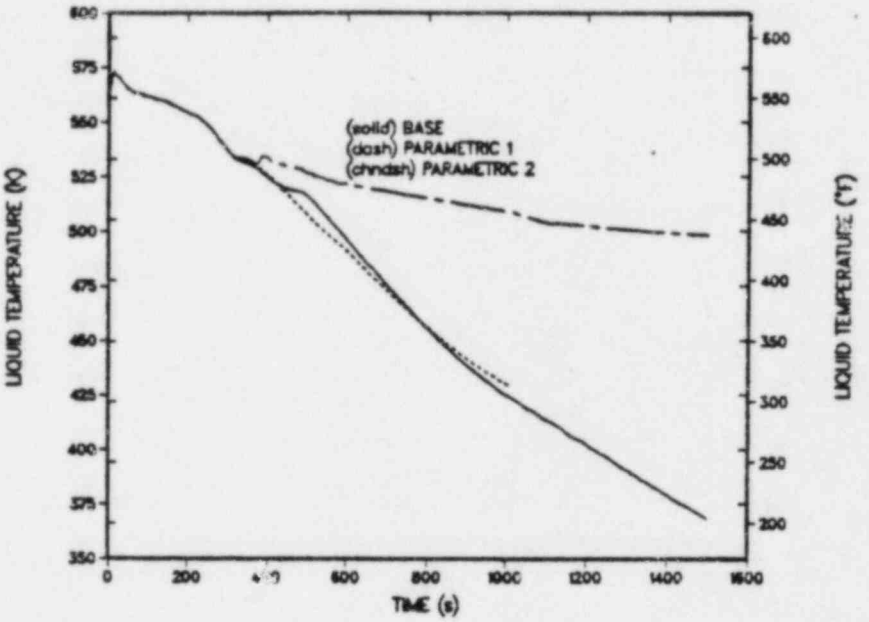

Fig. 158.
Cold-leg liquid temperatures - loop B2.

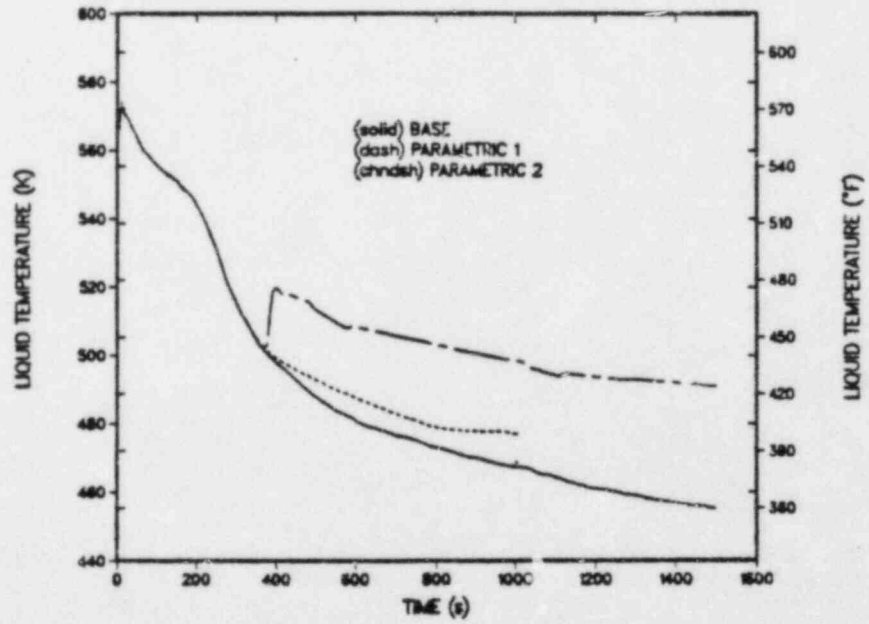

Fig. 159.
Cold-leg liquid temperatures - loop A1.

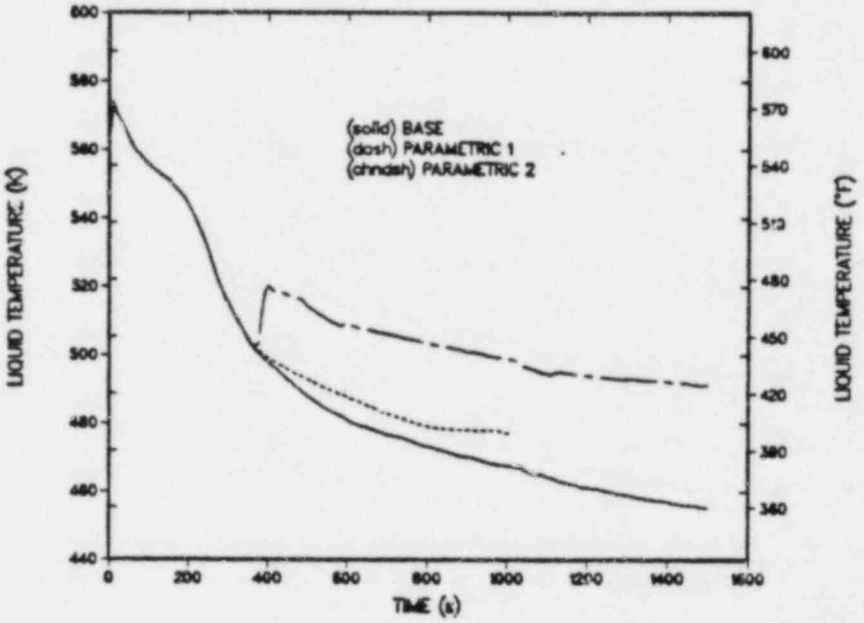

Fig. 160.
Cold-leg liquid temperatures - loop A2.

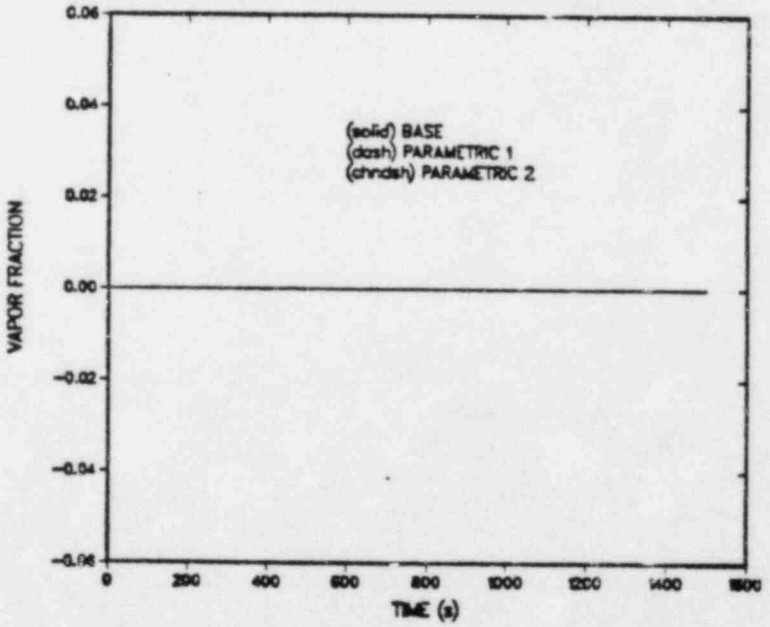

Fig. 161.
Candy-cane vapor fraction - loop A.

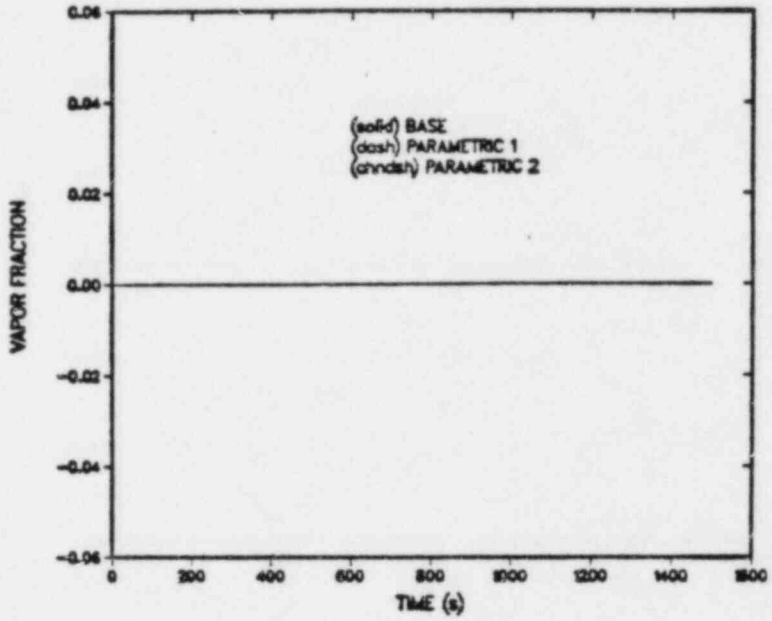

Fig. 162.
Candy-cane vapor fraction - loop B.

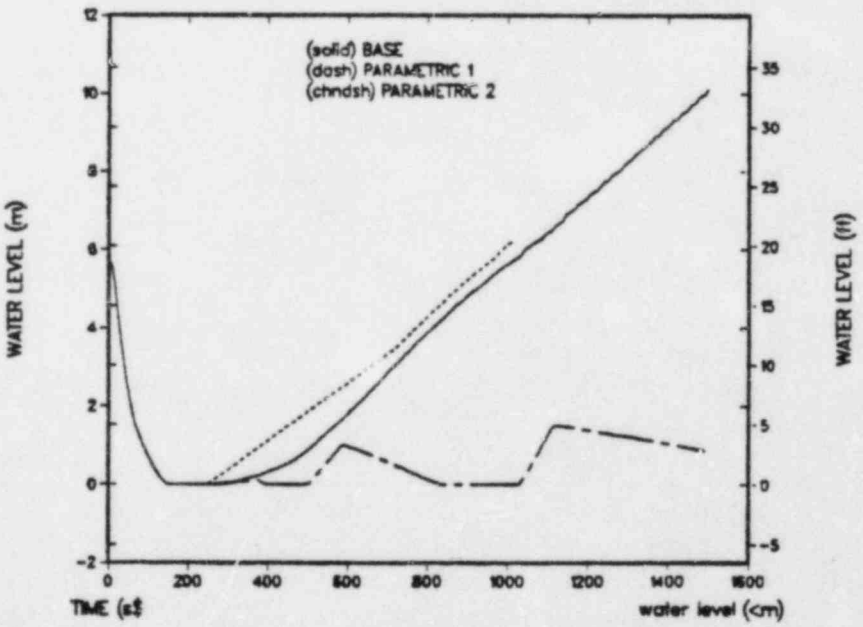

Fig. 163.
Pressurizer water level.

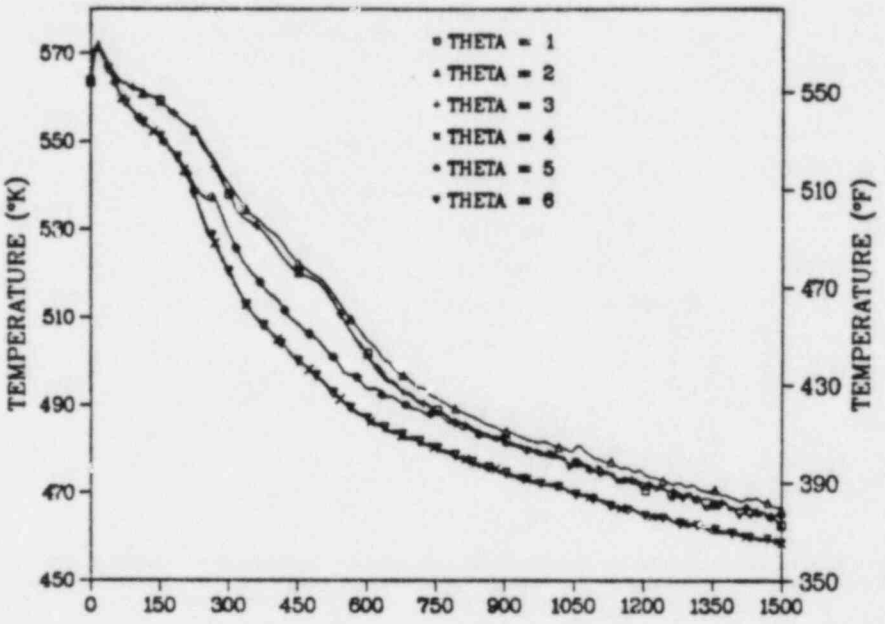

Fig. 164.
Downcomer liquid temperatures (base case) at vessel axial level 6 (all azimuthal sectors).

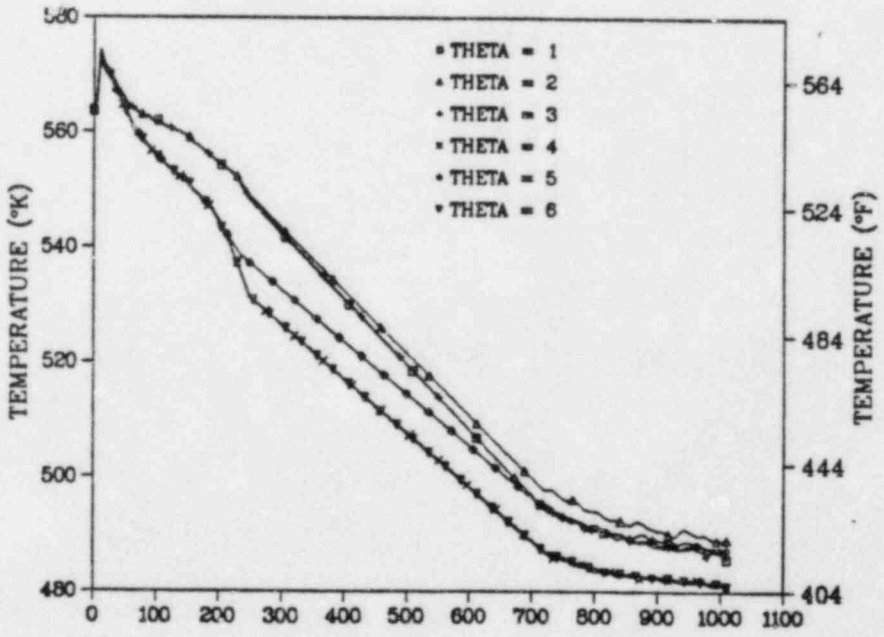

Fig. 165.
Downcomer liquid temperatures (parametric case 1) at vessel axial level 6 (all azimuthal sectors).

TABLE XXII

TBV EVENT SEQUENCE
Parametric Case 1

Event	Time(s)
1-10. Same as base case	0-209.1
11. Loop-A EFW valve shut on high SG liquid level	290.0
12. Loop-B EFW valve shut on high SG liquid level	460.8
13. PORV opens	975.0

operated on both steam generators. The closure of the loop A EFW valve limits the flow through the emergency-feedwater header as shown in Fig. 145. The remaining flow through the header comes through the loop-A SUFCV. The loop B emergency-feedwater header flow (Fig. 146) decreased to zero shortly after ~700 s with the closure of the SUFCV by ICS action. Downcomer liquid temperatures for Case 1 are presented in Fig. 165 at the top axial downcomer level (just below the cold-leg nozzles). At the end of the calculated transient (1015 s), the minimum temperature was ~482 K. The base case minimum temperature at the same time was ~471 K. The slightly increased downcomer temperature for Case 1 was caused by the reduced heat transfer to the loop-A steam-generator secondary with its reduced liquid inventory.

iii. Parametric Case 2. The specifications for this case differed from the base case as follows: the SG-A secondary liquid-level control did not fail; restart of one RCP in each loop was permitted on attainment of 75 F subcooling; and throttling the HPI was permitted on attainment of 75 ± 12.5 F subcooling. The event sequence for this transient is presented in Table XXIII. Events 1-10 were identical to the base case. One RCP in each loop was restarted at ~383 s after a 30 s delay following the subcooled-monitor trip. The HPI was throttled at ~485 s after a second subcooled-monitor trip at 75 ± 12.5 F subcooling.

Results for Case 2 are presented in Figs. 138 through 163 and may be compared directly to the base case. Case 2 displayed significant differences from the base case. A major consequence of throttling the HPI was that primary-system repressurization did not occur and thus the PORV did not open. The absence of repressurization is seen in Fig. 138. Restart of the loop-A1 and -B1 RCPs can be observed in Figs. 153 and 155, respectively. Operation of the RCPs

TABLE XXIII

TBV EVENT SEQUENCE
Parametric Case 2

	Event	Time(s)
1-10.	Same as base case	0-209.1
11.	Loop-A EFW valve shuts	290.2
12.	Restart RCPs in one loop after subcooling-monitor trip	383.5
13.	Loop-B EFW valve shuts on high SG liquid level	395.1
14.	HPI throttled after subcooling-monitor trip	484.7

induced a reverse flow through the cold legs with non-operating pumps. The influence of RCP restart on heat transfer to the loop-A steam-generator secondary can be observed in Fig. 139. The pressure increased with RCP restart (~383 s) and remained higher than the other cases for the remainder of the calculated transient. The same influence can be seen in the loop-A steam-generator-secondary water inventory (Fig. 149) as a marked reduction in the rate-of-inventory increase caused by increased evaporation of inventory with RCP operation. A different trend was observed in the loop-B steam-generator-secondary water inventory (Fig. 150) with the Case 2 inventory generally exceeding the base-case inventory. This suggests decreased energy transfer to the loop-B steam generator. The summed heat transfer to the A- and B-loop steam generators is less than in the base case, and this is evident in the primary-system temperature. Downcomer liquid temperatures for Case 2 are presented in Fig. 166 at the top axial downcomer level (just below the cold-leg nozzles). At the end of the calculated transient (1500 s), the minimum temperature was ~491 K. This was ~33 K higher than the base case. At 1015 s the minimum temperature was ~499 K, which compared with ~482 K for Case 1 at the same time.

d. Conclusions. The response of the Oconee-1 plant to a secondary-system depressurization transient was simulated using TRAC-PF1. The transient studied was failure of one bank of turbine bypass valves (two valves) to close after initially opening following reactor and turbine trips. The base-case transient included additional failures caused by failure of the level control in the affected steam generator, no operator restart of the reactor-coolant pumps, and

no operator throttling of the HPI system. A minimum liquid temperature in the downcomer of ~458 K at 1500 s was calculated. If correct operation of the steam-generator level control, operator restart of the reactor-coolant pumps, and throttling of the HPI flow were assumed, the primary system did not repressurize, and a minimum downcomer liquid temperature of ~491 K was calculated at 1500 s.

2. Two Banks of Two TBVs

a. Introduction and Summary. This case differs from the previous case (Sec. III.D) by assuming two banks of TBVs fail instead of one bank. For this study, the performance of the Oconee-1 plant following a secondary-side depressurization was predicted. The base case analyzed was the failure of two banks of TBVs to reseat after initially opening following reactor and turbine trips from full power. Additional failures assumed for the base case were failure of the level control in the affected steam generators, failure of the operator to restart the RCPs, and failure of the operator to throttle the HPI system. The lowest downcomer liquid temperature (~445 K) and hence the smallest margin against the NDT limit was again calculated for the base case. Repressurization of the primary system to the PORV setpoint was also predicted

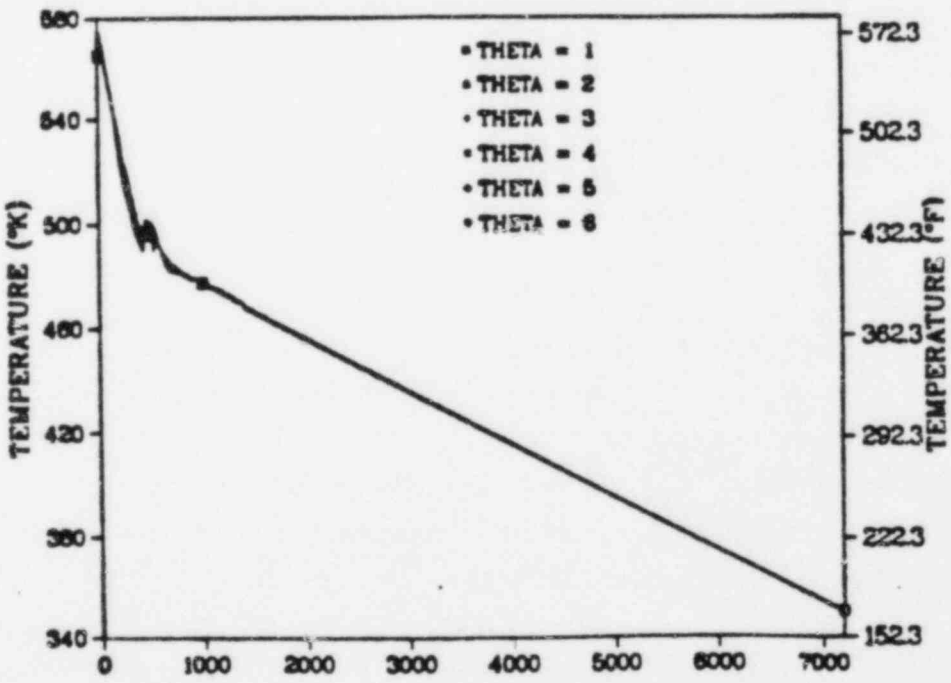

Fig. 166.
Downcomer liquid temperatures (parametric case 2) at vessel axial level 6 (all azimuthal sectors).

for the base case. For the parametric cases examined, a reduced number of failures were taken, and a greater margin against the NDT limit was calculated.

The same model used for the TBV transients described previously (Sec. III.D) was also used for this study. The significant features of the TBV failure transient are (two banks of two TBVs):

1. Reactor and turbine trips cause the TBVs to open.
2. Failure of two banks of TBVs to close causes a secondary-side depressurization through both loops.
3. Failure of the SG liquid-level control in the affected loops follows initiation of EFW.
4. The operator does not restart the RCPs.
5. The operator does not throttle the HPI.

Two parametric cases were also calculated. The steam-generator liquid-level controls in the affected loops operate correctly in Case 1. The steam generator liquid-level controls also operate correctly in Case 2. In addition, operator actions to restart the RCPs and throttle the HPI are permitted if the primary system subcooling-monitor trip points are exceeded.

b. Results.

i. Base Case. Table XXIV presents the calculated event times for the base case. Following the reactor and turbine trips, the TSVs closed (0.5 s), secondary pressures rose, and the TBVs opened for the first time at ~4 s. The secondary pressure peaked and then decreased, but both banks of TBVs (four valves; two on each line) failed to reseat. Continued flow through the TBVs resulted in a secondary-side depressurization.

The pressurizer pressure is presented in Fig. 167. The PORV opened at ~1175 s when its pressure setpoint was exceeded. The PORV then cycled for the remainder of the calculated transient to maintain the primary-system pressure at or below the PORV setpoint.

The loop-A and -B secondary pressures are shown in Figs. 168 and 169 respectively. The depressurization characteristics for the two loops were nearly identical. MFW flows for both loops are shown in Figs. 170 and 171, respectively. Per the problem specifications[3] the ICS failed to run back MFW to the SGs and thus the flows did not decrease until the MFW tripped on high SG B [illegible] level at ~91 s. A higher mass flow was predicted for loop B prior to tripping the MFW pump because the MFCV area under ICS control was ~6% greater

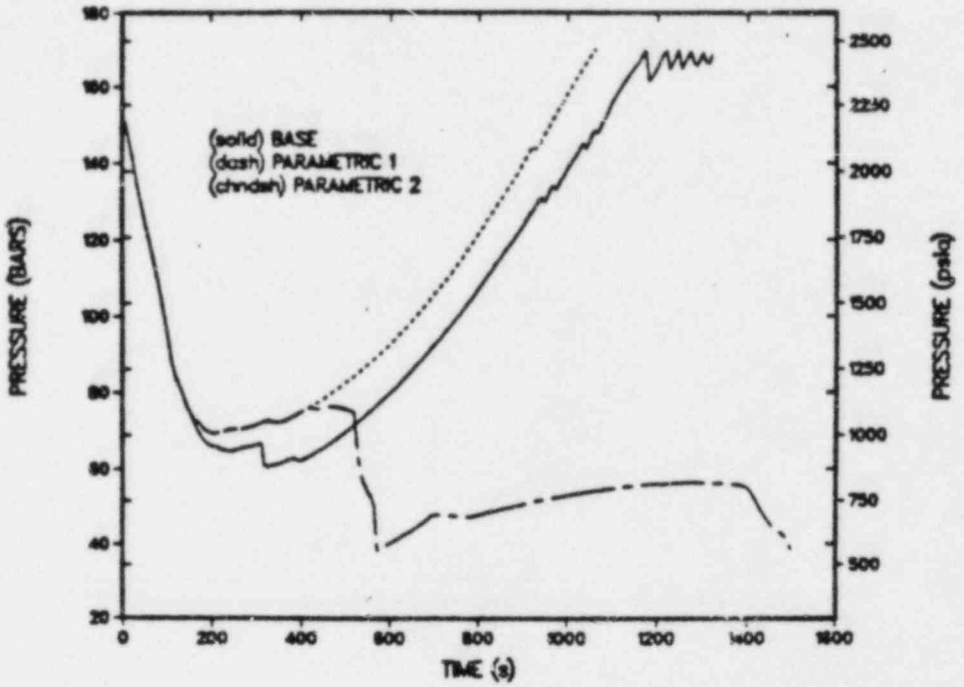

Fig. 167.
Pressurizer pressure.

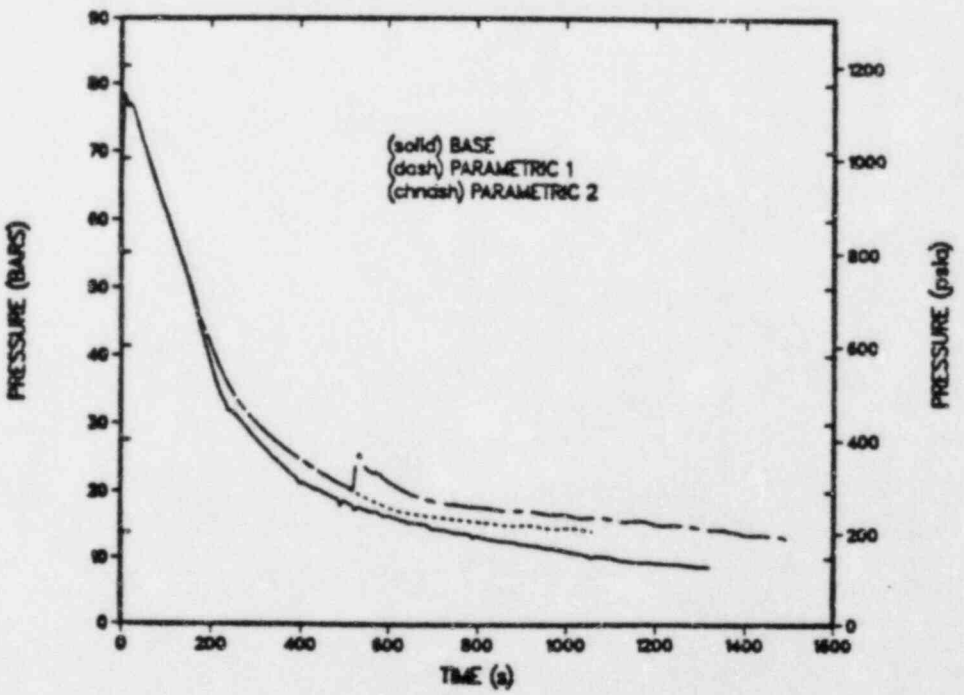

Fig. 168.
Steam-generator-secondary pressure - loop A.

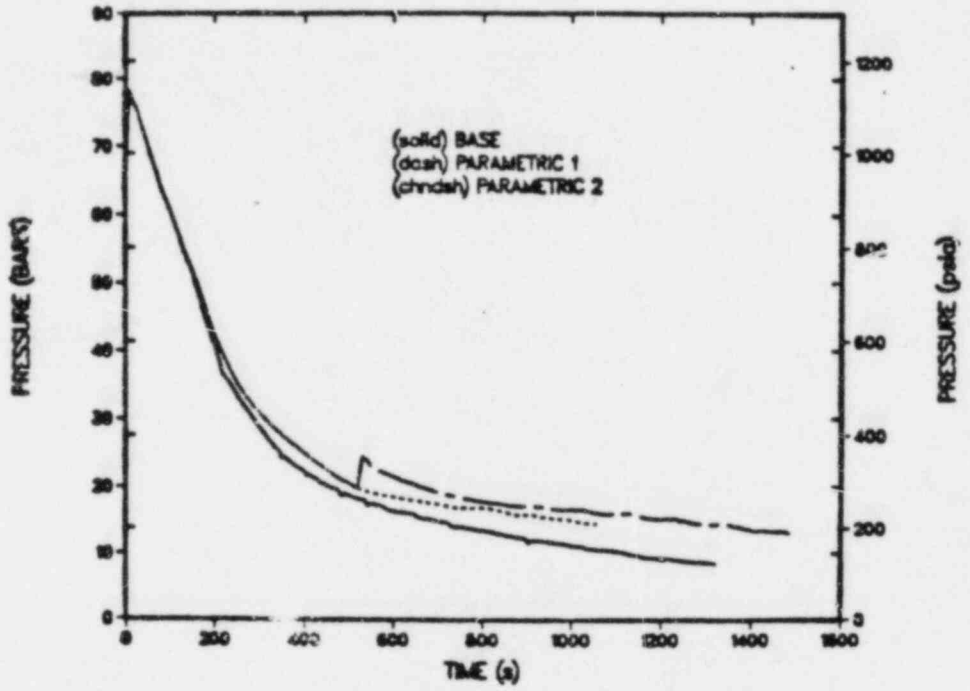

Fig. 169.
Steam-generator-secondary pressure - loop B.

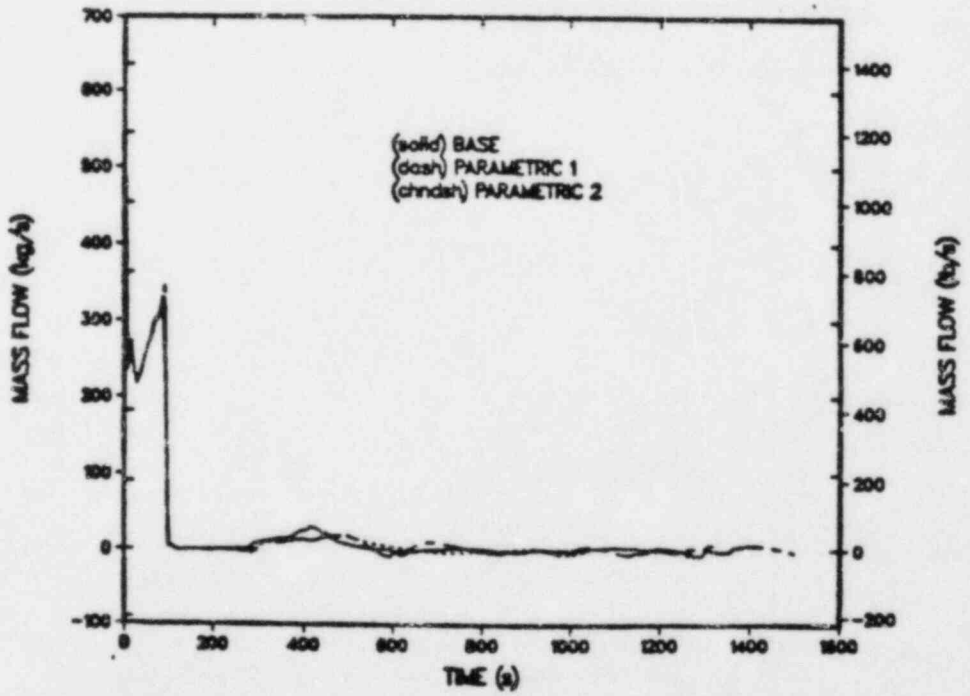

Fig. 170.
Main-feedwater flow - loop A.

TABLE XXIV

TBV EVENT SEQUENCE
Base Case

Event		Time (s)
1.	Turbine and reactor trip	0.5
2.	Turbine stop valves close	0.5
3.	Loop-A TBV opens (fails to reseat thereafter)	4.1
4.	Loop-B TBV opens (fails to reseat thereafter)	4.3
5.	HPI begins following trip on low system pressure	87.5
6.	MFW pump trip off following high SG B liquid level	91.2
7.	RCPs trip on 30 s delay after HPI actuation	117.4
8.	Feedwater realignment trip	117.4
9.	Main-flow control valves trip	117.4
10.	Emergency feedwater pump on	147.0
12.	PORV opens	1175.7

than in loop A. Loop-A and -B MFW temperatures are presented in Fig. 172 and 173, respectively.

EFW flows through loops A and B are shown in Figs. 174 and 175. EFW flows were initiated at ~150 s. Because the EFW level-control system failed, the EFW flow continued until the end of the calculated transient. Loop-A and -B EFW temperatures are presented in Figs. 176 and 177. Before ~150 s stagnant conditions prevailed, and the liquid temperatures were near the initial conditions. The EFW flow induced a flow of liquid through the SUFCVs that mixed with the EFW before entering the SGs. The temperature rise beginning near 200 s reflects mixing of these two flows.

The water inventories in the loop-A and -B SG secondaries are shown in Figs. 178 and 179. Although the fill characteristics were similar, SG B filled more rapidly before the MFW trip because, as previously discussed, the loop-B MFCV opened to a larger flow area by the ICS. With no liquid level control, the SG secondaries continued to fill and oscillations developed as the liquid level reached ~12.4 m (top of the generators).

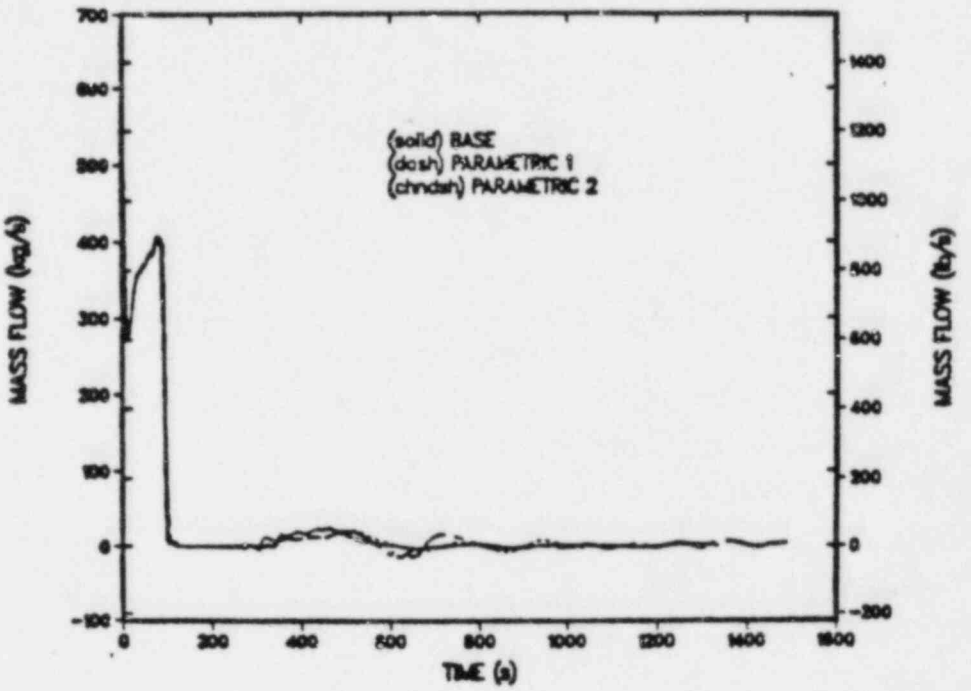

Fig. 171.
Main-feedwater flow - loop B.

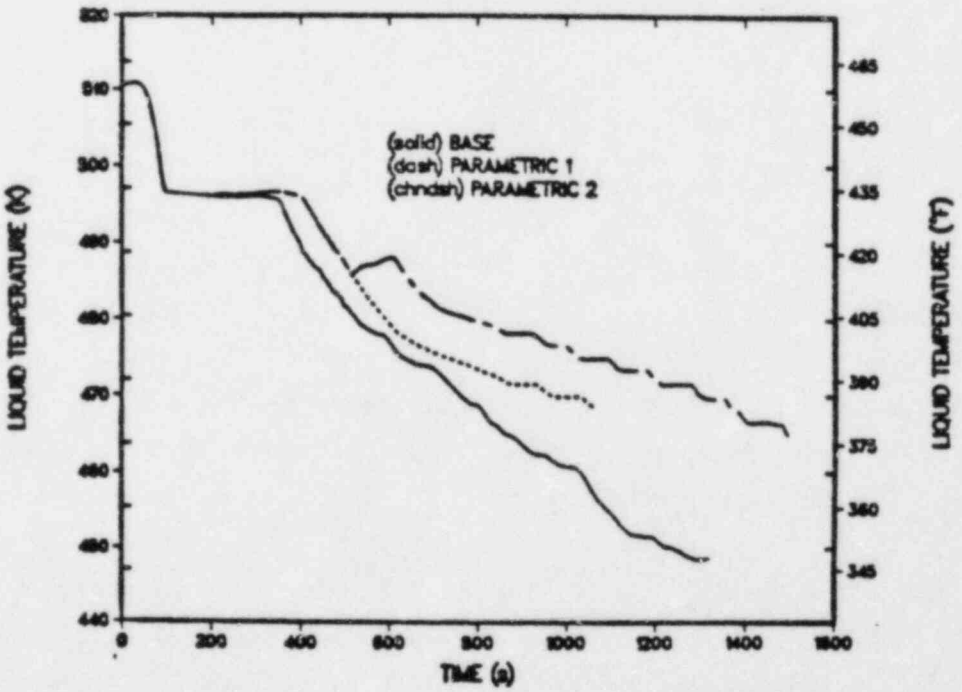

Fig. 172.
Main-feedwater liquid temperatures - loop A.

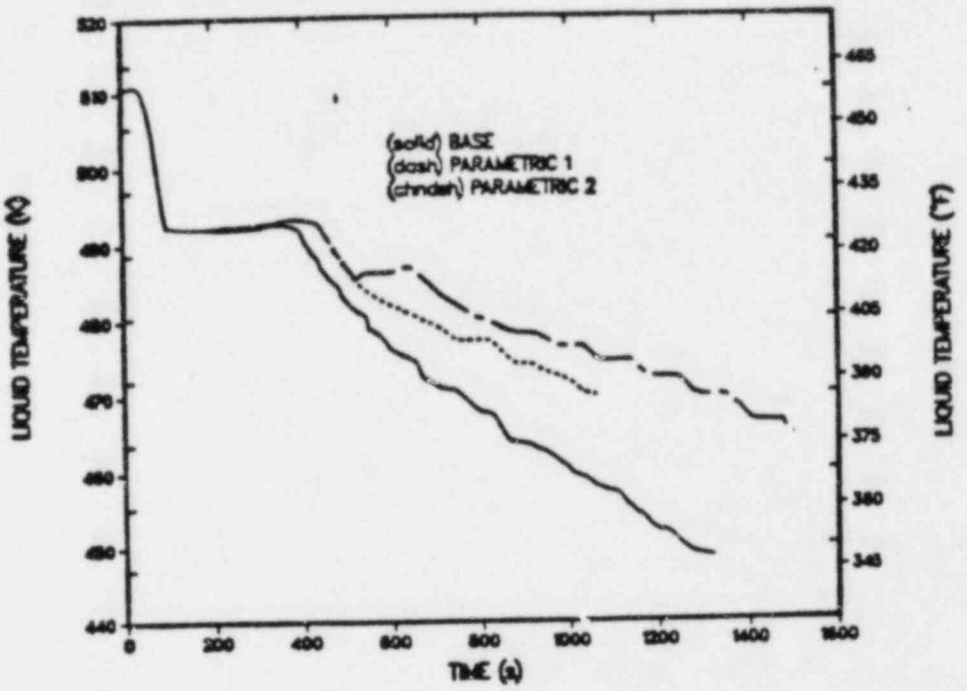

Fig. 173.
Main-feedwater liquid temperatures - loop B.

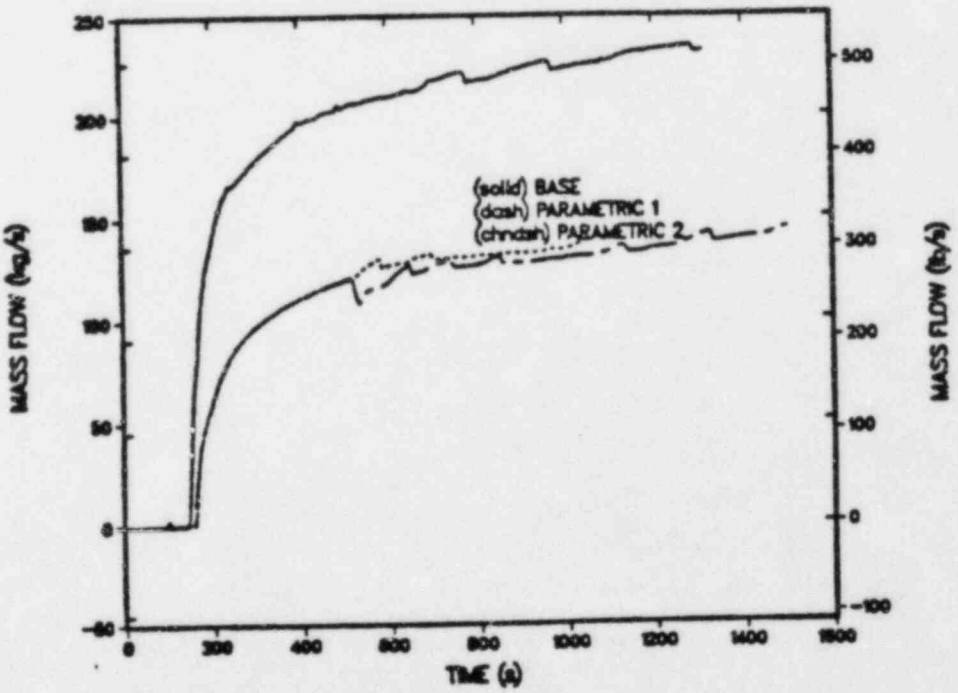

Fig. 174.
Emergency-feedwater flow - loop A.

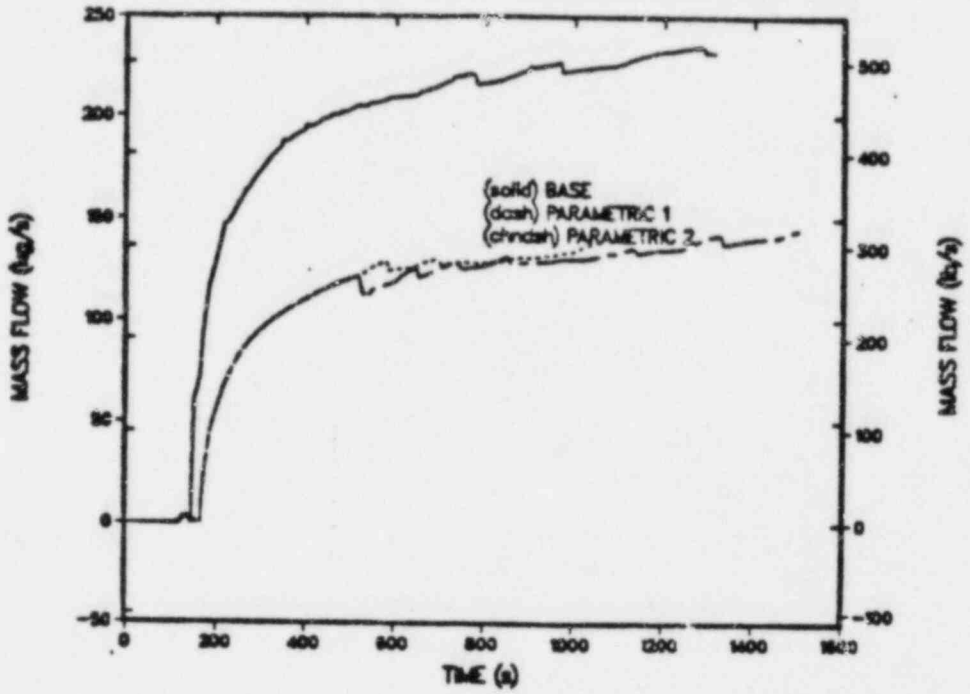

Fig. 175.
Emergency-feedwater flow - loop B.

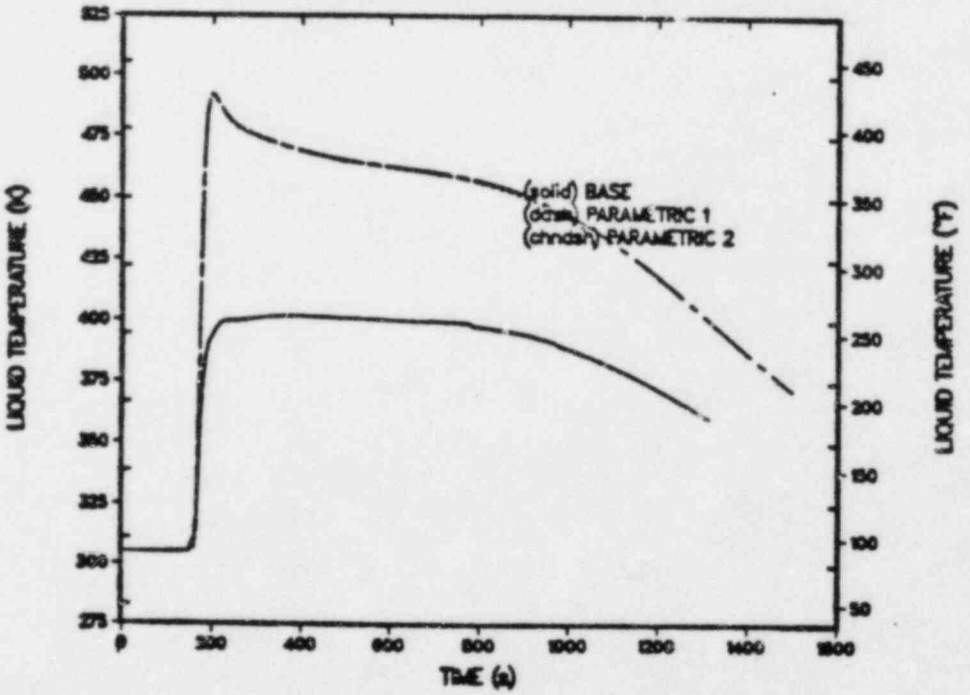

Fig. 176.
Emergency-feedwater liquid temperatures - loop A.

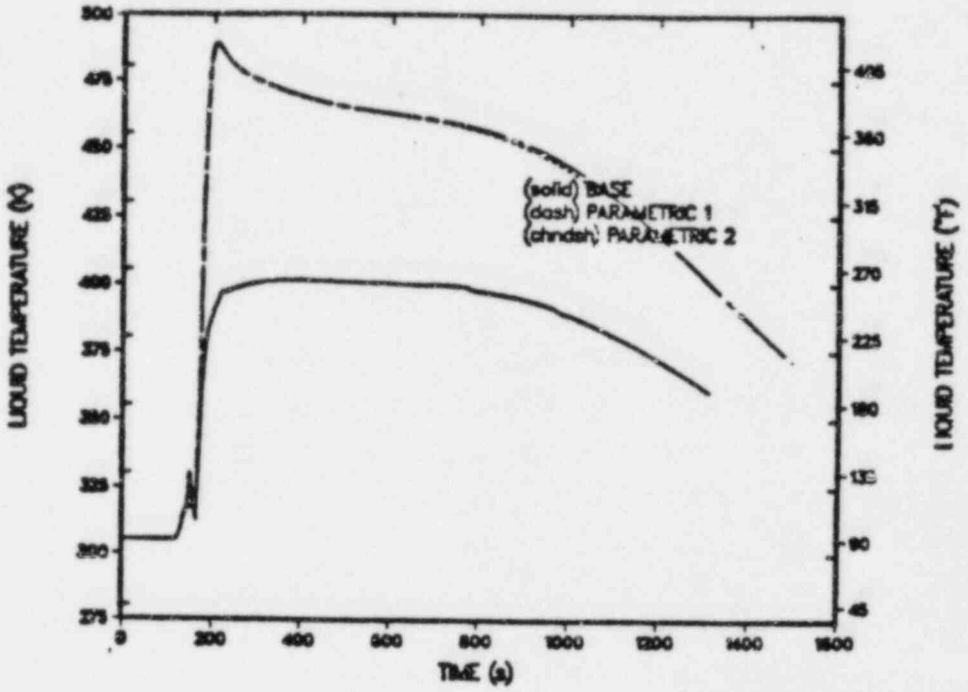

Fig. 177.
Emergency-feedwater liquid temperatures - loop B.

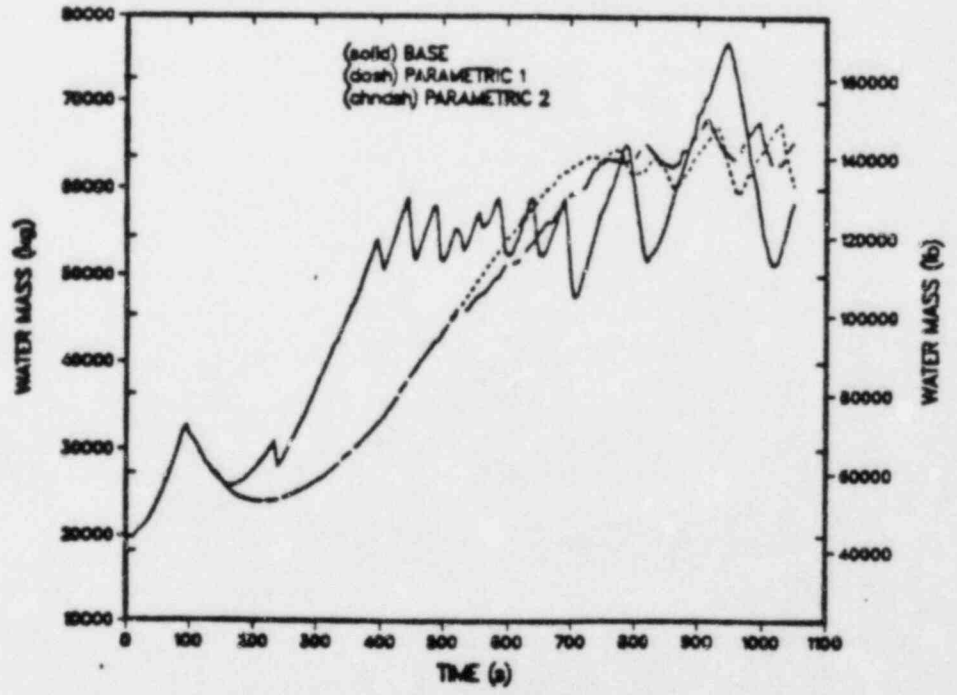

Fig. 178.
Steam-generator-secondary inventory - loop A.

Mass flows through the primary-loop hot legs are shown in Figs. 180 and 181. Following the RCP trips at ~117 s, the flows coasted down and natural circulation flows through both loops were established. Similar phenomena were observed in the cold legs as shown in Figs. 182 and 185. The corresponding loop cold-leg temperatures are presented in Figs. 186 through 189, respectively. Vapor fractions in the loop-A and -B candy-cane sections are shown in Figs. 190 and 191, and it can be seen that no voiding occurred during the transient. The pressurizer water level is presented in Fig. 192.

Downcomer liquid temperatures for the base case are presented in Fig. 193 at the top axial downcomer level (just below the cold-leg nozzles). At the end of the calculated transient (1320 s), the minimum temperature was ~445 K. The minimum downcomer temperature for the base-case failure of one bank of two TBVs was ~465 K at 1320 s. The lower temperature predicted for the base-case failure of two banks of two TBVs was the result of enhanced heat transfer to two, as compared to one, steam generators.

ii. Parametric Case 1. A single specification was changed for this parametric study. The loop-A and -B SG level controls following EFW activation were assumed to operate to maintain the secondary-liquid level at or below 6.2 m. It was assumed that the operator does not restart the RCPs and does not throttle the HPI. The event sequence for this case is presented in Table XXV. The event sequence was identical to the base case through event 9. At ~147 s the loop-B EFW valve shut on high SG-B secondary-liquid level. The loop-A EFW valve shut on high SG-A secondary-liquid level at ~373 s. The PORV opened ~13 s early in the Case 1 because of reduced heat transfer to the two SGs.

TABLE XXV

TBV EVENT SEQUENCE
Parametric Case 1

	Event	Time(s)
1-9.	Same as base case	0-117.4
10.	Loop-B EFW valve shut on high SG B liquid level	147.0
11.	Loop-A EFW valve shut on high SG A liquid level	372.6
12.	PORV opens	1062.1

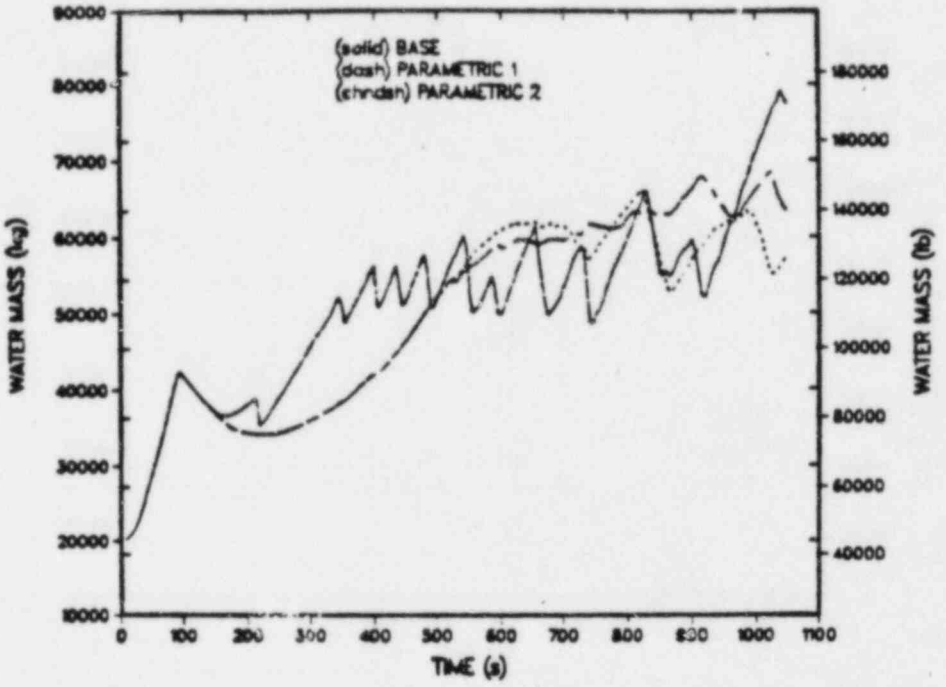

Fig. 179.
Steam-generator-secondary inventory - loop B.

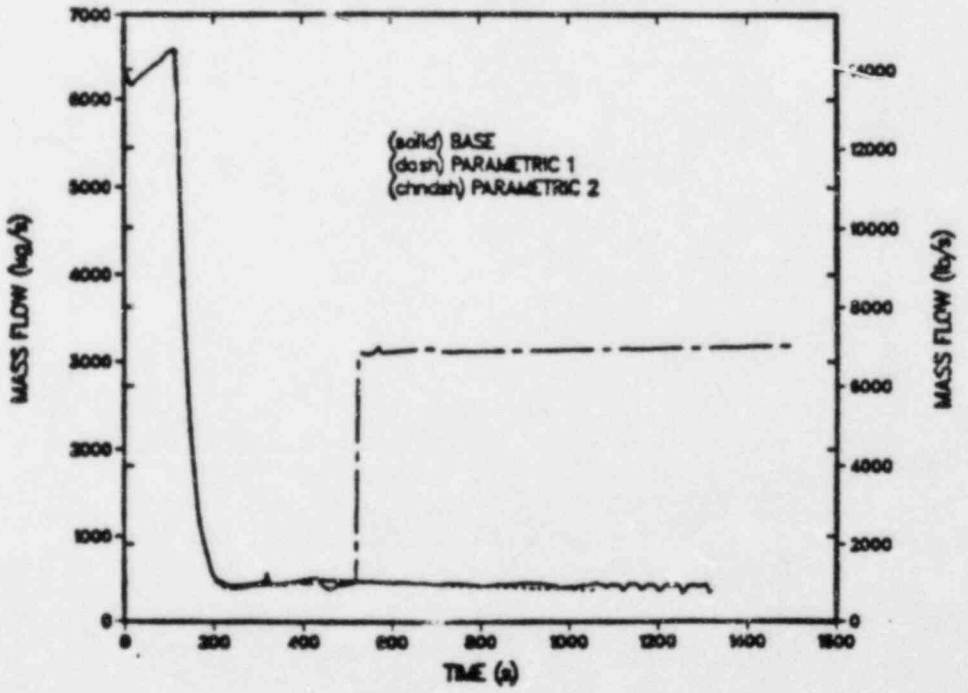

Fig. 180.
Hot-leg flow - loop A.

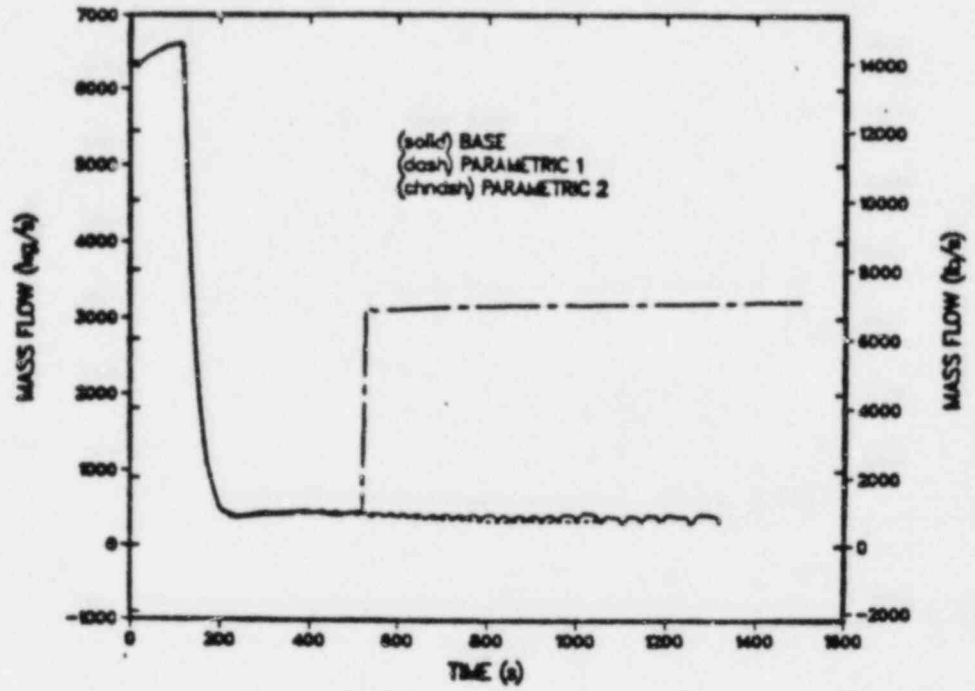

Fig. 181.
Hot-leg flow - loop B.

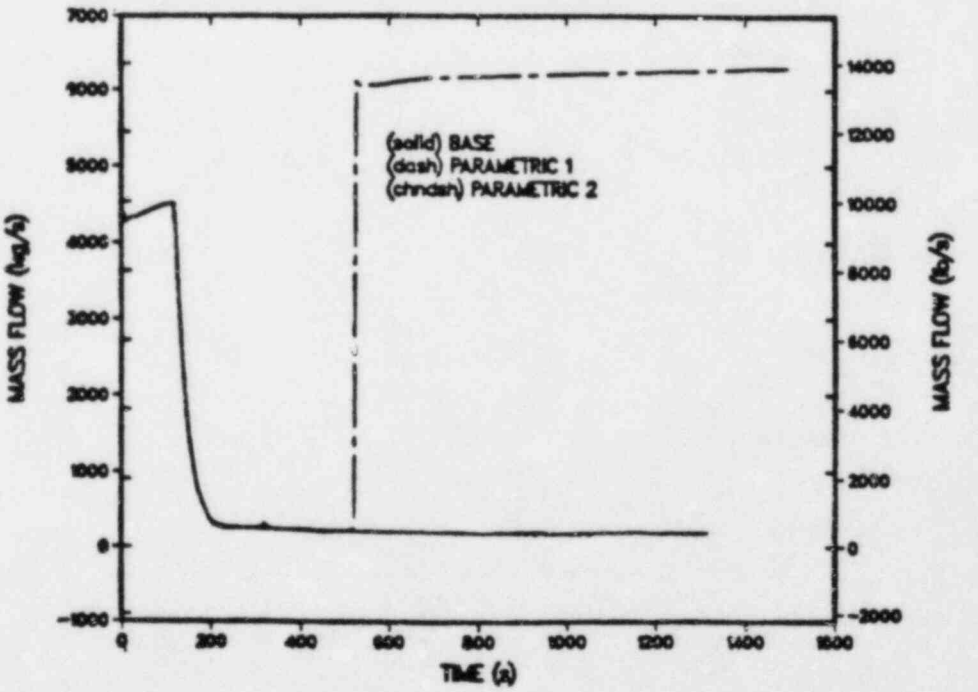

Fig. 182.
Cold-leg flow - loop A1.

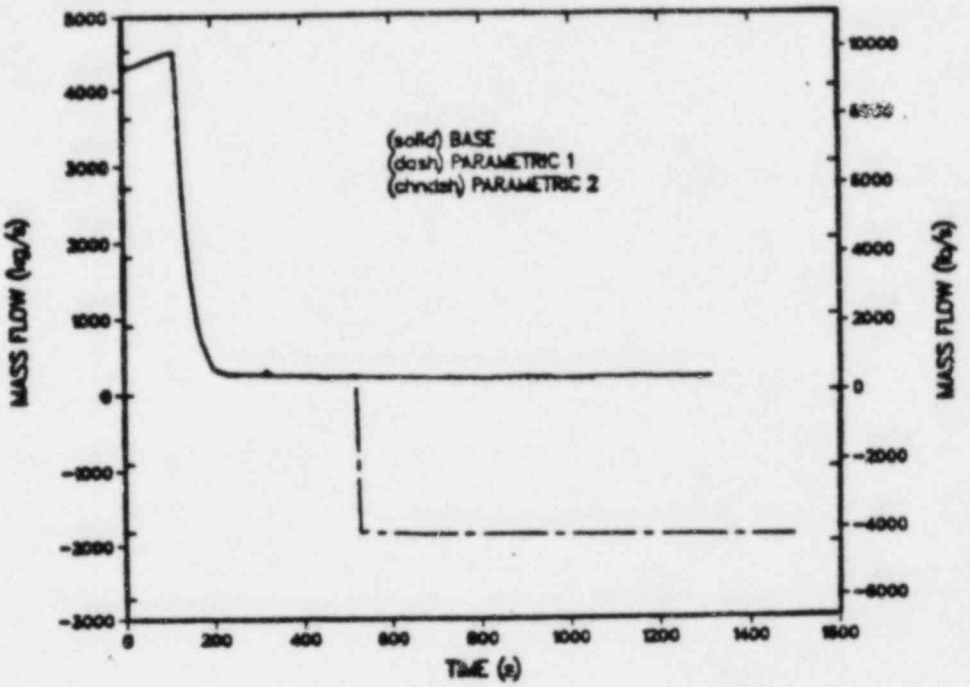

Fig. 183.
Cold-leg flow - loop A2.

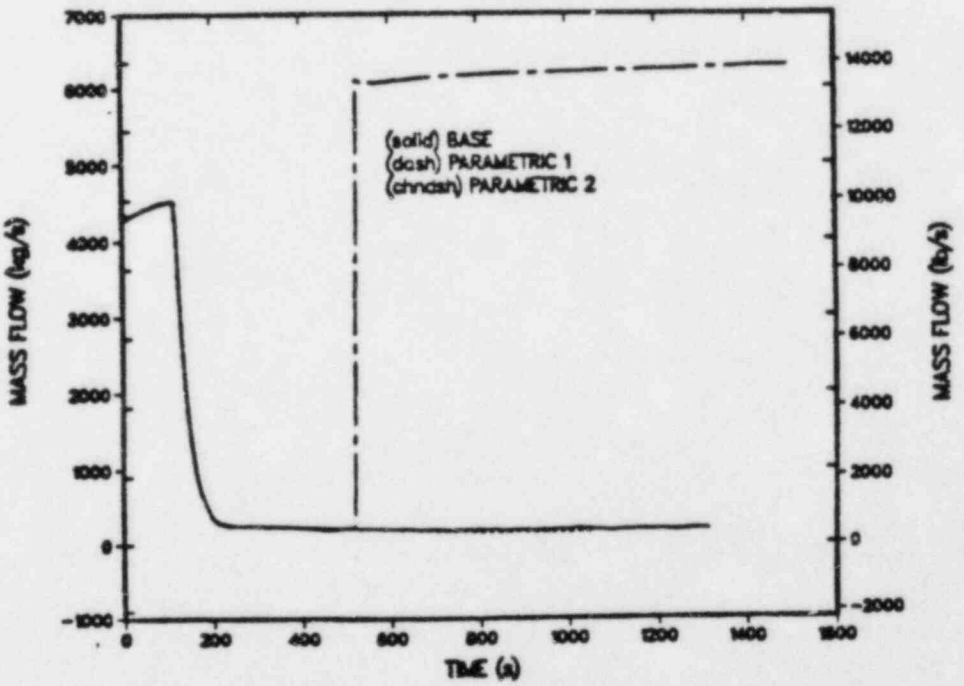

Fig. 184.
Cold-leg flow - loop B1.

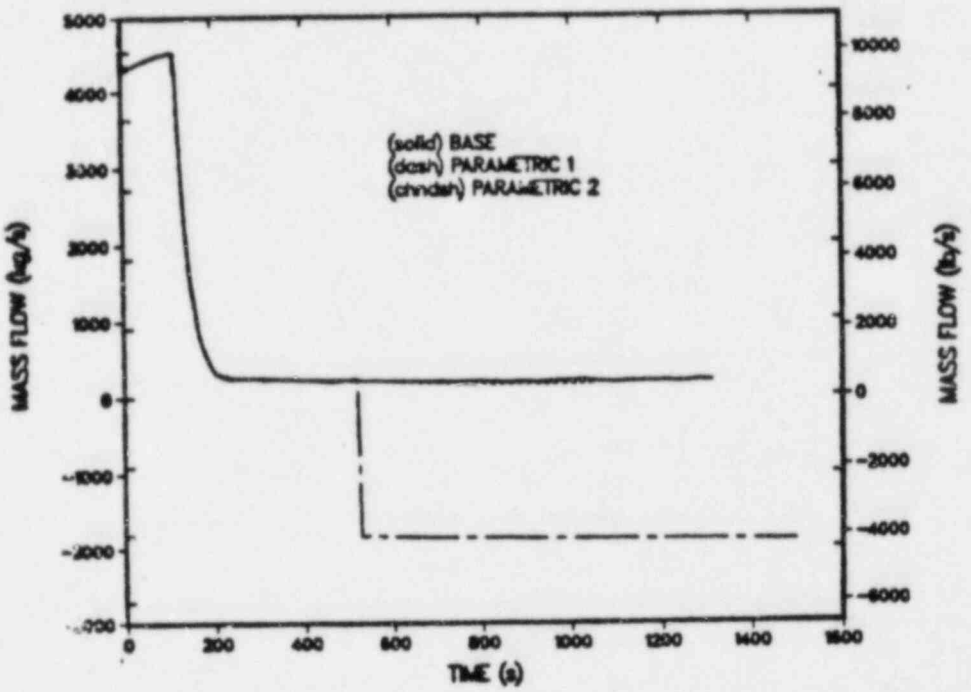

Fig. 185.
Cold-leg flow - loop B2.

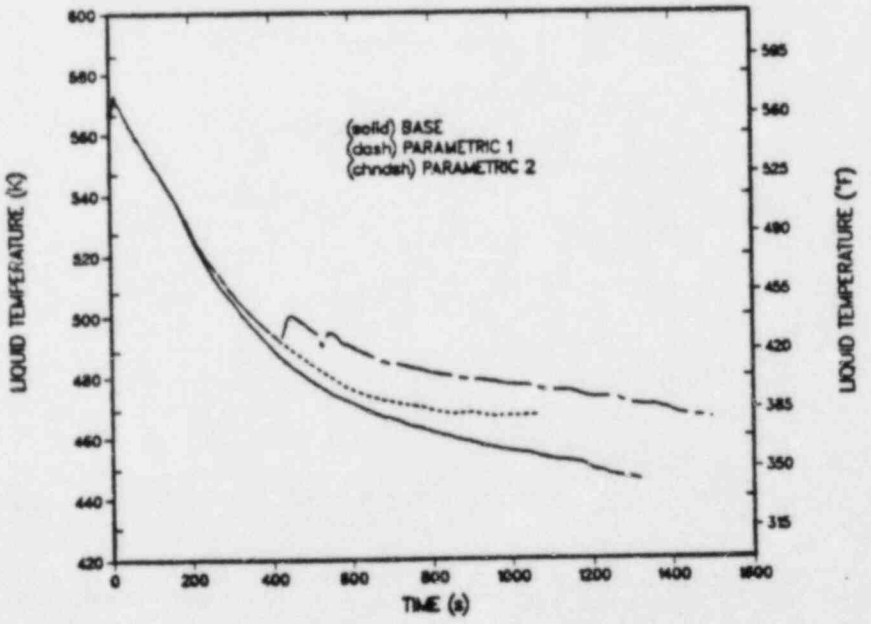

Fig. 186.
Cold-leg liquid temperature - loop A1.

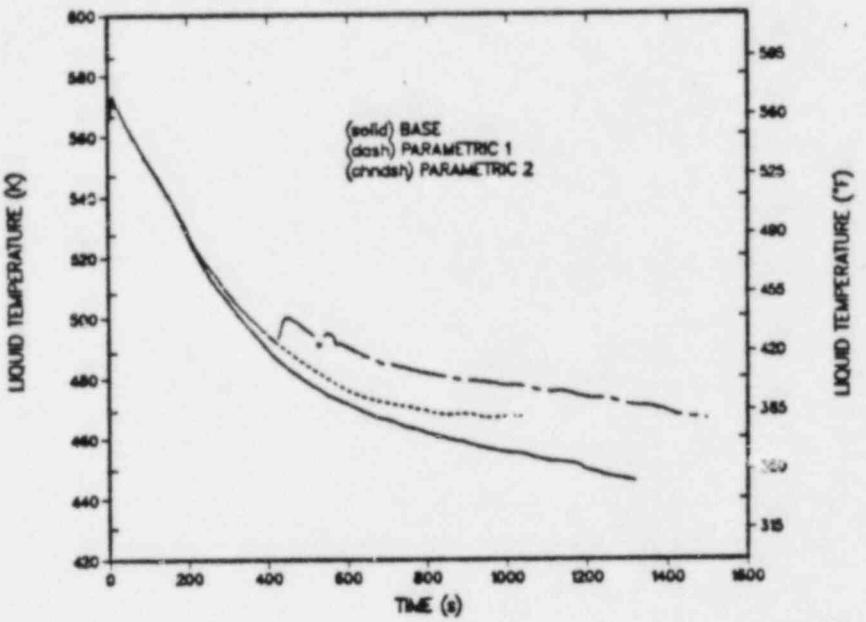

Fig. 187.
Cold-leg liquid temperature - loop A2.

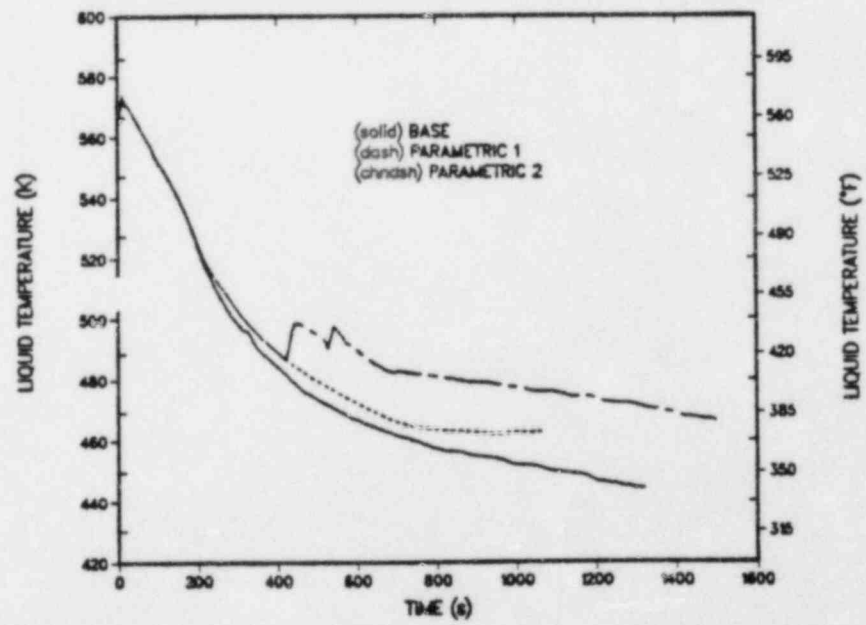

Fig. 188.
Cold-leg liquid temperature - loop B1.

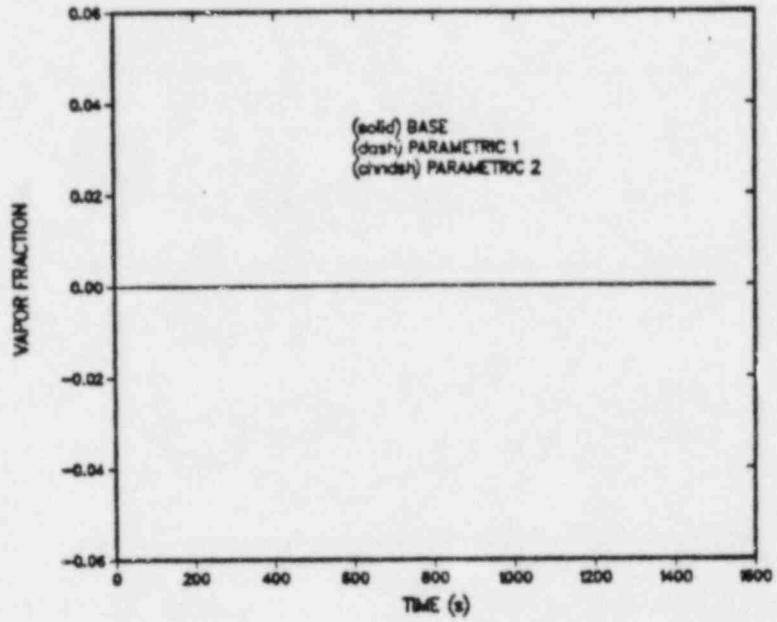

Fig. 189.
Cold-leg liquid temperature - loop B2.

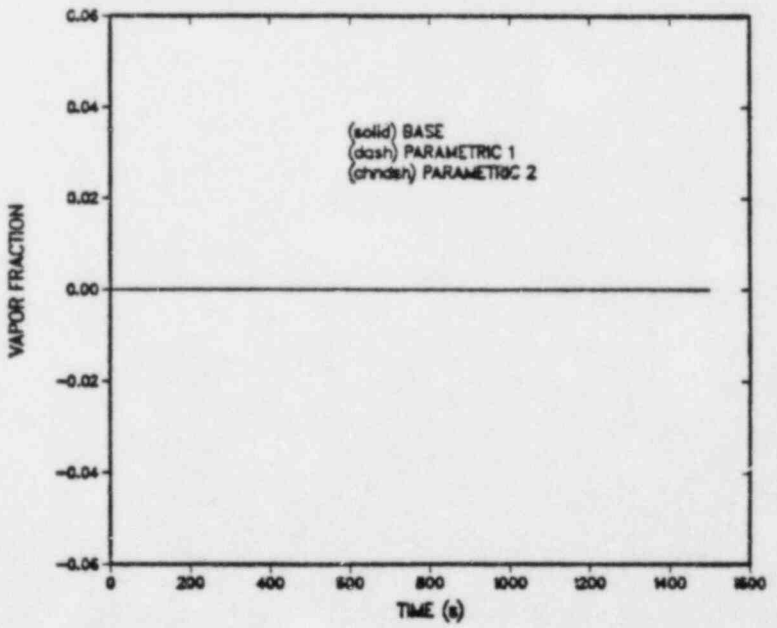

Fig. 190.
Candy-cane vapor fraction - loop A.

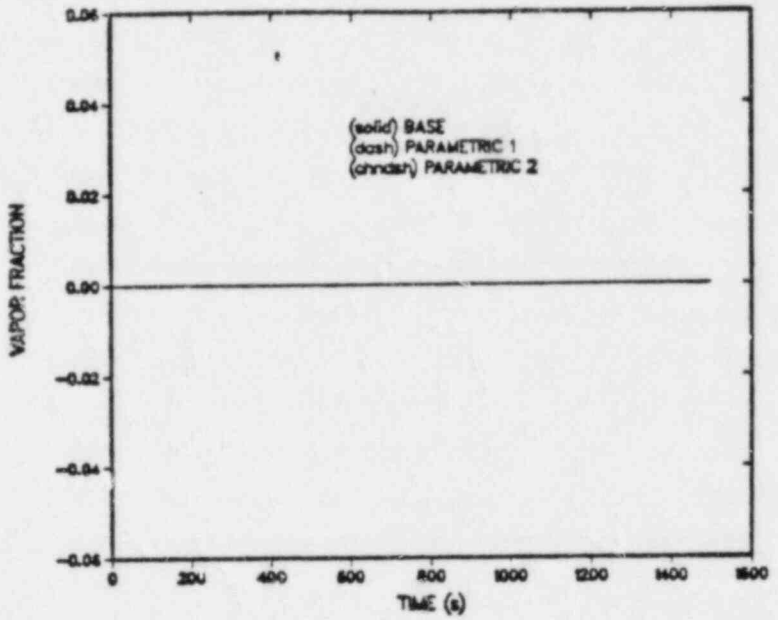

Fig. 191.
Candy-cane vapor fraction - loop B.

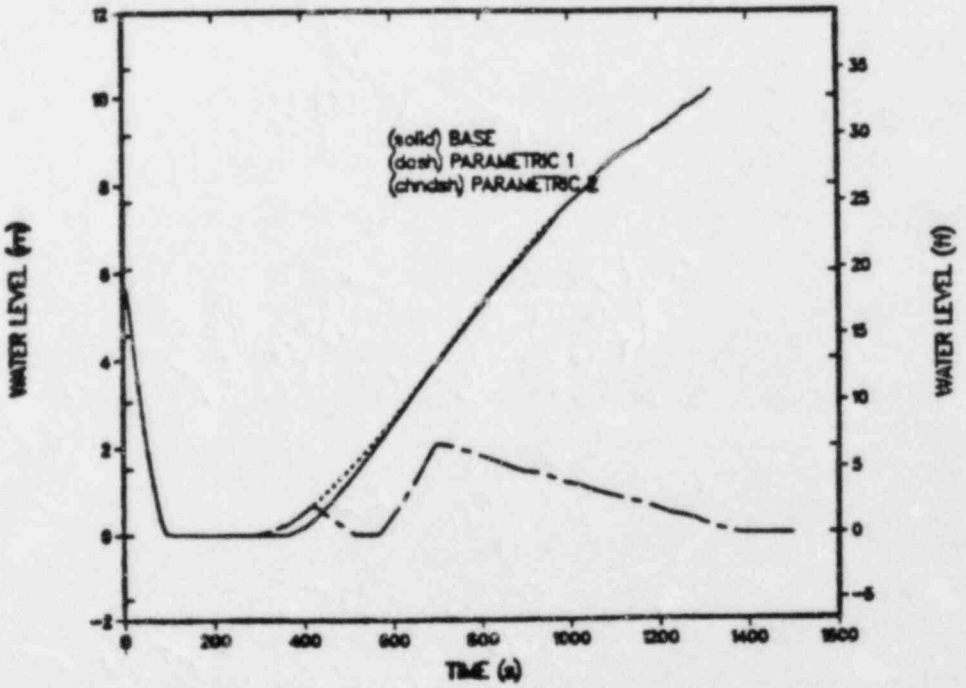

Fig. 192.
Pressurizer water level.

Results for Case 1 are presented in Figs. 167 through 192 and may be compared directly to the base case. The general trends of Case 1 were similar to the base case. The major differences appeared in the secondary sides of loops A and B and were caused by shutting the EFW valves on high SG liquid levels. The reduced EFW flow affected the primary side also. Compared to the base case, the pressurizer pressure increased more rapidly to the PORV setpoint as shown in Fig. 167. This was caused by reduced primary-to-secondary heat transfer associated with reduced loop-A and -B steam-generator secondary inventories (Figs. 178 and 179).

Downcomer liquid temperatures for Case 1 are presented in Fig. 194 at the top axial downcomer level (just below the cold-leg nozzles). At the end of the calculated transient (1062 s), the minimum temperature was ~465 K. The base case minimum temperature at the same time was ~453 K.

iii. Parametric Case 2. The specifications for this case differed from the base case as follows: the SG A and B secondary liquid-level controls did not fail, restart of one RCP in each loop was permitted on attainment of 75 F subcooling, and throttling the HPI was permitted on attainment of 75 ± 12.5 F subcooling. The event sequence for this transient is presented in Table XXVI. Events 1-9 were identical to the base case. The HPI was throttled at ~421 s after a subcooled-monitor trip at 75 ± 12.5 F. One RCP in each loop was restarted at ~517 s after a 30-s delay following a second subcooled-monitor trip.

Results for Case 2 are presented in Figs. 167 through 192 and may be compared directly to the base case. Case 2 displayed significant differences from the base case. A major consequence of restarting the RCPs and throttling the HPI was that primary-system repressurization did not occur, and thus the PORV did not open. The absence of repressurization is seen in Fig. 167. Restart of the loop-A1 and -B1 RCPs can be observed in Figs. 182 and 184, respectively. Operation of the RCPs induced a reverse flow through the cold legs with non-operating pumps. The influence of RCP restart on heat transfer to the loop-A and -B steam-generator secondaries can be observed in Figs. 168 and 169, respectively. The pressure increased with RCP restart and continued to increase to the end of the calculated transient. The increase of the primary system pressure (Fig. 167) was terminated after the HPI was throttled at ~420 s. The primary pressure decayed rapidly to the accumulator setpoint of 4.168 MPa at ~565 s. Water at 305 K was then injected into the primary for ~20 s. The primary pressure then increased until it was turned around by the increased heat transfer to the secondaries by RCP operation. The accumulators again discharged

TABLE XXVI

TBV EVENT SEQUENCE
Parametric Case 2

	Event	Time(s)
1-9.	Same as base case	0-117.4
10.	Loop-B EFW valve shut on high SG B liquid level	147.0
11.	Loop-A EFW valve shut on high SG A liquid level	372.6
12.	HPI turned off	421.0
13.	Restart RCPs A1 and B1 after subcooled monitor trip	517.0
14.	Loop-A accumulator begins discharging	565.5
15.	Loop-B accumulator begins discharging	565.5

near the end of the calculated transient, thereby increasing the rate of downcomer temperature decrease. This was the only TBV transient that experienced accumulator discharge and it markedly influenced the extrapolated downcomer temperatures at 7200 s.

Downcomer liquid temperatures for Case 2 are presented in Fig. 195 at the top axial downcomer level (just below the cold-leg nozzles). At the end of the calculated transient (1500 s), the minimum temperature was ~467 K. At 1062 s the minimum temperature was ~477 K, which compares with ~465 K for Case 1 and ~453 K for the base case at the same time.

c. Conclusions. The response of the Oconee-1 plant to a secondary-system depressurization transient was [illegible] using TRAC-PF1. The transient studied was failure of two banks of turbine-bypass valves (four valves; two on each steam line) to close after initially opening following reactor and turbine trips. The base-case transient included additional failures caused by failure of the level control in the affected steam generator, no operator restart of the reactor-coolant pumps, and no operator throttling of the HPI system. A minimum liquid temperature in the downcomer of ~495 K at 1020 s was calculated. If correct operation of the steam-generator level control, operator restart of the reactor coolant pumps, and throttling of the HPI flow were assumed, the primary

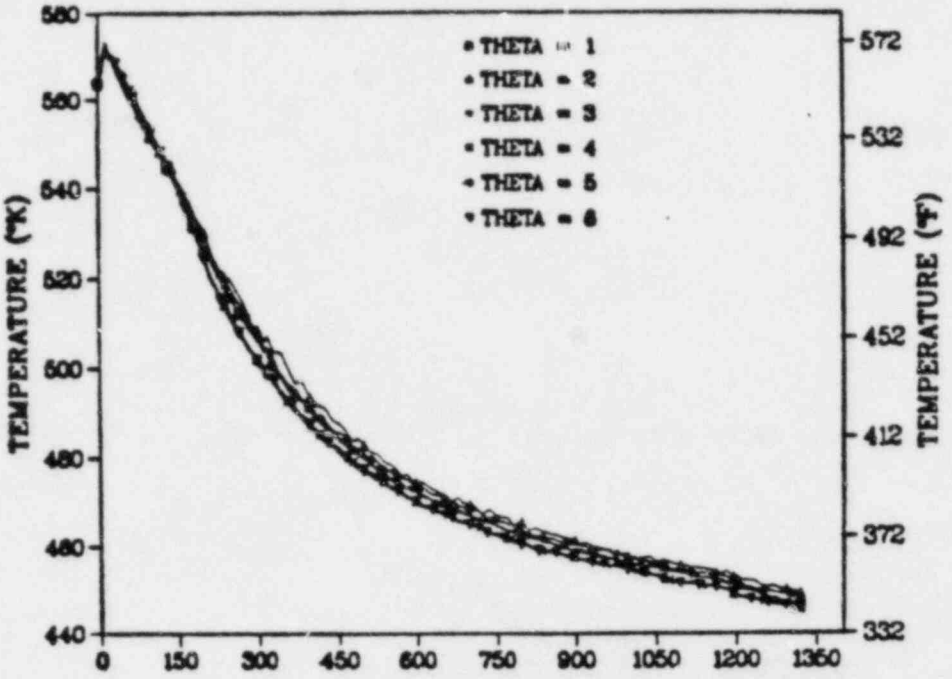

Fig. 193.
Downcomer liquid temperatures (base case) at vessel axial level 6 (all azimuthal sectors).

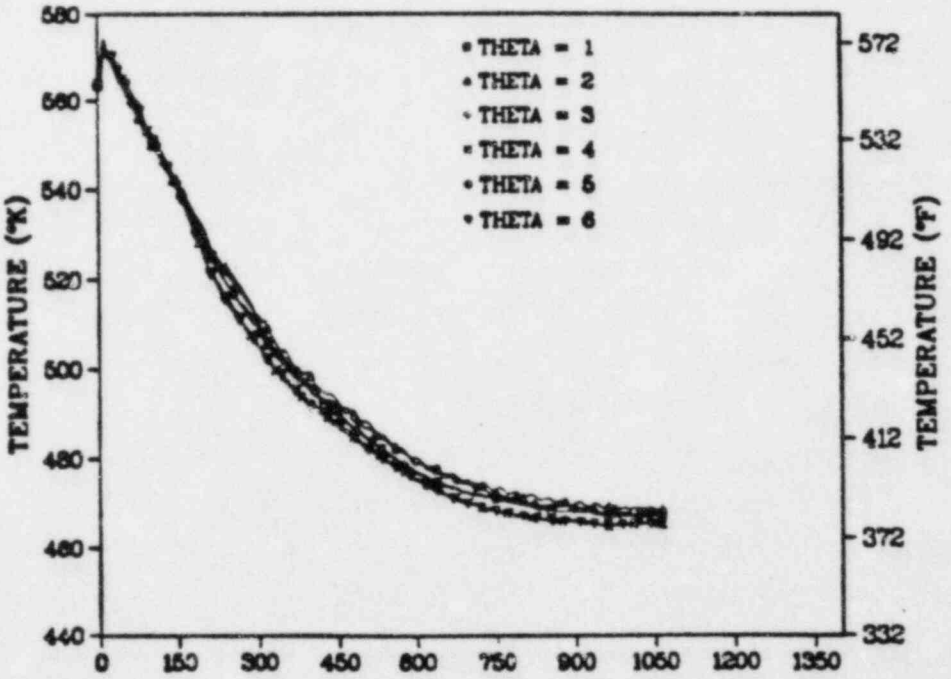

Fig. 194.
Downcomer liquid temperatures (parametric case 1) - vessel axial level 6 (all azimuthal sectors).

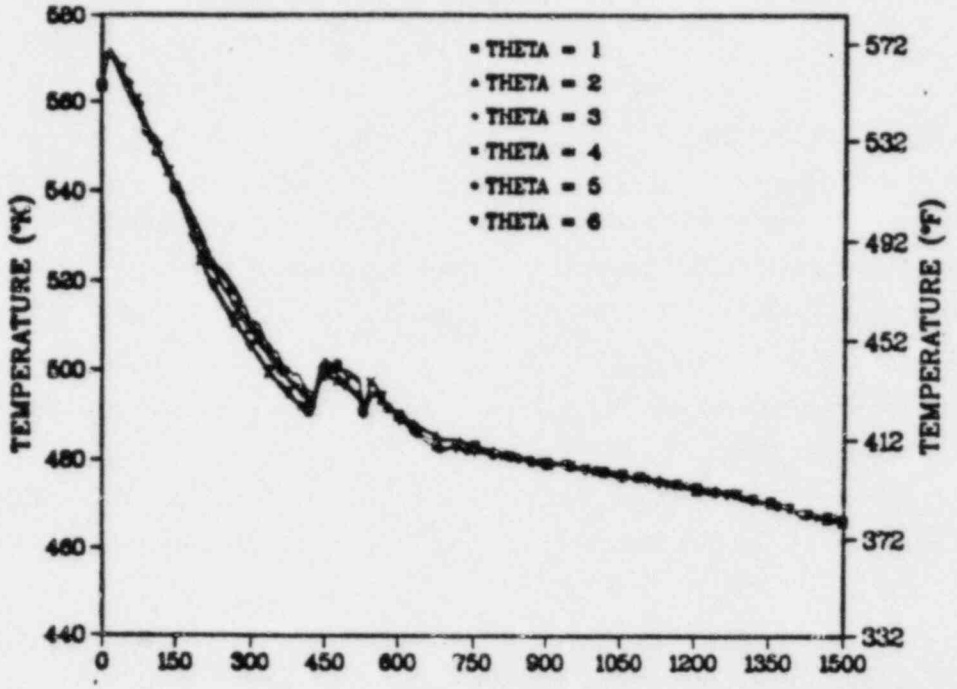

Fig. 195.
Downcomer liquid temperatures (parametric Case 2) - vessel axial level 6 (all azimuthal sectors).

system did not repressurize, and a minimum downcomer liquid temperature of ~472 K was calculated at 1320 s.

E. Hot-Leg Break LOCAs

1. 2 in. Break

a. Introduction and Summary. This report presents the Oconee-1 plant response to a 2-in. break in the surge line midway between the pressurizer and the riser of the candy cane. Following the initiation of the break, the reactor and turbine trip from full power. Reactor decay heat was specified as 1.0 times the ANS standard. For this transient calculation, the ICS and all key system components were assumed to function correctly. The only specified operator action was the RCPs trip 30 s after HPI actuation. Two cases involving HPI throttling to system subcooling were investigated. One calculation investigated the effects of HPI throttling to 42 ± 12.5 K subcooling and the other investigated the effects of no HPI throttling. The throttled HPI case was not run because the subcooling margin was never achieved.

TRAC calculated a relative minimum in temperature at approximately 1000 s into the transient; the pressure at 1000 s was ~6.2 MPa. The temperature and pressure were both decreasing at the end of the calculation at 3760 s and had values of ~450 K and ~2.1 MPa, respectively.

Because the reactor should not have been tripped until the low-pressure reactor trip setpoint was reached, and because the calculation was not run to 7200 s, it is recommended that the RELAP5 calculation[5] be used for the ORNL study.

b. Model Description and Assumptions. A complete description of the primary-side, secondary-side, and ICS modeling can be found in Section II. The steady-state operating conditions are also presented in that section.

The 2-in. break LOCA specification containing the initial conditions, event sequence, and assumed failures is presented in Ref. 3. The TRAC transient event sequence is presented in Table XXVII. Because the ICS and major system components were specified to function correctly, it was not necessary to make any overriding assumptions.

c. Transient Calculation. Figures 196 and 197 present the SG secondary side pressures for loops A and B. Following the initiation of the break, the reactor and turbine tripped from full power, the TSVs closed causing a temporary increase in secondary-side pressure. The TBVs for both loops were activated ~4.2 s to relieve the initial secondary-side pressure increase. The initial relief of secondary-side pressure caused a sudden drop in the SG secondary-side inventories shown in Figs. 198 and 199. As the SG secondary-side inventories continued to decrease, the RCPs tripped (30 s after HPI actuation) and the MFW

TABLE XXVII

HOT-LEG BREAK LOCA - 2 IN. BREAK
SEQUENCE OF EVENTS

	Event	Time (s)
1.	Break opens	0.0
2.	Reactor and turbine trips	0.5
3.	TSVs close (both loops)	0.5
4.	TBVs open (both loops)	~4.2
5.	HPI actuation	43.1
6.	TBVs open/close (both loops)	51.0
7.	RCPs trip	71.0
8.	MFW realignment	73.1
9.	TBVs open/close (both loops)	75.7
10.	Vent valves open	~100
11.	ICS closes SUFCVs	~350
12.	Candy canes remain voided	~500
13.	Minimum downcomer temperature (~470 K; 6.2 MPa)	~750
14.	Loop oscillations begin	~1200
15.	Accumulator injection begins	~1750
16.	End of calculation	3670

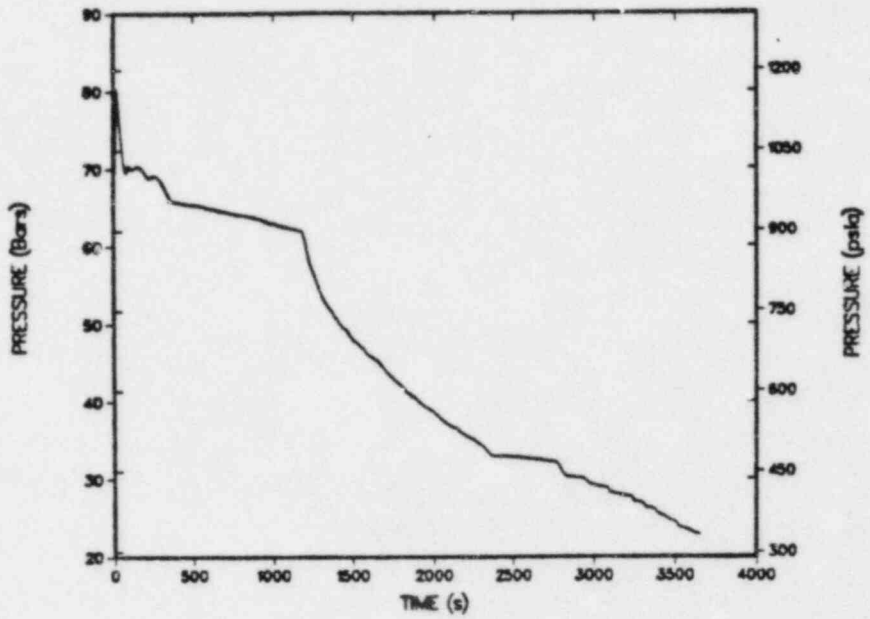

Fig. 196.
Steam generator secondary-side pressure - loop A.

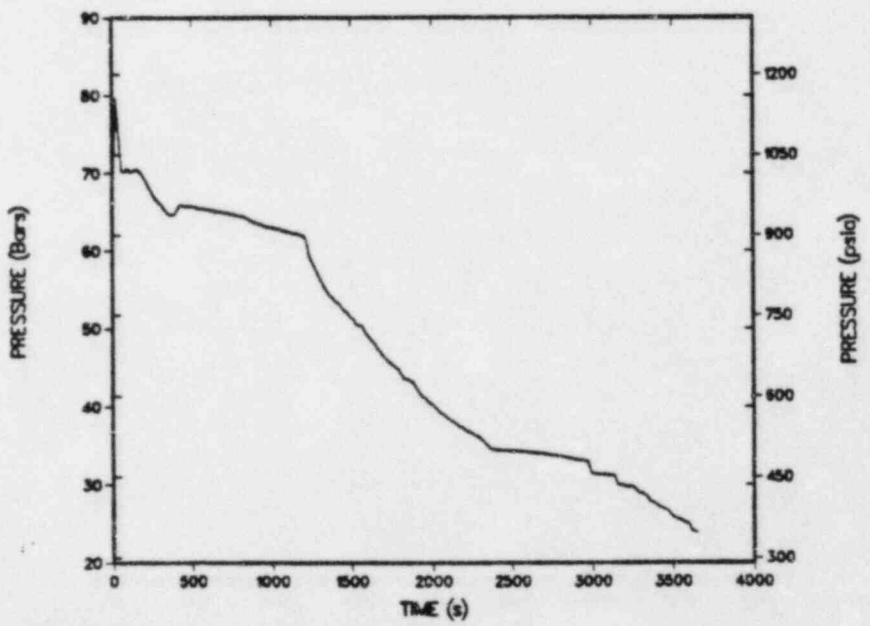

Fig. 197.
Steam generator secondary-side pressure - loop B.

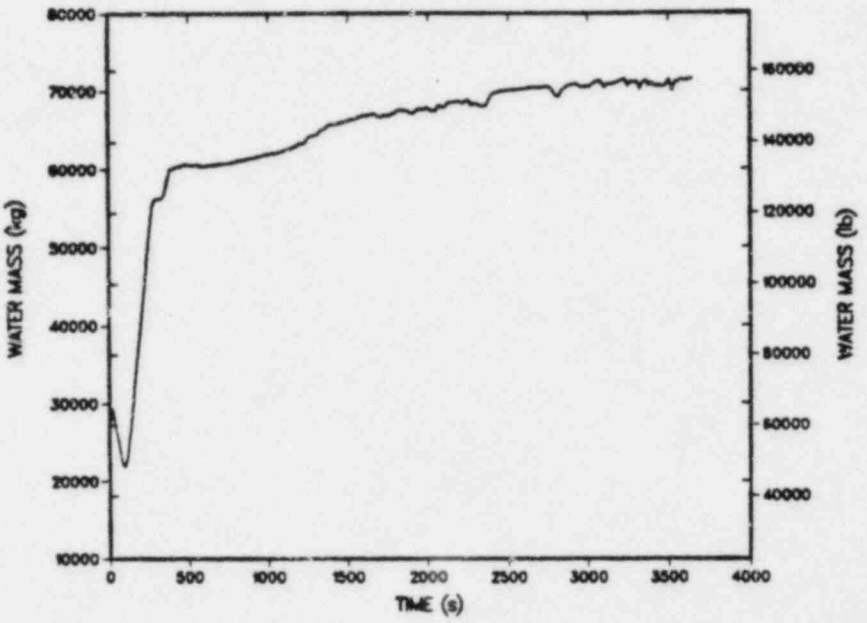

Fig. 198.
Steam generator secondary-side inventory - loop A.

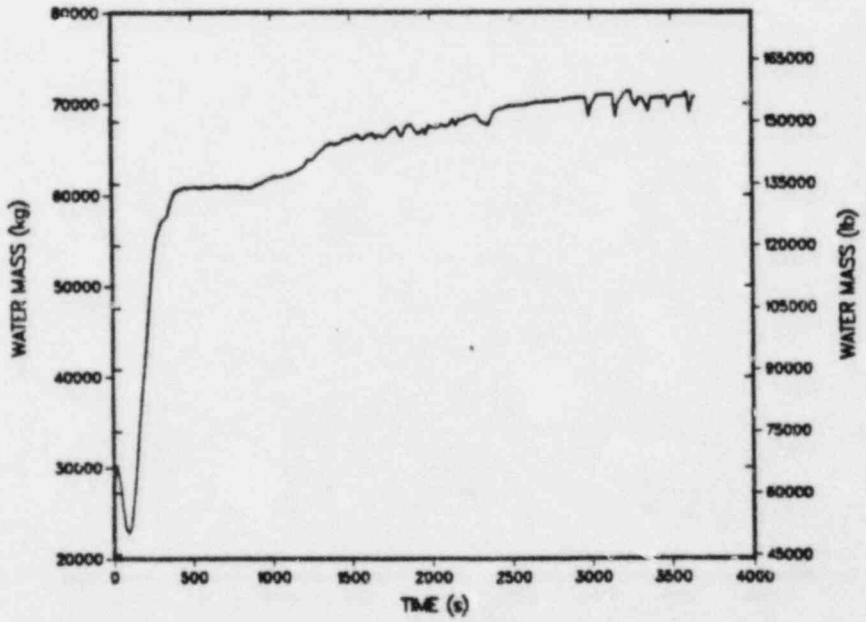

Fig. 199.
Steam generator secondary-side inventory - loop B.

was realigned to the EFW header. The loop-A and -B MFW mass flows and liquid temperatures are presented in Figs. 200 and 201. The realigned mass flows reduced the secondary pressures about 0.7 MPa between ~100 s and ~187 s and increased the SG inventories. The ICS continued to supply MFW to the SG upper header until ~350 s. At this time, the SUFCVs were closed by the ICS based on the SG inventory. Realigned mass flows and liquid temperatures are shown in Figs. 202 and 203, respectively. The EFW pump was not activated in this transient as it was not needed.

The pressurizer pressure and water level are presented in Figs. 204 and 205 respectively. The primary system depressurized rapidly until HPI actuation at ~43 s and remained above ~6.0 MPa until ~1200 s. From 1200 s to the end of the calculation the pressure decreased steadily to ~2.1 MPa. The pressurizer water level also dropped rapidly, and was zero by ~50 s. Figures 206 and 207 present the break mass flow and void fraction. The break mass flow was greater than ~100 kg/s for ~1000 s into the transient until the primary slowly voided. The mass flow decreased to ~70 kg/s as the void fraction increased to ~0.8. The candy-cane void fractions in Fig. 208 show that the loops did not refill in the course of the calculation.

Mass flows for the loops A and B cold-legs are shown in Figs. 209 and 210, respectively. As the primary-system flows began to decrease following the RCPs trip at ~73 s, the HPI fluid began to flow toward the vessel and fell into the downcomer as shown in the cold-leg mass flows and temperature profiles. Figures 211 and 212 present the cold-leg liquid temperatures for loops A and B. The hot-leg mass flow and liquid temperatures shown in Figs. 213 and 214 reflect the cold-leg response to the HPI. The mass flow and corresponding liquid temperature fluctuations that occurred after ~1000 s will be discussed later. TRAC calculated a minimum cold-leg temperature of ~420 K and ~440 K for loops A and B, respectively. The minimum hot-leg temperature was calculated to be ~495 K at the end of the calculation (3670 s).

An important feature of the B&W PWR design is the vent valves located around the upper plenum of the vessel (level 7 in the TRAC model) that provide the upper plenum region access to the downcomer. After the RCPs have tripped, the vent valves are capable of providing a source of hot fluid for mixing with cold HPI fluid that may flow toward the downcomer during these stagnant periods in the cold legs. Between ~200 s and ~1000 s of this calculation HPI fluid did flow toward the downcomer and was mixed with the vent-valve flow in the downcomer at the cold-leg junction.

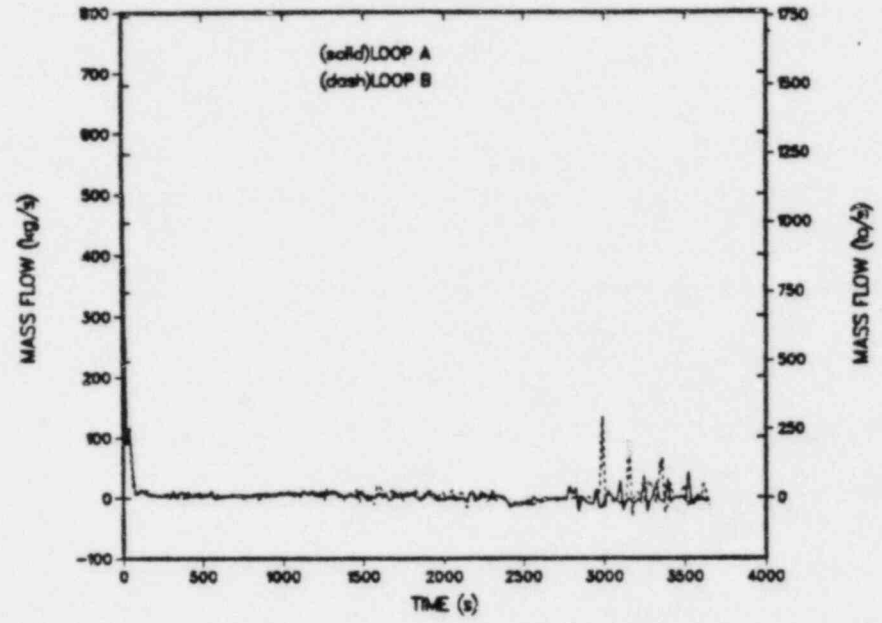

Fig. 200.
MFW mass flows - loops A and B.

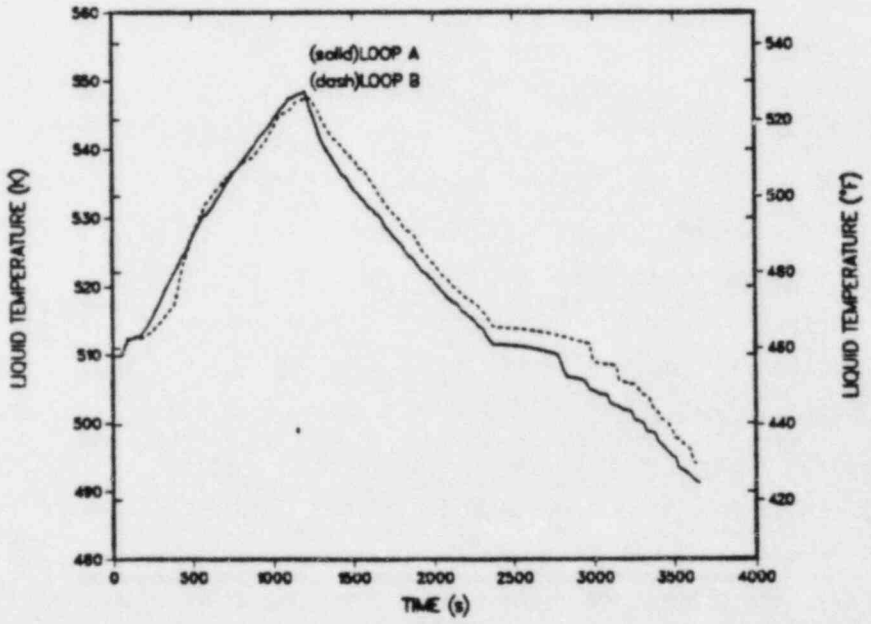

Fig. 201.
MFW liquid temperatures - loops A and B.

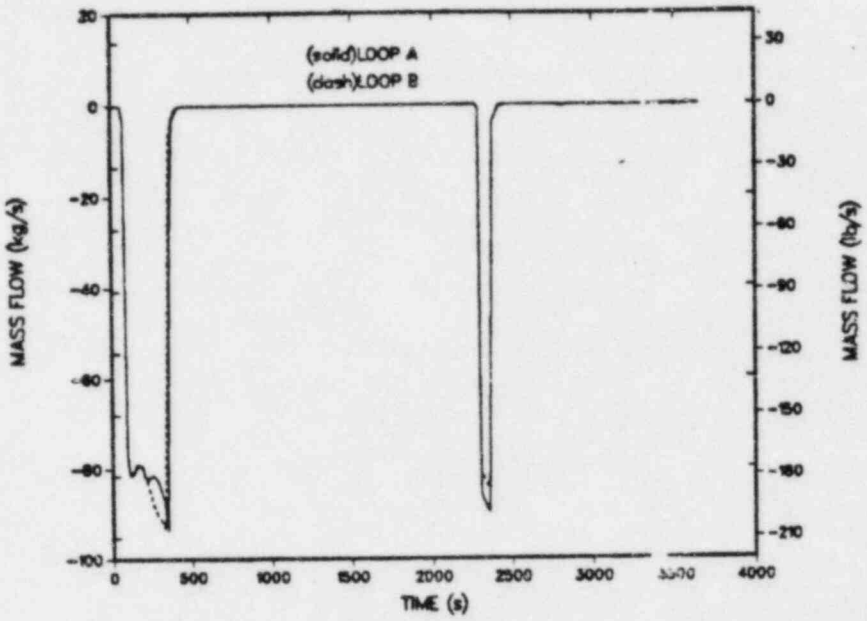

Fig. 202.
Emergency/realigned mass flows - loops A and B.

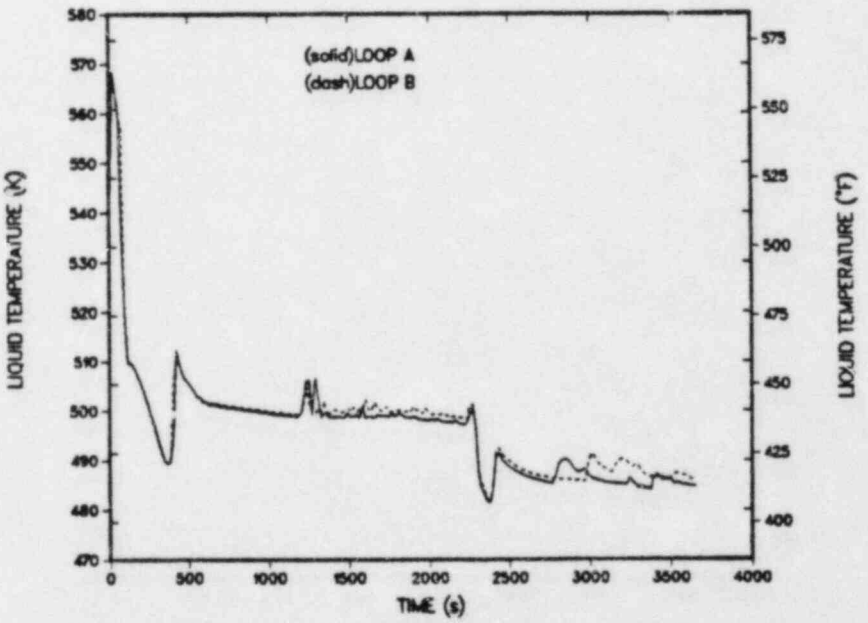

Fig. 203.
Emergency/realigned liquid temperatures - loops A and B.

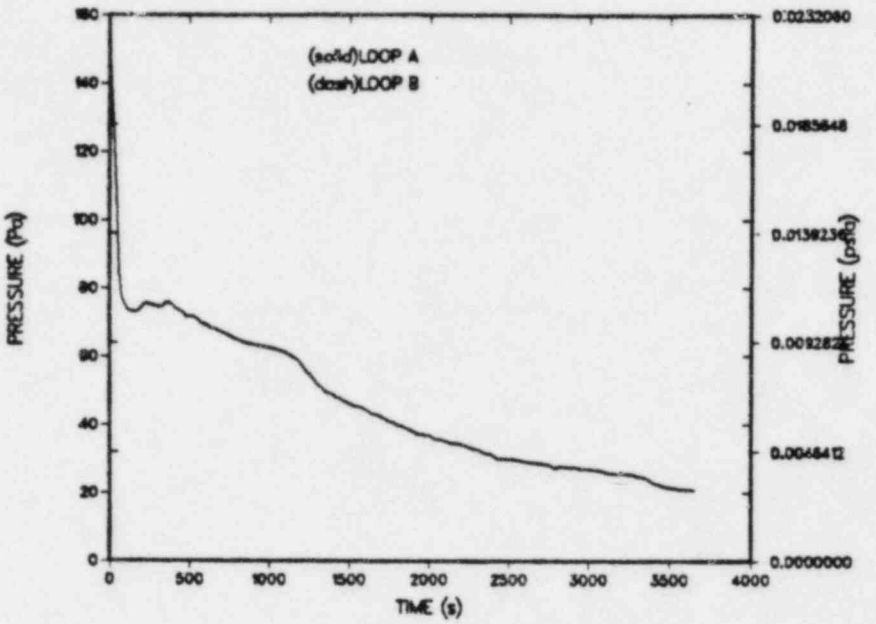

Fig. 204.
Pressurizer pressure.

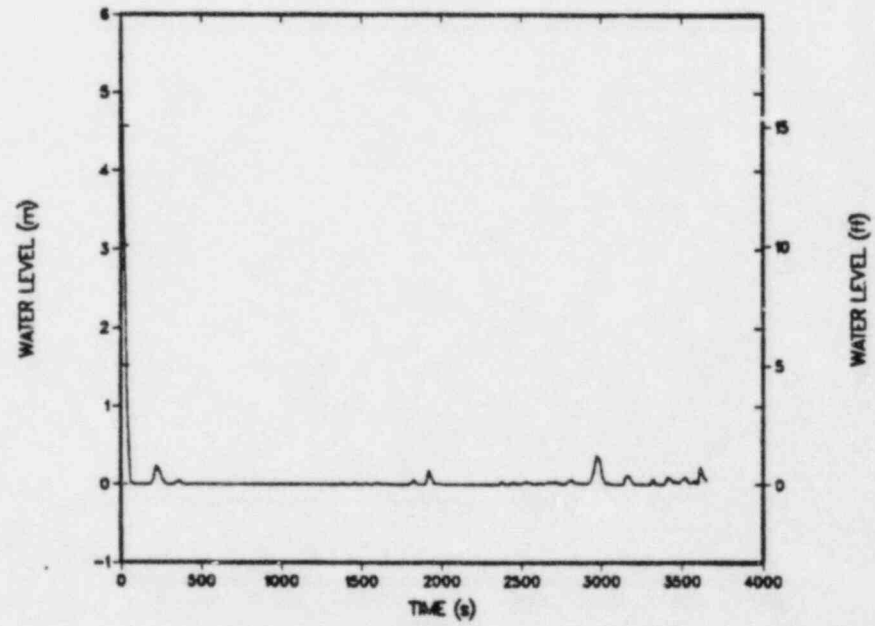

Fig. 205.
Pressurizer water level.

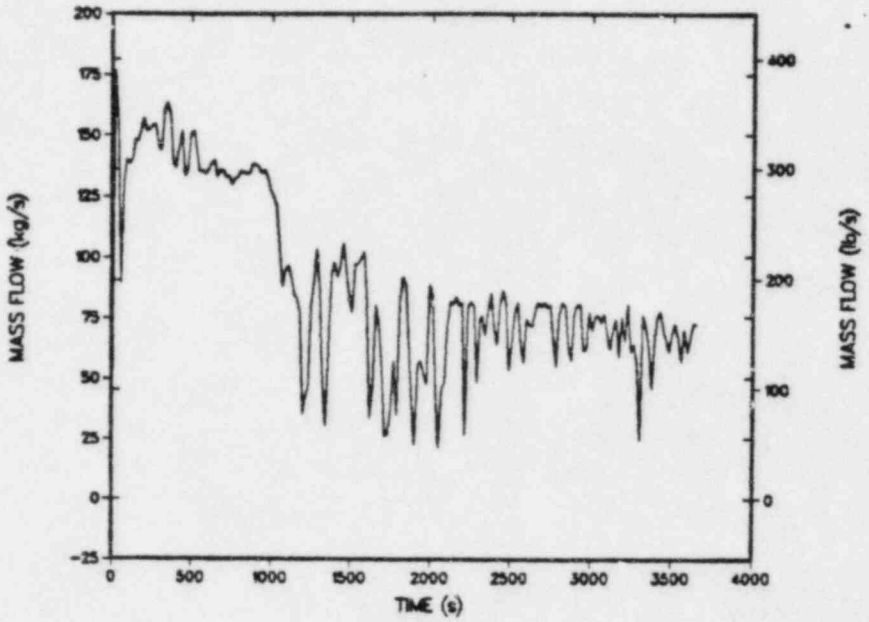

Fig. 206.
Break mass flow.

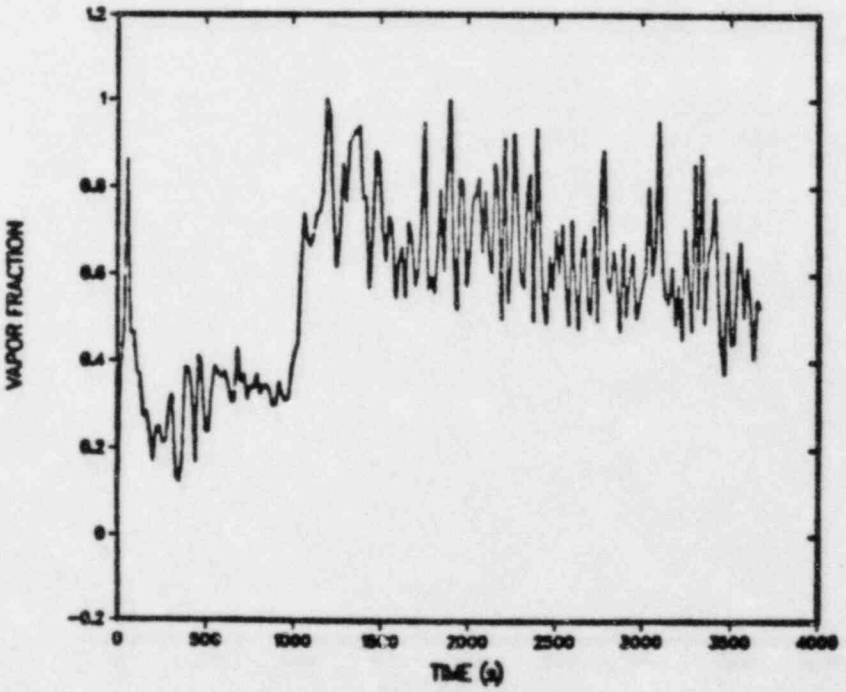

Fig. 207.
Break void fraction.

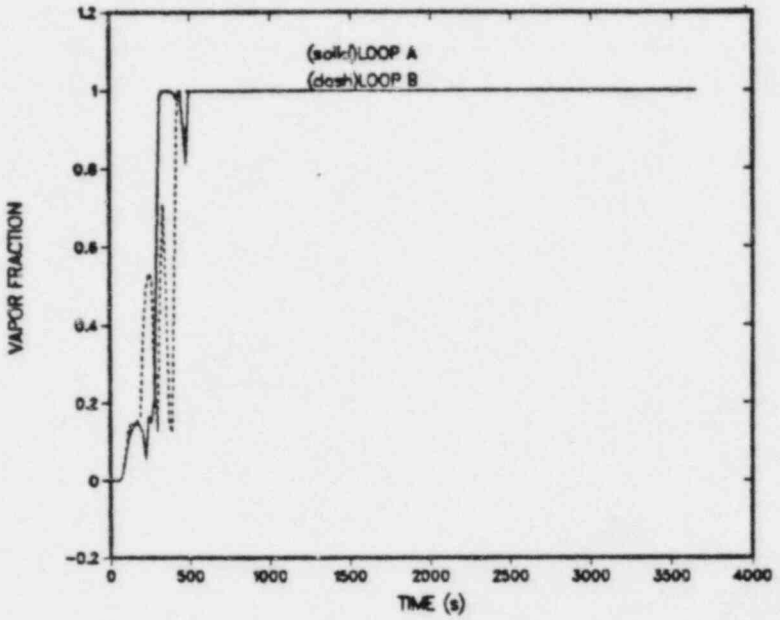

Fig. 208.
Candy-cane void fractions - loops A and B.

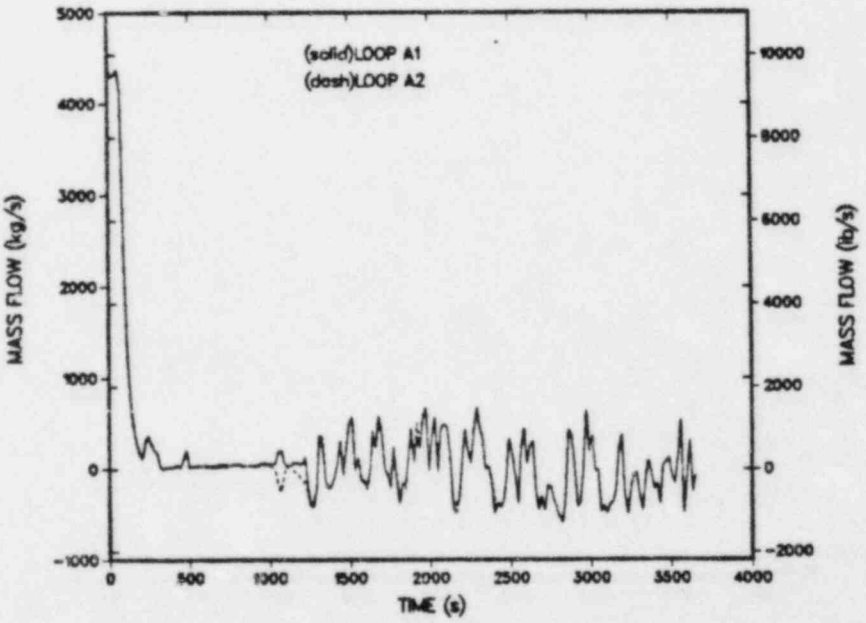

Fig. 209.
Cold-leg mass flows - loops A1 and A2.

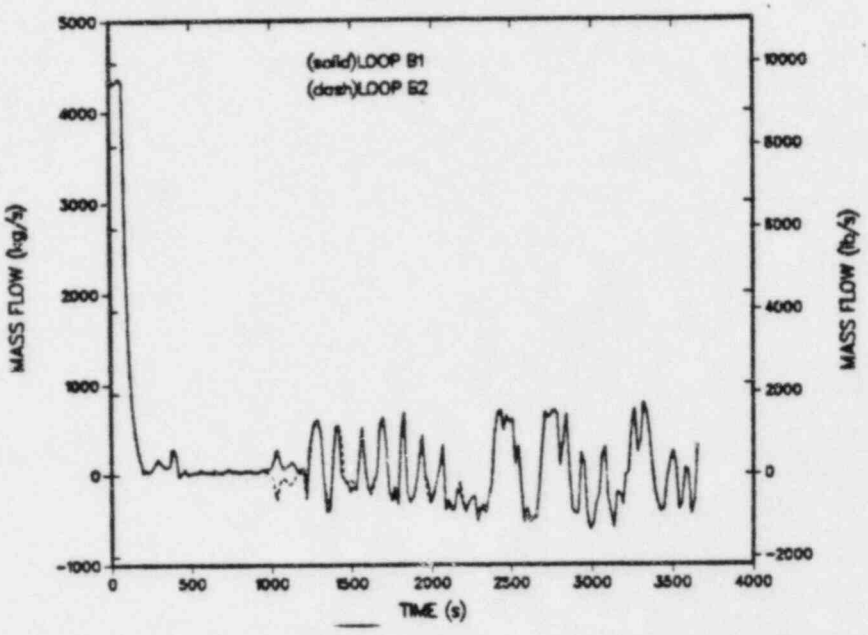

Fig. 210.
Cold-leg mass flows - loops B1 and B2.

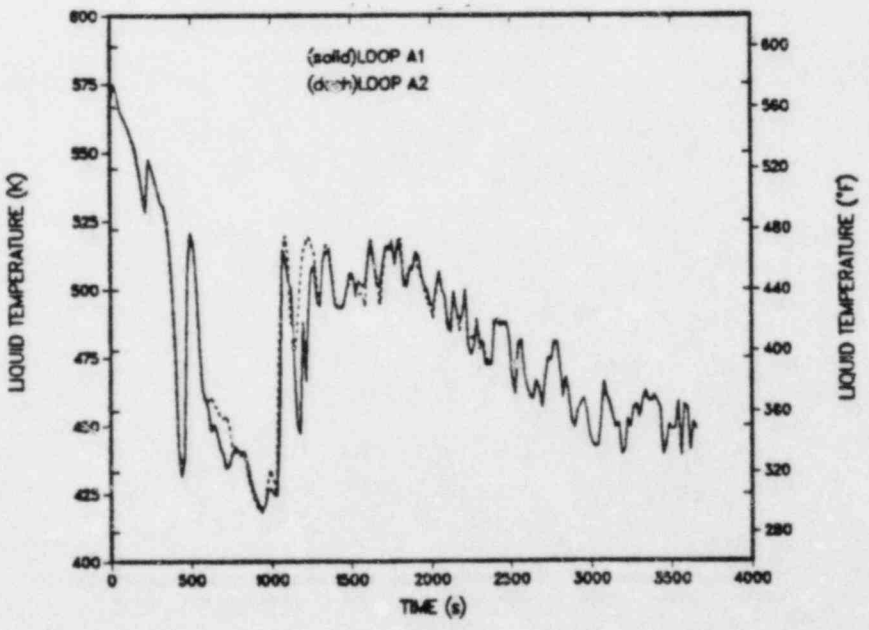

Fig. 211.
Cold-leg liquid temperatures - loops A1 and A2.

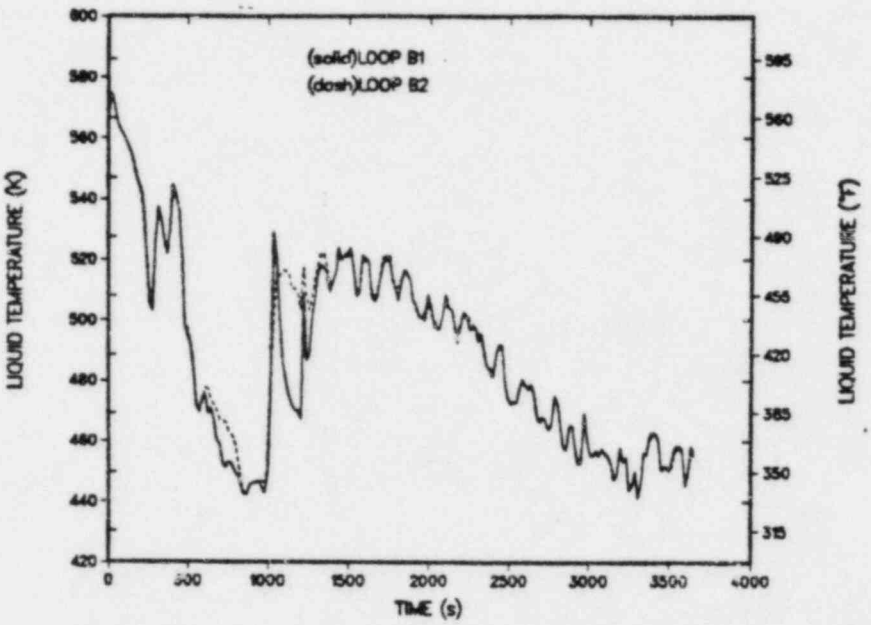

Fig. 212.
Cold-leg liquid temperatures - loops B1 and B2.

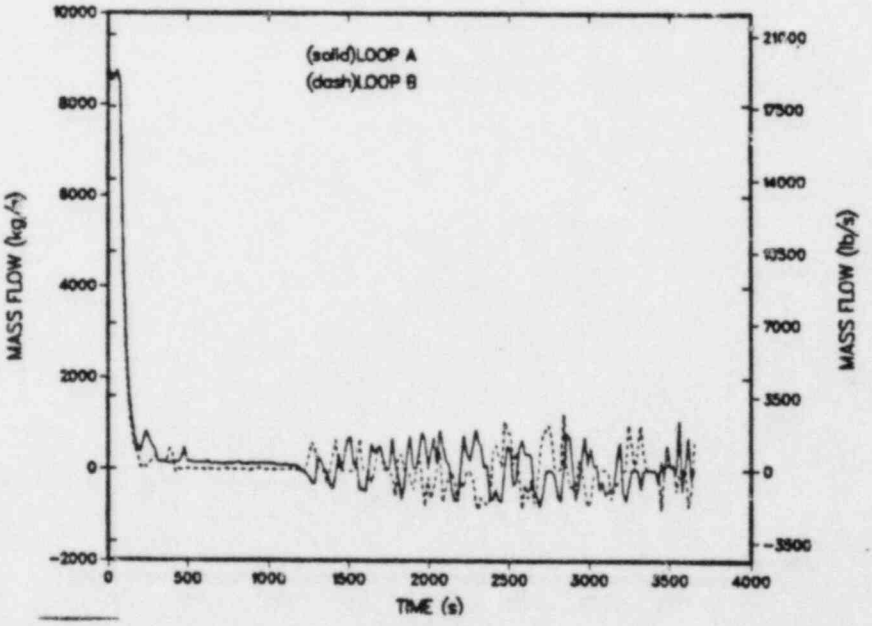

Fig. 213.
Hot-leg mass flows - loops A and B.

Downcomer liquid temperatures at the top axial downcomer level (just below the cold-leg nozzles) are presented in Fig. 215. TRAC calculated a minimum downcomer liquid temperature of ~470 K at approximately 1000 s. This was followed by heating until 1800 s. At 1800 s, additional cooling provided by increased HPI flow as the system pressure decreased and accumulator flow once again decreased the liquid temperatures. At the end of the calculation, the downcomer temperature was approximately 450 K.

From the results of a previous calculation in which the vent valves were accidently isolated from the downcomer (input error), the importance of the vent valves for this particular transient was determined. Figure 216 presents an azimuthal comparison of selected downcomer liquid temperatures at axial level 6 for both calculations. When the vent valves were modeled properly, TRAC calculated downcomer liquid temperatures that were at least 25 K warmer. From the PTS viewpoint, the vent valves were an asset in maintaining "warmer" downcomer liquid temperatures. The total positive vent-valve mass flow is shown in Fig. 217.

d. Analysis of the Loop-flow Oscillations. The loop oscillations that were calculated in the primary system were initiated in the loop B cold-legs. Similar oscillations have been calculated in other small-break transients for B&W plants.[6] The oscillations began after the liquid levels in the primary system decreased to the cold-leg/hot-leg elevations. At ~1100 s, cool HPI fluid dropped into the loop seal from the loop B2 cold leg, and as a result produced a sustained (for ~200 s) positive mass flow (toward the vessel) in loop B1 and a negative mass flow (away from the vessel) in loop B2. Between ~1200 s and ~1250 s a similar occurrence happened in loop A. Cool HPI fluid from the loop A1 cold leg dropped into the loop seal in loop A. Immediately following this occurrence, the loops A and B mass flows and liquid temperatures came in phase and began oscillating. Initially, the loop B oscillations were regular with a period of ~17 s and an amplitude of ~600 kg/s. The loop A oscillations were not initially regular.

In order to explain the loop oscillations, several case studies were conducted. These cases included: turn the HPI off before the oscillations begin, turn the core power off with the SG heat transfer on, turn the SG heat transfer off with the core power on, close the break, and renode the middle-to-upper levels of the vessel and SGs. The oscillations presented in this report were calculated with the renoded vessel and SGs.

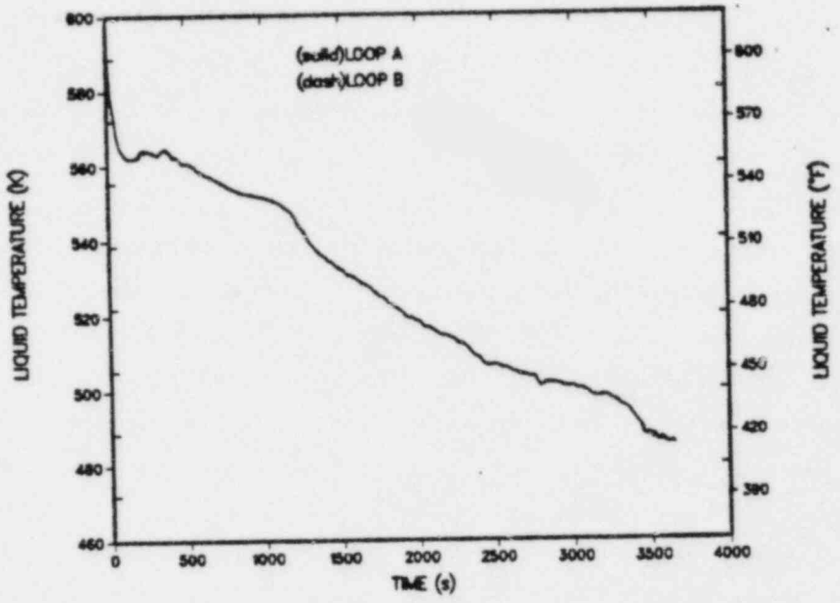

Fig. 214.
Hot-leg liquid temperatures - loops A and B.

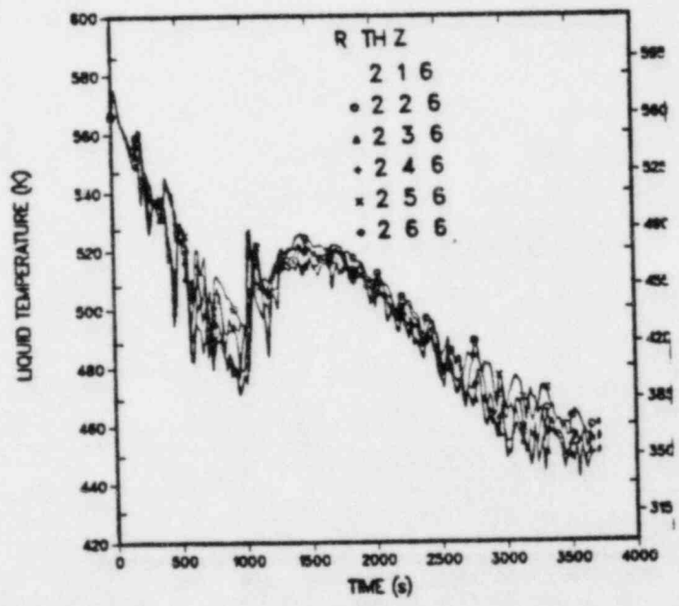

Fig. 215.
Downcomer liquid temperatures - vessel axial level 6 (all azimuthal sectors).

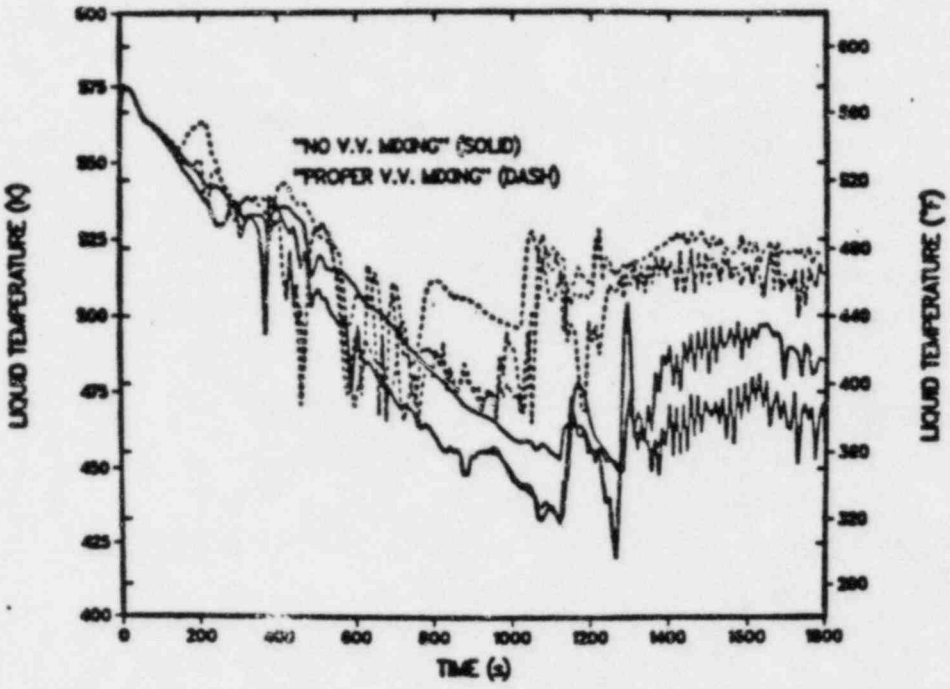

Fig. 216.
Downcomer liquid temperature comparison for 2-in. break case (vent valves versus no vent valves).

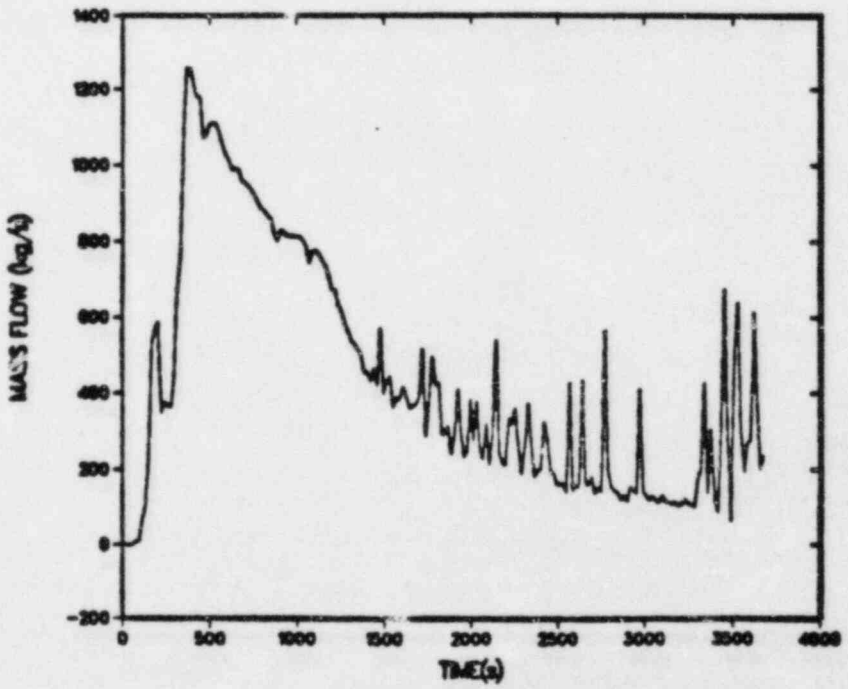

Fig. 217.
Total vent valve mass flow.

Briefly, the results of the parametric-case studies indicated that the HPI coupled with secondary-to-primary heat transfer in the SGs were the forcing functions that caused the oscillations to persist once initiated. The oscillations were manometer-type and the columns of liquid that oscillated included the legs of the loop seals, lower half of the SGs, and the vessel. After the HPI dropped into the loop seal, the elevation head in the loop seal increased because of the denser HPI liquid. This increased elevation head pushed the column of liquid in the loop seal down and up the lower-half of the steam generator. Because of reverse SG heat transfer (secondary to primary), this additional liquid was heated thus changing the effective elevation head in the SG. Thus, because of these changing elevation heads in the loop seals and steam generators, the oscillations persisted.

e. Summary. The Oconee-1 plant response to a 2-in. break in the surge line was calculated using TRAC-PF1. For this small-break transient, the ICS and all key system components were assumed to function correctly. Also, the operators were assumed to trip the RCPs 30 s after HPI actuation. TRAC calculated a minimum vessel downcomer liquid temperature of ~470K at 1000 s. The primary system pressure at this minimum liquid temperature was calculated to be ~6.2 MPa. HPI flow and accumulator injection reduced the temperature at the end of the calculation at 3670 s to ~450 K.

The calculated minimum downcomer liquid temperatures never approached the current NDT value of Oconee-1 for two reasons; (a) vent valve flow mixing with the fluid in the downcomer region, and (2) calculated loop oscillations. However, if the calculation were continued the LPI system will actuate as a result of the depressurization. The addition of LPI would probably result in downcomer liquid temperatures that may approach or exceed the current NDT of the Oconee-1 plant. However, this transient may not be important in terms of PTS because the primary system pressure will be quite low when the downcomer liquid temperature falls below the NDT limit.

2. 4 in. Break

a. Introduction and Summary.

This report presents the Oconee-1 plant response to a 4-in. break in the surge line midway between the pressurizer and the riser of the candy cane. Following the initiation of the break, the reactor and turbine trip from full power. Reactor decay heat was specified as 1.0 times the ANS standard. In this transient, the ICS and all key components are assumed to function correctly. The only specified operator action was the RCPs trip 30 s after HPI actuation. Two cases involving HPI throttling to system subcooling were to be investigated

for this transient. At the end of the base-case calculation (~1433 s), the subcooling condition had not been achieved; therefore, only one calculation was required.

TRAC calculated a minimum vessel downcomer liquid temperature of ~350 K; the primary system pressure at this minimum temperature was ~1.0 MPa.

b. Model Description and Assumptions. A complete description of the primary-side, secondary-side, and ICS modeling can be found in Section II. The steady-state operating conditions are also presented in that section.

The 4-in. break specification containing the initial conditions, event sequence, and assumed failures is presented in Ref. 3. The TRAC transient event sequence for this transient is presented in Table XXVIII. Because the ICS and major system components were specified to function correctly, it was not necessary to make any overriding assumptions.

c. Transient Calculation.

Following the initiation of the break, the reactor and turbine tripped from full power and the TSVs closed, causing an increase in secondary-side pressure. Between ~17 s and ~92 s, the TBVs for both loops functioned normally and relieved the increases in secondary-side pressure. The SG secondary-side pressures for loops A and B are shown in Figs. 218 and 219, respectively. At ~300 s the secondary pressures in both SGs remained momentarily constant just below ~6.0 MPa following the closure of the SUFCVs based on the increasing secondary-side inventories. After ~400 s the loop A secondary-side pressure decreased at a much faster rate as the primary cooled the secondary. This heat-transfer mechanism lowered the loop-A secondary pressure and produced a larger loop-A secondary-side inventory as a result of condensation. Figures 220 and 221 show the loop A and B SG secondary-side inventories.

Loop A and B MFW mass flows and liquid temperatures are shown in Figs. 222 and 223, respectively. The SUFCVs continued to deliver feedwater to the lower SG header until ~47 s when the MFW was realigned to the SG upper header. The MFCVs were closed by the ICS ~10 s into the transient. Figures 224 and 225 show the loop A and B realigned mass flows and liquid temperatures. The EFW pump was not activated in this transient as it was not needed.

Pressurizer pressure and water level are shown in Figs. 226 and 227, respectively. The primary system pressure fell very rapidly until the HPI was actuated at ~17 s. The system pressure was almost stabilized after ~800 s at ~2.0 MPa as the HPI mass flow approached the break mass flow. The pressurizer emptied immediately and was never refilled because of the relatively large break. Figures 228 and 229 present the break mass flow and void fraction.

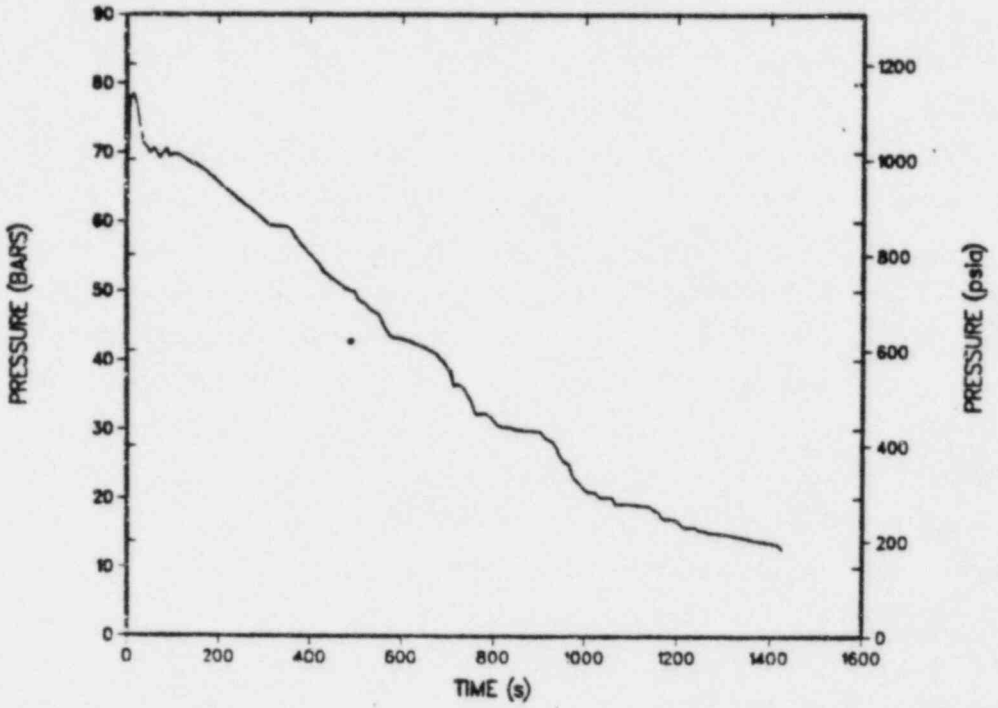

Fig. 218.
Steam generator secondary-side pressure - loop A.

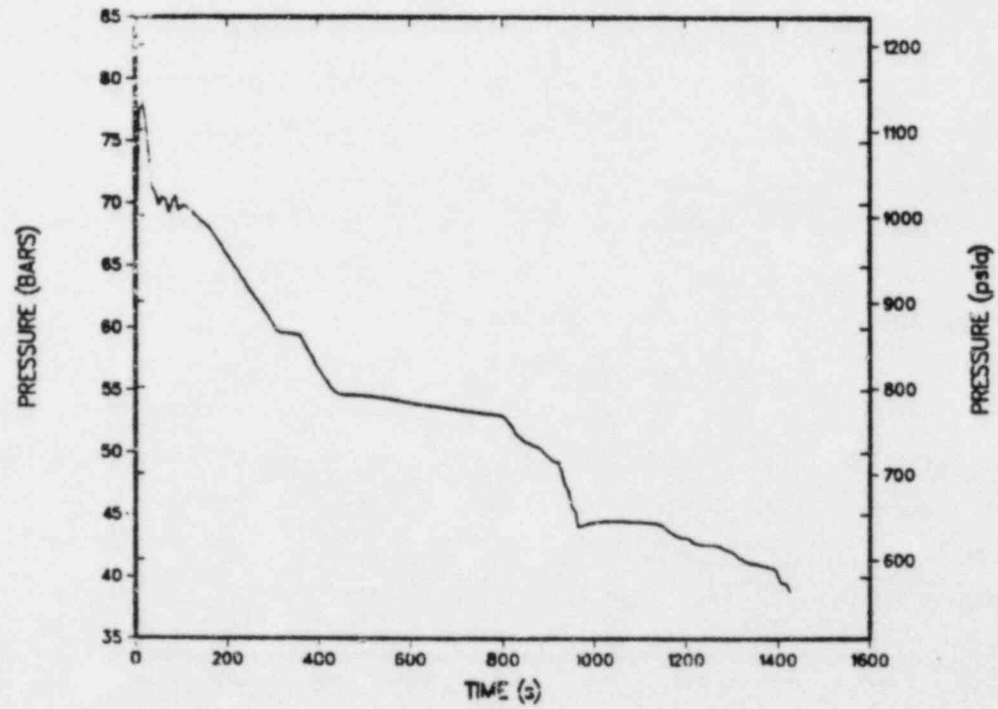

Fig. 219.
Steam generator secondary-side pressure - loop B.

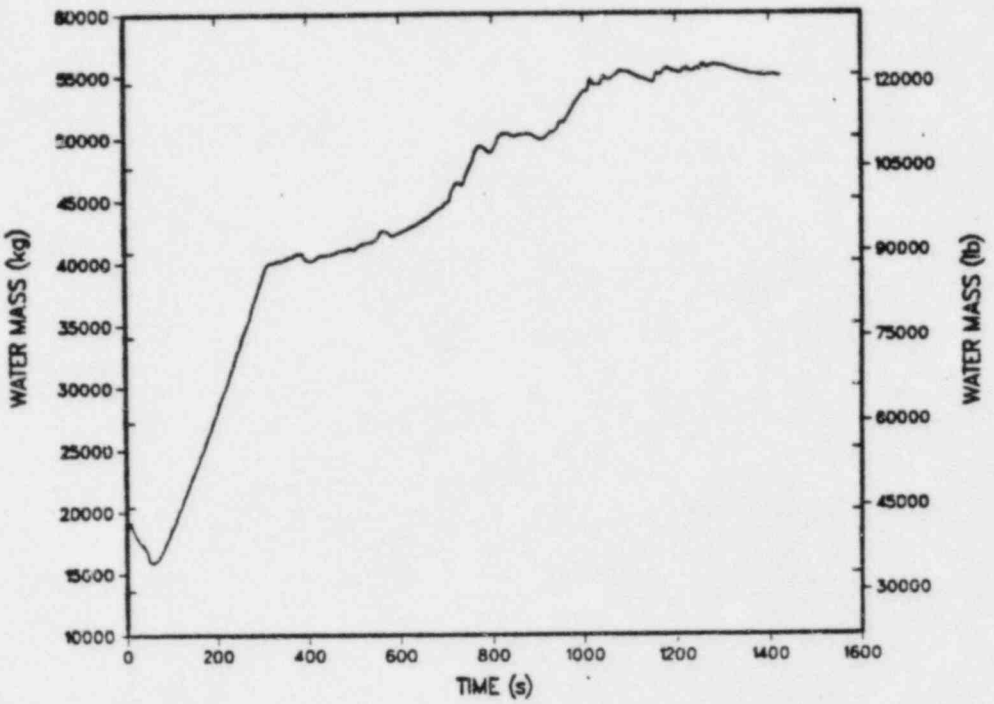

Fig. 220.
Steam generator secondary-side inventory - loop A.

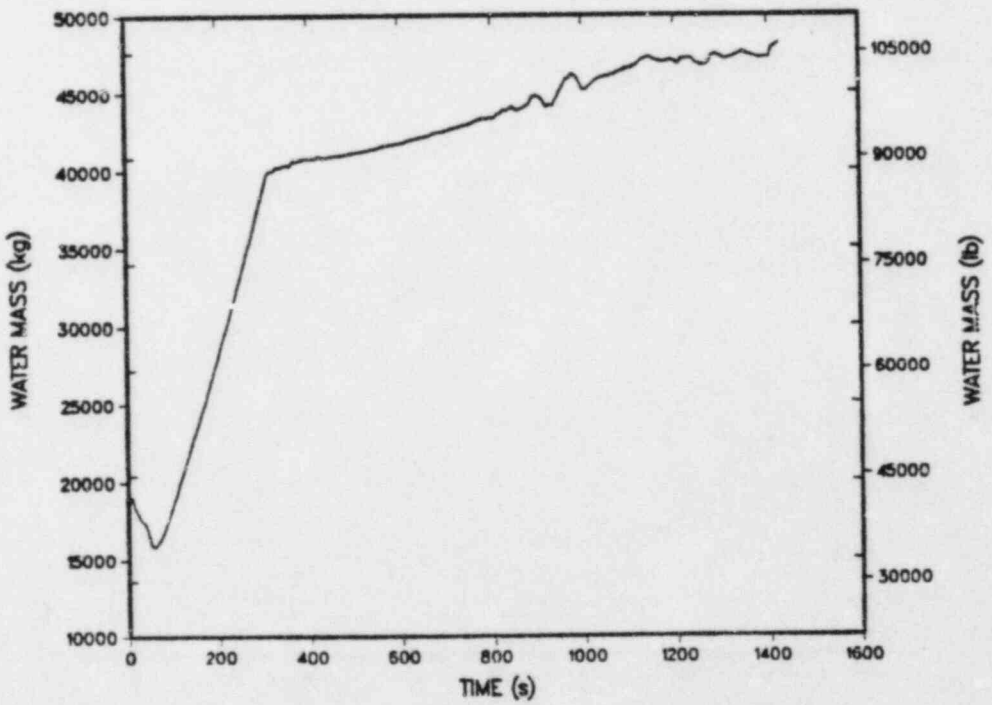

Fig. 221.
Steam generator secondary-side inventory - loop B.

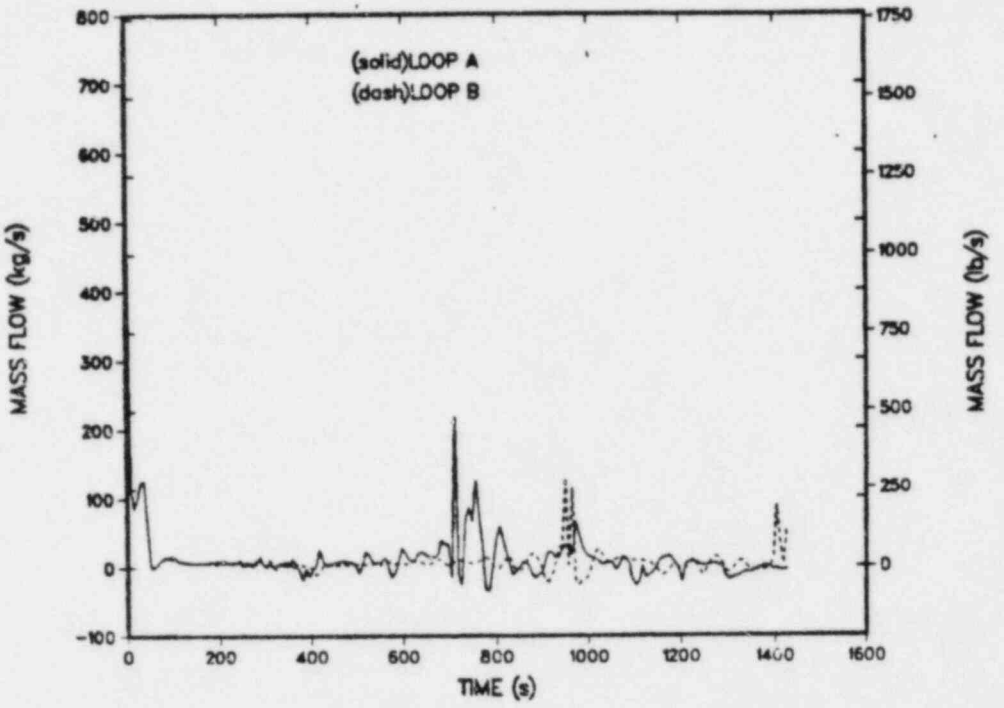

Fig. 222.
MFW flows - loops A and B.

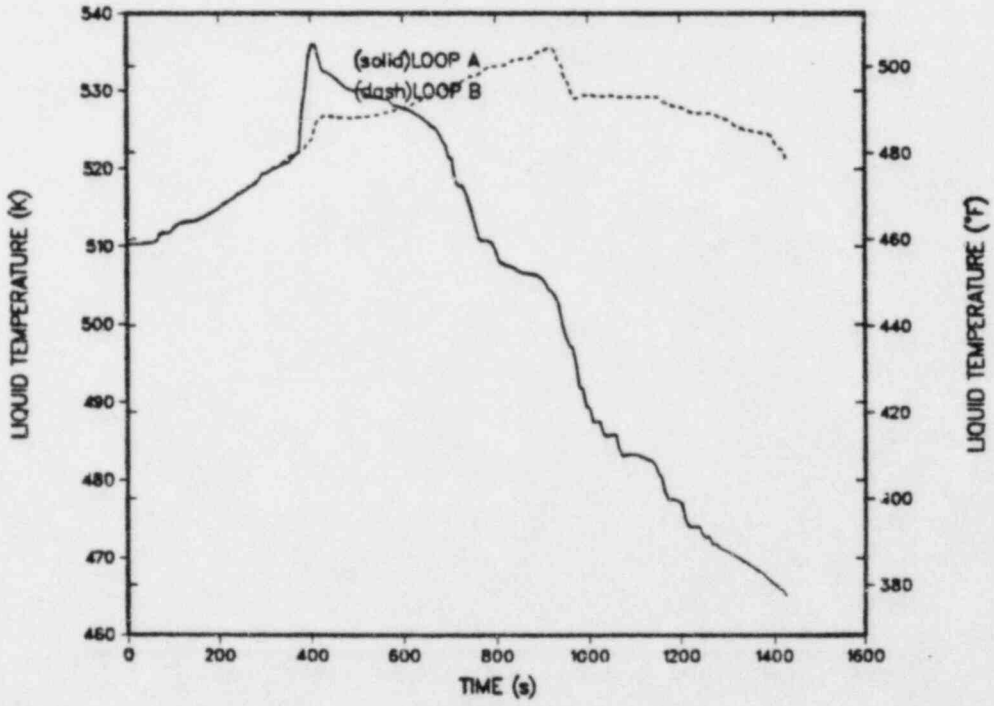

Fig. 223.
MFW liquid temperatures - loops A and B.

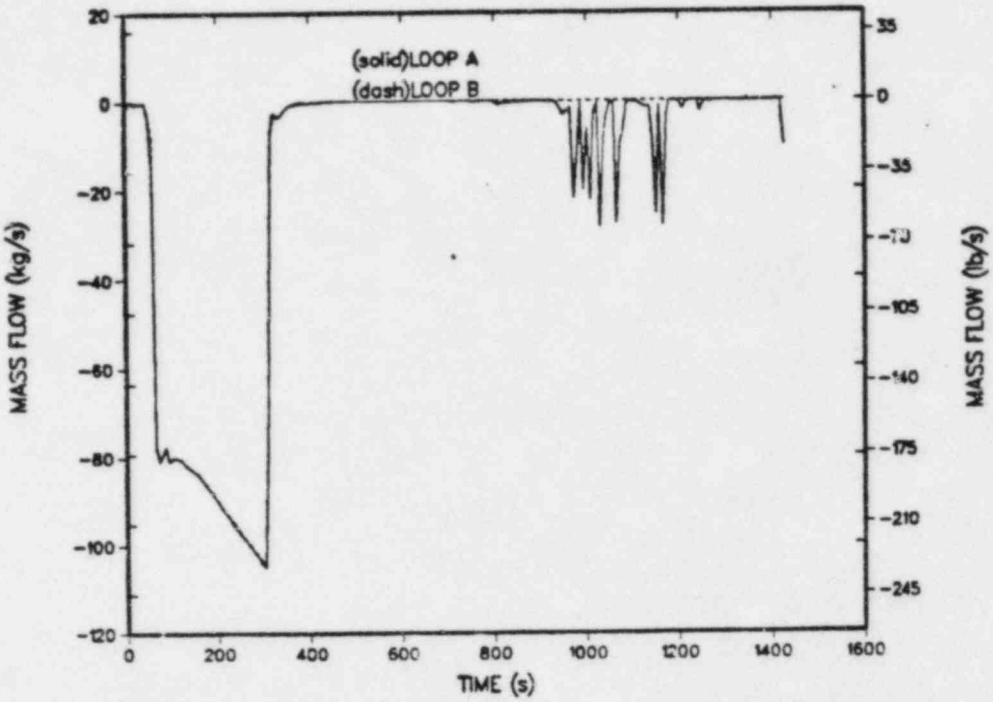

Fig. 224.
Realigned mass flows - loops A and B.

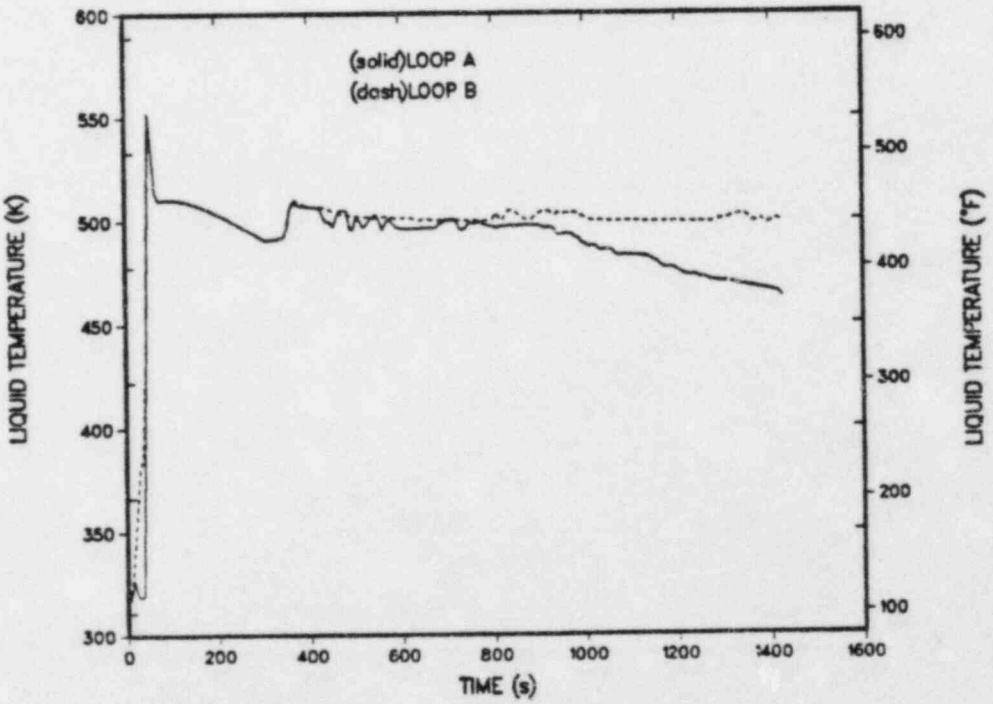

Fig. 225.
Realigned liquid temperatures - loops A and B.

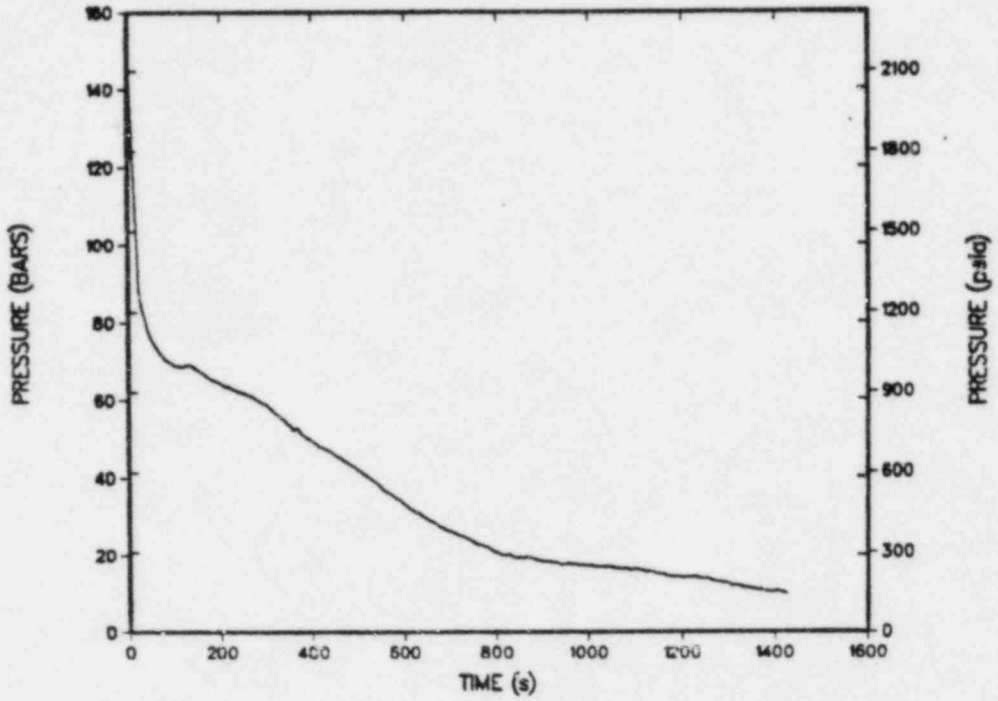

Fig. 226.
Pressurizer pressure.

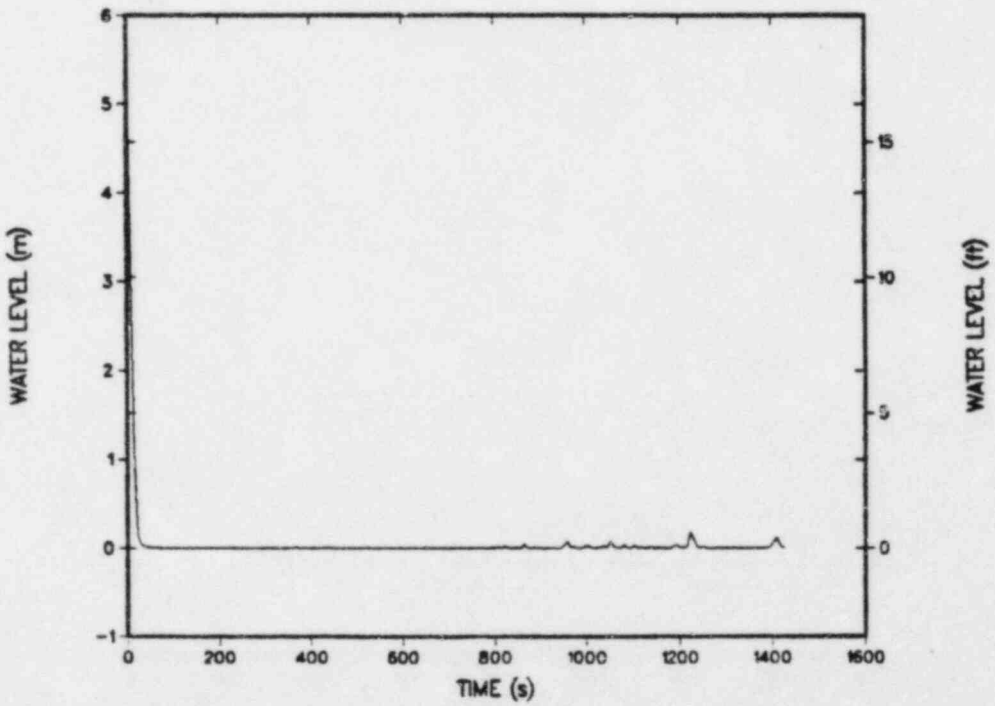

Fig. 227.
Pressurizer water level.

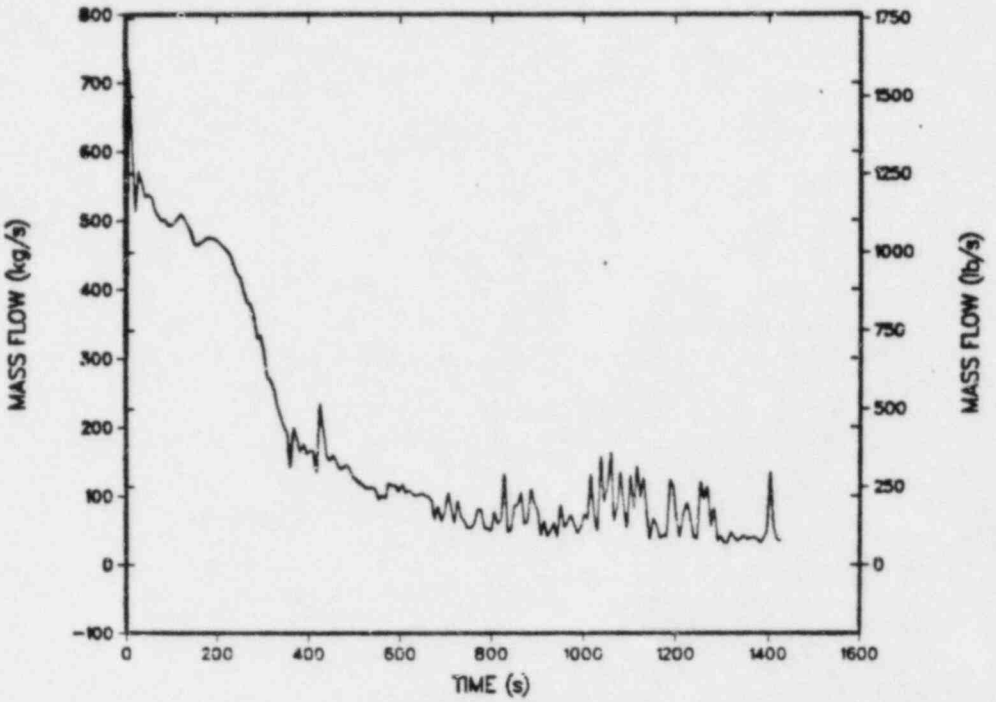

Fig. 228.
Break mass flow.

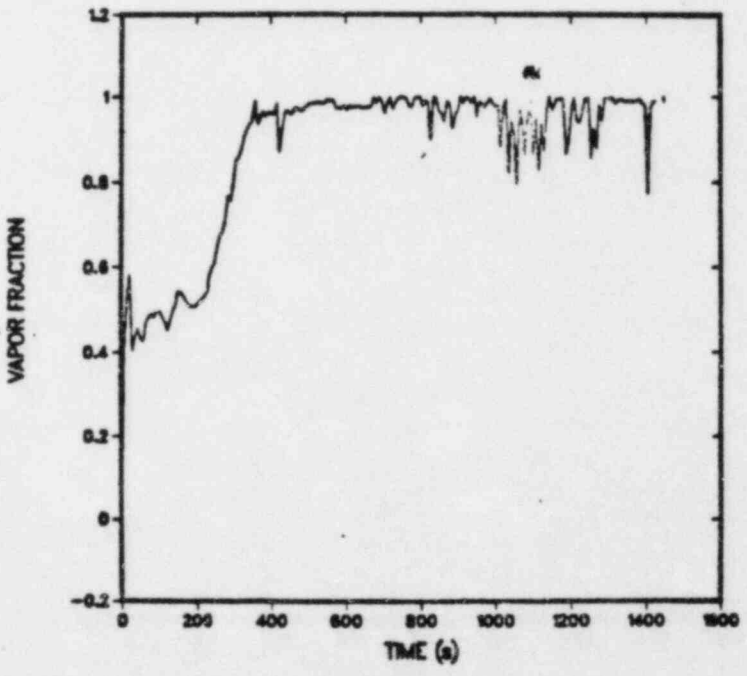

Fig. 229.
Break void fraction.

TABLE XXVIII

HOT-LEG BREAK LOCA - 4 IN. BREAK
EVENT SEQUENCE BASE CASE

	Event	Time (s)
1.	Break opens	0.0
2.	Turbine and reactor trip	0.5
3.	Turbine-stop valves close	0.5
4.	Secondary-side heater and heater-drain trip	1.0
5.	Condenser feed from turbine trip	1.5
6.	TBV loop A opens for first time	4.4
7.	TBV loop B opens for first time	4.8
8.	HPI system actuation on low primary system pressure	16.8
9.	TBV loops A and B open/close	
10.	RCPs trip 30 s after HPI actuation	46.8
11.	MFW is realigned to SGs upper header	46.8
12.	MFCV override trip	46.8
13.	TBV loops A and B open/close	92.1
14.	Candy-canes void	125.0
15.	ICS closes SUFCVs	300.0
16.	Accumulator injection loop A (first time)	54C 7
17.	Accumulator injection loop B (first time)	541.0
18.	Accumulator injections loop	678.6
19.	Accumulator injection loop A	726.1
20.	Accumulator injection loop B	784.5
21.	Accumulator injection ceases loop A	828.7
22.	Accumulator injection loop A	921.4
23.	Accumulator injection loop B	925.7
24.	Accumulator injection ceases loop B	947.5
25.	Accumulator injection ceases loop A	947.7
26.	Accumulator injections (both loops)	~1100.0
27.	LPI system actuation on low primary system pressure	~1236.0
28.	End of calculation	~1400.0

Initially, the break mass flow was quite large (> 450 kg/s) until ~200 s. Following this time, the upper regions of the primary became significantly void causing the break mass flow to decrease. The candy-canes for both loops were completely voided by ~125 s as shown in Fig. 230.

Mass flows and liquid temperatures for the loop-A and -B hot legs are shown in Figs. 231 and 232, respectively. The primary system flows decreased to approximately zero following the RCPs trip. The loop-B hot leg flow became stagnant as the candy-cane voided; however, the loop-A hot leg did not stagnate and continued to feed the break with vapor. Hot-leg liquid temperatures decreased in accordance with the primary system depressurization. TRAC

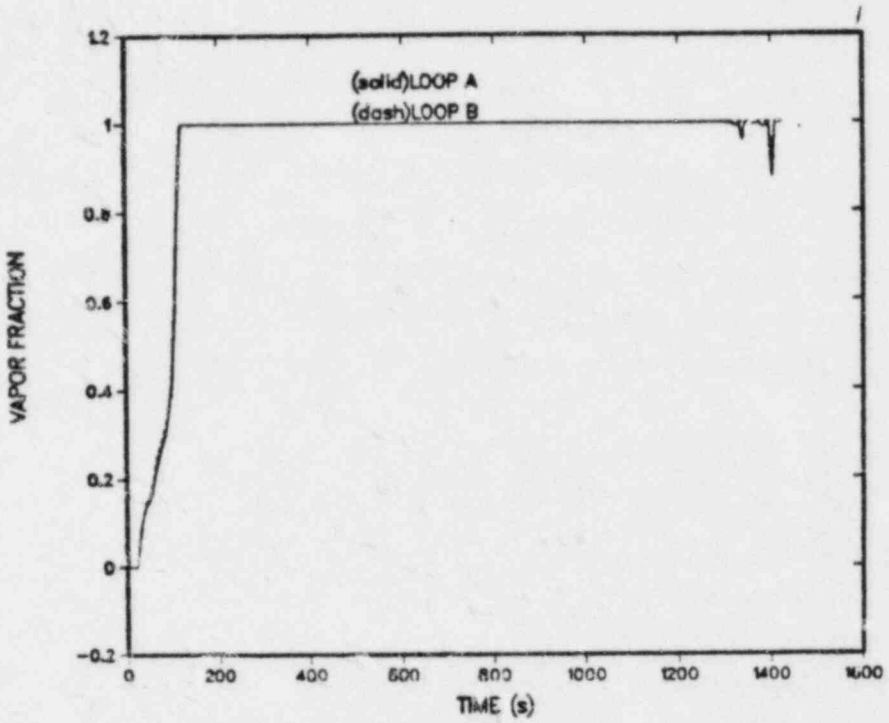

Fig. 230.
Candy-cane void fractions - loops A and B.

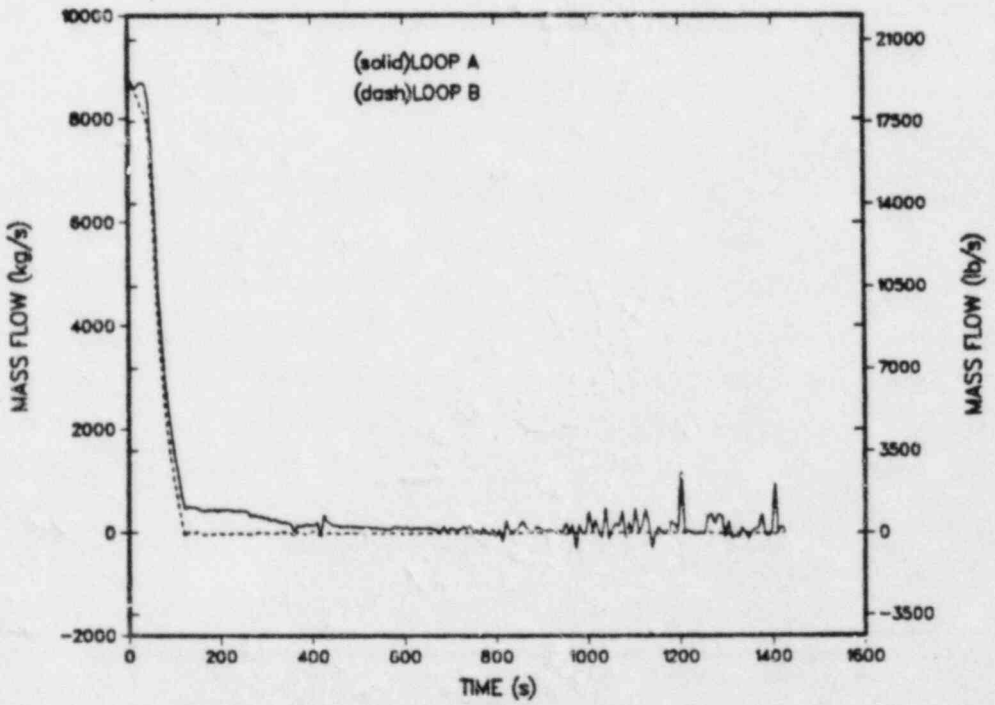

Fig. 231.
Hot-leg mass flows - loops A and B.

calculated a minimum hot-leg temperature of ~455 K. The loop -A and -B cold-leg mass flows are presented in Figs. 233 and 234, and exhibited trends similar to the hot legs. The corresponding cold-leg liquid temperatures are shown in Figs. 235 and 236. Minimum cold-leg temperatures (before LPI actuation) were calculated to be ~430 K at ~650 s for loop A1 and ~430 K at ~600 s for loop A2. During the stagnant period in the cold-legs (between ~400 and ~700 s), HPI flow into the downcomer along with accumulator injection at ~540 s and a decreasing vent valve vapor mass flow rate were responsible for the calculated minimum temperatures. The vent valves opened at ~50 s immediately following the RCP trip. The vent valve total mass flow is presented in Fig. 237. The loop B cold-leg liquid temperatures had trends similar to those found in loop A but with the minimums (before LPI actuation) occurring at times corresponding to loop-B accumulator injection. TRAC calculated minimum cold-leg temperatures of ~425 K at ~770 s for loop B1 and ~445 K at ~950 s for loop B2. The initiation of the low-pressure injection (LPI) system at ~1240 s on low primary system pressure dropped the cold-leg liquid temperatures near or below ~400 K. The LPI system injected directly into the vessel downcomer in axial level 7.

As identified in Sec. I, transients involving system repressurization and overcooling have been identified as events that could damage and possibly cause the failure of a PWR vessel. Thus, the key PTS parameters are pressure and liquid temperature in the vessel downcomer region around the weld locations. For this particular transient, the primary concern is thermal shock because the primary system will not repressurize. In this plant, the welds located in vessel level 6 in the TRAC model are the weld locations that are considered important for this study. TRAC calculated a minimum downcomer liquid temperature of ~350 K in level 6. The system pressure at this minimum downcomer liquid temperature was calculated to be ~1.0 MPa. The minimum temperature values calculated for downcomer level 6 (between ~540 s and ~1200 s) directly correspond to accumulator injections. The LPI system actuation produces the minimum temperatures after ~1200 s. Downcomer liquid temperatures at the top axial downcomer level (just below the cold-leg nozzles) for each azimuthal segment are presented in Fig. 238.

d. Summary. The Oconee-1 plant response to a 4-in. break in the surge line was calculated using TRAC-PF1. For this transient, the ICS and all key components were assumed to function correctly. Also, the operators were assumed to trip the RCPs 30 s after HPI actuation. TRAC calculated a minimum downcomer liquid temperature of ~350 K; the system pressure at this minimum temperature was ~1.0 MPa.

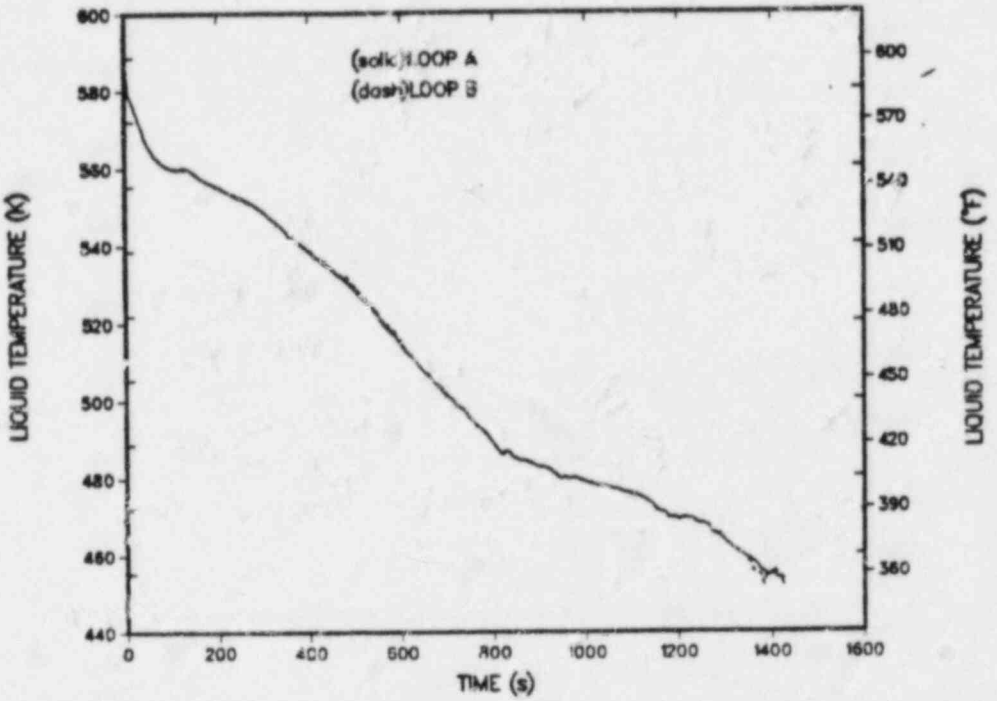

Fig. 232.
Hot-leg liquid temperatures - loops A and B.

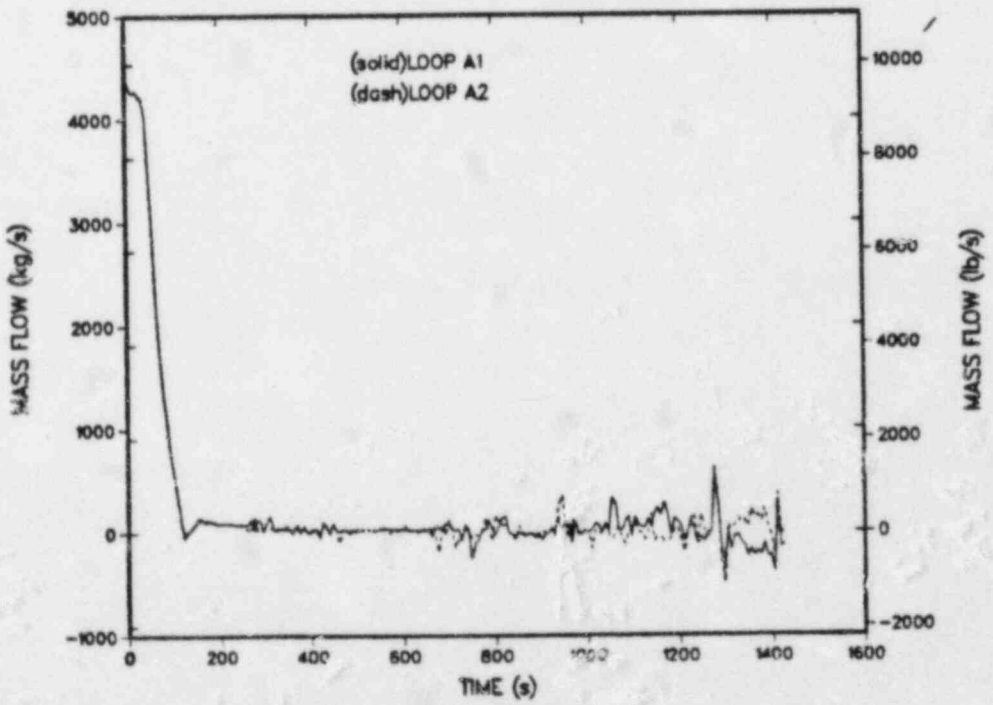

Fig. 233.
Cold-leg mass flows - loops A1 and A2.

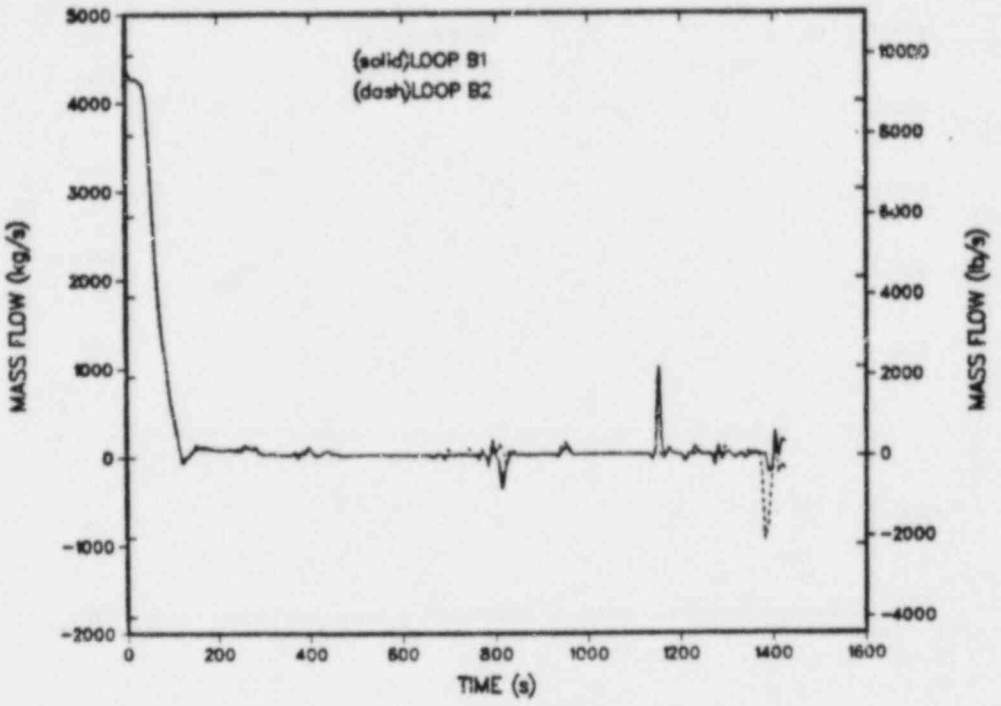

Fig. 234.
Cold-leg mass flows - loops B1 and B2.

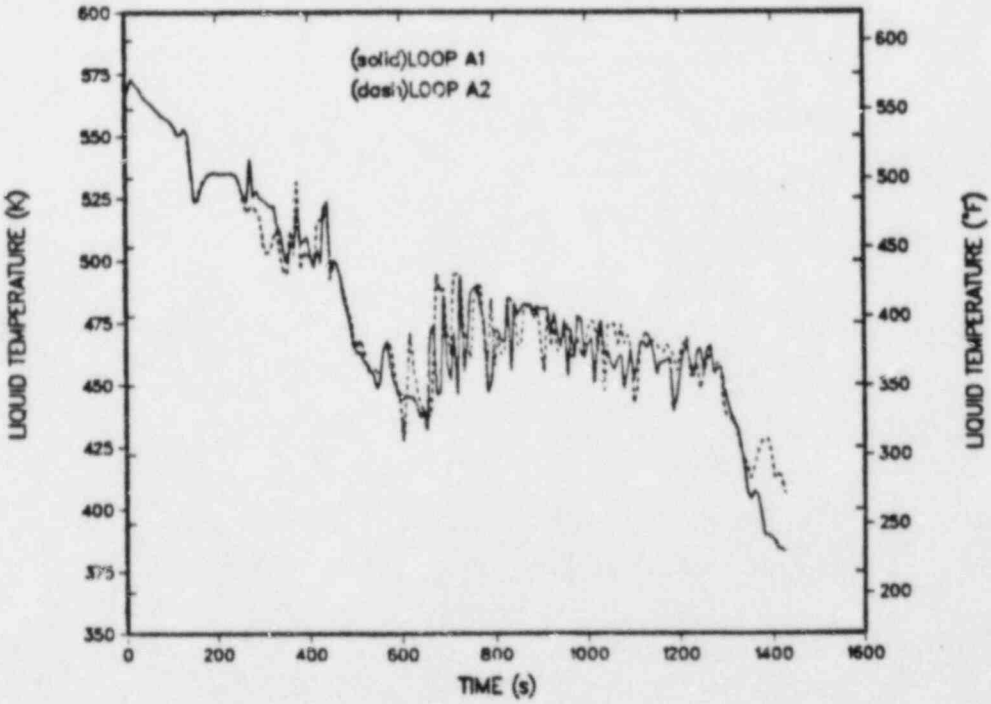

Fig. 235.
Cold-leg liquid temperatures - loops A1 and A2.

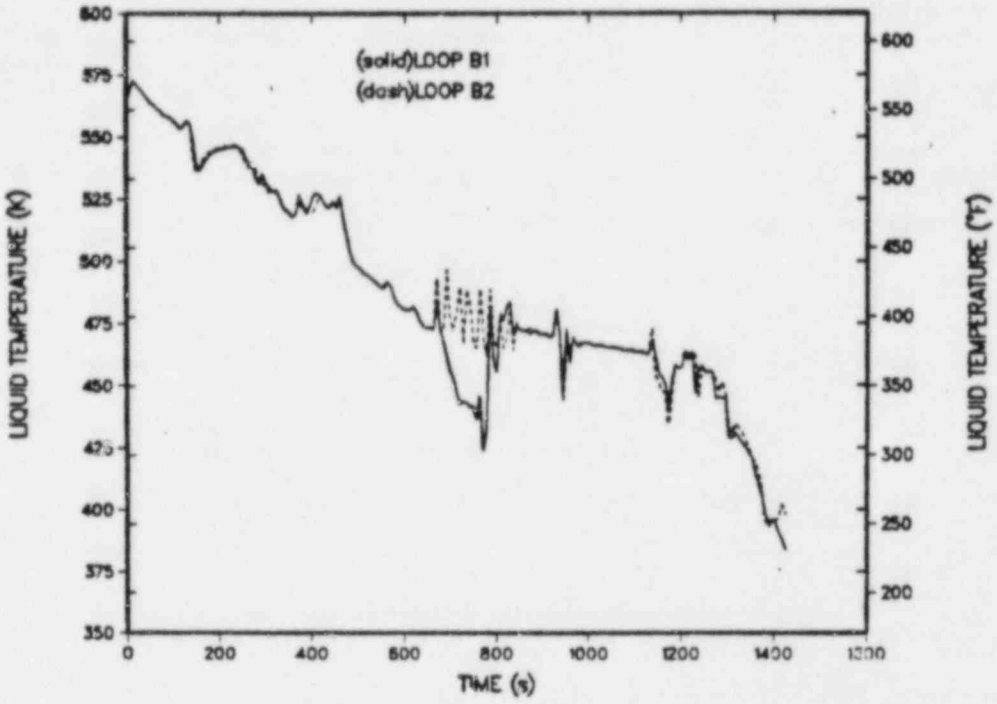

Fig. 236.
Cold-leg liquid temperatures - loops B1 and B2.

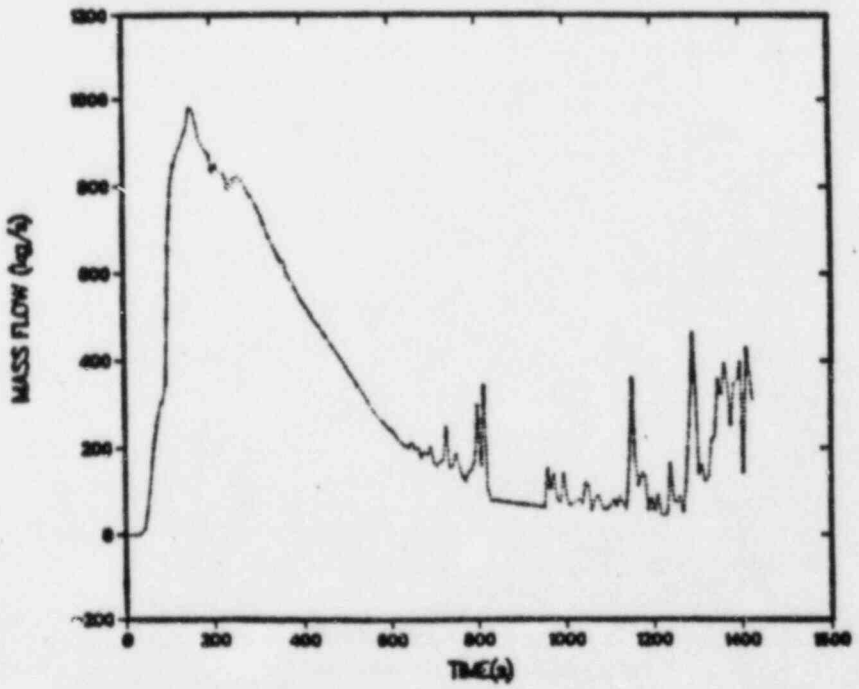

Fig. 237.
Total positive vent-valve vapor mass flow.

Adequate fluid mixing between the vent-valve fluid and the cold-leg (HPI) fluid in the downcomer at the cold-leg junction maintained the downcomer liquid temperatures above ~450 K. However, the actuation of the LPI system at ~1240 s dropped the downcomer temperatures very rapidly and below the current NDT value (~365 K) for the Oconee-1 plant. Even though the downcomer liquid temperatures were calculated to be below the current NDT for Oconee-1, this calculation could not be considered a significant PTS transient because repressurization did not occur.

F. Rancho-Seco Type Transient (SG Dryout Followed by EFW Overfeed)

1. Introduction and Summary. The thermal-hydraulic response of the Oconee-1 plant to a Rancho-Seco type overcooling transient, that is, steam generator (SG) dryout followed by emergency-feedwater overfeed, has been analyzed. The accident sequence began as a loss-of-main feedwater transient (MFW pumps trip). The EFW-control valves failed to open on demand but were subsequently manually opened by the operator. Also, the RCPs remained on during the transient, and the EFW to the SGs was not terminated until 4200 s. The primary system repressurization was limited to ~13.8 MPa as a result of the operator throttling the HPI system.

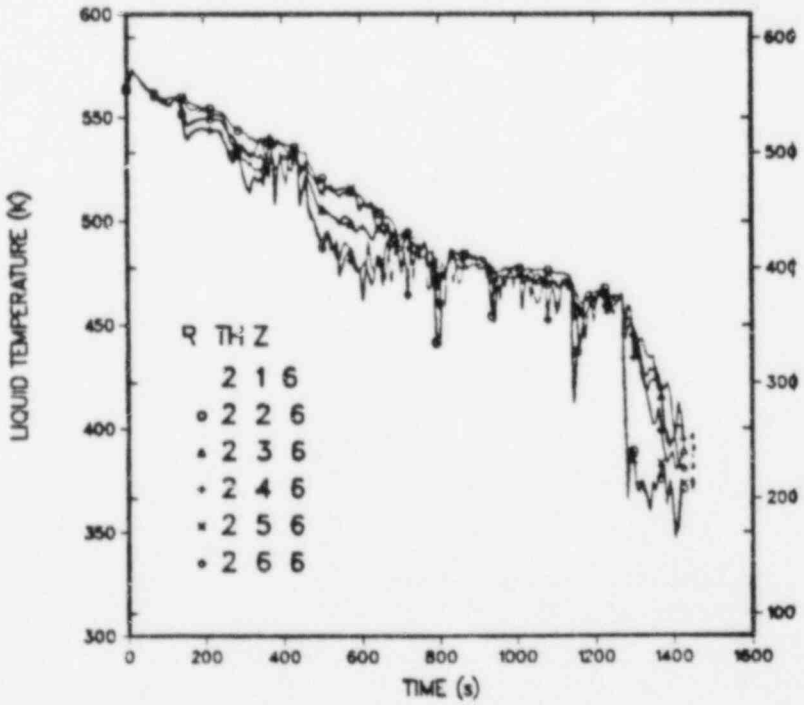

Fig. 238.
Downcomer liquid temperatures - vessel axial level 6 (all azimuthal sectors).

TRAC calculated a minimum downcomer liquid temperature of ~452°K at 4200 s. Repressurization of the primary system to ~13.8 MPa was also calculated.

2. Model Description and Assumptions. A complete description of the primary system, secondary system, and ICS modeling can be found in Section II. The steady-state operating conditions are presented in that section also. The SG dryout followed by EFW overfeed accident specification containing the assumed plant initial conditions and postulated event sequence is presented in Table XXIX. The calculated event sequence is presented in Table XXX. In order

TABLE XXIX

RANCHO-SECO TYPE TRANSIENT
INITIAL CONDITIONS AND POSTULATED EVENT SEQUENCE

Initial Conditions:

1. Reactor at 100% power
2. Nominal temperatures and pressures
3. Decay heat: 1.0 ANS standard
4. Pressurizer spray/heaters function as designed

Postulated Sequence of Events:

1. MFW pumps trip
2. Turbine trip (TSVs close)
3. EFW pumps start (on low MFW discharge pressure)
4. Reactor trip (on high pressure)
5. Both EFW control valves fail close
6. SG dryout
7. PORV (primary) function as designed
8. Turbine bypass system operates as designed
9. Operator fully opens EFW control valves at 9 minutes
10. HPI activates on low pressure
11.[a] Accumulator and LPI function as designed
12. Operator fully opens EFW control valves at 9 minutes
13. Operator limits pressurization to 13.8 MPa by throttling HPI flow
14. EFW flow terminated at 70 minutes
15. Operator restores SG level by throttling EFW flow (aligned to hotwell if necessary)
16. Operator throttles HPI to maintain 42 K subcooling after SGs are restored to proper level

[a]May be phenomenologically dependent

TABLE XXX

RANCHO-SECO TYPE TRANSIENT
SEQUENCE OF EVENTS

	Event	Time (s)
1.	MFW pumps trip, MFCVs and SUFCVs close	0.0
2.	TSVS close (both loops)	0.0
3.	Reactor trips on high pressure	4.4
4.	TBVs actuated	~4.6
5.	PORV actuated	226.4
6.	EFW initiated to both SGs	540.0
7.	HPI actuated on low pressure	~738.0
8.	HPI throttled to limit repressurization	~1255.0
9.	EFW terminated to both SGs	4200.0
10.	Minimum vessel downcomer liquid temperature (~452 K) calculated	~4200.0
11.	Calculation terminated	4300.0

to ensure the correct plant response to the postulated sequence of events, significant portions of the TRAC ICS model were used.

3. Results. Following the loss of MFW and coincident turbine trip, the reactor tripped from full power on high RCS pressure at ~4.4 s. The PORV functioned properly between ~226 s and ~550 s and relieved the pressure increase in the primary system as the SGs dried out. The primary system pressure, pressurizer water level, and PORV mass flow rate are presented in Figs. 239, 240, and 241, respectively. On the secondary side, the TBVs functioned properly and relieved secondary-side pressure increases that occurred also during the SG dry-out period. Figures 242 and 243 present the secondary-side pressures for loops A and B, respectively. At 540 s, the EFW valves were opened fully and EFW began to refill the SGs. EFW mass flow rates and liquid temperatures at the point of injection are presented in Figs. 244 and 245, respectively. The SG inventories for loops A and B are shown in Figs. 246 and 247, respectively. As the EFW was injected into the SGs, the secondary-side inventories began to recover and the primary system began to depressurize. Cold-leg liquid temperatures for loops A and B are presented in Figs. 248 and 249, while Fig. 250 presents the hot-leg liquid temperatures for both loops.

As a result of the depressurization, the HPI system was actuated at ~738 s on low pressure. At ~1255 s, the HPI system flow was throttled to limit RCS repressurization to ~13.8 MPa as specified in the event sequence. The HPI system flow was continually throttled to limit system repressurization

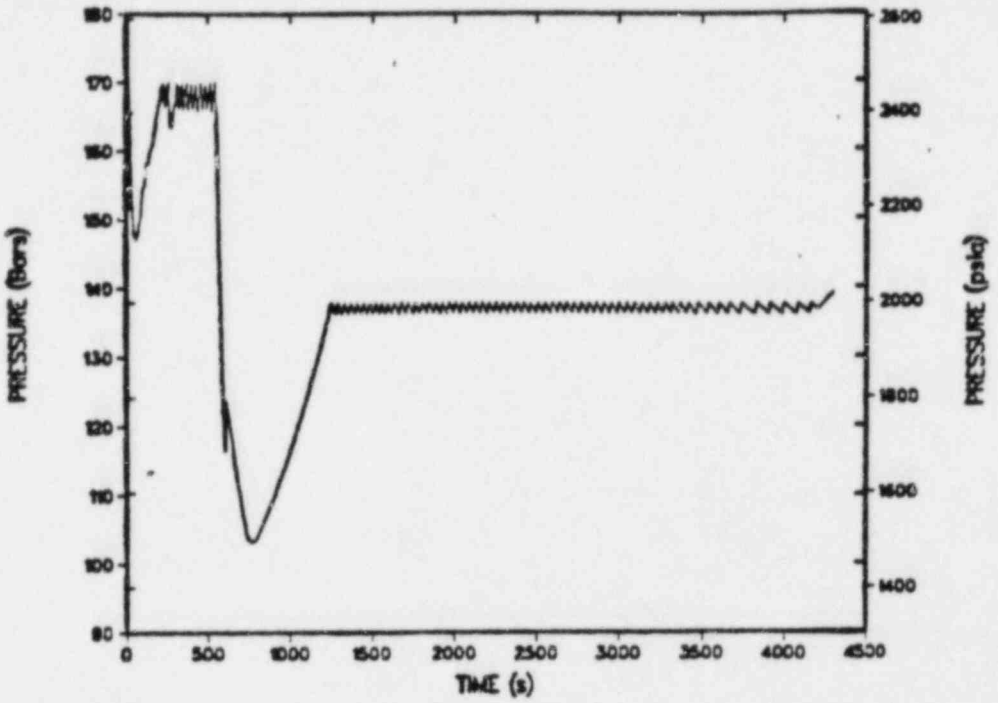

Fig. 239.
Primary system pressure.

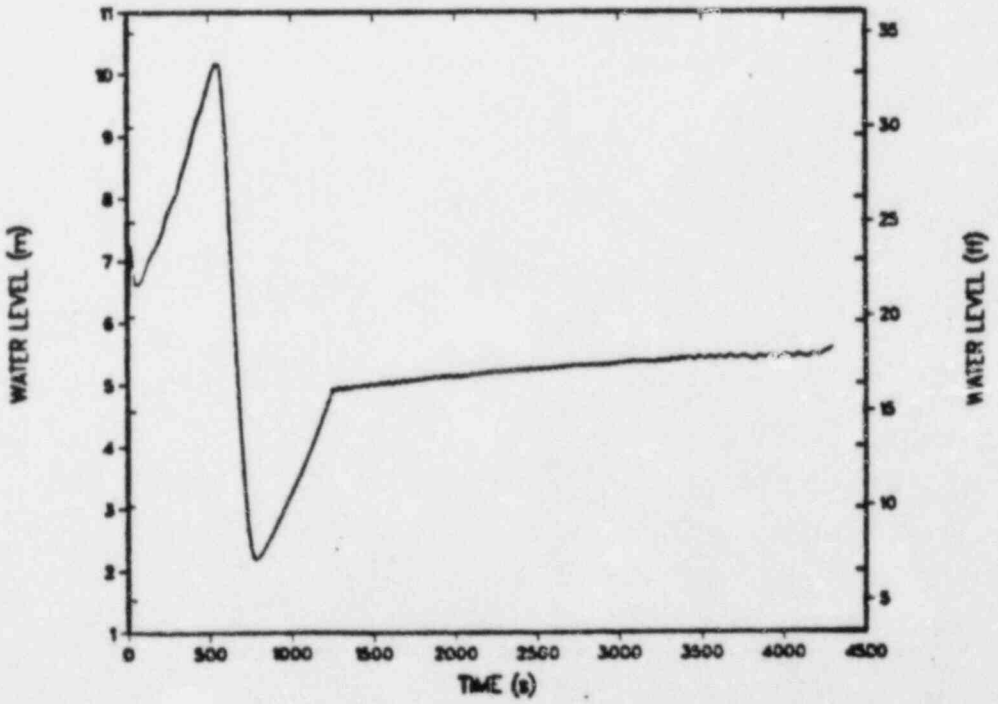

Fig. 240.
Pressurizer water level.

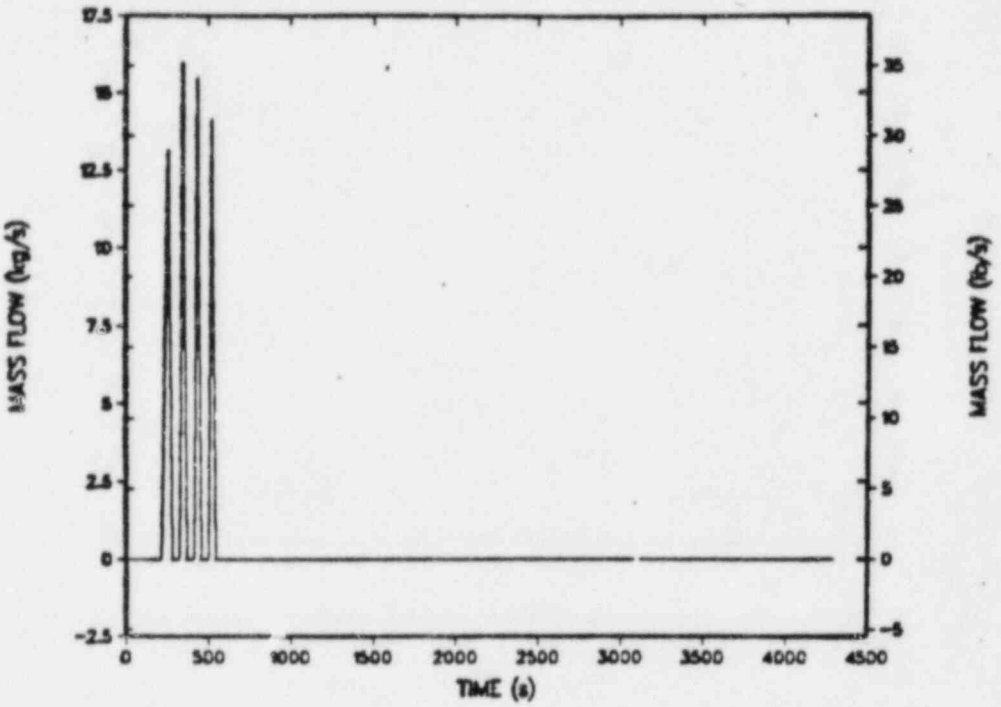

Fig. 241.
PORV mass flow.

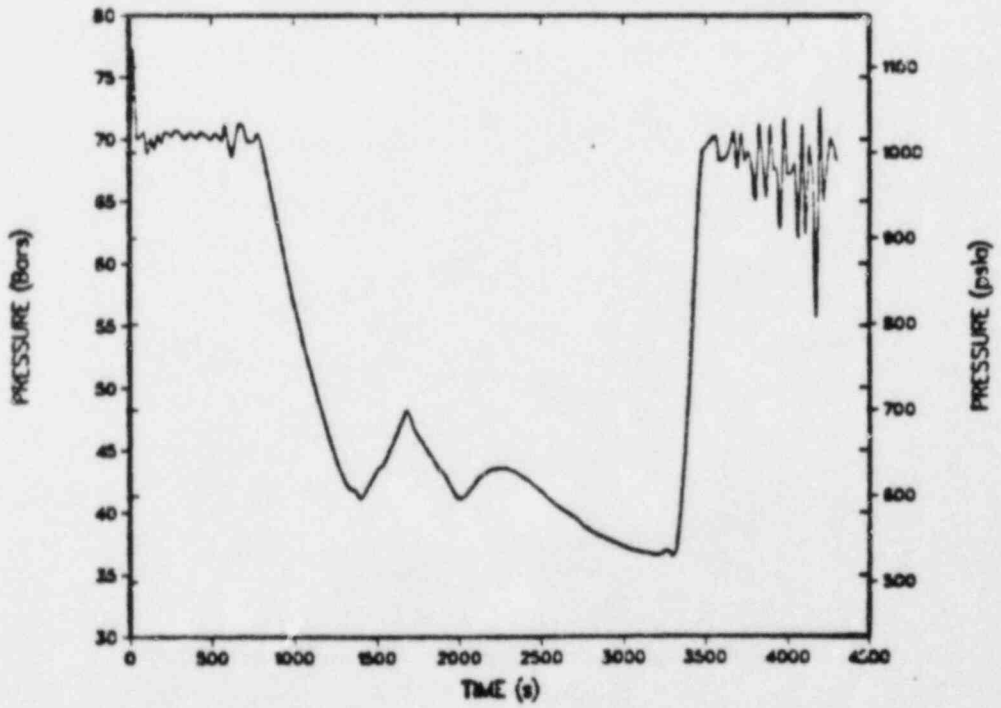

Fig. 242.
SG-A secondary-side pressure.

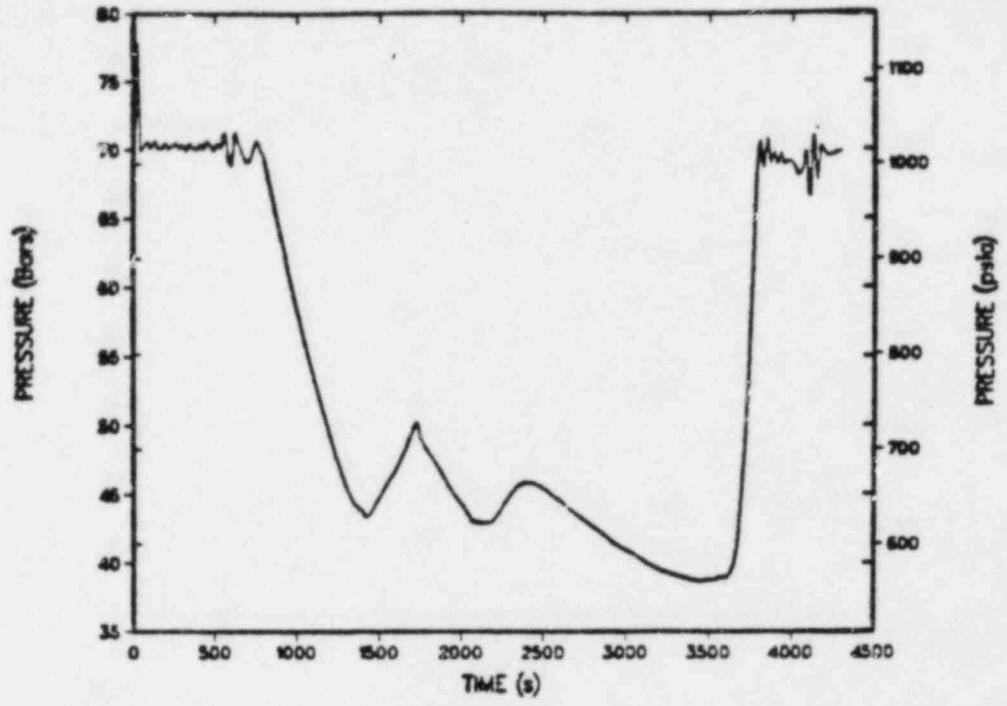

Fig. 243.
SG-B secondary-side pressure.

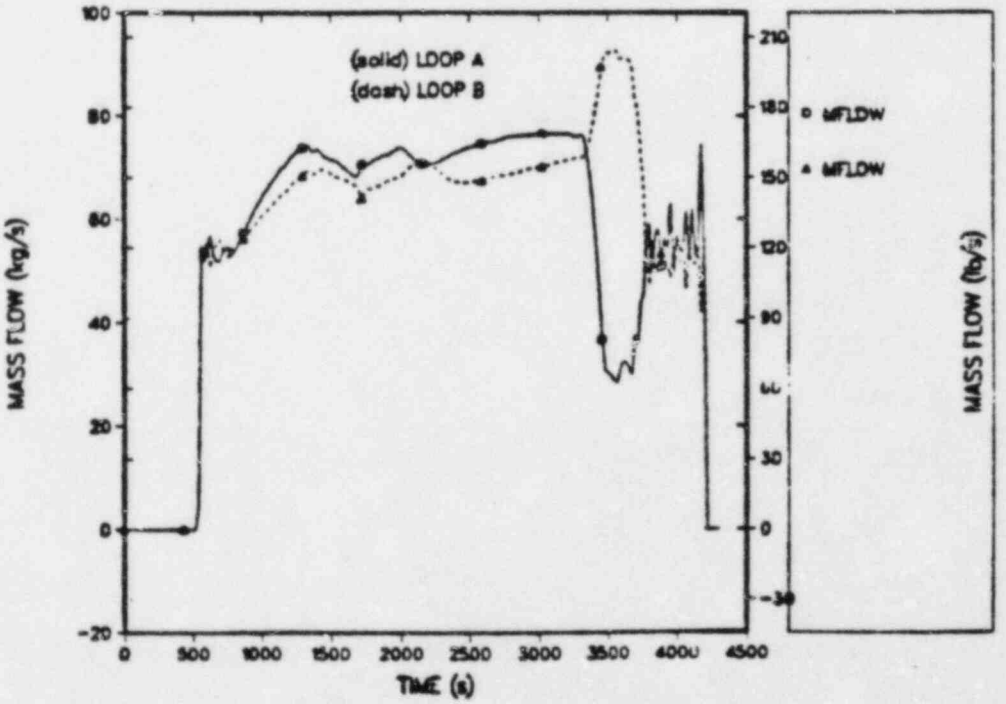

Fig. 244.
EFW mass flows.

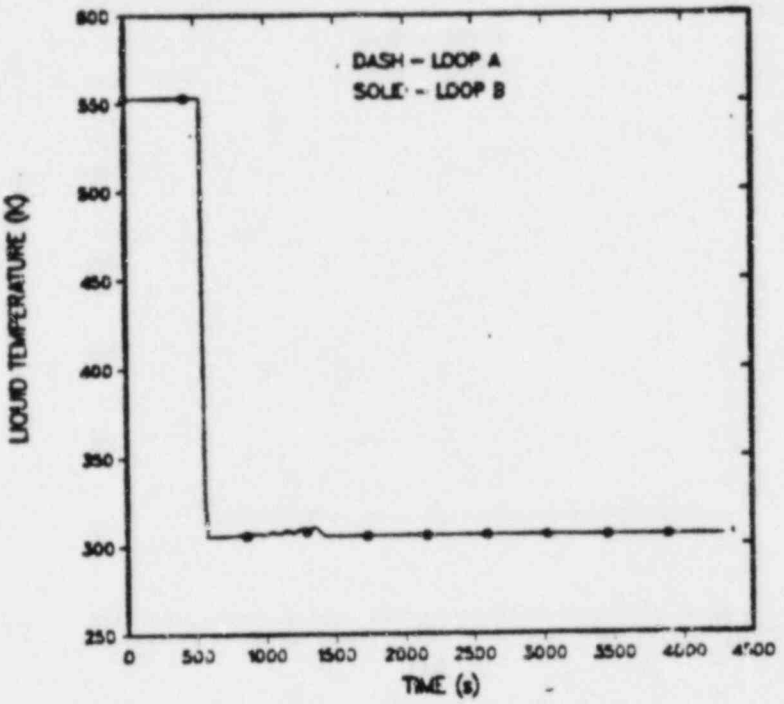

Fig. 245.
EFW liquid temperatures at injection point.

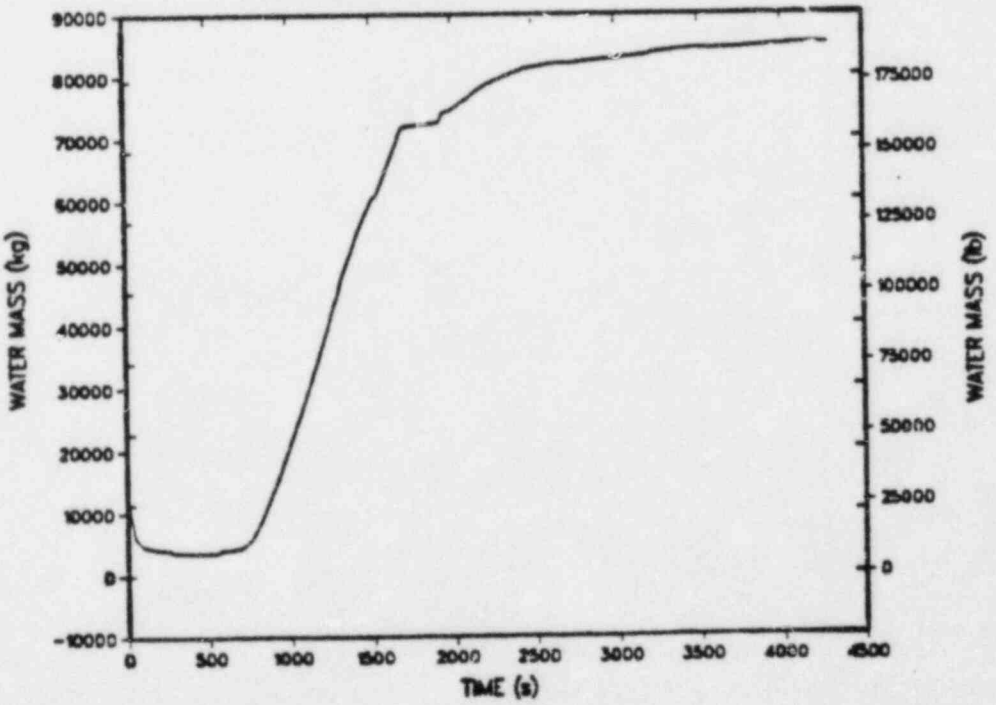

Fig. 246.
SG-A secondary-side inventory.

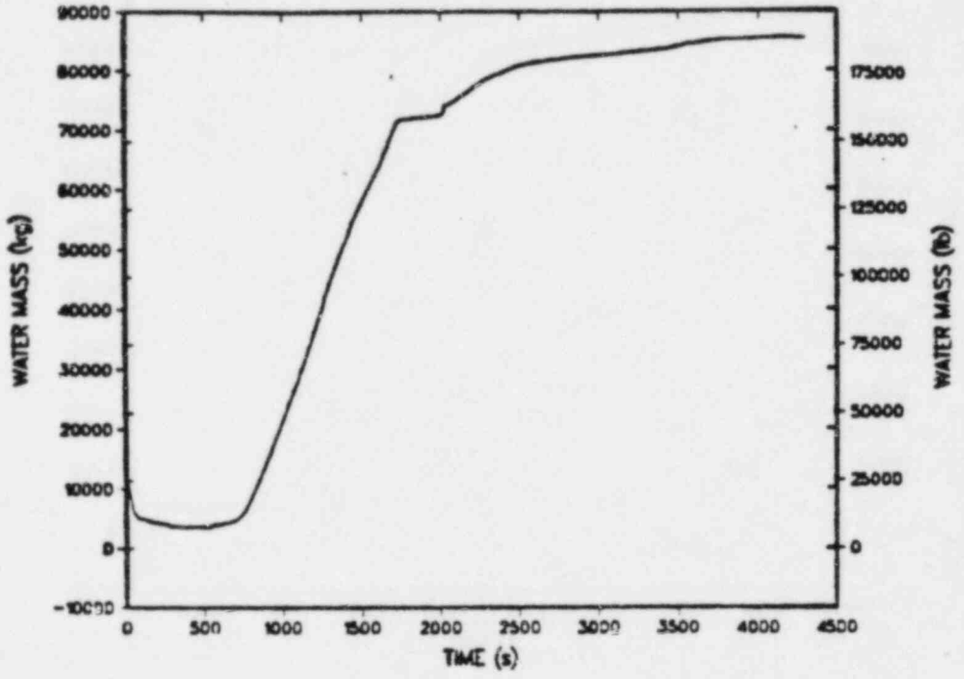

Fig. 247.
SG-B secondary-side inventory.

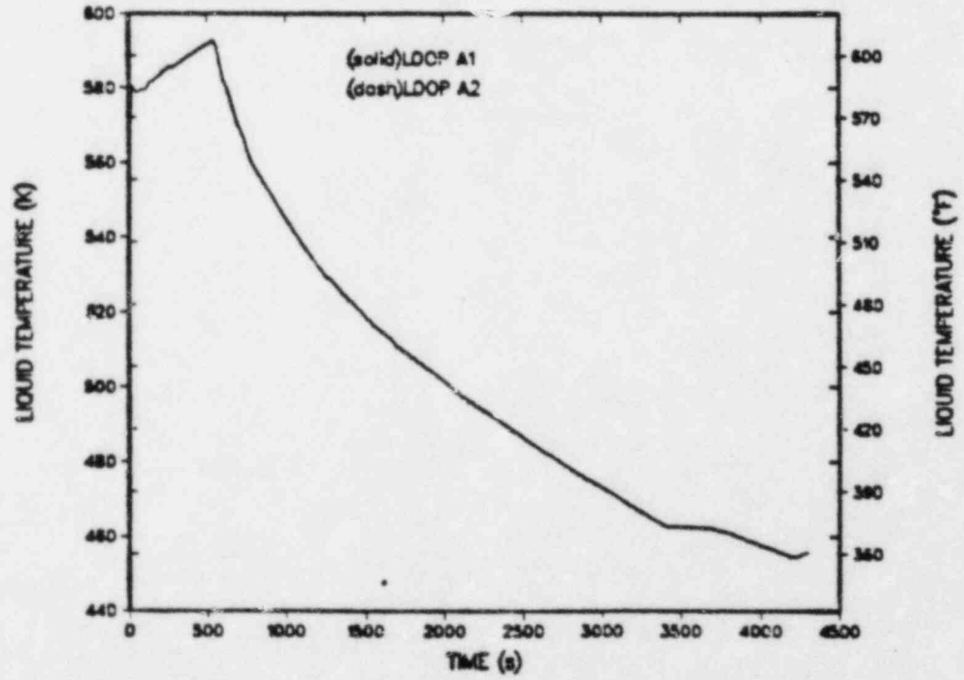

Fig. 248.
Loop A cold-leg liquid temperatures.

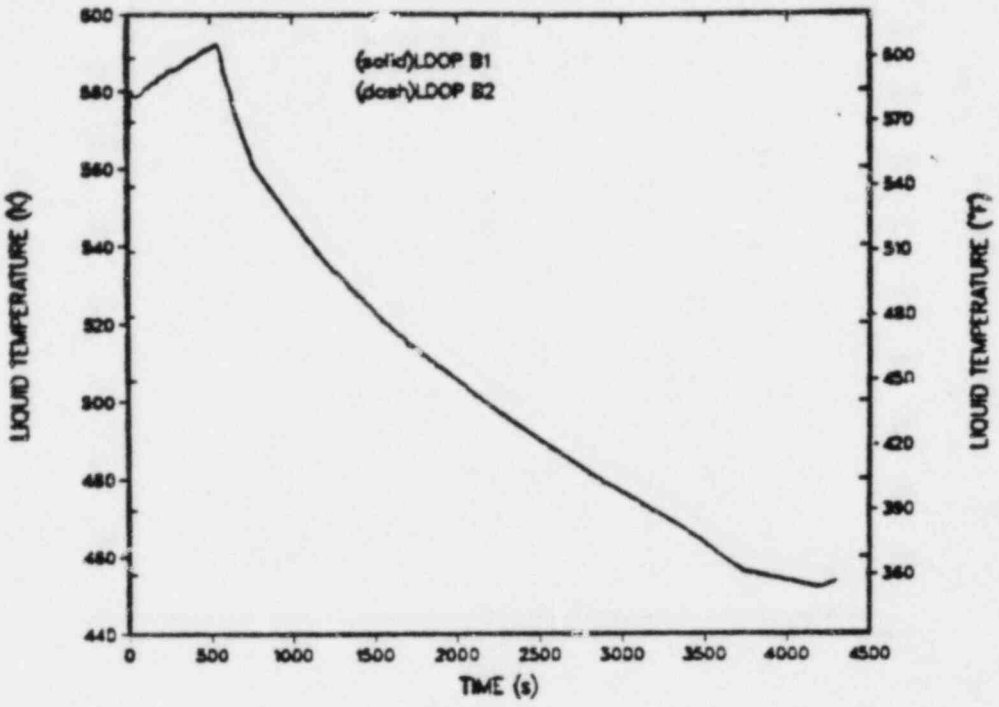

Fig. 249.
Loop B cold-leg liquid temperatures.

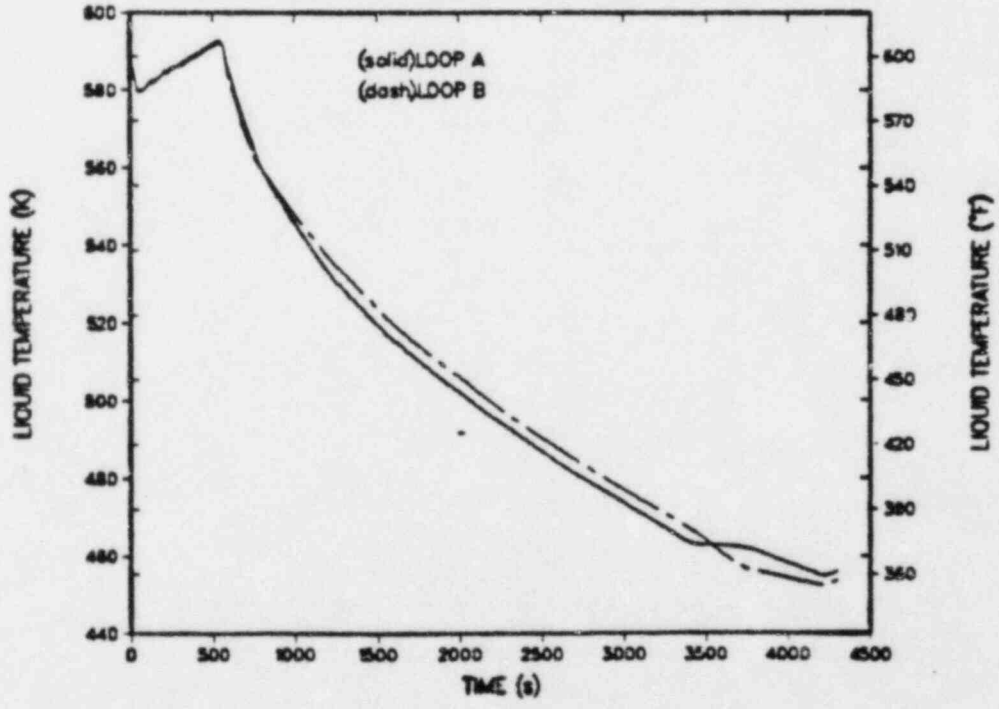

Fig. 250.
Hot-leg liquid temperatures.

throughout the transient as indicated by the loops A and B HPI mass flows shown in Figs. 251 and 252. The RCPs were not tripped following the actuation of the HPI system, and continued to operate as specified in the event sequence. Cold-leg mass flows for loops A and B are presented in Figs. 253 and 254, respectively. Figure 255 presents the hot-leg mass flows for both loops.

The continued operation of the RCPs provided forced convective heat transfer on the primary side that assisted in the rapid cool down of the primary system as indicated by the cold-leg and hot-leg liquid temperature profiles between ~540 s and ~3500 s.

At ~3500 s into the transient, the loop A secondary side (SG and steam lines) had been completely filled with EFW and began to repressurize as shown in the SG secondary-side pressure profiles. Also, the loop B secondary side was calculated to repressurize ~200 s later than the loop A side. Both secondary sides were repressurized to the TBV setpoints as EFW continued to feed the system. As a result of the secondary-side repressurization, the primary side began to cool at a slower rate. At 4200 s, the EFW was terminated to both SGs (as specified). It was at this point in the transient that TRAC calculated a minimum vessel downcomer liquid temperature of ~452°K. The system pressure at this calculated minimum downcomer liquid temperature was ~13.8 MPa. Vessel downcomer liquid temperature profiles for all six azimuthal sectors at axial level 6 (at the weld locations) are shown in Fig. 256.

4. Conclusions. The overcooling of the primary side of the Oconee-1 plant caused by a SG dryout followed by EFW overfeed (Rancho-Seco type transient) was simulated with TRAC-PF1. The TRAC simulation calculated most of the plant response and occurrences as outlined in the postulated sequence of events. A minimum vessel downcomer fluid temperature of ~452 K was calculated at 4200 s. Repressurization of the primary system to ~13.8 MPa was also calculated.

IV. CONCLUSIONS AND RECOMMENDATIONS

The response of the Oconee-1 plant for several overcooling transients has been predicted using TRAC-PF1. The complete plant including the primary and secondary sides was modeled so that accurate predictions of system thermal-hydraulic conditions could be made. The plant control and protection systems were also modeled in sufficient detail to simulate actual plant response during these postulated overcooling transients. The results of these calculations are to be used for PTS analyses at ORNL.

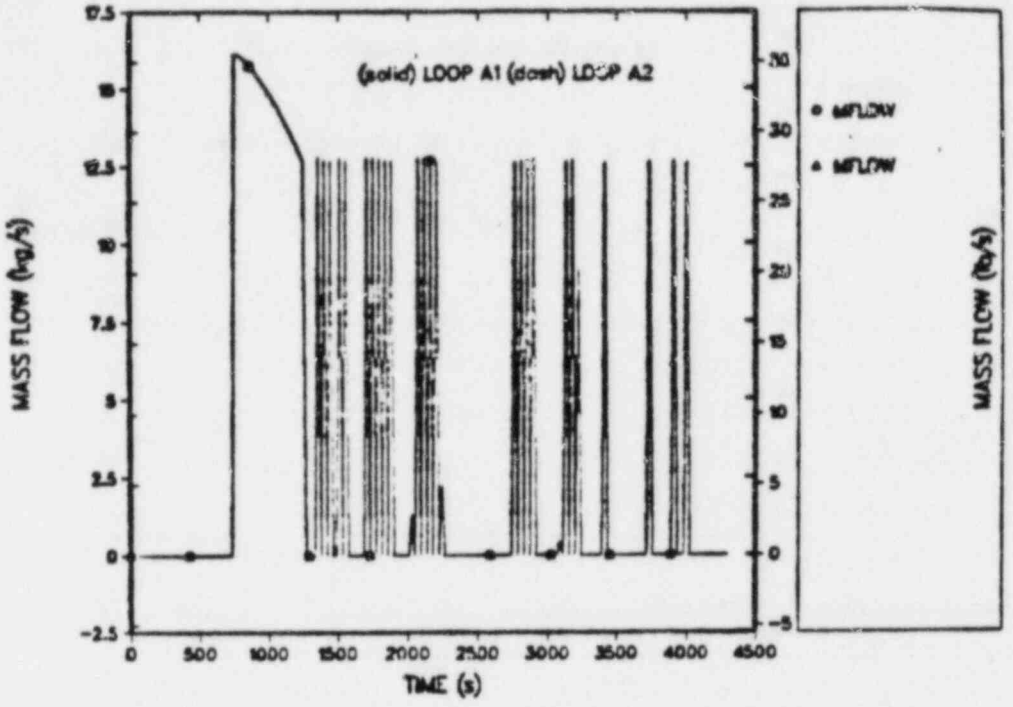

Fig. 251.
Loop A HPI mass flows.

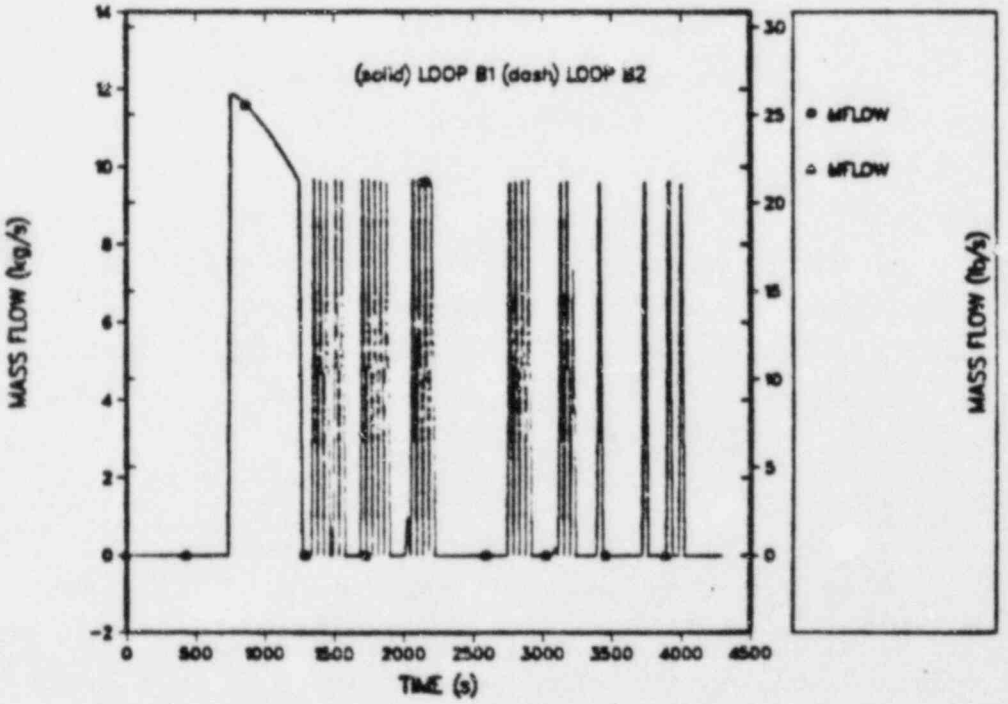

Fig. 252.
Loop B HPI mass flows.

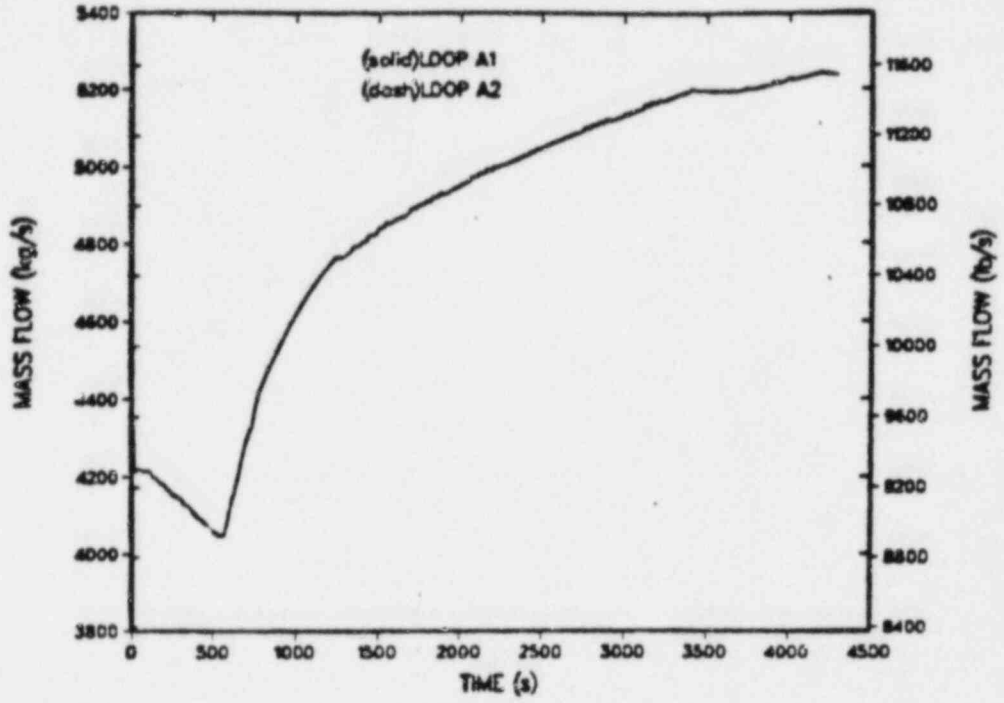

Fig. 253.
Loop A cold-leg mass flows.

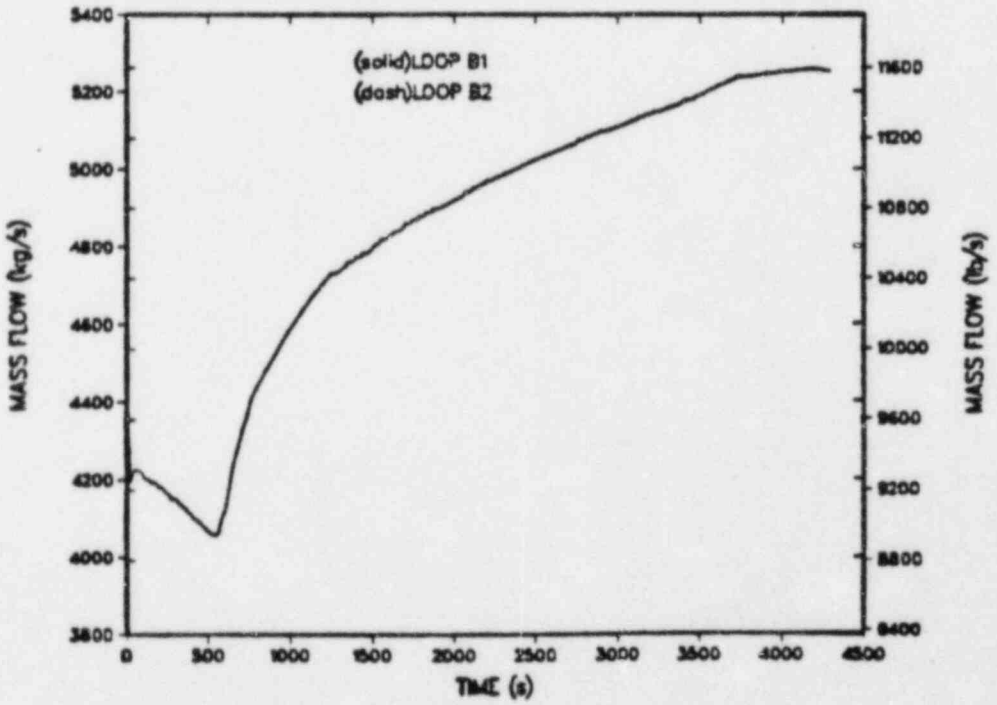

Fig. 254.
Loop B cold-leg mass flows.

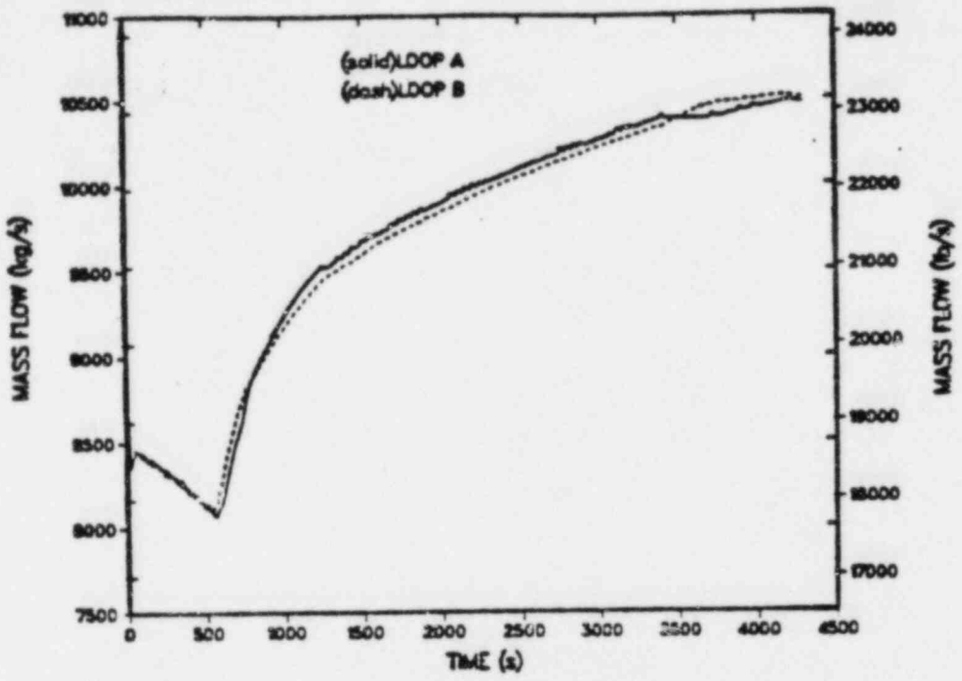

Fig. 255.
Hot-leg mass flows.

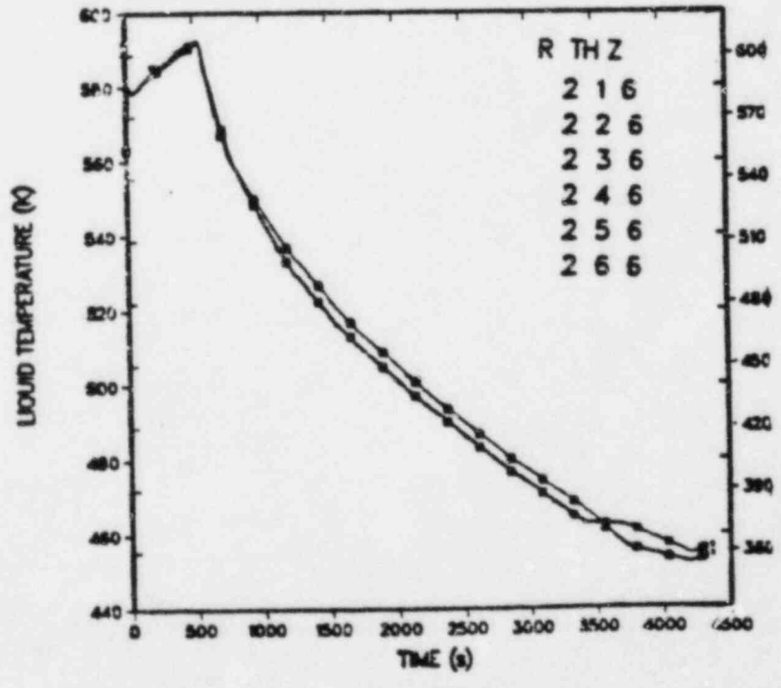

Fig. 256.
Downcomer liquid temperatures-vessel axial level 6 (all azimuthal sectors).

Several overcooling transients were analyzed. The transients calculated included a MSLB with a delay in isolating the affected steam generator, a small-break PORV LOCA with failure of the ICS to throttle MFW flow and RCP trip, and TBV transients with SG overfeed. An actual plant transient (Oconee-3 turbine trip) was also simulated by TRAC to compare with actual plant data. Two small hot-leg breaks were also analyzed to investigate the effects of vent-valve flows on downcomer fluid mixing. Finally, a Rancho-Seco type transient was investigated.

The results of the calculations indicate that some overcooling was obtained in all of the cases analyzed as evidenced by highly subcooled liquid temperatures in the downcomer. The most severe transient in terms of overcooling and system repressurization was the TBV transients. For the TBV case (two banks of TBVs), the minimum calculated downcomer fluid temperature was ~350 K, and the primary system repressurized. The least severe transient was the PORV-LOCA transient, which had a predicted minimum downcomer fluid temperature of ~528 K. The final NDT temperature for Oconee-1 is ~365 K after 32 effective full-power years of operation.

It is recommended that other calculations be performed to fully address the Oconee-1 PTS concern. Specifically, other operation actions should be considered to fully cover the spectra of overcooling scenarios. In the case of the small-break LOCAs, other break sizes and locations should be investigated. Additional failures of the ICS and protection systems should also be analyzed to see if more severe overcooling transients could occur. For example, a MSLB calculation with run-away MFW flow and all other plant systems operating would possibly lead to a more severe overcooling transient.

REFERENCES

1. Safety Code Development Group, "TRAC-PF1: An Advanced Best-Estimate Computer Program for Pressurized Water Reactor Analysis," Los Alamos National Laboratory report (to be published).

2. R. C. Kryter, et. al., "Evaluation of Pressurized Thermal Shock," Oak Ridge National Laboratory report ORNL TM-8072, NUREG/CR-2083 (October 1981).

3. J. D. White, "List of Oconee-1 Transients for Thermal-Hydraulic Calculations," Oak Ridge National Laboratory letter, (December 1982).

4. "Transient Assessment Report for Oconee Nuclear Station Unit III Reactor Trip of March 14, 1980," Duke Power Company report (No date).

5. C. D. Fletcher, "RELAP 5 Thermal-Hydraulic Analysis of Pressurized Thermal Shock Sequences for the Oconee-1 Pressurized Water Reactor," Idaho National Engineering Laboratory report EGG-NSMD-6343 (July 1983).

6. J. R. Ireland and R. J. Henninger, "Analyses of B&W Small-Break LOCA TRAC Calculations," Los Alamos National Laboratory report LA-UR-82-3294 (November 1982).

APPENDIX A

OCONEE ICS CONTROLLER FOR LOOP A

(all signals input are in SI units)
(initialization of valves is for steady state only)
(Letters indicate boxes in the previous figure)

BTU LIMITER

A = 0.00204083 * RCFLOWA

B = -605.4459 + 1.04092 * RCTEMPA , -10.0 < B < 9.080

C = 82.549 - (1.16958e-05) * SGPRESA , -1.0 < C < 9.080

D = -11.036 + 0.037260 * FWTEMP , -1.270 < D < 9.080

E = -16.0 + B + C + D , -10.0 < E < 12.0

F = 0.55555 + 0.055555 * E

H = -10.0 + A * F

* hold initial value for H until 10 s have passed

IF(TIME .LT. 10.0) H = 8.0

"TOP" OF LAYOUT

* -20%/min ramp after trip

A1 = TIME - (TIME OF REACTOR TRIP)

B1 = 1.0 - (0.2/60.0) * A1 , 0.0 < B1

* f.w. demand function

C1 = 18.0 * B1

D1 = f(C1) :

C1	D1
0.0	204.0
0.562	240.0
3.6	320.0
5.4	356.0
9.36	402.0
18.0	460.0
21.42	483.0

```
* f.w. temperature compensation

  E1 = -460.0 - D1 + 1.8 * FWTEMP

  F1 = 1.0 + 0.0013 * E1

  G1 = F1 * C1

* hold initial value of G1 for 10 s

  IF(TIME .LT. 10.0) G1 = 18.0


* neutron power cross limiter
* initialize signal

  IF(TIME .LT. 10.0) POWER = 2568.0E6

* bias signal back to zero

  SP = POWER - 2568.0E6

* 1st order lag of power with 4.5 s time constant

  JL = JL + ((SP - JL)/4.5) * DELT

* remove bias

  J1 = JL - 2568.0E6

  H1 = 1.6 + 14.4 * B1

  I1 = -1.0 * (H1 - 6.23053E-9 * J1) , -10.0 < I1 < 10.0

  K1= f(I1)    :    I1        K1
                  -10.5    -10.0
                  - 0.5      0.0
                    0.5      0.0
                   10.5     10.0

* sum f.w. temperature and power limiters

  SG = -10.0 + K1 + G1

* take the smallest value - SG or H

  R = min(SG,H)

* initialize signal

  IF(TIME .LT. 10.0) FWFLOWA = 680.4

* bias signal to zero
```

```
  FWB = FWFLOWA - 680.4

* 1st order lag of f.w. flow error with 1.0 s time constant, loop A

  FSL = FSL + ((FWB - FSL)/1.0) * DELT

* remove bias

  SL = FSL + 680.4

  S1 = 10.0 + R - 0.026455 * SL
```

STGEN OPERATING LEVEL LIMITERS

```
* high level limiter, Loop A
* operating level scale, 96 to 388 in   (level in meters)

  HL1 = f(ALEV)     :
```

ALEV	HL1
2.438	-10.0
9.855	10.0

```
  P1 = -2.0 * (HL1 - 7.0)

* take the smallest between signals S1 and P1

  Q1 = min(S1,P1)

* low level limiter, Loop A
* startup level scale, 0.0 to 250 in

  LL1 = f(ALEV)     :
```

ALEV	LL1
0.0	-10.0
6.350	10.0

```
* decide which setpoint to use depending on pump trip
* pumps tripped:  240 in = 6.096 m = 9.2v

  IF(PTRIP .EQ. 1) STP = 9.2

* pumps running :  24in = 0.61m = -8.08v

  IF(PTRIP .NE. 1) STP = -8.08

* low level error function

  P2 = -2.0 * (LL1 - STP)

* take the largest signal - P2, Q1

  T1 = max(P2,Q1)
```

"BOTTOM END" OF FLOW CONTROL

```
* choose which constants to use depending on whether the STGEN
* is low level limited or not
* if P2 < 0, low limit has not been hit

  IF(P2 .GE. 0.0) CNST1 = 0.12
  IF(P2 .LT. 0.0) CNST1 = 0.1125

  IF(P2 .GE. 0.0) CNST2 = 2.4
  IF(P2 .LT. 0.0) CNST2 = 0.9

* integrate, T1_o is the last timestep value of signal T1

  U1 = U1 + CNST1 * (T1 + T1_o)/2.0 * DELT  ,  -18.0 < U < 2.0

  X11 = U1 + CNST2 * T1

  X1 = X11 + 8.0  ,  -10.0 < X1 < 10.0

* startup control valve function, Loop A

  SUA = 64.1164 + 7.44164 * X1  ,  -10.0 < SUA < 10.0

* normalized flow area for SUFV-Loop A
* this signal sent to valve

  SUFVA = 0.1 * SUA  ,  0.0 < SUFVA < 1.0

* Main flow control valve function, Loop A

  MFA = 0.5555 * X1 - 4.4444  ,  -10.0 < MFA < 10.0

* normalized flow area for MFCV-Loop A
* this signal sent to valve

  MFCVA = 0.5 + 0.5 * MFA  ,  0.0 < MFCVA < 1.0
```

Oconee ICS Controller for Loop B

(balance of signals come from Loop A sections)

BTU LIMITER

```
BA = 0.00204083 * RCFLOWB
BB = -605.4459 + 1.04092 * RCTEMPB , -10.0 < BB < 9.080
BC = 82.549 - (1.16958e-05) * SGPRESB , -1.0 < BC < 9.080
BE = -16.0 + BB + BC + D , -10.0 < BE < 12.0
BF = 0.55555 + 0.055555 * BE
BH = -10.0 + BA * BF
* hold value of BH at 8.0 until 10 s passes
IF(TIME .LT. 10.0) BH = 8.0
```

"TOP" OF LAYOUT SECTION

```
* take the smallest value - SG or BH
BR = min(SG,BH)
* initialize signal
IF(TIME .LT. 10.0) FWFLOWB = 680.4
* bias signal to zero
FWC = FWFLOWB - 680.4
* 1st order lag of f.w. flow with 1.0 s time constant, Loop B
FBL = FBL + ((FWC - FBL)/1.0) * DELT
* remove bias
BSL = FBL + 680.4
BS1 = 10.0 + BR - 0.026455 * BSL
```

STGEN OPERATING LEVEL LIMITERS

```
* high level limiter, Loop B
* operating level scale, 96 to 388 in   (level in meters)

  BHL1 = f(BLEV)    :      BLEV       BHL1
                           9.855      10.0
                           2.438     -10.0

  BP1 = -2.0 * (BHL1 - 7.0)

* take the smallest between signals BS1 and BP1

  BQ1 = min(BS1,BP1)

* low level limiter, Loop B
* startup level scale, 0.0 to 250 in

  BLL1 = f(BLEV)    :       BLEV     BLL1
                           6.350     10.0
                           0.0      -10.0
* low level error function

  BP2 = -2.0 * (BLL1 - STP)

* take the largest signal - BP2, BQ1

  BT1 = max(BP2,BQ1)
```

"BOTTOM END" OF FLOW CONTROL

```
* choose which constants to use depending on whether STGEN B
* is low level limited or not
* if BP2 < 0, low limit has not been hit

  IF(BP2 .GE. 0.0) BCNST1 = 0.12
  IF(BP2 .LT. 0.0) BCNST1 = 0.1125

  IF(BP2 .GE. 0.0) BCNST2 = 2.4
  IF(BP2 .LT. 0.0) BCNST2 = 0.9

* integrate, BT1_o is the last timestep value of signal BT1

  BU1 = BU1 + BCNST1 * (BT1 + BT1_o)/2.0 * DELT  ,  -18.0 < BU1 < 2.0

  BX11 = BU1 + BCNST2 * BT1

  BX1 = BX11 + 8.0  ,  -10.0 < BX1 < 10.0

* startup control valve function, Loop B

  SUB = 64.1164 + 7.44164 * BX1  ,  -10.0 < SUB < 10.0
```

```
* normalized flow area for SUFV-Loop B
* this signal sent to valve

  SUFVB = 0.1 * SUB   ,  0.0 < SUFVB < 1.0

* Main flow control valve function, Loop B

  MFB = 0.5555 * BX1 - 4.4444   ,  -10.0 < MFB < 10.0

* normalized flow area for MFCV-Loop B
* this signal sent to valve

  MFCVB = 0.5 + 0.5 * MFB   ,  0.0 < MFCVB < 1.0
```

FEEDPUMP CONTROL

```
* DELPA is the pressure drop for the Loop A MFCV, DELPB for Loop B
* initialize signal

  IF(TIME .LT. 10.0) DELPA = 3.55E5

*  bias signal to zero

  DPAB = DELPA - 3.55E5

* 1st order lag of DELPA with a 1.0 s time constant
* 40 psi limit on both sides

  DPAL = DPAL + ((DPAB - DPAL)/1.0) * DELT   ,  -2.44e5 < DPAL < 2.4E5

* remove bias

  DPA = DPAL + 3.55E5

  FA = 2.90074e-5 * DPA - 10.0

* initialize signal

  IF(TIME .LT. 10.0) DELPB = 3.55E5

* bias signal to zero

  DPBB = DELPB - 3.55E5

* 1st order lag of DELPB with a 1.0 s time constant
* 40 psi limit on both sides

  DPBL = DPBL + (DPBB - DPBL)/1.0) * DELT   ,  -2.44e5 < DPBL < 2.44E5
```

* remove bias

DPB = DP3L + 3.55E5

FB = 2.90074e-5 * DPB - 10.0

* take the smallest of these

FC = min(FA,FB)

FD = FC - 0.2975

FE = 0.2 * FD * ABS(FD) , -10.0 < FE < 10.0

* integrate once per timestep, FE_o is last timestep value of signal FE

FF = FF + 0.2333 * (FE + FE_o)/2.0 * DELT , -10.0 < FF < 10.0

FG = FF + FE , -10.0 < FG < 10.0

* signal R is from "top of layout" section, Loop A
* signal BR would be the identical signal from Loop B

FI = 0.5 * (R + BR) - FG

* FP is required pump speed (523.6 rad/sec = 5000 rpm)
* this signal sent to MFW pump

FP = f(FI)

FI	FP (rad/sec)
-2.0	370.4
0.0	392.8
6.0	460.0
10.0	586.43

* internal limit on rate of change of pump speed is set to 27 rad/sec per sec

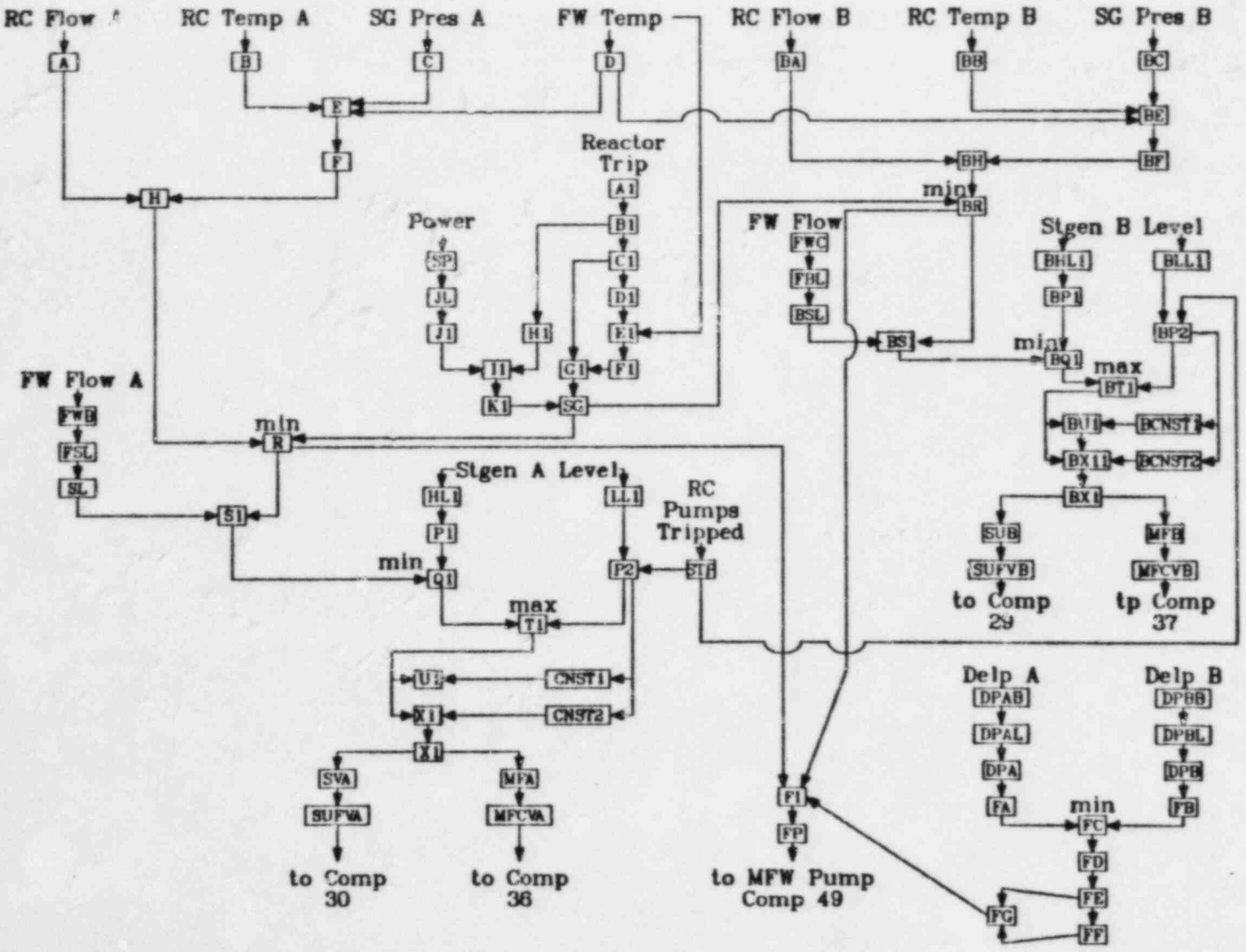

TRAC-PF1 ICS MODEL FOR OCONEE-1

Trip System Legend
(for Section II.C)

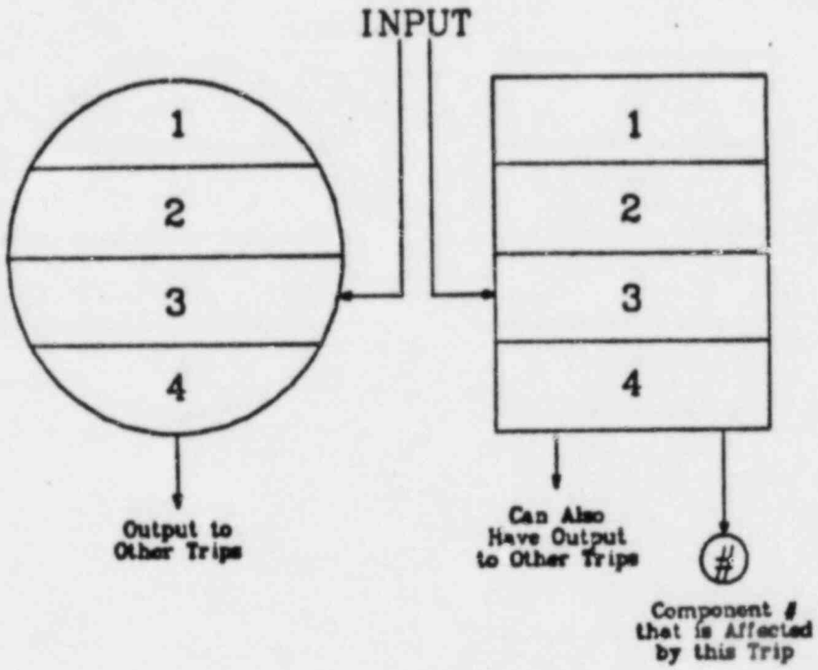

1. the trip #
2. description of trip
3. input to trip, four kinds available:
   - S.V. ≡ signal variable input
   - T.S.E. ≡ trip signal expression, a mathematical operation of S.V.'s
   - C.B. ≡ a control block
   - # ≡ any leading # means it is a trip controlled trip defined in the input deck by this #. Following a trip cont. t. #, the condition that the input must meet to change the trip set status is indicated:
     - $\sum$ ≡ summation
     - M ≡ product
4. trip output (the trip ISET value)
   can only be -1 ≡ on-reverse
   0 ≡ off
   +1 ≡ on-forward

APPENDIX B

EXTRAPOLATIONS

I. MSLB TRANSIENT

Because the MSLB calculation was run to 7200 s, no extrapolation of the results is necessary. The pressurizer pressure, downcomer liquid temperatures, and heat-transfer coefficients are shown in Figs. B-1 through B-3 respectively.

The uncertainties in the MSLB calculation are categorized as follows.

1. Steam generator (SG) secondary-side water level - TRAC used a collapsed-level calculation to approximate the ΔP measurement.
2. Main feedwater (MFW) pump trip - because collapsed liquid level used, MFW pump tripped later than if ΔP were used.
3. HPI throttling - core exit temperatures should have been used after RCPs tripped - TRAC used hot-leg temperatures. HPI should have been throttled at ~275 s instead of ~525 s as calculated.
4. RCP restart - 42 K subcooling margin must be reached in all loop locations before RCPs restarted - TRAC only used one location (hot leg); therefore, RCPs should not have been restarted at ~525 s.

The first two uncertainties regarding the liquid-level calculation do not appear to affect the primary-side overcooling calculated by TRAC. The reason for this is because the flow into the affected SG prior to the feedwater realignment trip (~50 s) is only through the start-up flow control valve (main flow control valves closed because of reactor trip) which limits the flow to ~15% of normal. So, even if the main feed pumps are running, the flow is limited to approximately the same rate as if they are not running. Therefore, the primary-side overcooling rate during this period (0-50 s) is essentially independent of whether or not the main feed pumps are running. Also, the emergency feedwater pump operation during the first ~85 s of the transient has no effect on the primary-side overcooling because all of this liquid is bypassed out the break (refer to Section III.B of report for further details).

The effect of throttling the HPI on primary-system overcooling at ~275 s instead of ~525 s is expected to be small. This is because the overcooling caused by the energy removal through the affected SG is much greater than the cooling provided by the HPI. Therefore, the effects of HPI throttling in the MSLB transient are believed to be insignificant for this time period.

The effects of restarting or not restarting the RCPs are perhaps the most difficult to estimate. In the TRAC calculation, the RCPs were restarted at ~525 s because the subcooling monitor was not modeled correctly. In reviewing the results, it appears that the RCPs should not have been restarted at that time, and probably would have not been restarted at all if modeled correctly. This is because the candy cane in loop B voided in the calculation and remained voided for a considerable time. Also, the region in the vertical part of the hot leg where the fluid temperatures are measured was also voided. Therefore, the subcooling criteria for restarting the RCPs would not have been met. What most likely would have happened in the TRAC calculation if the subcooling monitor was modeled correctly is that the RCPs would not have been restarted at ~525 s, and the downcomer temperatures would have continued to decrease at the same rate as prior to ~525 s until steam generator isolation at 600 s. Then the downcomer fluid temperatures would begin to increase and continue to increase for the remainder of the transient. Also, the system would repressurize to the PORV setpoint as shown in Fig. B-1.

Because there is only ~75 s worth of additional cooling if the RCPs had not been restarted, there probably will not be much difference in the minimum downcomer fluid temperature calculated. Therefore, if all of these

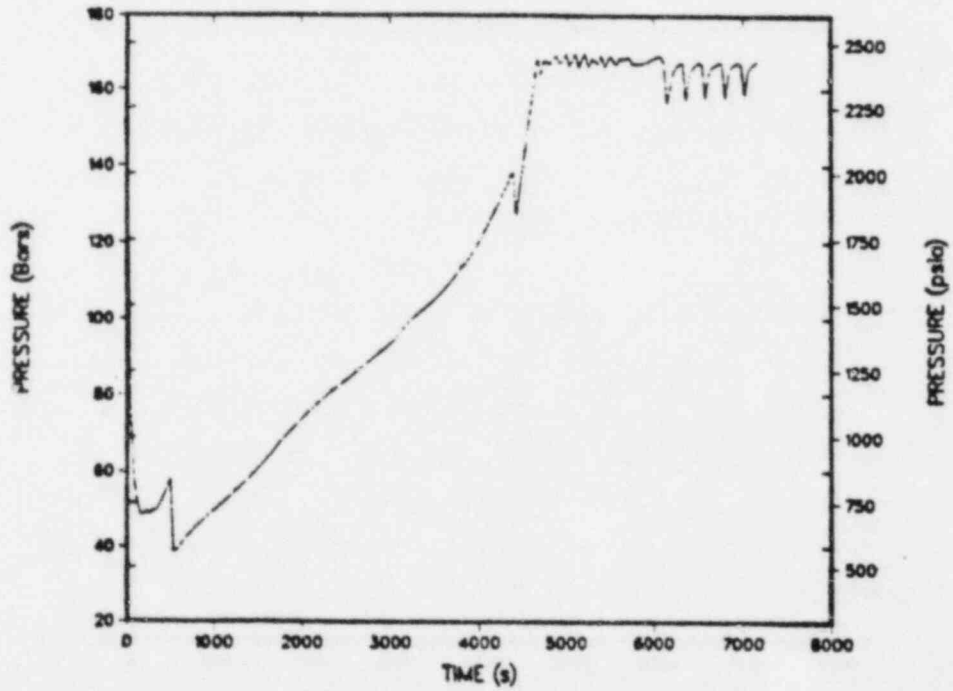

Fig. B-1.
Pressurizer pressure.

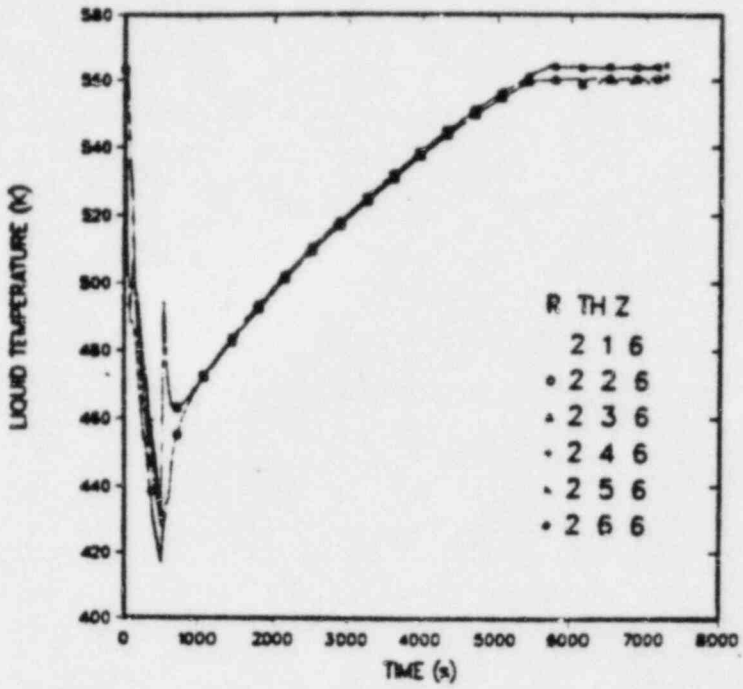

Fig. B-2.
Downcomer liquid temperatures at vessel axial level 6 (all azimuthal sectors).

uncertainties were removed, it is estimated that the minimum downcomer fluid temperature would be ~405 K ± 25 K.

II. TBV TRANSIENTS

The TRAC-PF1 calculated results of six TBV failure transients are presented in the body of the report (Sec. III.D and Sec. III.E). Each of the calculated transients ended at a time equal to or less than 1500 s. In this section, these results are extrapolated to 7200 s. The parameters extrapolated are the system pressures, downcomer liquid temperatures, and the heat-transfer coefficients in the downcomer.

The extrapolated pressure histories are presented in Figs. B-4 and B-5. Following an initial depressurization, the system repressurized to the PORV setpoint in four cases; 5A, 5B, 6A and 6B. The system did not repressurize in cases 5C and 6C because the HPI was throttled upon attainment of sufficient primary-system subcooling.

The extrapolated downcomer liquid temperatures are presented in Figs. B-6 through B-11. A discussion of factors expected to influence the transient histories through the extrapolation period are presented below.

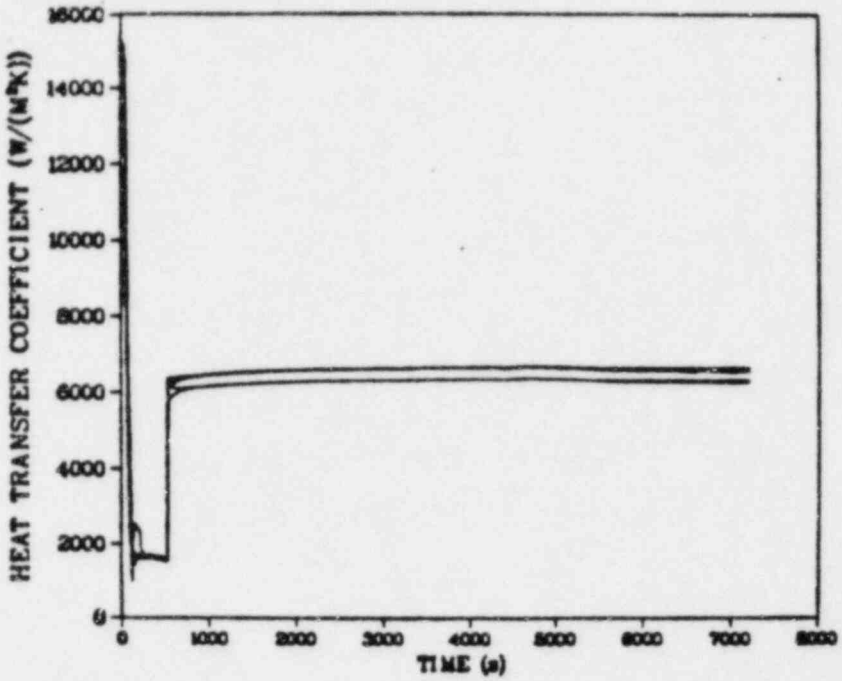

Fig. B-3.
Heat-transfer coefficients at vessel axial level 6 (all azimuthal sectors).

The extrapolated heat-transfer coefficients in the downcomer are presented in Figs. B-12 through B-17.

A. General

For the TBV failure transients, ICS failure to run back MFW to the affected SG(s) was specified. The method chosen to simulate this failure was to fix the MFW pump at its specified value and fix the SUFCV and MFCV in the affected loop(s) in the steady-state position. These valves were maintained in that position throughout the transient. The open position of the SUFCV(s) has proven to be significant. Although the MFW pump is tripped and the EFW pumps are operating, a significant flow from the hotwell and through the MFW pump continues. This flow continues to the affected SG(s) even following tripping of the EFW pumps.

Case 5A

The EFW pumps begin operation at ~210 s. The two motor-driven and one turbine-driven EFW pumps take suction from the surge tank, which empties at ~2500 s. At this time the suction of the turbine-driven pumps only is switched to the hotwell and continues to operate to the end of the transient. Before ~2500 s, the flow through the EFW header is ~255 kg/s of which ~117 kg/s is provided by the EFW pumps and ~138 kg/s comes through the MFW pump and SUFCV.

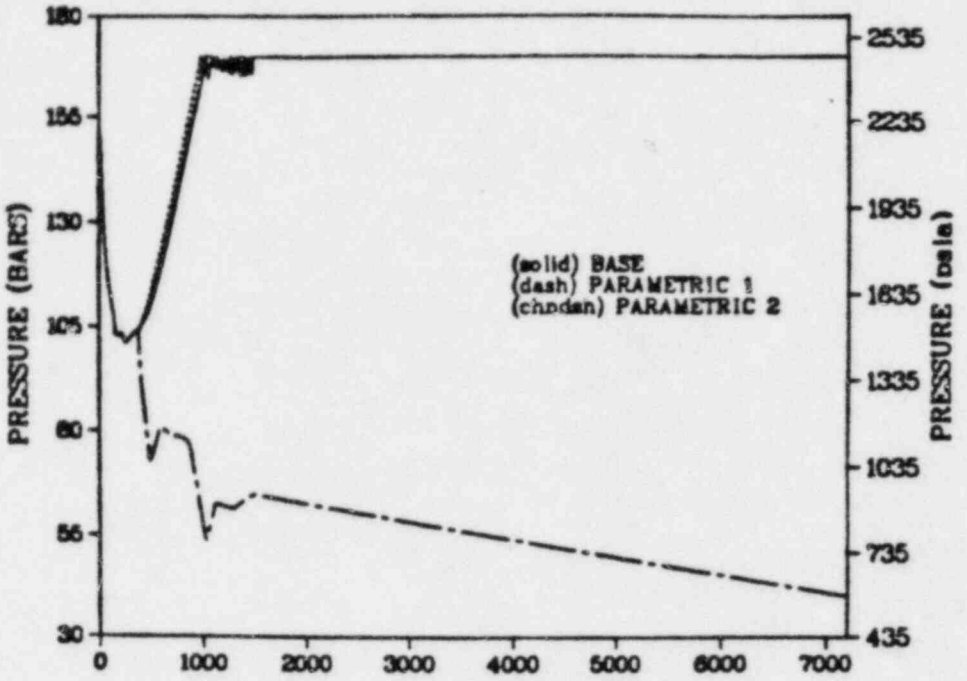

Fig. B-4.
Pressurizer pressure histories for Case 5 (Case 5A-base; Case 5B-parametric 1; Case 5C-parametric 2).

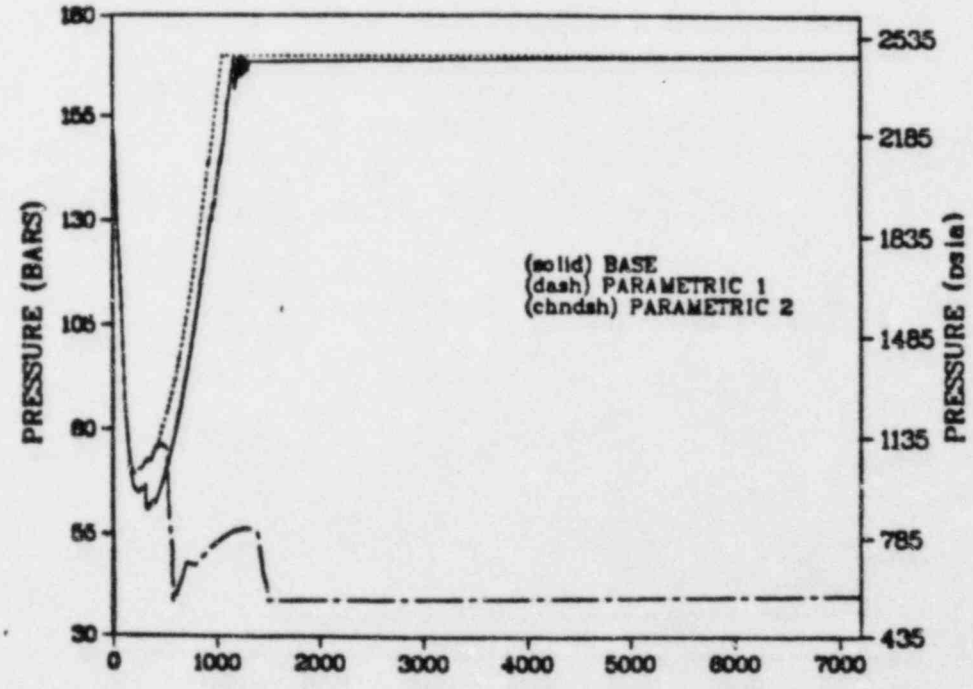

Fig. B-5.
Pressurizer pressure histories for Case 6 (Case 6A-base; Case 6B-parametric 1; Case 6C-parametric 2).

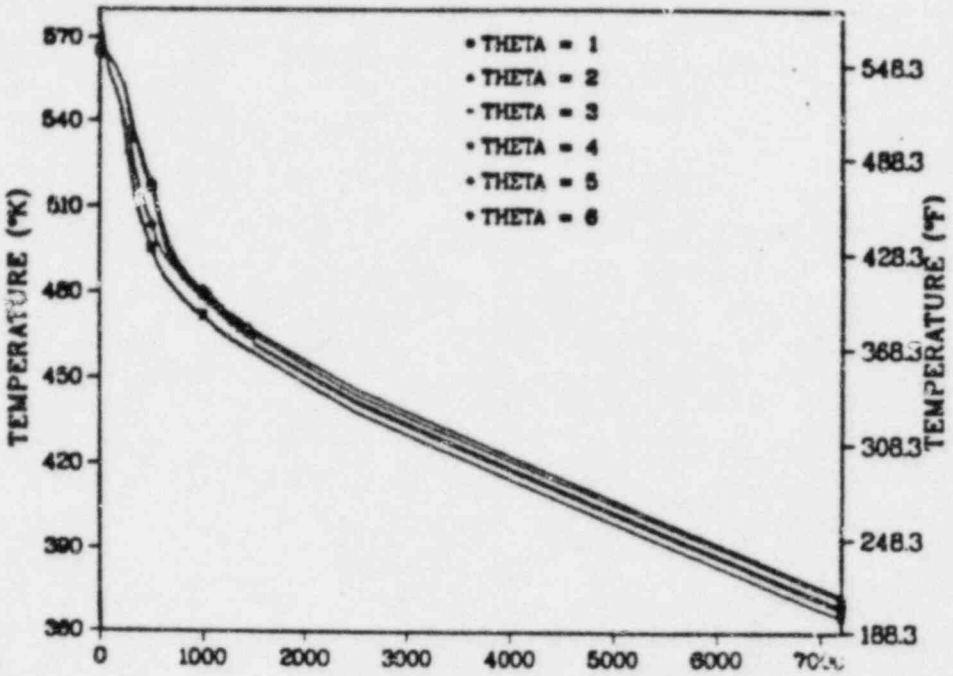

Fig. b-6.
Downcomer liquid temperatures at vessel axial level 6 (all azimuthal sectors) for Case 5A.

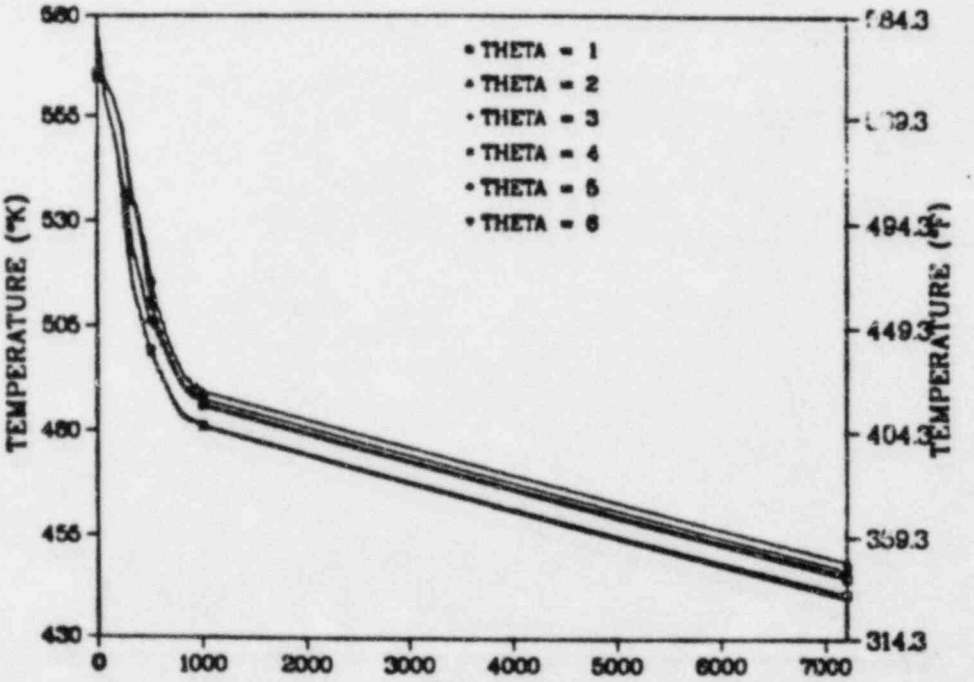

Fig. B-7.
Downcomer liquid temperatures at vessel axial level 6 (all azimuthal sectors) for Case 5B.

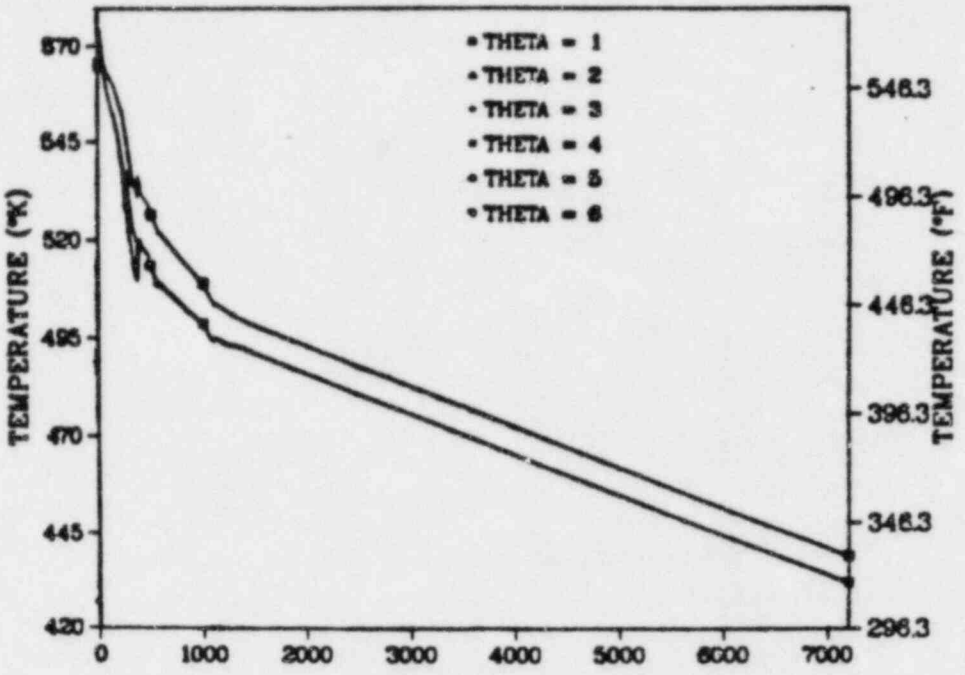

Fig. B-8.
Downcomer liquid temperatures at vessel axial level 6 (all azimuthal sectors) for Case 5C.

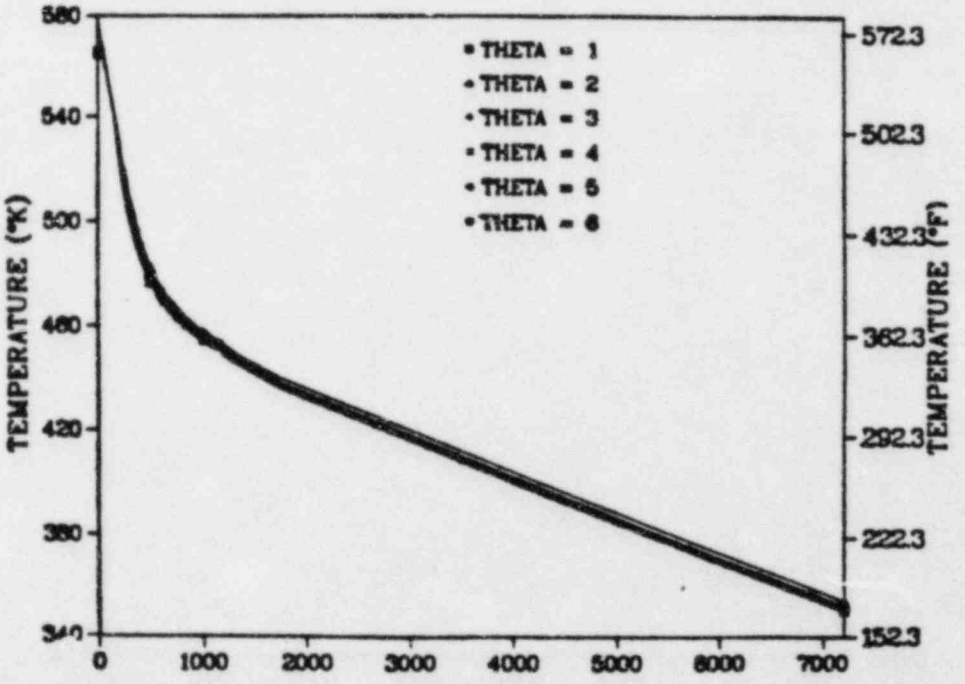

Fig. B-9.
Downcomer liquid temperatures at vessel axial level 6 (all azimuthal sectors) for Case 6A.

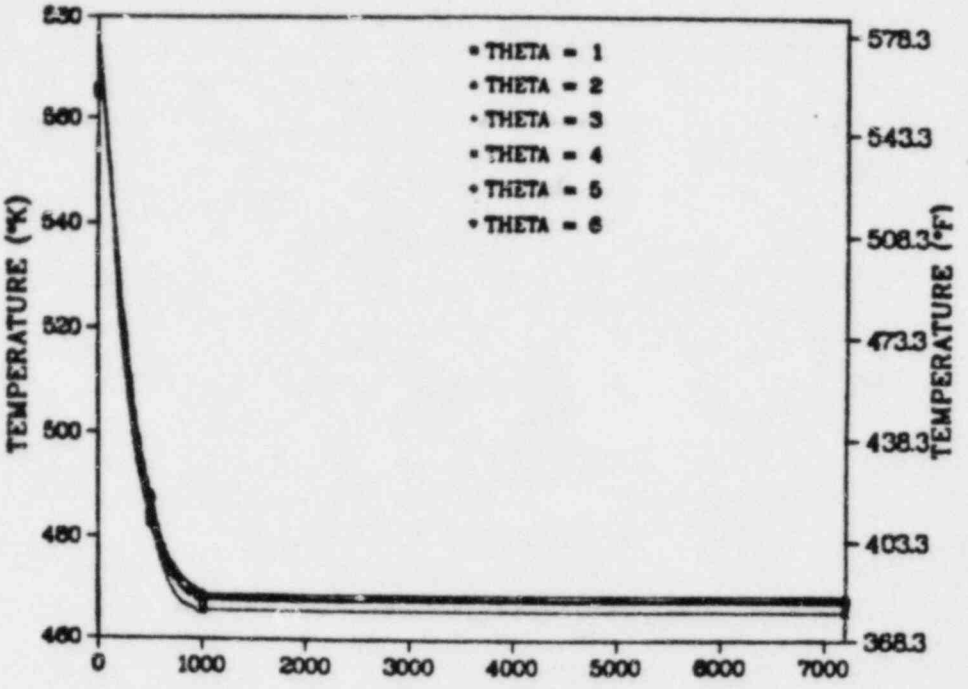

Fig. B-10.
Downcomer liquid temperatures at vessel axial level 6 (all azimuthal sectors) for Case 6B.

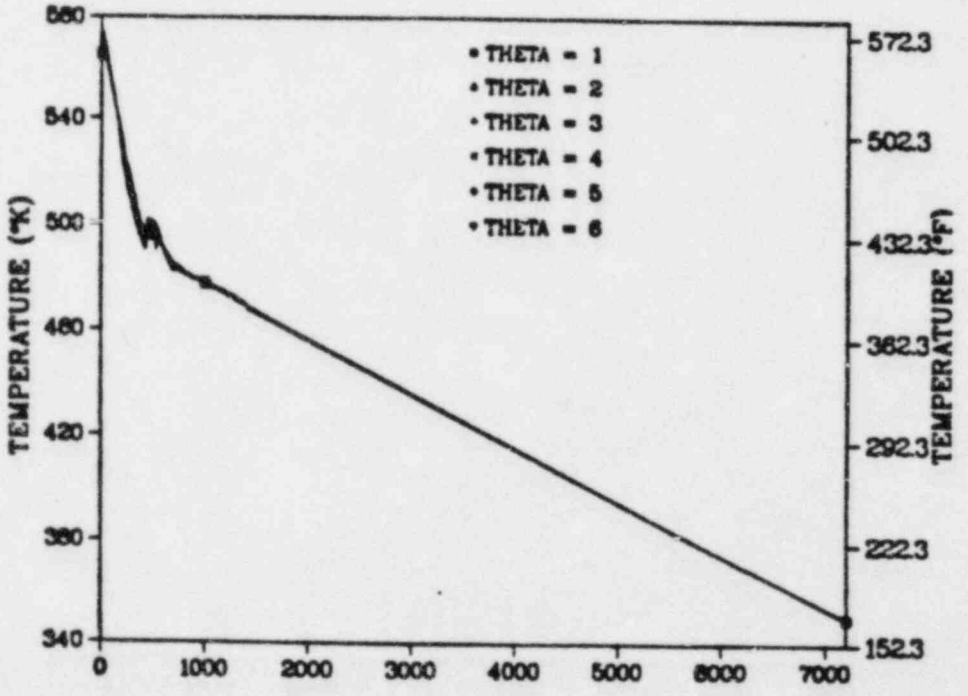

Fig. B-11.
Downcomer liquid temperatures at vessel axial level 6 (all azimuthal sectors) for Case 6C.

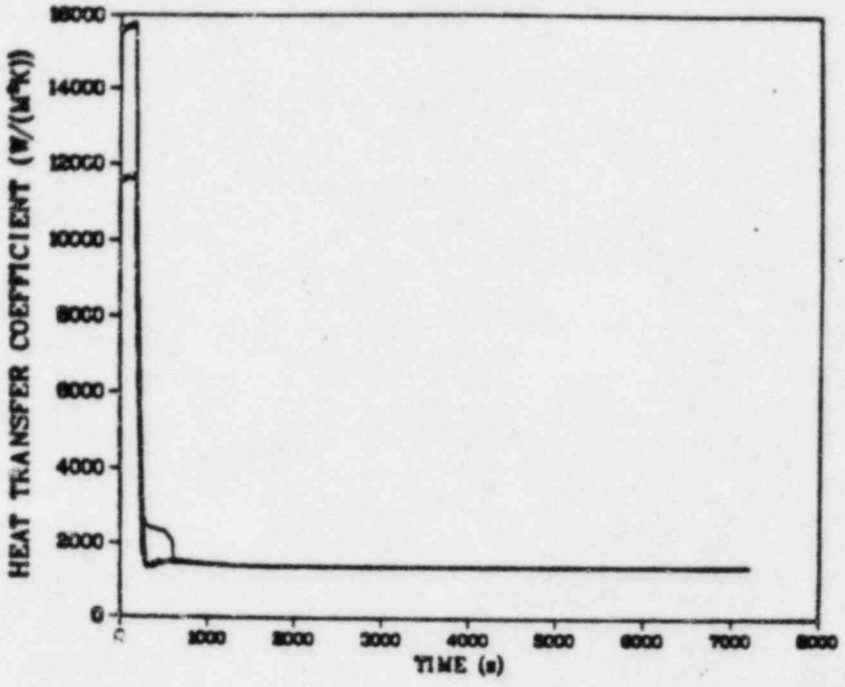

Fig. B-12.
Heat-transfer coefficients at vessel axial level 6 (all azimuthal sectors) for Case 5A.

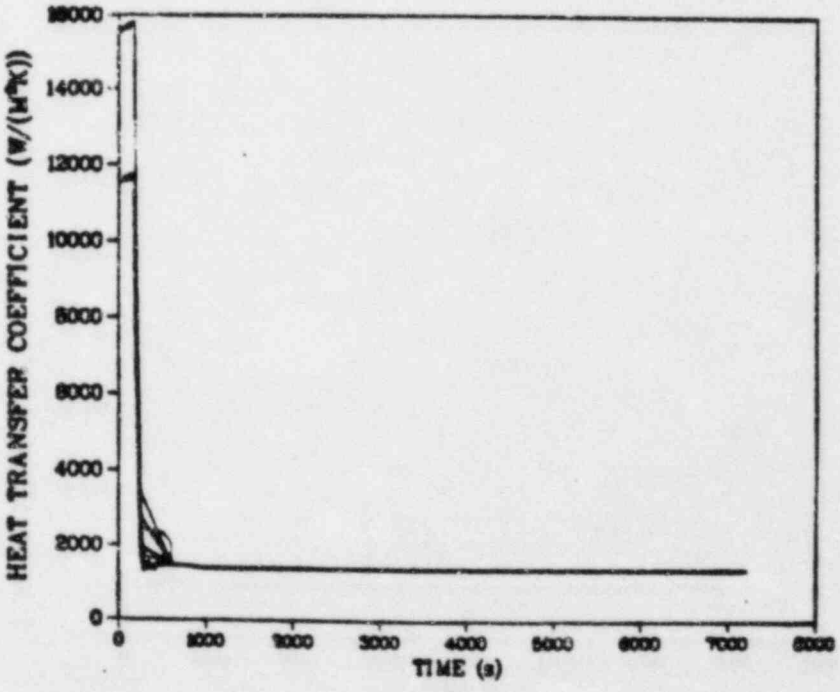

Fig. B-13.
Heat-transfer coefficients at vessel axial level 6 (all azimuthal sectors) for Case 5B.

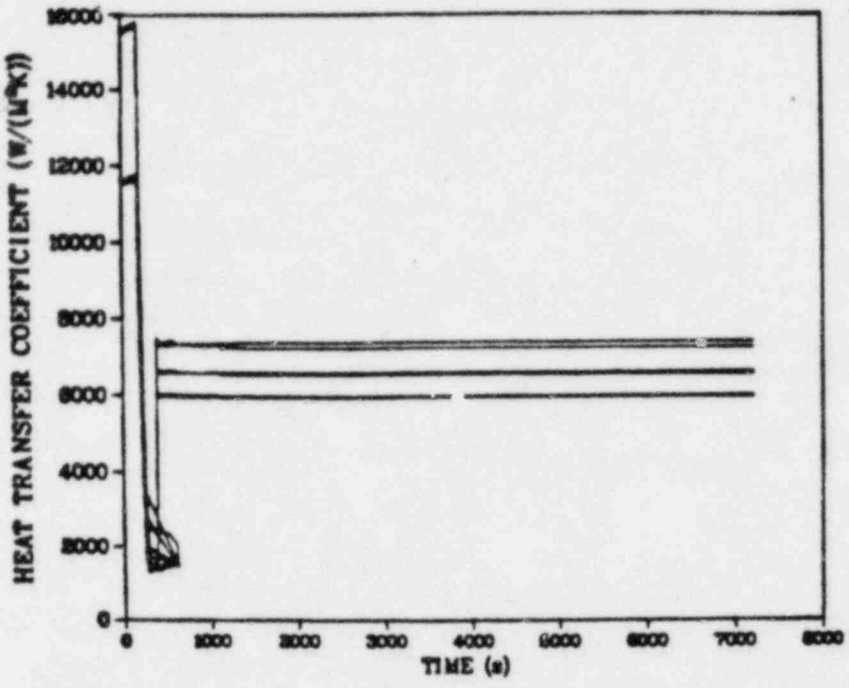

Fig. B-14.
Heat-transfer coefficients at vessel axial level 6 (all azimuthal sectors) for Case 5C.

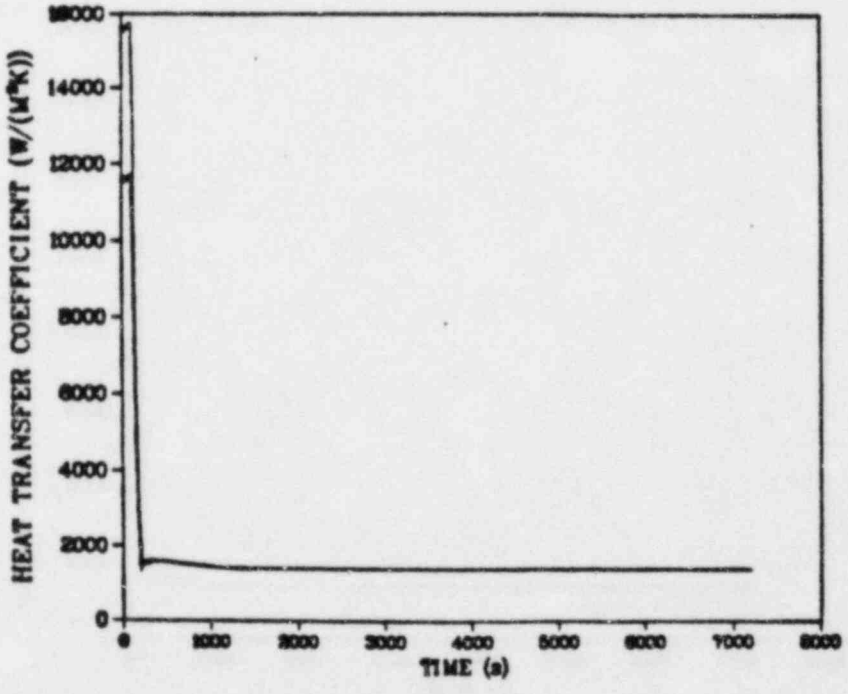

Fig. B-15.
Heat-transfer coefficients at vessel axial level 6 (all azimuthal sectors) for Case 6A.

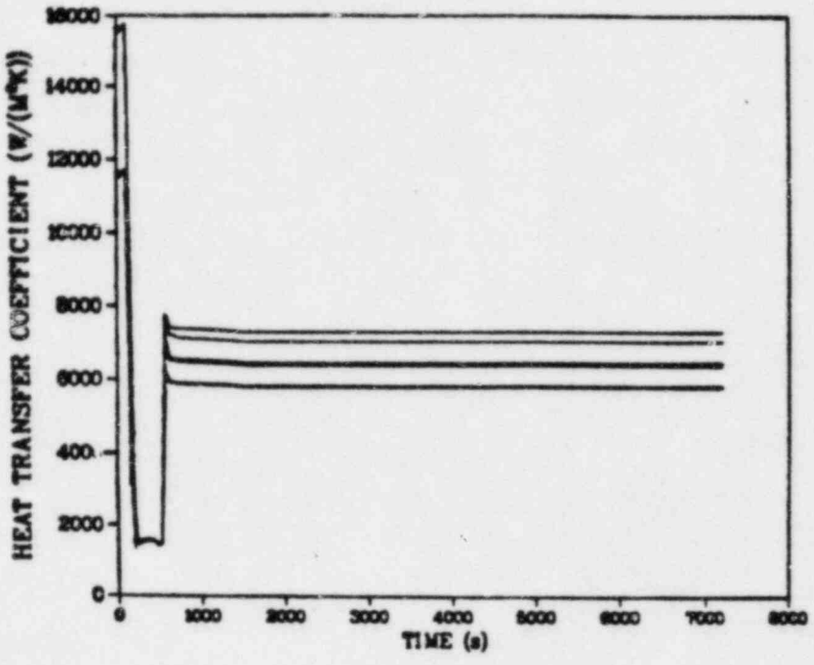

Fig. B-16.
Heat-transfer coefficients at vessel axial level 6 (all azimuthal sectors) for Case 6B.

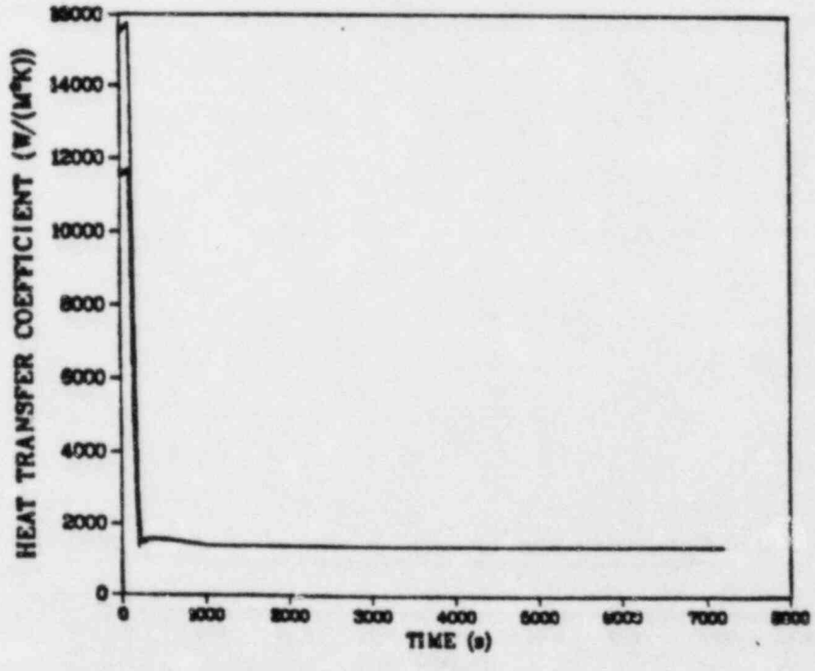

Fig. B-17.
Heat-transfer coefficients at vessel axial level 6 (all azimuthal sectors) for Case 6C.

Following surge tank depletion only the turbine-driven EFW pump operates, delivering ~59 kg/s. Total flow through the EFW header is estimated at ~196 kg/s. After ~2500 s the cooldown rate is reduced by two factors. First, the reduced flow to the SG reduces the secondary-side heat-transfer coefficient. Second, reduced flow from the EFW pumps results in a higher mixed-mean temperature for the flow through the EFW header. These two effects reduce the cooldown rate by ~25% after 2500 s. The estimated extrapolated downcomer liquid temperature at 7200 s is ~365 ± 30 K.

Case 5B

The EFW pumps begin operation at ~210 s, but EFW flow is terminated at ~400 s following closure of the loop-B EFW valve on high SG liquid level. Flow through the SUFCV continues at ~125 kg/s. The cooldown rate between ~800 and ~1100 s is -0.0130 K/s. This rate is used to estimate the downcomer liquid temperature at 7200 s. The estimated temperature is ~440 ± 30 K.

Case 5C

The EFW pumps begin operation at ~210 s, but EFW flow is terminated at ~400 s following closure of the loop B EFW valve on high SG liquid level. Flow through the SUFCV continues at ~120 kg/s. The estimated cooldown rate between ~1200 and ~1500 s is -0.0103 K/s. This rate is used to estimate the downcomer liquid temperature at 7200 s. The estimated temperature is ~430 ± 30 K.

Case 6A

The approach used to estimate the downcomer liquid temperature is similar to that discussed for Case 5A. The EFW pumps begin operation at ~150 s. The surge tank empties at ~1750 s. Before ~1750 s the flow through the EFW header to one SG is ~225 kg/s of which ~88 kg/s comes from the EFW pumps. Following surge tank depletion at ~1750 s, total flow through the EFW header is ~180 kg/s of which ~44 kg/s is from the turbine-driven EFW pump. After ~1750 s the cooldown rate is reduced by ~37%. The estimated extrapolated downcomer liquid temperature is ~350 ± 30 K.

Case 6B

The EFW pump does not operate during this transient because the liquid level in both SGs is too high following MFW pump trip. The downcomer liquid temperature cooldown has stopped by the end of the calculated transient. The minimum downcomer liquid temperature of ~465 K occurs at ~950 s.

Case 6C

The EFW pump does not operate during the transient. The estimated cooldown rate between ~750 and ~1500 s is -0.0203 K/s. This rate is used to estimate the downcomer liquid temperature at 7200 s. The estimated temperature is ~350 ± 30 K.

B. Summary

The extrapolated results for the TBV transients are summarized in Table B-I.

III. SBLOCA TRANSIENTS

Extrapolations of the key parameters (primary system pressures, vessel downcomer liquid temperatures, and downcomer heat-transfer coefficients) to 7200 s are presented in Figs. B-18 through B-23 for the PORV and 4-in-diam. SBLOCAs. For each transient, the extrapolation assumptions, modeling assumptions/uncertainties, and effect of the assumptions/uncertainties are described. Also, uncertainties on the extrapolated results are estimated.

A. PORV LOCA Extrapolation

Extrapolation Assumptions

The extrapolation of the PORV LOCA primary system pressure, vessel downcomer liquid temperatures, and vessel downcomer heat-transfer coefficients presented in Figs. B-18 through B-20 assume the following:

1. HPI continues to operate
2. PORV remains open
3. Accumulators and LPI will not actuate

TABLE B-I

EXTRAPOLATED RESULTS FOR TBV TRANSIENTS AT 7200 s

Case	Downcomer Liquid Temperature (K)	Pressure (bars)	Heat-Transfer Coefficient (W/m^2 K)
5A	~365 ± 30	~170 ± 5	~1200 ± 400
5B	~440 ± 30	~170 ± 5	~1200 ± 400
5C	~430 ± 30	~40 ± 20	~6000-7500 ± 400
6A	~350 ± 30	~170 ± 5	~1200 ± 400
6B	~465[a] ± 30	~170 ± 5	~1200 ± 400
6C	~350 ± 30	~40 ± 20	~6000-7500 ± 400

[a]minimum occurs at ~950 s

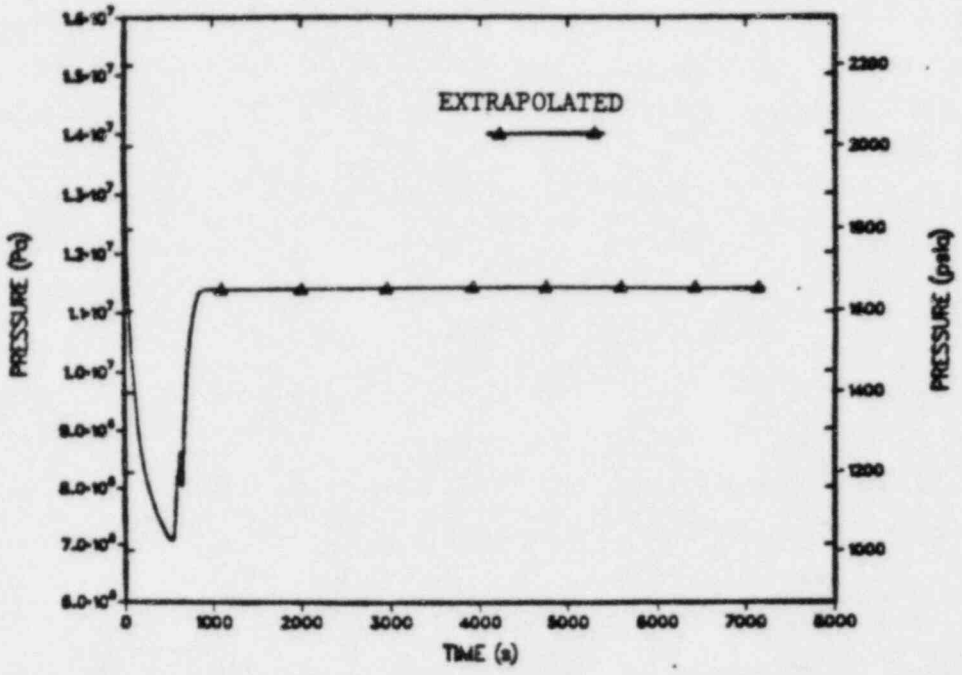

Fig. B-18.
PORV LOCA extrapolated system pressure.

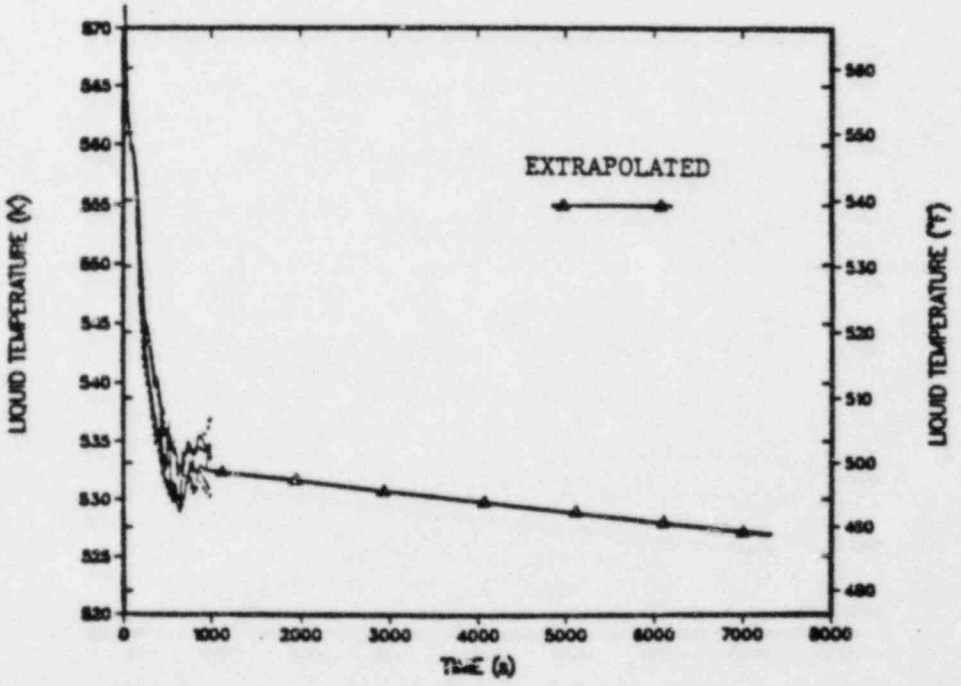

Fig. B-19.
PORV LOCA extrapolated downcomer liquid temperature.

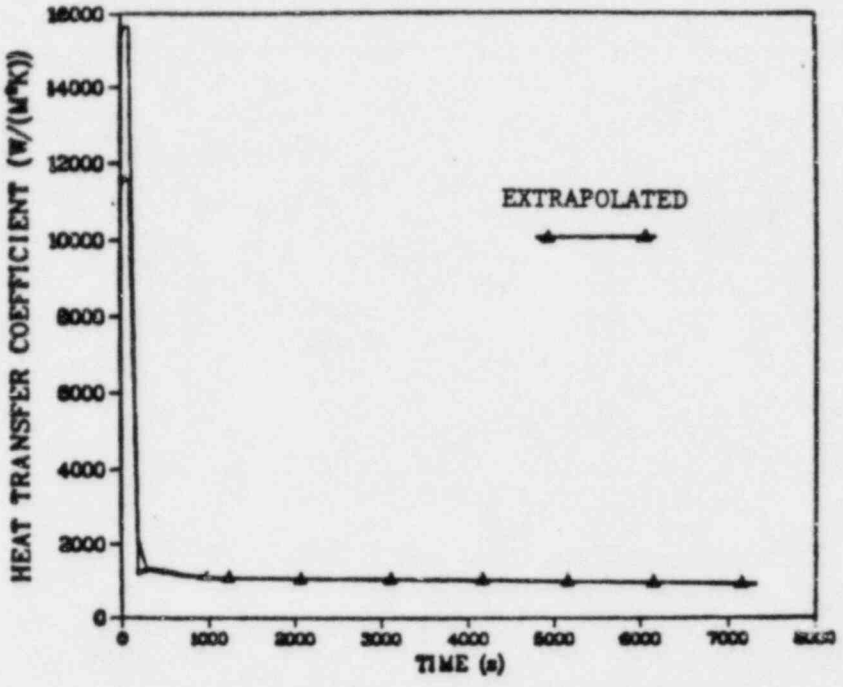

Fig. B-20.
PORV LOCA extrapolated downcomer heat-transfer coefficient.

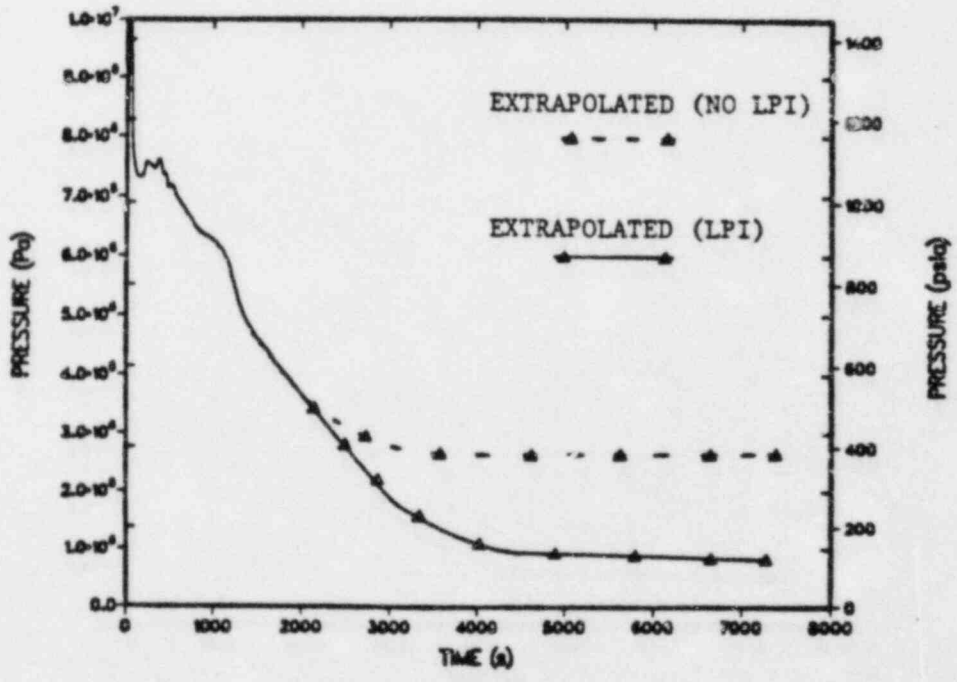

Fig. B-21.
4-in-diam. SBLOCA extrapolated system pressure.

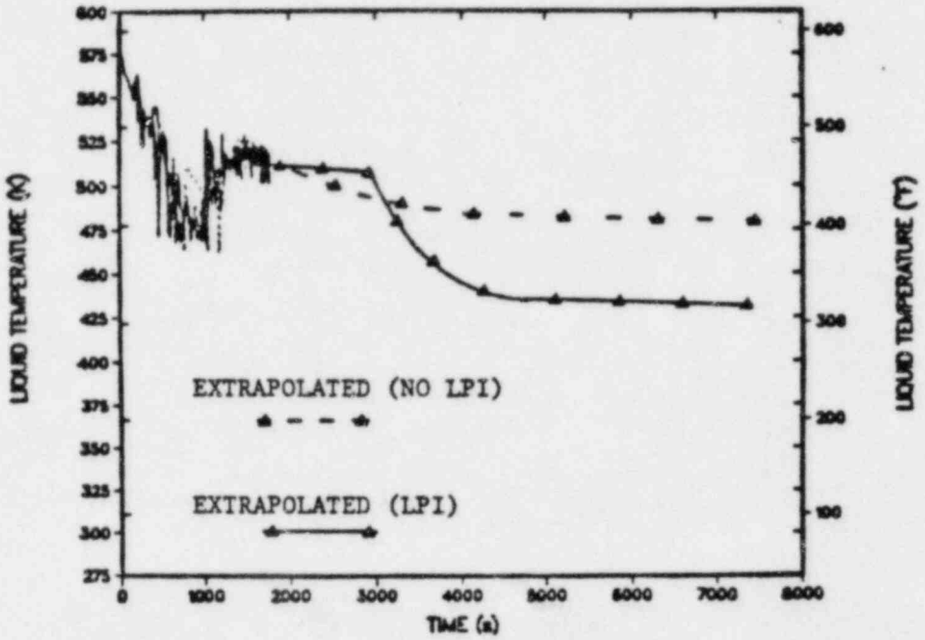

Fig. B-22.
4-in-diam. SBLOCA extrapolated downcomer liquid temperature.

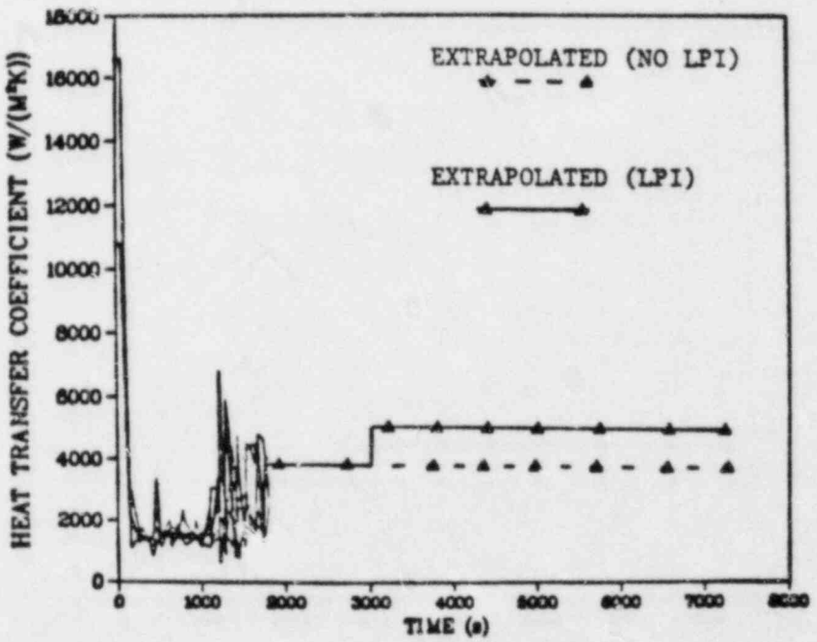

Fig. B-23.
4-in-diam. SBLOCA extrapolated downcomer heat-transfer coefficient.

3. Accumulators and LPI will not actuate
4. No operator actions taken
5. ICS, trips, and system components function correctly.

Modeling Assumptions/Uncertainties

The following modeling assumptions possibly affected the calculated results:

1. MFW pump speed increased to maximum rated speed
2. MFCVs fixed open (at steady-state flow area) until realignment trip.

No uncertainties in the TRAC modeling such as, failure of the TRAC ICS/trips to function as the B&W ICS/trips would function for this particular accident sequence were found.

Effect of Modeling Assumptions/Uncertainties

The modeling assumptions listed probably would not significantly affect the calculated final vessel downcomer liquid temperature results. The uncertainty of the modeling has essentially no effect on the calculated downcomer liquid temperature. Based on the modeling assumptions described, a downcomer liquid temperature uncertainty of ±15 K has been estimated for the extrapolated results.

B. 4-In-Diam. SBLOCA Extrapolation

Extrapolation Assumptions

The extrapolation of the 4-in-diam. SBLOCA primary system pressure, vessel downcomer liquid temperatures, and vessel downcomer heat transfer coefficients presented in Figs. B-21 through B-23 assume the following:

1. HPI, accumulators, and LPI continue to operate
2. Break is not isolated (closed)
3. No operator actions taken
4. ICS, trips, and system components function correctly.

Modeling Assumptions/Uncertainties

The following modeling assumption affected the calculated results: Total LPI volumetric flow rate of 6000 gpm (2 pumps) at 50 °F.

No uncertainties in the TRAC modeling such as, failure of the ICS/trips to function as the B&W ICS/trips would function for this particular accident sequence were found.

Effect of Modeling Assumptions/Uncertainties

The LPI modeling assumption does affect the calculated final system pressure, vessel downcomer liquid temperature, and heat-transfer coefficient results. The LPI volumetric flow of 6000 gpm (2 pumps) at 50 °F reflects the maximum discharge rate and temperature for the LPI system obtained from the

FSAR. Variations in the volumetric flow (as a function of system pressure) would somewhat alter the slope of the system pressure curve, the downcomer liquid temperature profiles, and calculated heat-transfer coefficients. The extrapolation of the three key parameters following the LPI actuation (~1265 s) is very difficult and should be recognized as a rough approximation. Based upon the modeling assumptions made, the following uncertainties were estimated for the extrapolated results:

1. System pressure - ± 2.0 x 10^5 Pa
2. Downcomer liquid temperature - ± 30 K
3. Downcomer heat-transfer coefficient - ± 2000 W/cm^2 K.

C. SG Dryout Followed by EFW Overfeed (Rancho Seco-Type Transient)

Extrapolation Assumptions

The extrapolation of the SG dryout followed by EFW overfeed transient primary system pressure, vessel downcomer liquid temperatures, and vessel downcomer heat-transfer coefficient presented in Figs. B-27 thru B-29 assume the following:

1. SG level will not be restored to correct level by 7200 s.
2. HPI will not be throttled to maintain 50°F subcooling by 7200 s.
3. No further operator action taken.
4. ICS, trips, and system components function correctly.

The following uncertainties were estimated for the extrapolated results:

1. System pressure - ± 2.0 x 10^5 Pa
2. Downcomer liquid temperature - ± 30 K
3. Downcomer heat-transfer coefficient - ± 500 w/m^2 K.

Modeling Assumptions/Uncertainties

No modeling assumptions or uncertainties in the TRAC model were found to affect the calculated results.

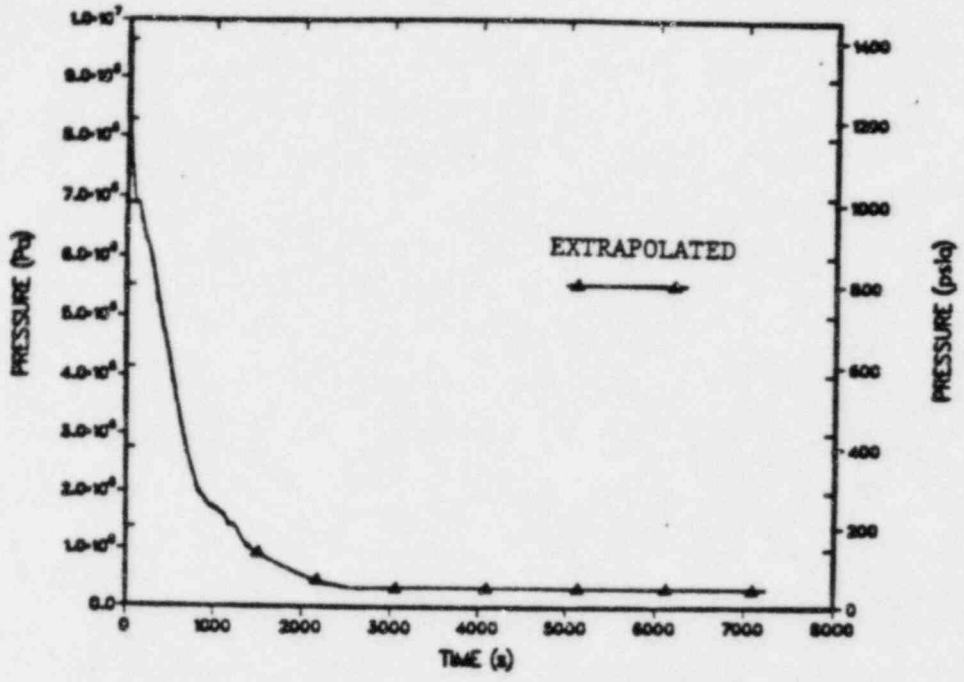

Fig. B-24.
4-in-diam. SBLOCA extrapolated system pressure.

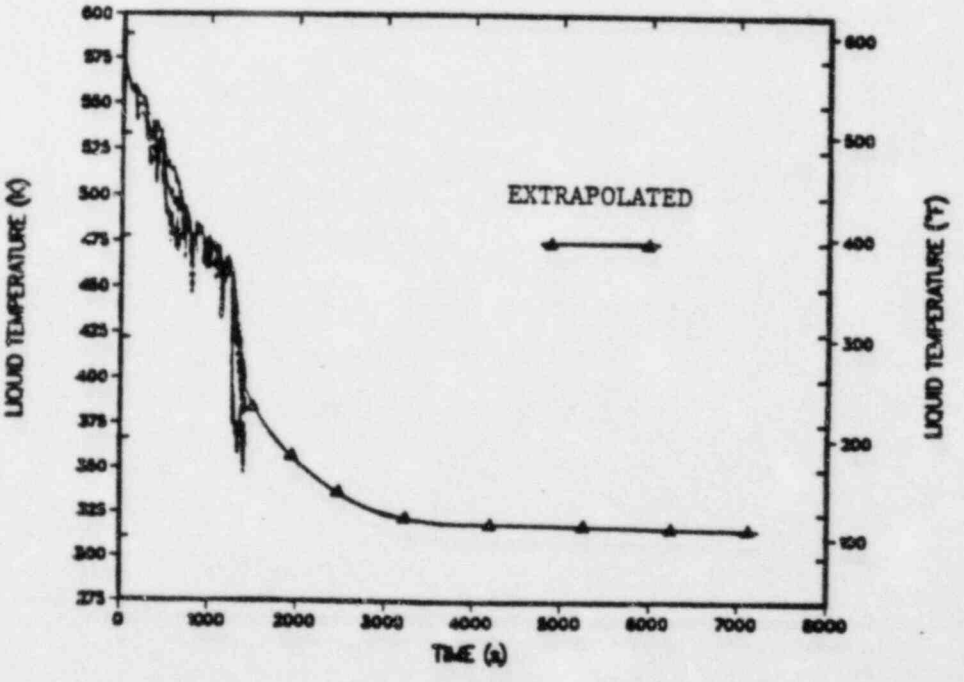

Fig. B-25.
4-in-diam. SBLOCA extrapolated downcomer liquid temperature.

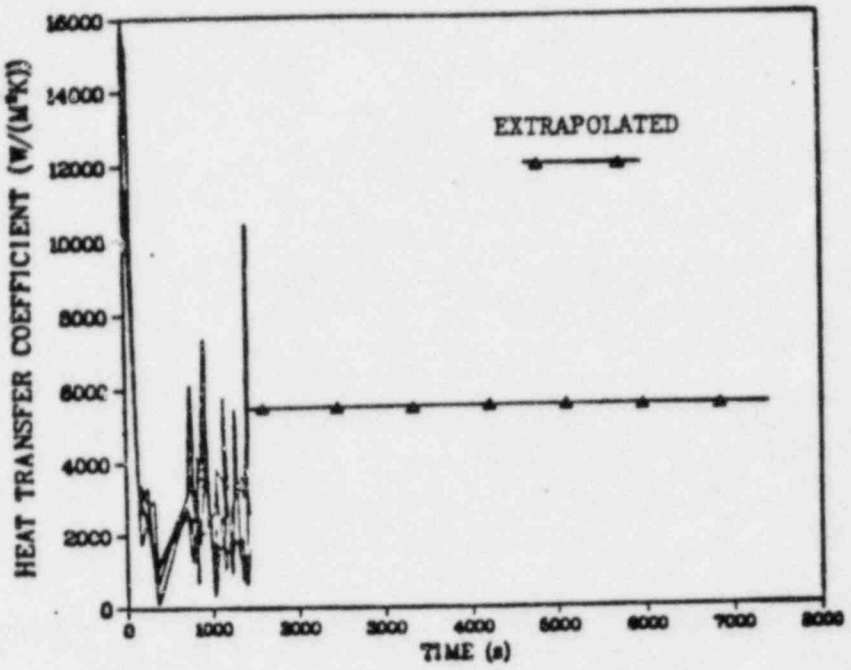

Fig. B-26.
4-in-diam. SBLOCA extrapolated downcomer heat-transfer coefficient.

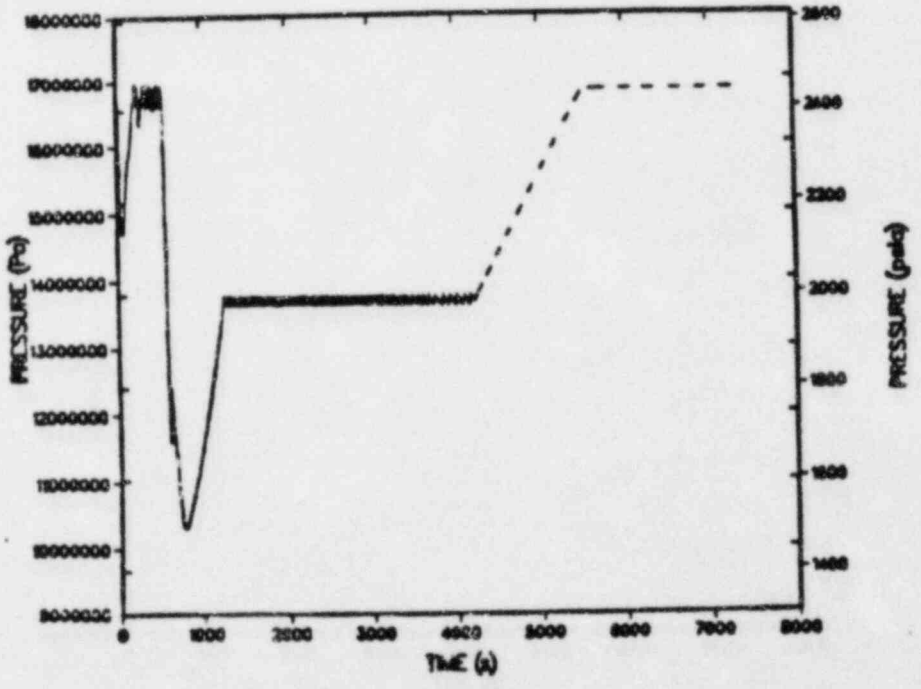

Fig. B-27.
Rancho-Seco type transient extrapolated system pressure.

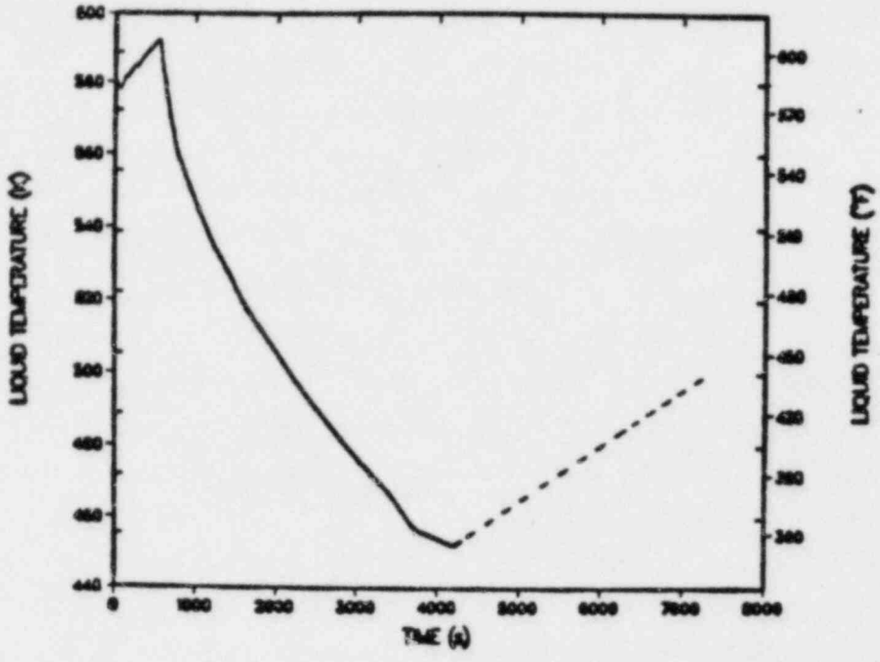

Fig. B-28.
Rancho-Seco type transient extrapolated downcomer liquid temperature.

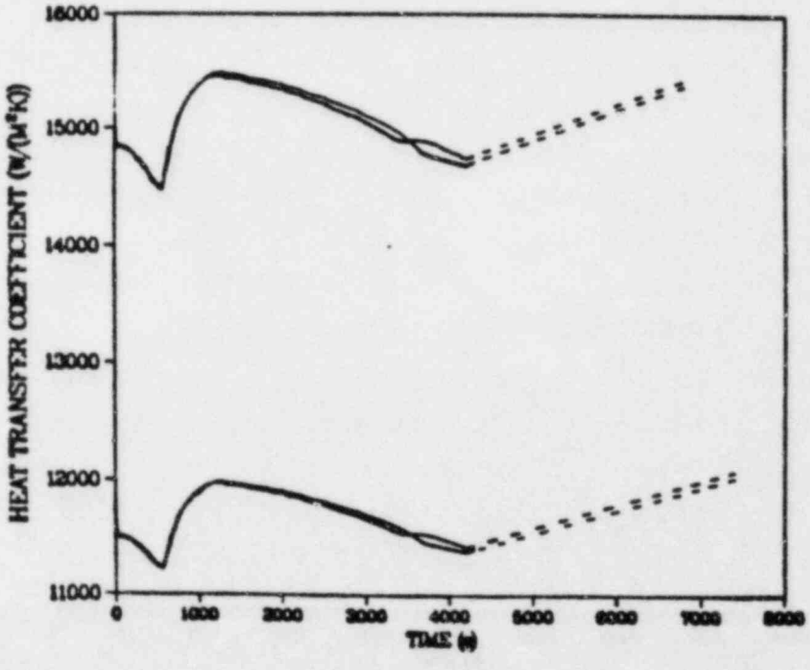

Fig. B-29.
Rancho-Seco type transient extraplated downcomer heat-transfer coefficients.

APPENDIX C

UNCERTAINTIES IN OCONEE PTS CALCULATIONS

I. INTRODUCTION

Any realistic evaluations in uncertainties occurring in the Oconee PTS calculations should be obtained by sensitivity analyses. Such analyses require time, manpower, and money, none of which were available to assess the uncertainties in this study. In the absence of such resources, we used an algorithm that has a weak basis, but can be used to estimate the influence of uncertainties on the calculations.

Contributors to uncertainty in the calculations include (1) physical models (heat transfer, flow regime, choked flow, equation of state, condensation, frictional losses), (2) component models (fuel rod, steam generator, valves, pumps), (3) initial conditions (operating power, system pressure, primary flow rate, steam generator inventory, pressurizer inventory), (4) plant model (noding, combined components, setpoints, control delays, shutdown margin), (5) operator actions, and (6) numerical methods. For the same accident initiator, changes in these contributors can cause a wide spread in results, particularly if one focuses on the results at a given instant in time. One can, by definition, fix the transient by declaring that the only uncertainties in which we have interest are those arising from the TRAC code, i.e., physical models, component models, numerical methods, and plant input deck (excluding setpoints etc.). Even with this restricted definition, the temperature and pressure uncertainties can cause a setpoint to be reached earlier or later such that the transient takes a different path and the subsequent uncertainty at a given instant in time can still be large.

Such nonlinear behavior and the overall nonlinearity of the equations being solved make estimating uncertainties extremely difficult. One must also be careful about arbitrarily picking temperatures and pressures from within the uncertainty ranges; they are not necessarily independent because the uncertainties that may cause the temperture to be lower than the best estimate will probably cause the pressure to behave in a like manner.

II. UNCERTAINTY ALGORITHM

If we concentrate on physical models, we know that heat-transfer correlations match the data to within 10-20%. We have also used TRAC to predict PORV flowrates to within 15-25%. Other uncertainties may be within similar ranges. On the other hand, we knew we were within 2-5 K on initial temperatures, and we set the pressure to be the normal operating pressure. Thus, we assumed that the initial uncertainty was close to zero given that the initial conditions were defined.

Our algorithm ignored the nonlinear effects and accounted for the initially small uncertainty. Basically we assumed that the uncertainty was proportional to the deviation from the steady-state conditions. For the proportionality constant, we relied on the uncertainties seen in heat-transfer and choked-flow correlations, 10-20%. We used 20% for this study. Please note that in testing TRAC against data from integral experiments, we have been able to predict results to better than 20% but usually only after adjustment of the input model to obtain better resolution in specific regions of the calculations.

Thus, our algorithm for the temperature uncertainty was

$$\delta T = 0.2\ |T_t - T_s|,$$

and the pressure uncertainty was

$$\delta p = 0.2\ |p_t - p_s|,$$

where T_t and P_t are the transient temperature and pressure, respectively, and T_s and p_s are the steady-state temperature and pressure, respectively.

As the transient values began to approach the steady-state values, then the maximum uncertainty predicted so far was used. These algorithms were used directly to obtain the uncertainty in the primary-system pressure and the downcomer liquid temperature. The initial primary system pressure was 15.03 MPa, and the initial downcomer temperature was 563 K. We used a 20% uncertainty in heat-transfer coefficient at all times.

III. UNCERTAINTY EFFECTS ON PTS TRANSIENTS

We examined each transient to determine how these uncertainties might affect certain system trips listed in Table C-I. Almost all of these systems were tripped by pressure. We did not account for overlapping uncertainties arising from uncertainties in both the setpoints and the pressure. Table C-I also includes the effective uncertainty range for this trips. For example, our best-estimate calculations used 10.44 MPa to trip on high-pressure injection. However, at 11.21 MPa, 20% uncertainty might also cause the HPI to trip on, or with 20% uncertainty, the trip might be delayed until the best-estimate pressure reached 9.29 MPa. In other words the effective uncertainty range is not the uncertainty in the setpoint, but how the pressure uncertainty can be translated into an effective setpoint uncertainty. In the following we examine the possible effect of these uncertainties on the transients.

A. Main Steam-Line Break

The loop-B TBV was tripped (7.064 MPa) open at 5 s; the loop-B pressure increased so rapidly that its uncertainty should have little effect on the transient. At 21.2 s the HPI was tripped on (10.44 MPa); the cooling effect of the MSLB so overwhelmed the calculation that an advance or delay in HPI should have little effect. Advance or delay of the RCP trip, which occurred 30 s later, may have some effect because the high flows associated with RCPs on enhance the heat transfer to the steam generator. However, the pressures dropped so rapidly that the advance or delay would be only a few seconds. At 526 s the subcooling margin 42 K was reached, and the HPI was shut off and the RCPs were restarted. A delay would have given colder downcomer temperatures at a time when the pressure was increasing. An advance may have had the opposite effect. The accumulators were predicted (4.17 MPa) to inject at 531 s. The

TABLE C-I

SYSTEMS AFFECTED BY UNCERTAINTIES

System	Setpoint	Effective Uncertainty Range
Turbine Bypass Valve (TBV)	7.064 MPa	6.94-7.26
High Pressure Injection (HPI) on	10.44 MPa	9.29-11.21
Reactor Coolant Pumps (RCPs)	30s after HPI on	
Accumulators	4.17 MPa	1.46-5.98
PORV	16.9 MPa	16.59-17.37
Low Pressure Injection (LPI)	1.0 MPa	0.0-3.34
High Pressure Injection Off	42 K + 12.5 K subcooling	

uncertainty is such that they could have begun dumping as early as ~70 s. This could have caused more cooling, possibly more subcooling with the additional possibility for the RCPs to be restarted earlier. The PORV setpoint was hit at 4678 s; the results are insensitive to the uncertainty in when the PORV opened.

B. PORV LOCA

The trips observed in this transient were TBV opens at 4.4 s, the HPI comes on at 70 s and the RCPs are shut off at 100 s. The transient would be insensitive to the uncertainties that might change the timing of these trips. No accumulator injection occurred and none would be expected, even with the pressure uncertainty.

C. TBV Failure-One Bank

All three transients would be insensitive to the uncertainty in the opening of the loop-A TBV at 4.1 s. The HPI was initiated at 153 s with subsequent RCP shutoff at 183 s. The pressure uncertainty may advance or delay this trip, but it should have no effect on the transient. The pressure plateau from 180 s to 380 s could be shortened or lengthened. In the second parametric case, the RCPs were restarted when the subcooling margin was reached at 383 s. Uncertainty in the subcooling margin could advance or delay this restart, which causes the pressure to drop and the downcomer temperature to increase. Although the accumulators were not predicted to actuate, the pressure uncertainty could cause accumulator actuation at approximately 900 s in the second parametric case.

D. TBV Failure-Two Banks

Again all three transients would be insensitive to the uncertainty in the timing of the TBV at 4.1 s. The HPI is tripped on at 87.5 s, with the RCPs tripped off 30 s later. With the rapidly decreasing pressure at 87.5 s, these trips and their effects would be insensitive to the pressure uncertainty. In the second parametric case, RCP restart caused a rapid pressure decrease such that at 565 s the accumulators were actuated. Again the pressure decreases rapidly and the accumulator actuation would be insensitive to the pressure uncertainty. Uncertainty in the subcooling monitor trip could advance or delay the RCP restart or the HPI throttling at 485 s. This would be expected to have little effect on the transient. The pressure uncertainty in the base case approaches the accumulator setpoint at approximately 300 s. The pressure increase that occurs immediately thereafter indicates that the accumulators would probably shut off almost immediately.

E. Two-Inch SBLOCA

The transient would be insensitive to the timing of the TBV opening at 4.1 s. HPI is initiated at 43 s and RCP trip at 73 s; again this timing is not very sensitive because the pressure is decreasing so rapidly. Accumulator actuation is predicted at 1800 s; uncertainty in pressure could lead to actuation as early as 1200 s.

F. Four-Inch SBLOCA

Again the timings of the TBV opening, HPI initiation, and RCP trip would be insensitive to the pressure uncertainties. The pressure uncertainty could lead to accumulator actuation as early as 280 s instead of the predicted 540 s, or it could be delayed until approximately 1200 s. Low pressure injection could have started as early as approximately 600 s instead of the predicted 1236 s.

G. Rancho Seco

The Rancho Seco transient is fairly insensitive to the pressure uncertainties. The timing of HPI initiation, predicted at 738 s, would be changed by the uncertainties, but would have little effect on the overall transient.

IV. CONCLUSIONS

Overall, it is probable that uncertainties in the timing of the actuation of the engineered safety features, arising from thermal-hydraulic uncertainties, would have little effect on pressurized thermal shock results for these transients. Only a more extensive sensitivity study could verify this conclusion.